Cortical - Basal Ganglia Circuits: Control of Behaviour and Alcohol Misuse

Laurel Sophia Morris
Downing College
March 2017

This dissertation is submitted for the degree of
Doctor of Philosophy of Letters PhD.

Preface

This dissertation is the result of my own work and includes nothing which is the outcome of work done in collaboration except as declared in the Preface and specified in the text. It is not substantially the same as any that I have submitted, or, is being concurrently submitted for a degree or diploma or other qualification at the University of Cambridge or any other University or similar institution except as declared in the Preface and specified in the text. I further state that no substantial part of my dissertation has already been submitted, or, is being concurrently submitted for any such degree, diploma or other qualification at the University of Cambridge or any other University or similar institution except as declared in the Preface and specified in the text. It does not exceed the prescribed word limit for the relevant Degree Committee.

Acknowledgements

I would like to thank my excellent PhD supervisors, Dr Valerie Voon and Professor Trevor Robbins, who massively supported all of my work and decisions and taught me innumerable technical, professional and career-based lessons. Both provided me with incredible opportunities to advance my academic and research work throughout my PhD and offered me absolute freedom to pursue my own interests. I would like to thank the Medical Research Council, the Behavioural and Clinical Neuroscience Institute and the Department of Psychology for supporting my PhD.

I would like to thank everyone in the Voon group during my time there who contributed significantly to my growth, learning and achievement, particularly Kwangyeol Baek, as well as Mike Irvine, Pauline Favre, Yee-Chien Chang-Webb, Daisy Mechelmans, Daniela Strelchuk for supporting the research activities of the group.

I would like to thank my parents; seven brothers and sisters; and numerous nieces and nephews, for being extremely supportive. Thanks to mum in particular for being the head of the family and motivating me to achieve my absolute best at all times.

I would like to thank Downing College for taking me on as student and as the Middle Combination Room (MCR) social secretary, along with my fellow committee members, child Audrey Valreau, James McTavish and Jordan Rush. The MCR community at Downing gave me some of the most memorable dinners, swaps, balls, mini-balls, garden parties, boat races, whiskey tastings and seminar nights one could hope to experience in Cambridge.

I would like to thank Winnets & Co., for hanging around, magically uniting and for developing and running the annual Princess Cake Day. I would like to thank the Alma for the pub quiz, the opportunity to watch Man City smash other teams in the Premier League and of course, for the free champagne. I finally thank Gael for being there for the final stages of my PhD in Hong Kong and Japan.

Contents

Abbreviations

4-CSRT	4-Choice Serial Reaction Time Task
ACC	Anterior Cingulate Cortex
AD	Alcohol dependence
BA	Brodmann's Area
BD	Binge Drinker
BDI	Beck Depression Inventory
BOLD	Blood Oxygenation Level Dependent
DBS	Deep Brain Stimulation
dlpfc	Dorsolateral Prefrontal Cortex
dmpfc	Dorsomedial Prefrontal Cortex
fMRI	Functional Magnetic Resonance Imaging
FWE	Family-Wise Error
HV	Healthy Volunteer
Hz	Herz
IFC	Inferior Frontal Cortex
IQ	Intelligence Quotient
K	Cluster Extent Size
MNI	Montreal Neurological Institute
NAc	Nucleus Accumbens
OFC	Orbitofrontal Cortex
p	Probability of obtained versus expected value
P	Probability
PD	Parkinson's Disease
PFC	Prefrontal Cortex
ROI	Region of Interest
rsfMRI	Resting State fMRI
RT	Reaction Time
SD	Standard Deviation
SMA	Supplementary Motor Area
SPM	Statistical Parametric Mapping
SSRT	Stop Signal Reaction Time
SST	Stop Signal Task
SVC	Small Volume Corrected
vmpfc	Ventromedial Prefrontal Cortex
xyz	Peak Coordinates in MNI Space
Z	Z-Score

Introduction

Cortical – Basal Ganglia Circuitry

The systematic elucidation of neural organizational architecture is crucial for the understanding of diverse higher cognitive functions of the brain. The most highly evolved neural structure, the neocortex, is densely connected in a specific and deliberate pattern with the evolutionarily older subcortical structures, like the basal ganglia (and cerebellum). These circuits form and unite to link the frontal cortex with the basal ganglia and thalamus to mediate movement, cognition and behaviour[1, 2].

While the basal ganglia function were traditionally associated with motor functions, myriad subsequent evidence from lesion and neuroimaging studies has argued for more diverse roles in a range of cognitive and behavioural faculties, from skill learning[3], to language[4], to attention and planning[5, 6]. The basal ganglia have been suggested to serve a general computational role in the brain, to integrate functionally diverse information received from cortical regions to devise and implement goal-directed behaviour[7, 8]. Additionally, the PFC also maintains a 'top-down' regulatory role over the basal ganglia, to fine tune attention, inhibition and emotional tone[9]. Behaviour is therefore modulated via patterns of temporal and spatial activation and inhibition, allowing subtle modulation of behavioural programs[10, 11]. Together, these cortical – basal ganglia circuits work to accomplish diverse behaviours, from steering the cognition required to select an appropriate behaviour, to motivating and organizing their implementation, and finally to execute them.

Components

The cortex is broadly divided into frontal, temporal, parietal and occipital lobes. The majority of work on cortical and basal ganglia interactions implicates the frontal lobe as the major cortical site for the cortical – basal ganglia circuit loops. The PFC mediates executive function, a general term that includes diverse functions and processing that

broadly mediates goal selection, planning, anticipation and implementation[12]. It is also involved with maintaining active and online representations of goals for the guidance of behaviour (working memory), and providing 'top-down' regulation of attentional, inhibitory and emotional processes. The frontal cortex can be broadly anatomically divided into two distinct functional systems. A dorsal system processes sequential, sensory and spatial information and a ventral system regulates emotional and limbic tone. The frontal cortex crucially works to integrate and regulate the information processing through these discrete functional systems to orchestrate behaviour[13].

Dissociations between frontal cortical regions in humans remain a subject of debate. Frontal cortical regions can be defined based on cytoarchitechtonic [14-16], characteristics, functions [17, 18] or latent network organization[19, 20]. While there is ongoing debate, this thesis defines OFC as the most ventral portion of the frontal cortex, above the orbits of the skull, with a dorsal extent to the dorsal tip of the olfactory sulcus. The ventromedial PFC is directly dorsal to the OFC and includes only the medial frontal gryri, with a dorsal extent to the mid genu of the corpus callosum, not including ACC. The dorsomedial PFC occupies the medial frontal wall directly dorsal to the vmpfc. The dlpfc is typically defined as Brodmann areas 9 and 46. The IFC is defined as dorsal to the OFC, lateral to the vmpfc and inferior of the dlpfc. A schematic depiction of these subdivisions in humans is demonstrated in Figure 1 and further details of cortical subregion definitions are provided in full in Data Chapter 1.

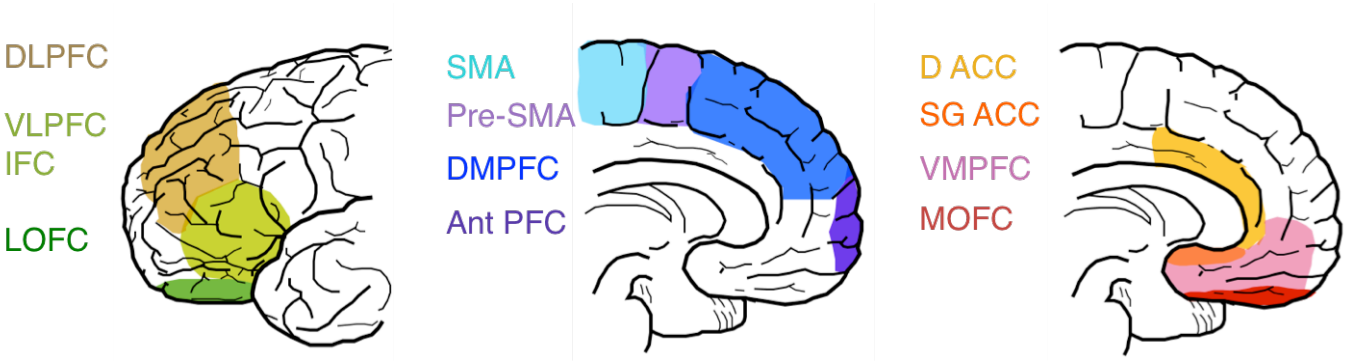

Figure 1. Schematic depiction of frontal cortical subdivisions in humans.
Abbreviations: dorsolateral prefrontal cortex (DLPFC), ventrolateral prefrontal cortex (VLPFC), inferior frontal cortex (IFC), lateral orbitofrontal cortex (LOFC), supplementary

motor area (SMA), dorsomedial prefrontal cortex (DMPFC), anterior prefrontal cortex (Ant PFC), dorsal anterior cingulate cortex (D ACC), subgenual ACC (SG ACC), ventromedial prefrontal cortex (VMPFC), medial orbitofrontal cortex (MOFC).

The dlpfc and IFC inhibit attention to irrelevant or distractor stimuli or information, and sustain attention on goal-relevant representations, working to coordinate attentional resources in an appropriate manner depending on the task in hand, and in particular working with the caudate nucleus via the associative circuit[9, 21]. The IFC also regulates the inhibitory control of behaviour, particularly in the face of interference, with the right IFC more involved with inhibitory control and motor impulsivity, working with other cortical regions (SMA, motor cortex) and basal ganglia structures (STN)[9, 22]. The OFC and vmpfc, via connections with limbic structures outside of the basal ganglia like amygdala and hippocampus, regulate emotional responses to arousing or fearful environmental information by activating or inhibiting behavioural responses and flexibly updating emotional responses to rewards and punishments [23-25]. Together, regions within the PFC regulate a plethora of functional processes, guiding and mediating attentional, inhibitory and emotional responses.

The basal ganglia are strongly implicated in general reward-related learning and decision making to guide both automatic and controlled behaviour[11, 26]. Adaptive behaviour in a dynamic world requires an ability to adjust behaviour in light of changing environmental information like rewards in the pursuit of current or future goals and basal ganglia – mediated learning of contingencies between actions and outcomes forms the basis of instrumental conditioning, required for rapid behavioural choice[27, 28]. The basal ganglia are made up of several interconnected structures including the striatum, globus pallidus, substantia nigra, subthalamic nucleus and thalamus. Each of these structures can be further subdivided based on inputs, function and outputs, in a similar manner to frontal cortical regions. For example, the striatum can be divided into dorsomedial caudate nucleus, dorsolateral putamen and ventral striatum including nucleus accumbens. The use of this terminology broadly covers both human and rodent studies. The term ‘ventral striatum’ is used to describe a region in humans that includes the

nucleus accumbens core and shell, as well as some small surrounding portion of ventral caudate and anterior ventral putamen, due to the low spatial resolution of MRI.

The striatum is comprised primarily of medium spiny GABAergic projection neurons[7, 29] and sends inhibitory projections to the GABAergic cells of the globus pallidus interna and externa. The globus pallidus interna is the primary output structure of the basal ganglia and sends GABAergic projections to the thalamus. The thalamus in turn relays excitatory glutamatergic projections to the cortex and striatum. This is commonly described as the 'direct' pathway[30] and uses substance P as a co-neurotransmitter within the GABA projection[2, 7]. In the 'indirect' pathway, the globus pallidus externa sends inhibitory GABA-ergic projections (along with the co-transmitter enkephalin)[2, 7] to the glutamatergic cells of the subthalamic nucleus, which emits excitatory projections back to the globus pallidus externa and also relays to the output structure of the globus pallidus interna. Activity through the direct pathway therefore causes disinhibition of the thalamic excitatory outputs to the cortex, allowing glutamatergic activation of cortical target regions and in the case of the motor circuit, movement[1, 30, 31]. Activity through the indirect pathway however, results in inhibition of the thalamic outputs to the cortex and for motor target cortical regions, this can result in slowing or stopping of movement[13, 30, 31]. Thus, the parallel circuits can have opponent effects, depending on the pathway recruited.

The ventral tegmental area provides dopaminergic afferents to the ventromedial striatum, including medial nucleus accumbens shell[7, 32, 33], acting as a 'Go' signal for foraging or exploration[34]. Stimuli that trigger ventral tegmental area release of dopamine to the ventral striatum include natural rewards (food, sex) and drug rewards (cocaine, nicotine)[33, 35, 36]. The substantia nigra provides a parallel dopaminergic input to the dorsal striatum, including caudate and putamen, for the initiation and execution of motor programs and motivational processing[7, 34, 37]. The direct pathway expresses predominantly dopamine D1 receptors whereas the indirect pathway expresses predominantly dopamine D2 receptors[2, 38] and their activation facilitates and inhibits cortico – striatal transmission, respectively[38, 39]. Therefore, increased dopamine in the

direct pathway activates this circuit, leading to inhibition of globus pallidus interna, disinhibition of thalamus and increased thalamo – cortical excitation. Increased dopamine in the indirect pathway leads disinhibition of globus pallidus external, inhibition of STN, which allows the globus pallidus interna to inhibit the thalamus, blocking the excitatory projections from thalamus to cortex.

Dopaminergic projections to the striatum and striatal activity have been shown to encode rewarding properties of unconditioned and conditioned stimuli, as well as an unexpected presence or absence of reward and its magnitude[40-43]. This neural encoding of expected and actual rewarding outcomes, and importantly, the difference between the two, forms the basis of evidence for computational reinforcement learning in the brain[26, 44]. In artificial intelligence algorithms, the 'temporal difference' between the expected and actual outcome is used to update the predicted value of a relevant action[26, 45]. This parameter closely mirrors the signals observed in the striatum [26, 40, 41] and it follows that such striatal reward-related signaling is critical for updating and guiding reward-related decision making[26, 28]. Indeed, basal ganglia dopamine is also implicated in the flexible updating of cognitive or behavioural programs in the face of changing task demands or environmental information[46]. The role of the basal ganglia in gating motor[47] and cognitive[48-50] processing means that they are well poised to halt, shift or stop behaviour when an update in strategy is required. Indeed, the basal ganglia are active during attentional and task shifting and reversal learning [51, 52], It has been proposed that, at least for attentional shifting, the basal ganglia adheres to a threshold for salient information and when that threshold is met, it allows the PFC to direct or shift attention[46], a hypothesis that requires further evidence before being accepted.

There are some differences between rodent and primate anatomy that should be noted. The ventral striatum is made up of more complex neurochemical organization in primates compared to rodents [53-55]. The division between the nucleus accumbens core and shell is well established in rodents but there has been some debate as to separate regions in primates. A study examining immunoreactivity in the marmoset, rhesus and human brain demonstrated a distinction between the semi-circle shaped outer shell

region commonly observed in rats, and an inner core region [56]. While the core and shell is difficult to definitively dissociate in humans, the core-shell distinction has been suggested in primates [57-59]. Other basal ganglia nuclei have been compared in a study assessing rats, marmosets, macaques, baboons and humans [53]. Volumes and numbers of neurons for the major components of the basal ganglia network were compared relative to whole brain volumes. Neuronal numbers were equivalent across species, corrected for brain size, for the globus pallidus interna and externa, striatum, substantia nigra and STN [53]. Humans had fewer substantia nigra dopaminergic neuronal populations compared to other species. Taken together, these studies suggest that while there are differences between species in anatomy, major features of basal ganglia nuclei are broadly equivalent.

In summary, the output of the basal ganglia and subsequent control of movement can be mediated via the direct cortico-striatal-globus pallidus interna pathway; the indirect cortico-striatal-globus pallidus externa-STN-globus pallidus interna pathway; and the cortico-STN- globus pallidus interna hyperdirect pathway[31]. Indeed, the globus pallidus interna displays a characteristic triphasic response following stimulation of motor cortical regions [31, 60]. This consists of an initial excitation, followed by inhibition and a late excitation in the globus pallidus interna. These three phases reflect processing through the hyperdirect pathway, and then presumably the direct pathway, and the indirect pathway, respectively[61]. Importantly, alongside these uni-directional feed-forward circuits, there are feedback pathways that create a cascading loop of functional influence. The primary example of this is the output of the nucleus accumbens core which can modulate dorsal striatal processing via projections to substantia nigra[62, 63]. The significance of this ‘cascading’ set of pathways is explored further in later sections.

Circuits

The flow of information follows a cortical – basal ganglia – thalamic – cortical path, with the progressive convergence of the multiple initial cortical inputs and integrated passage through basal ganglia structures before reaching the thalamus, which in turn relays the

information to a single cortical region[1, 2]. Cortical regions project long range excitatory glutamatergic efferents to the striatum[64, 65], the primary input structure of the basal ganglia, in a segregated and organised manner[65, 66]. As well as receiving afferents from the cortex, the striatum receives excitatory inputs from the thalamus, amygdala and hippocampus, and dopaminergic inputs from the substantia nigra (dorsal striatum) and ventral tegmental area (ventral striatum). An example of the spatial organization of the circuits following a conserved pattern is demonstrated by the dlpfc, which projects to the dorsolateral portion of the caudate nucleus[2]. See Figure 2 for a schematic depiction of the cortical – basal ganglia – thalamic – cortical connections described in the following text.

The classical view of the basal ganglia circuitry is that cortical inputs to the striatum, including the hippocampus and the basolateral amygdala converge with other inputs, to be integrated and processed, before being sent through the downstream structures of the basal ganglia[7]. Previous assertions that the basal ganglia primarily acted to filter cortical information to facilitate motor outputs have since given way to an understanding of the basal ganglia as a relay and gating structure with functionally and structurally segregated inputs, functions and outputs[1, 30]. Early studies suggested that this circuit could be divided into two, representing “motor” and “association” functions[67]. Building upon that, Alexander et al[1] suggested that there were in fact five parallel circuits, including motor, oculomotor, dorsolateral prefrontal, lateral orbitofrontal and anterior cingulate. Later, two additional circuits were proposed[68, 69] but have been suggested to equate to sub-circuits of a broader motor circuit[69]. Indeed, distinctions can be made between caudal and rostral cortical motor regions, SMA, motor cingulate and premotor cortex and their projections to striatum, although they collectively project to the more caudal putamen, missing the more rostral portions of the striatum, whereas the dlpfc projects to the caudate nucleus and not the putamen[70]. While there is still debate as to the extent that these circuits are ‘closed’, this framework of segregated loops has been widely accepted and provides a useful way of conceptualizing the functional organization underlying behaviour. More recently, studies have collated these segregations into comprising of three broadly separable functional domains, mediating motor, cognitive, and limbic

processes [71-74]. There is certainly convergence, integration and crossover between these distinct domains at all levels of the circuit. However, separating the system into three is a useful way to test the distinct functions they serve. The choice of examining the circuit as three rather than five or seven domains allows this separation into the three broad functional domains of motor, cognitive and limbic processing.

There is some agreement that the circuits can be separated into three dissociable loops. Cortical regions traditionally associated with specific cognitive functions make segregated projections into three distinct striatal regions, with this tri-loop segregation being maintained at the pallidal level too[75-77]. The apparent separation of these circuits supports the organizational dissociation of circuit-specific behaviours[2] and there is some evidence that disruption of loci within the same circuit can result in selective cognitive or behavioural changes[2, 78], broadly associating each circuit with certain behavioural or cognitive process. Early evidence for the dissociation of the three circuits into specific cognitive or behavioural roles came from lesion studies. Lesions to nodes or regions within the same circuit produced similar behavioural deficits in non-human primates. For example, gross lesions of the dlpfc and dorsal caudate both resulted in deficits in delay response and alternation tasks[79] and lesions to the OFC and ventral caudate both resulted in response inhibition deficits[80], highlighting that distinct nodes within the same circuit are responsible for the same types of cognitive tasks. It should be noted still that nodes of the cortical basal ganglia circuitry are involved with a range of other functions too, for example lesions to the caudate can have broad cognitive effects, including on avoidance behaviours[81, 82], general cognitive ability [83] and social cognition [84].

The motor circuit has been most widely described[1, 2] and includes topographic projections from the primary motor cortex, SMA and premotor area to the dorsolateral striatum or putamen[7, 85, 86]. The putamen in turn projects topographically to specific regions of the globus pallidus that can thus be described as ‘motor’ portions, and thence to specific subnuclei of the thalamus[30, 87]. Thalamic subnuclei connect with motor cortex (ventral lateral and ventral anterior), SMA (ventral lateral, ventral anterior, lateral

posterior) and premotor cortex[30, 87]. Activation through the motor circuit broadly results in execution and preparation of movement[30]. Also, activity through the dorsolateral striatum has been broadly associated with stimulus-response learning and habit formation[29].

The associative or cognitive circuit is involved with executive function, broadly including goal selection, planning, anticipation and implementation[12]. This circuit originates in the dlpfc, Brodmann areas 8, 9, 10 and 46 [7]. Projections from the dlpfc terminate on the dorsolateral head of the caudate[65], which in turn projects to lateral mediodorsal globus pallidus interna and anteriolateral substantia nigra in the direct pathway and the dorsal globus pallidus externa and lateral subthalamic nucleus in the indirect pathway[2, 88]. The globus pallidus interna and substantia nigra terminate on the anteroventral and mediodorsal thalamic nuclei, respectively[2, 89]. The mediodorsal thalamus then projects back to the PFC, particularly the dlpfc to complete the circuit[90]. Via the associative circuit through the caudate, the dlpfc is thought to mediate executive function, planning, working memory and attentional shifting or guiding behaviour appropriately in the face of a changing environment[2, 75, 91]. Lesions to the dlpfc perturb attention regulation, focus, maintenance and shifting in response to changing task demands[80] and memory search and organizational strategies[13], with similar disturbances in individuals with lesions to regions subcortically downstream of the same circuit, including caudate[92] and mediodorsal thalamus[93, 94]. Circuits involving the dorsomedial striatum are broadly associated with action-outcome learning and goal-directed behaviour[29].

The so-called limbic circuit is the third broadly distinguishable circuit and is involved with reward and reinforcement[75, 91]. The OFC, infralimbic and prelimbic cortices, ACC, amygdala and hippocampus project to ventromedial caudate and ventral striatum or nucleus accumbens[7, 65, 76, 95]. The OFC and ACC mediate reward-based learning and goal directed behavioural control, motivation, and modulate appropriate responses to social cues and mood[2]. The lateral and medial OFC can be dissociated, with divergence anatomical and functional properties, including projections to ventromedial caudate and ventral striatum / nucleus accumbens, respectively[70, 96]. The medial OFC

combines visceral information with internal state representations[13, 96]. OFC lesions result in a disconnection between frontal control systems and limbic tone that leads to behavioural disinhibition, distractibility and inappropriate social behaviour and judgment[13, 80, 97], while other executive functions remain intact[97]. The ventral striatum in turn projects to the medial globus pallidus interna, the ventral pallidum, the anterior substantia nigra and medial subthalamic nucleus[2, 62, 98]. The ventromedial caudate also has an indirect projection to the dorsal globus pallidus externa which projects to lateral subthalamic nucleus[2, 99]. Behavioural deficits similar to those observed following OFC lesion are observed in individuals with ventral caudate lesions[92]. Lesions to the ACC can result in reduced motivation and drive, as demonstrated by the emergence of 'akinetic mutism' which includes symptoms of apathy and indifference, even to hunger and pain[13, 78, 100, 101]. Again, similar disturbances in motivational drive are observed with deficits in functioning of ventral striatum[13], ventrolateral and dorsomedial thalamus[102], substantia nigra and VTA[103]. Output projections for this pathway converge on the anteroventral and mediodorsal thalamus and back to the lateral OFC[2, 65] or ACC[104, 105]. This set of evidence from lesion studies pinpoints the characteristic behavioural control responsibilities of these circuits, demonstrating comparable deficits in response to lesions of nodes within the same circuits.

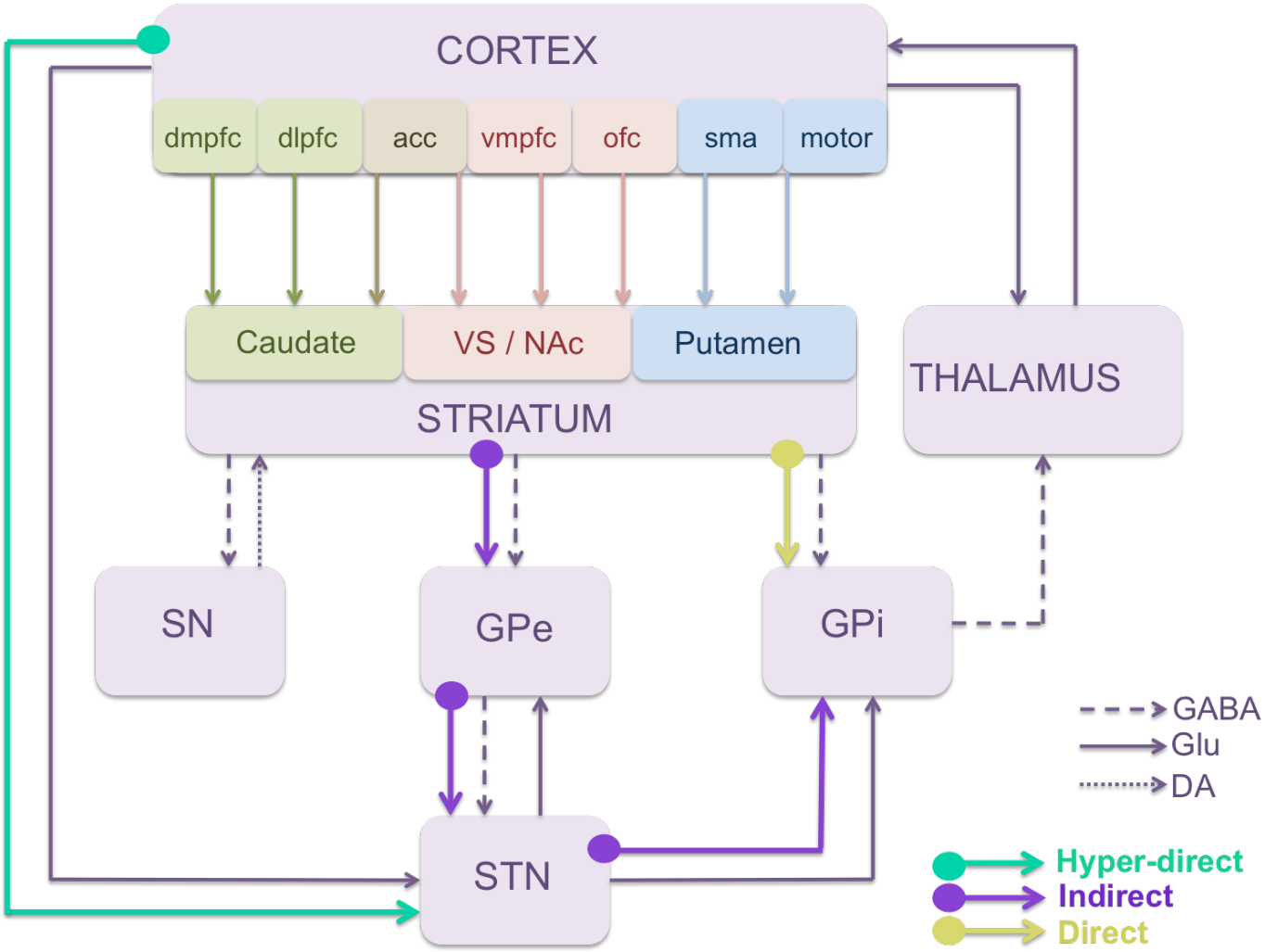

Figure 2. Schematic depiction of cortical – basal ganglia – thalamic – cortical connections. *This is a highly simplified and schematized depiction of major efferents in the cortical basal ganglia circuitry. Cortical and striatal regions in green, pink and blue boxes represent the cognitive-associative, limbic and motor pathways, respectively. The turquoise, purple and gold arrows indicate the hyperdirect, indirect and direct circuits, respectively. The dashing of the line indicates the primary neurotransmitter for that projection. Abbreviations: dorsomedial prefrontal cortex (dmPFC), dorsolateral prefrontal cortex (dlpfc), anterior cingulate cortex (acc), ventromedial prefrontal cortex (vmpfc), orbitofrontal cortex (ofc), supplementary motor area (sma), ventral striatum / nucleus accumbens (VS / NAc), substantia nigra (SN), globus pallidum externa (GPe) and interna (GPi), subthalamic nucleus (STN), γ-Aminobutyric acid (GABA), glutamate (Glu), dopamine (DA).*

The Subthalamic Nucleus

Evidence demonstrates that different portions of the STN receive and emit projections from different sites of the cortical – basal ganglia circuitry. Specifically, the posterior and dorsolateral STN projects to the motor pallidum and motor striatum, whereas the anterior, ventromedial STN projects to the associative pallidum, associative striatum, substantia nigra, and to an extent, the limbic pallidum[77]. Likewise, pallidal projections to STN follow a similar topological pattern[106], which broadly equates the most posterior, dorsolateral portion of the STN to motor function and the anterior ventromedial portion to associative-limbic function[77, 106]. While there are fewer STN projections to striatum compared to globus pallidus and substantia nigra, they seem to follow a similar segregated pattern. Projections originate primarily from anterior, lateral and dorsal portions of STN, terminating on dorsolateral striatum, and there are some projections arising from ventromedial STN terminating in anterior medial caudate[77, 107]. Therefore, different regions within the STN show different connectivity patterns. Based on this evidence, several studies have suggested a tri-partite organization of the STN, suggesting dissociable motor, limbic and cognitive-associative subdivisions[99, 108-112]. However, a report of a review of the relevant literature published before 2010 suggested that there was insufficient evidence to justify such a tri-partite model of the STN [111]. While researchers have rebutted this claim, suggesting separate limbic and motor subzones and a mixed, overlapping central associative zone [113-115], a more likely model is that there are heterogeneous gradient patterns of connectivity and function along the three axes of the STN, with some STN regions being more implicated in motor function than limbic processing for example but without a clear distinction between the two. Indeed, targeting the most anterior medial portion of the STN with DBS has evidenced effects on limbic-cognitive functioning in patients with obsessive-compulsive disorder[116, 117] whereas targeting the most posterior lateral portion is effective for motor symptoms of PD[118, 119]. Therefore while these clusters or ‘subzones’ are not divided by strict anatomical or even functional divisions within the STN, evidence suggests that the extreme posterior-lateral tip is more involved with motor function and less with limbic functioning and the extreme anterior-medial tip shows the opposite pattern [113]. When examining motor, cognitive and limbic function it can be useful to

consider these extreme sites of the STN, with the continual consideration that gradient patterns do exist in between.

The discussed broad divisions of STN efferents are also reflected in the pattern of cortical affferents to STN. Motor cortices project primarily to posterior, dorsolateral motor STN, and motor striatum; and the associative PFC, including area 8 and area 9 project to the anterior, ventromedial STN as well as the associative striatum[77]. More extensive fronto-cortical mapping of projections to STN was recently examined in non-human primates[109]. This revealed vmpfc and OFC projections to the medial tip (but mostly in adjacent lateral hypothalamus); slightly more dorsal projections from dorsal ACC to the anterior and medial tip extending into the medial half; slightly more lateral dorsal PFC projections primarily to the anterior STN pole, with projections entering the anterolateral STN and extending to the dorsal anterior portion of the medial half of the STN, as well as the ventromedial central third; and motor cortical projections in the posterior third, entering the STN via the dorsolateral portion, with primary motor cortex axons terminating at the dorsolateral region, and cortical area 6 axons terminating topographically in the central and posterior portions, avoiding the medial tip, and in the dorsal anterior portion[109]. Thus there exists an anterior – posterior and ventromedial – dorsolateral topographical gradient of cortical inputs to STN, although there also appears to be overlap and convergence of projections from neighboring cortical regions including vmpfc, dorsal PFC and dorsal ACC, as well as some overlap from more diffuse projections from primary motor cortex and dorsal PFC[109]. A recent study attempted to divide the STN into three functional subzones (anterior limbic; posterior motor; and a more mixed central associative subzone) using diffusion tractography, a technique that arguably does not have the spatial resolution to confirm such a hypothesis, but an anterior – posterior topological gradient was implicated[114].

The functional role of the hyperdirect pathway and the STN can be first assessed in relation to movement. Voluntary movement can be examined in terms of information processing through the three cortical – basal ganglia pathways (hyperdirect, direct and indirect). In order for a voluntary motor program to be carried out, the cortical motor region initiates a hyperdirect signal to inhibit thalamic and cortical motor regions

processing unwanted movement. Secondly, the direct pathway disinhibits a portion of the thalamo-cortical motor system that controls the intended or desired movement, such that that motor program is executed in isolation. Thirdly, the indirect pathway again extensively inhibits the thalamo-cortical motor system. This sequence ensures that only the intended or chosen motor program is initiated and executed while other competing movements are blocked[61]. The hyperdirect pathway plays an important role here as a mediator of voluntary movements, suppressing involuntary and unnecessary movements so that an intended and appropriate movement can be carried out[47, 61].

Beyond motor functions, it is becoming clear that the hyperdirect pathway mediates other cognitive or behavioural programs, whether they are motor, associative or limbic, by modulating the output of the basal ganglia in this rapid and cortically-mediated fashion. Diverse frontal cortical innervations of STN point towards a more mixed role in cognitive and behavioural control, rather than simply gating motor function. Any cognitive or behavioural programs that pass through the cortical – basal ganglia circuitry can be subject to filtering by the STN[109], as the hyperdirect pathway can mediate the output of the globus pallidus interna before the direct and indirect pathways reach this output structure. As such, the most appropriate cognitive or behavioural program can be selected and allowed expression via the thalamus and onto the cortical target regions. Because of this gating or mediating function, it is unsurprising that the STN has been implicated in inhibition of ongoing behaviours[120, 121], conflict processing[122, 123] and switching behaviour[124].

Impulsivity

Cognitive constructs can provide useful conceptual frameworks for the characterization of the cognitive or behavioural capacities of cortical – basal ganglia circuits. Cognitive constructs define a discrete measure of cognition or behaviour along a dimensional spectrum, allowing a transpathological understanding of a certain behaviour across seemingly disparate psychiatric groups[125, 126]. Two cognitive constructs that transcend inter-individual differences and neuropsychiatric states are impulsivity and

compulsivity[125]. Both are multi-dimensional constructs and are associated with a range of overlapping neural, cognitive and neurochemical processes and are broadly discussed in the following two sections. As discussed, the basal ganglia are involved in inhibiting, filtering or halting motor, cognitive or behavioural programs that pass through the cortico – basal ganglia circuitry. As such, this system provides an essential gating mechanism important for behavioural control, not just in terms of the motor system, but also for the control of impulses and emotions.

Impulsivity, a tendency towards rapid, unplanned behaviour that is divorced from sufficient forethought, risky or inappropriate and occurs despite potential negative consequences, is well documented in healthy individuals and across a range of psychiatric disorders[127, 128]. Impulsivity can be decomposed into several discrete yet often overlapping constructs, subserved by dissociable neural systems[128]. Briefly, motor impulsivity describes a capacity for response inhibition or action cancellation; decisional impulsivity describes impulsive choice, modulated either by the influence, or lack, of prior evidence (reflection impulsivity) or by the temporal features of an outcome (delay discounting); and finally, waiting impulsivity describes the propensity towards disadvantageous premature responding. This heterogeneity implicates differing neural representations, which are explored further here.

Motor impulsivity

In experimental psychology, active or willed inhibition can eb conceptualized as a form of cognitive control and encompasses motor or behavioural inhibition, selective attention, emotion inhibition or memory item inhibition[120].A distinction can be made between cognitive and behavioural inhibition, with the former associated with a suppression of cognitive processes, contents and attention and the latter associated with overt behavioural or motor suppression to resist temptation or impulses or delay gratification[129]. However this notion of active inhibition has been disputed, with claims that appropriate behaviours or cognitive processes might be amplified, rather than inappropriate ones inhibited[120, 130]. Inhibition may not be a unitary dampening of

neural activity and therefore behaviour but instead a process by which one brain region or network biases the response or activity of another region or network, to increase or decrease a certain behaviour or cognitive process. Through time, this biasing towards the task goal and simultaneous inhibition of unwanted or unintended cognitive/behavioural processes, can lead to tonic inhibition that is not under the control of an active and dedicated 'stop' network but rather a result of long-running selective facilitation[130-132].

However, it is widely agreed that individuals can actively inhibit a motor response or suppress a psychical action given enough warning[120, 133]. Appropriate methods to examine whether one region has an active inhibitory effect on another region are by studying region pairs with known anatomical connectivity including frontal-striatal projections, frontal-subthalamic projections and frontal-thalamic projections; and by recording the target region (for example with intracranial neurophysiological recordings or TMS) [120]. For example, a study using TMS revealed that the primary motor cortex increases in excitability of inhibitory neurons at around 130msec after a stop cue[134] and provides evidence for the conceptualization of stopping of a motor response as an active inhibitory process.

The ability to control motor responses can also be captured by cognitive/behavioural tasks that can be collectively termed measures of motor impulsivity. Two commonly used tasks to measure active inhibitory control or motor impulsivity are the Go/NoGo task and the SST (described further in Chapter 2), in which responses are inhibited before or after response initiation, marking action restraint or action cancelation, respectively.

The Go/NoGo task requires individuals to respond to a Go cue and withhold a response to a NoGo cue. Responding to the Go cue elicits recruitment of primary sensorimotor cortices, SMA, thalamus and cerebellum[135]. Responding to the NoGo cue engages the PFC[135, 136], in particular the lateral OFC[137], right lateral PFC[138, 139], pre-SMA[139] and premotor cortex[135]. As the pre-SMA is seemingly involved in both Go and NoGo responses, its role in selection of an appropriate behaviour is clear, whether

that behaviour is to execute an appropriate and necessary action or to inhibit an unnecessary action.

The SST has been widely used to study the behavioural and neural processes that govern motor response inhibition[132]. This task uses a Go signal, which participants must respond to and an infrequent Stop signal, to which subjects must withhold their response. The current studies used the CANTAB (Cambridge Cognitive Ltd.) version of the SST, henceforth referred to as the SST. During the currently employed SST, participants respond to a Go signal in the form of a left or right arrow image that requires a left or right arrow key press, respectively. The Stop signal is a sound presented after the onset of the Go signal and participants must inhibit their prepotent response. Algorithms have been developed to measure response inhibition reliably [132, 140]. The time delay between the go and the stop signals (the stop signal delay) is varied on a trial-by-trial basis according to performance, such that subjects correctly stop around half of the trials [132]. The SSRT can then be estimated by subtracting this average stop signal delay from the median response time for go trials without a stop signal. This measure therefore captures the point at which that participant is able to successfully stop [132] [141].The calculation of the SSRT assumes that the Go and Stop processes are independent and that they race for completion, and while there is some suggestion of an interaction between the two systems[142], their independence has been supported by computational modeling that demonstrates independent processes until a certain late point of interaction[121, 143]. This race between Go and Stop processes has been suggested to reflect the parallel basal ganglia pathways mediating movement (direct pathway) and inhibition of movement (indirect pathway)[50, 144, 145] and the selective gating of basal ganglia output has been suggested to depend on the direct and indirect pathway's computation of evidence for the facilitation or inhibition of each motor program[146]. As phasic increases and decreases in striatal dopamine signals encode reward receipt or prediction errors, this signal is thought to amplify Go or NoGo activity states subserved by the direct and indirect pathways, respectively[146]. Tonic striatal dopaminergic state changes may conversely shift the balance of background or intrinsic state towards either Go or NoGo systems, equating to learned associations and

influencing more rapid responding[146]. It is important to note that stopping ability or performance on the SST can also be modulated by motivational states[147] or attentional salience[148].

In situations where rapid behavioural change is necessary, for example when an activated response must be suppressed, or in situations of conflict, a different system is required to rapidly overcome more automatic or habitual responding[146]. As discussed, activity or processing through the motor circuit of the cortico – basal ganglia circuitry equates to preparation and execution of movement. As an action is prepared or initiated, the primary motor cortex increases in excitability[149]. Stopping an initiated action (for example during the SST) therefore requires interference with this motor program, or its 'hijacking'. This stopping ability seemingly requires interference by the PFC, specifically the right IFC, as individuals with lesions[150, 151] or temporary lesions via transcranial magnetic stimulation[152] demonstrate deficits in the ability to stop executed actions rather than initiating the actions themselves. Patients with lesions to the right pre-SMA also demonstrate disrupted stopping ability during the SST [153] and in the face of conflict[154]. To inhibit the initiated actions, the right IFC or pre-SMA must act to block the Go program that is presumably passing through the direct pathway of the motor cortico – basal ganglia circuitry (motor circuit)[143]. Indeed, at the time of the Stop signal, the primary motor cortex excitability decreases (the output of the cortico – basal ganglia motor circuit)[149] and cortical inhibition takes over.

The STN is the expected point of intersection for this rapid, frontally-mediated control of basal ganglia output due to its positioning within the circuitry as a target of frontal innervations and rapid mediator of basal ganglia output. This PFC and STN-mediated rapid stopping process halts the striatum-mediated movement process mediated via the basal ganglia[145]. The STN does indeed respond to the stop signal during the SST in rodents[145], whether the action was successfully cancelled or not, and while STN lesions do not affect the SSRT itself, lesions do reduce the accuracy of stopping following a Stop signal[155], indicating a generalized impairment in stopping ability. Furthermore, the STN is active at the time of successful stopping during the SST in humans[156] and

direct anatomical connectivity between the PFC regions implicated (right IFC and pre-SMA) with STN has been demonstrated in humans using diffusion tractography[121]. This rapid, hyperdirect interference and halting of the motor program is then followed by dlpfc-mediated dampening of striatal Go signals and enhancement of striatal NoGo signals, via top-down cortical regulation systems[146].

Decisional impulsivity

Decisional impulsivity describes impulsive choice. Individuals tend to prefer smaller immediate rewards over larger but delayed rewards, a tendency known as delay discounting[157]. A distinct measure that can be described as decisional impulsivity is reflection impulsivity, which describes a tendency towards decision making with low or minimal information accumulated prior to decision.

Lesions to the nucleus accumbens[158] and OFC[159] in rats lead to impulsive choice in the form of enhanced preference for the smaller, immediate reward. Indeed, the ventral striatum and vmpfc seems to track subjective value during this task[160] as well as the magnitude or value of future rewards[161]. In humans, this ventral striatal tracking, as measured by neural responses to positive feedback, is associated with the extent of delay discounting[162]. The higher the ventral striatal neural responses to positive feedback, the higher the discounting rates or preference for the smaller, immediate and impulsive choice[162], which might reflect increased processing through the limbic direct pathway. Similarly, lower response activity of the ventral striatum to future rewards is also associated with more impulsive choice[161]. Examining the temporal delay aspects of the task implicate the striatum, with anterior ventral striatum responding to immediate and posterior dorsal striatum responding to delayed rewards[163]. Parahippocampal gyrus and frontal polar cortex are also sensitive to delay[164]. The PFC has been implicated in tracking both the magnitude and delay of the expected reward, with a suggested functional role of monitoring and influencing the choice of the delayed and larger reward option[165], with the dlpfc being particularly implicated[165]. This role of the dlpfc in the exertion of behavioural control for longer term benefits may not only be relevant to

decisions of temporal choice but might extend to behavioural control over choice in more general terms. For example, the role of the dlpfc has been demonstrated in other situations, like choosing a healthy over an unhealthy dietary option[166].

The Information Sampling Task measures the tendency to sample or gather information before making a decision[167], indicative of reflection impulsivity. Individuals tend to sample less evidence than necessary[168] but increase evidence sampling in uncertain or potentially negative environments[168]. The dlpfc has been implicated in the neural process of information gathering and evidence accumulation, and plays an integrating role for processing of inputs from sensory regions[169-171]. Lower dlpfc grey matter volume is associated with reduced evidence accumulation during the Information Sampling Task [172]. When individuals accumulate enough evidence and make a choice, the insula, ACC and striatum are implicated[168].

Waiting Impulsivity

Waiting impulsivity has been well characterized in rodents through the use of the 5-choice serial reaction time task[173]. The rodent is presented with five openings. A light is presented above one of the openings and the rodent must learn to poke its nose into that opening in order to obtain a reward. A premature nose-poke before the illumination of a light represents a form of impulsivity, termed here as ‘waiting impulsivity’.

Work in rodents has provided evidence for candidate neural regions for waiting impulsivity. Lesion studies have identified a specific network underlying premature responding or waiting impulsivity implicating the nucleus accumbens, infralimbic cortex (probably equivalent to the human subgenual ACC) and the STN. Lesions of the nucleus accumbens attenuate amphetamine-induced increases in premature responding[174]. Highly impulsive rodents have lower dopamine D2/D3 receptor availability in the nucleus accumbens [175] and lower left grey matter density in the nucleus accumbens core[176]. Furthermore, lesions of the rodent infralimbic cortex and the STN also enhance premature responding[177-180]. In rodents, increasing amplitudes of STN DBS at high

frequencies increases premature responding[181]. Finally, enhanced premature responding is observed during a gambling task in rodents with STN lesions[178-180].

Preclinical evidence supports the role of waiting impulsivity as a predictor for the development of disorders of addiction[182-184]. High premorbid premature responding in rodents predicts greater nicotine use[183] and greater addiction-like behaviour to cocaine[182]. Mice acutely exposed to alcohol[185], in the early stages of alcohol abstinence[186] and with greater preference for alcohol[187] all exhibit enhanced premature responding or waiting impulsivity.

A novel translational task has been recently developed for humans, the 4-Choice Serial Reaction Time task, which was designed with high fidelity to the rodent task[188, 189]. The rodent and human tasks do however have some differences. For example, if the rodent makes a premature response they are usually punished in the form of a five second period of darkness, whereas there is no punishment in the human task[188, 190]. Punishment also occurs for omission and commission errors. Furthermore, rodents are usually trained on a certain wait period but are subsequently tested on a slightly longer wait period, in order to encourage premature responses[190]. These more explicit task features are needed for rodents to learn and perform this task properly. Humans however are instructed and understand that they should not make a premature response and do not require explicit punishment to correctly perform the task. However, this effect of punishment is therefore not assessed with the human task, a process that would be interesting in disorders of addiction where the drug-seeking behaviour can persist despite negative consequences. While these discrepancies mean that the human and rodent tasks are not exactly equivalent, an overall primary measure of interest, premature responses, can be obtained using both. Previous studies have indeed used this human analogue task to demonstrate heightened premature responses in individuals with alcohol and methamphetamine dependence and in smokers and recreational cannabis users[188]. How these premature responses might change in the face of negative feedback is a question yet to be answered. However, the underlying neural correlates of the main outcome measure of premature responding are yet to be elucidated in humans.

Behavioural Flexibility and Compulsivity

The capacity to flexibly adapt behavior is a crucial aspect of human behaviour. As discussed, the cortico – basal ganglia circuitry is strongly implicated in reward-related learning and decision making to guide both automatic and controlled behaviour. Indeed, behaviour can be broadly dissociated into two, parallel systems. On the one hand, flexible goal-directed behaviour is guided by the assessment of a model of environmental contingencies and remains sensitive to outcome value or reward[191]. On the other hand, habitual behaviour or habit learning occurs when an environmental stimulus or previously reinforced action engenders an automatic response, usually after an extended period of training[192]. The process of formation of habits is evolutionary conserved and highly adaptive for animal behaviour and survival as automatisation of certain frequent behaviours liberates cognitive resources for other forms of information processing that might be necessary in the immediate environment. However, habit formation hypothetically can lead to or be associated with the development of compulsivity. Compulsivity can be described as the presence of persistent actions or behaviours that remain despite negative consequences and are divorced from any apparent goal[125, 128], and could reflect dysregulated stimulus-response learning.

Schools of instrumental learning theory distinguish goal-directed behaviour as relating to the action-outcome contingency and habit as stimulus-response learning[44, 191, 193, 194]. Recent computational theories further these models and describe two distinct forms of learning known as model-based and model-free reinforcement learning. These provide a computational framework that can be used to describe goal-directed and habitual behaviours, respectively[195].

Behavioural Flexibility and Goal-Directed Behaviour

Goal-directed behaviour is demonstrated by adaptive behavioural responses to changing outcomes, for example decreased and increased responding for decreasing and increasing outcome rewards, as well as remaining sensitive to action-outcome

contingencies[194]. The properties of the goal, such as reward magnitude or rate of reward delivery mediate behavioural responses rather than certain learned motor programs.

Reversal learning tasks can be used to measure a component of flexible goal-direct behaviour. During these tasks, participants must re-learn a previously acquired behaviour when there is new environmental information. During reversal learning tasks, an action that was previously rewarded is no longer rewarded and simultaneously an action that was not rewarded suddenly is. This requires disengagement from a previously reinforced stimulus and the engagement of learning for a previously unrewarded stimulus, a process related to learned irrelevance [196, 197]. Subjects are required to adapt their internal representations and choices according to changes in stimulus-reward contingencies: previously irrelevant stimuli can start to predict a rewarding outcome[198, 199]. This task typically measures the acquisition learning of a stimulus associated with an outcome, followed by a reversal. This behavioural updating or switching requires suppression of the previously rewarded response and initiation of a new response in a rapid, adaptive manner. While response inhibition is an important process involved with this behavioural updating, the neural correlates of response inhibition and reversal implementation have been dissociated[200], suggesting that the reversal process requires a different set of cognitive and neural functionality than response inhibition alone. This process of reversal learning is in contrast to stimulus-response behaviour in which the chosen action is divorced from the eventual outcome and the outcome acts only to strengthen or weaken the stimulus-response association. Therefore reversal-learning tasks simultaneously requires inhibition of a learned response alongside the acquisition of new learning, together allowing flexible updating of behaviour in a goal-directed manner.

Several elements of the cortical – basal ganglia circuitry have been implicated in flexible and adaptive goal-directed behaviour. A wealth of literature supports the role of the dorsomedial striatum or caudate in goal-directed learning and action. Lesions to the posterior portion of the dorsomedial striatum or caudate impair acquisition and expression of goal-directed actions as measured by outcome devaluation sensitivity[194]. The processing required for such learning is demonstrated in this region: action-outcome

contingency information is encoded in the caudate[201]. Also, the dorsomedial striatum encodes the preferred action choice that is contingent on reward outcome and changes or updates when reward contingencies change[202, 203]. Caudate encoding of changing reward outcome contingencies seems to occur even before the updated behaviour is expressed[204].

The role of the cortex in goal-directed behaviour has been explored using lesion studies in rodents and imaging studies in humans, particularly implicating the medial PFC, including ventromedial prefrontal and orbitofrontal cortices[194, 205]. The medial PFC projects primarily to the dorsomedial striatum and lesions to this cortical region in rats abolish sensitivity to outcome devaluation[206, 207]. Similarly, lesions to the mediodorsal thalamic nucleus, the major downstream target for dorsomedial striatal projections, also abolish outcome devaluation sensitivity[208]. Clearly, the circuit as a whole rather than a single component, is crucial for the development, maintenance and expression of goal-directed learning and behaviour.

Delving further into the role of the medial PFC in flexible goal-directed behaviour, this heterogeneous region can be further segregated based on its functional role in valuation. Broadly, the OFC is involved in the computation and updating of outcome value in the context of changes in current internal motivational states or feedback[209-211], whereas the vmpfc encodes action-outcome contingencies and action values to guide behaviour[194, 212-214]. The OFC, ventral striatum and also amygdala respond not only to primary (food, drugs), but also to secondary rewards (money)[215-217]. Medial-lateral divisions within the OFC are apparent, with medial regions involved with reward and value monitoring and lateral regions becoming recruited when an action previously associated with reward must be suppressed (important for reversal learning)[210, 218]. Goal-directed model-based behaviour has been associated with higher grey matter volume in the medial OFC[219].

The role of the ventral striatum in valuation however cannot be ignored, particularly due to its role in encoding anticipation and receipt of reward, tracking prediction error and linking motivationally-relevant reward properties with instrumental performance and response vigor[41, 220-222]. The nucleus accumbens or ventral striatum also receives

extensive anatomical connections from OFC[76, 95]. Indeed, ventral striatal activity has been linked to model-based valuation, as well as model-free reward prediction error[191]. Thus, the medial OFC and ventral striatum have been implicated in model-basedness and may act via linking outcome valuation-updating and reward-motivation, vital for such behavioural adaptations.

Habit Formation

In instrumental learning, there can be a shift from action-outcome to stimulus-response learning or behaviour, often depending on the amount of training or rewarded responses[194]. In the striatum, the shift from action-outcome to stimulus-response behaviour is thought to reflect an underlying shift in ventral to dorsal striatal engagement[63, 223]. While this thesis has mainly discussed the separable cortical – basal ganglia circuits, there are also intimate cross-links between the circuits, particularly between the ventral and dorsal striatum[63, 217]. Indirect connections between ventral and dorsal striatum exist via midbrain dopaminergic connections- the nucleus accumbens can innervate the dorsal striatum via the substantia nigra, again following a topographical organization[217, 224]. Medial substantia nigra and VTA are connected to ventral striatum and central and ventrolateral substantia nigra with dorsal striatum[217]. While the ventral striatum receives fewer dopaminergic projections compared to dorsal regions, it innervates a larger portion of substantia nigra compared to the dorsal striatum. This means that the ventral striatum is in a pivotal position to mediate or influence downstream dopaminergic modulation of the dorsal striatum due to extensive reciprocal connections between the striatum and substantia nigra[217]. This ascending spiral of connectivity forms the neural basis for the influence of reward or limbic ventral striatal processing on associative or motor dorsal striatal processes[63, 217].

The neural locus of habit formation within the dorsal striatum has been further analysed. As mentioned, the dorsomedial striatum or caudate is involved with flexible behavioural updating and goal-directed learning. The associative dorsomedial striatum responds initially during motor learning and involvement reduces after several months of motor

training in non-human primates[225] and humans[226, 227]. Inactivation of the dorsomedial striatum in non-human primates impairs learning but not execution of a learned motor sequence, suggesting that this is not the neural locus of the storing of habitual information or guiding habitual behaviour. In fact, lesions to the associative dorsomedial striatum in rodents speeds up stimulus-response learning[194].

On the other hand, the dorsolateral motor striatum responds after a motor sequence has been over-learned[225] and its inactivation disrupts execution of a learned sequence but not its acquisition [228], demonstrating an opposite role to the associative striatum and implicating the motoric striatum in habit formation, automatic responding and the shift from goal-directed to habitual processes[193].

Evidence of the influence of the ventral striatum on the dorsolateral striatum comes form a study demonstrating that disconnection of nucleus accumbens and dopamine transmission to the dorsolateral striatum reduces habitual cocaine seeking in rodents[229]. Indeed, conditioned stimuli increase dorsolateral striatal dopamine, not ventral striatal[230]. Furthermore, lesions of the dorsolateral striatum in rodents impair the ability to form and maintain habitual responding[231] and dopaminergic antagonism in the dorsolateral striatum diminished cue-induced drug seeking in rats[229, 232].

The shift of information processing from ventromedial to dorsolateral striatal (equivalent to posterior putamen) regions, which can occur during the course of affective learning[63], corresponds to actions progressing from goal-directed to habitual. These actions can become repetitive and reliant on previously reinforced actions which are divorced from an apparent goal and persist despite outcome devaluation[233].

Other properties of the striatum further implicate this structure in mediating the shift from goal-directed to habitual or stimulus-response responding. This is in part due to the principles of neuroplasticity within the cortical – basal ganglia circuitry. Simultaneous activation of dopaminergic projections to striatum that encode unexpected rewarding outcomes, and sensorimotor cortical projections to striatum that facilitate the initiation or

execution of a movement, creates a moment of concomitant and convergent striatal input that, with repetition, leads to synaptic strengthening (long-term potentiation)[234-236]. As such, dopamine-mediated reinforcement learning links with sensorimotor action programs to engender associative learning that, through repetition or training, leads to stimulus-response learning or habitual responding. The resultant habitual responding becomes unreliant on dopamine. As training progresses and habit formation ensues, the role of dopamine diminishes[236, 237]. Blocking dopamine D1 receptors in rodents has no effect on associative responding following extensive training[238, 239]. This role of dopamine in cortico-striatal synapses is unique in the cortico – basal ganglia system. In cortico-cortico dopaminergic synapses, dopamine is not cleared as quickly as in the striatum as there are fewer cortical dopamine transporters (DAT)[193, 240, 241]. This latency diminishes the temporal precision needed for dopamine-mediated reinforcement and associative learning in the cortex and restricts this process to striatal synapses.

Cortically, the process of habit formation has implicated several loci. Frontal and parietal attentional and executive networks seem to disengage with increased task performance or training[242-244]. Cortical regions involved with valuation (ventral PFC) also show a reduction in involvement as task training progresses[245, 246]. On the other hand, sensorimotor or premotor cortical regions increase their engagement[227, 247-249]. In humans, progressive instrumental conditioning[250] and habitual ‘slips of action’[251] following over-training are associated with a transition towards greater engagement of posterior putamen and its connectivity with premotor cortical regions[251]. The supplementary motor complex (comprising SMA and pre-SMA) primarily projects to putamen or dorsolateral striatum and is responsible for learning of stimulus-response contingencies[252, 253], associated with the development of inflexible and habitual behaviours towards drugs of abuse[63, 254, 255]. Thus, in terms of habitual model-free behaviour, a putaminal and supplementary motor network has been implicated.

Compulsivity

Compulsivity is a more elusive construct than impulsivity, with a less well-established

operationalization, perhaps due to a lack of obvious presentations of compulsivity in healthy individuals (unlike impulsivity which is variable across healthy individuals[256-258]). An understanding of compulsivity has been derived primarily from the study of neuropsychiatric groups, like obsessive-compulsive disorder[125, 126, 259], although lower goal-directed behaviour has been recently associated with traits of compulsivity in a large general population[260].

Habit formation and compulsivity overlap extensively, theoretically, behaviourally and neurally. However, compulsivity can be considered as the detrimental persistence of a habit, or a maladaptive stimulus-response function[63]. Urgency and anxiety is also relevant in compulsivity but not simply habits; compulsive behaviour can be performed to relieve a negative anxious state particularly in disorders of anxiety and obsessive-compulsive disorder[261], although anxiety can also be a product of obsessive-compulsive symptoms [262]. As mentioned, whereas habits can be useful and not clinically relevant, compulsive behaviour can be distressing and can negatively impact daily life. For example, the habit of switching on a light upon entry of a familiar room is helpful. This action would be considered a habit if the switch is known to be broken but the behaviour persists a few times. However, compulsivity might be more persistent repetition of this behaviour, long after the new association with the outcome of no light has been fully learned and in some cases combined with an urgency to switch the light to relieve a state of anxiety. Compulsivity is implied when the behaviour is no longer mediated by the ultimate goal[63] and is associated with the subjective state of ‘wanting’ or ‘must-do!’[63]. This behaviour is most clearly presented in obsessive-compulsive disorder but has marked homology to behaviours observed in substance or alcohol dependence too[63].

Compulsivity can be deconstructed into several aberrant processes including stimulus-response habit learning, reduced response inhibition and negative reinforcement[125]. This deconstruction allows a more objective measure of underlying deficits. While difficult, measures of some components of compulsivity can be obtained in healthy volunteers. As mentioned, reversal learning tasks provide a measure of an individuals’ ability to inhibit

an established response and flexibly switch when feedback demonstrates an outcome change[198]. This can be considered one process involved in compulsive behaviour. Perseveration (continuing to choose a response that is no longer rewarded for example) during reversal learning tasks can also represent a process encompassed by compulsivity[126, 263]. The lateral OFC processes punishment-related information and becomes involved when an action previously associated with reward must be suppressed[210, 264]. Lesions to the OFC in rodents[25] and humans[265] cause perseveration. Patients with obsessive compulsive disorder show reduced activity within the lateral OFC during reversal learning[266].

Perseveration during the intra-dimensional/extra-dimensional set shifting task can also indicate a component compulsivity[126, 263] and requires the dlpfc[25, 267]. The intra-dimensional/extra-dimensional set shifting task is a deterministic reward reversal task, testing rule acquisition and reversal that requires a conceptual, attentional shift and mirrors the Wisconsin Card Sorting Task[268, 269]. Subjects choose between stimuli for monetary rewards and after six correct choices, the contingencies reverse, requiring response suppression for the previously rewarded stimulus and flexible updating of responses to the previously unrewarded stimulus. Later in the task, stimuli become compound (shapes with overlying white lines) and subjects must first respond to the shape, which determines the outcome. Reversal of the shape–reward contingency is the intradimensional shift. Finally, the shape becomes redundant and the line type determines reward. Subjects must perform a conceptual, attentional shift from the shape to the line, described as an extradimensional shift. While the reversal learning task measures disengagement from a previously reinforced stimulus and the engagement of responding to a previously unrewarded stimulus, during the extradimensional shift the previously irrelevant stimulus is replaced by a novel stimulus meaning that continuation of responding there is not related to a problem with learning that a previously irrelevant stimulus is now relevant, but instead indicates perseverative responding [196, 197].

Damage to the dlpfc impairs inhibitory control for such attentional selection[25, 265, 270] and connectivity between dlPFC and striatum[25, 267] is associated with this attentional

shifting. On the other hand, OFC lesions impair reversal learning and inhibitory control for affective or emotional information[25, 265, 270]. Finally, as mentioned, computational measures of habitual model-free learning described can also indicate a component of compulsive choice behaviour and implicate sensorimotor and supplementary motor cortical and dorsolateral striatal or putaminal regions. Thus, while the lateral OFC and dlpfc are required for flexible updating of responses based on environmental changes and attentional shifting, respectively, cortical and subcortical motoric regions are engaged or 'take over' when an inflexible habit forms.

Anxiety relief and urgency are key components of compulsivity in obsessive-compulsive disorder [261]. The current thesis examines the more cognitive components of compulsivity rather than anxiety. In healthy populations, traits of compulsivity can be measured by lower goal-directed behaviour has been recently associated with traits of compulsivity in a large general population[260]. Examining the cognitive aspects of compulsivity highlights the more general role of the shift from impulsivity to compulsivity and allows the study of components of compulsivity in healthy populations where trait levels and endophenotypic markets of compulsivity may not include a strong anxiety component.

From Impulsivity to Compulsivity

As discussed, there are intimate links between the ventral and dorsal striatum [63, 217]. The nucleus accumbens innervates a large portion of the medial substantia nigra and VTA, and in turn, the ventrolateral substantia nigra extensively innervates dorsal striatum[217]. This creates an intersecting link from ventral striatum, through substantia nigra, to dorsal striatum, meaning that the ventral striatum can mediate the dopaminergic projections innervating the dorsal striatum, broadly allowing limbic-mediated modulation of associative or motor dorsal striatal processes[63, 217].

Through excessive activation of this pathway, there is a shift of information processing

from ventromedial to dorsolateral striatum. As the ventral striatum is responsible for reward processing to guide goal-directed behaviour and the dorsal striatum is important for habit formation and automatic responding processes[193], the spiraling activation up this system forms the neural basis of actions progressing from goal-directed to habitual[63]. This can also represent a shift from impulsive behaviour governed by ventral striatal systems to compulsivity[63, 217]. Indeed, impulsivity can act as an endophenotype to predict the development of compulsive behaviour [182-184, 271] and it is through this neural link that this transition is thought to take place. Indeed, disconnecting this link between the nucleus accumbens and dorsolateral striatum reduces habitual cocaine seeking in rodents[229] and dopaminergic antagonism in the dorsolateral striatum diminishes cue-induced drug seeking in rats[229, 232]. Therefore, impulsivity can be assessed in terms of its premorbid risk factor status for compulsive behaviour in subclinical or healthy groups.

Alcohol Misuse: Behavioural and Neurobiological Implications

Addiction is a chronic and relapsing disorder that involves loss of control over compulsive substance use, a behaviour that is divorced from an ultimate goal and persists despite negative consequences[63, 272, 273]. The Diagnostic and Statistical Manual of Mental Disorders – Fifth Edition (DSM-5) defines 11 criteria for substance use disorders, with the presentation of two or three symptoms indicating mild substance use disorder, four or five indicating moderate and six or more indicating severe[274]. These criteria include: 1. Taking the substance in larger amounts or for longer than you meant to; 2. Wanting to cut down or stop using the substance but not managing to; 3. Spending a lot of time getting, using, or recovering from use of the substance; 4. Cravings and urges to use the substance; 5. Not managing to do what you should at work, home or school, because of substance use; 6. Continuing to use, even when it causes problems in relationships; 7. Giving up important social, occupational or recreational activities because of substance use; 8. Using substances again and again, even when it puts you in danger; 9. Continuing to use, even when you know you have a physical or psychological problem

that could have been caused or made worse by the substance; 10. Needing more of the substance to get the effect you want (tolerance); 11. Development of withdrawal symptoms, which can be relieved by taking more of the substance.

While these criteria are commonly used, they focus on antiquated frameworks of personal and social functioning, stemming from an era of clinical interview –based psychiatric diagnostics. Recently, there has been encouragement for the establishment of biologically [275] or computationally [276] –based psychiatric diagnostics. For example, by determining the neurobiological underpinnings of impulsivity or anhedonia, we can more empirically classify patients, identify high risk-factor groups, and target treatment interventions more personally. By identifying and isolating a cognitive construct and demonstrating its relevance within and across psychiatric groups, we can start to build a more accurate picture of disorder state and severity.

The Research Domain Criteria (RDoC) project proposes that disorders can arise from dimensional factors across neural integrity and organization, behaviour and cognition [277]. Examples of dimensional measures that cut across disorder states and categories have already been discussed. Measures of impulsivity and compulsivity can be crucial factors that empirically describe a patient's condition, indicate the perturbed neural systems and highlight novel avenues for treatment targets. Furthermore, as impulsivity can act as an endophenotypic marker of a risk for compulsive behaviour[63, 182-184, 217], it can be measured in subclinical or subdromal groups to determine relative propensities for risk of disorder development. For example, siblings of chronic drug users show higher trait impulsivity[278, 279], suggesting an endophenotypic marker of the risk for drug dependence. Understanding endophenotypic marker and risk factors for such disorders will be a crucial step in psychiatry and personalized medicine, where a shift to prevention rather than just treatment is necessary.

This section first describes the main neural changes associated with chronic drug or alcohol use, before describing the role of measures of impulsivity and compulsivity in

alcohol dependent patients and young adult binge drinkers who are at heightened risk for the development of alcohol or substance use disorders.

Neural Effects of Drugs of Abuse

Drugs of abuse commonly increase ventral striatal dopamine transmission[280], the expected locus of the primary reinforcing effects of drugs of abuse[63]. Alcohol has several primary targets including glutamate, GABA, glycine, 5-HT, nicotinic acetylcholine receptors, with additional indirect effects on neuropeptides and neurotransmitters leading to disinhibition and sedation[281]. Alcohol causes release of endogenous opioids, facilitates the inhibitory effects of GABA and reduces the stimulatory effects of glutamate[282]. Acute ethanol enhances GABA release onto VTA dopaminergic neurons[283]. Therefore, short-term alcohol consumption enhances GABA (A) receptor function and inhibits glutamate (NMDA receptor) function. However, with chronic use, counter-adaptive processes engender opposite effects- glutamatergic cells increase their excitability via structural changes, receptor numbers at synapses and subunit composition, and GABA-A receptor density is reduced[281, 284]. Drugs of abuse in general alter the glutamatergic system causing long lasting neuroplastic changes[285]. Withdrawal from chronic ethanol results in increased in striatal glutamate in rats[286] and reduced striatal GABA transmission in mice and non human primates[287, 288] Anti-glutamatergic and pro-GABA strategies for alcohol withdrawal in humans is successful in reducing withdrawal severity[289-291].

Behaviourally, drugs of abuse also act as instrumental reinforcer's, meaning that they increase the frequency of the behaviour associated with them: drug seeking or taking[63]. As enhancing striatal dopamine enhances learning mechanisms[292, 293], abnormally strong learned associations can form between the behaviour of drug seeking or use and the neurobiologically rewarding effects of the drug[223]. This is also true for environmental stimuli that occur in close temporal and spatial proximity to the rewarding effects of the drug, causing the attribution of incentive salience to the previously neutral stimuli, which can eventually elicit expectation, craving and approach behaviours themselves[63]. Indeed, unexpected conditioned stimuli that have been paired with a

drug increase nucleus accumbens core dopamine release[294], invigorating Pavlovian approach responses[63].

Apart from nucleus accumbens or ventral striatal dopamine transmission, special attention has been given to the caudate's role in maintaining sensitivity to outcome devaluation (for goal directed behaviour) [223] and the putamen's role in autonomous instrumental responding following overtraining [231, 295]. As discussed previously, a shift occurs in the neurobiological mediation of goal-directed drug use to habitual or compulsive behaviour, from ventral to dorsolateral striatum involvement[63, 223]. Indeed, conditioned stimuli increase dorsolateral not ventral striatal dopamine[230] and dopaminergic antagonism in the dorsolateral striatum diminishes cue-induced drug seeking in rats [229, 232]. It has been suggested that drug use therefore shifts from goal-directed to habitual, ultimately becoming driven by stimulus-response associations, conditioned reinforces in the environment that trigger cravings, Pavlovian and incentive motivation processes, and also states of stress that facilitate negative reinforcement[63, 272, 273].

Alongside these drug-induced striatal adaptations, prefrontal executive control functions diminish[63, 223, 296], associated with attentional bias to drug cues, motivation, craving and reduced inhibitory control[296]. The following sections describe the cognitive and behavioural deficits observed in individuals with AD, with a particular focus on impulsivity and compulsivity. Such impairments in behavioural control and executive function act in parallel and interact with the lower-level striatal learning mechanisms described. For example, low dorsal striatal dopamine transmission is associated with reduced PFC integrity, particularly of OFC, cingulate and dlpfc[297]. Thus, the combination of diminished PFC-mediated executive behavioural control and enhanced striatal-mediated habitual behaviour, sums to strengthen the facilitation of maladaptive and compulsive drug seeking and taking.

Alcohol Misuse: The Cost of Harmful Drinking

Consumption of alcohol in public and in private has been a part of the British culture for centuries and while many individuals use alcohol sensibly, its misuse has become a serious public health issue, worsening with time[298]. Across the world, the number one risk factor for global mortality and disease burden for 15 – 49 year olds is alcohol use[299]. In England, over 24% of people consume a potentially harmful amount of alcohol, with widespread physical, psychological and social consequence. Despite recent trends towards reduced alcohol consumption, alcohol-related hospital admissions are on the rise (increase of 5% from 2013 to 2014)[300] and data from the National Health Service in England suggests that around 1.2 million admissions to hospitals are due to alcohol-related conditions and injuries. Alcohol-related healthcare, crime and productivity costs are estimated at around £21bn per year[298].

The pattern of alcohol intake may be a critical determining factor of the subsequent harms. There are probably three major drinking subgroups: harmful or hazardous drinking, binge drinking and dependent drinking or addiction. Binge drinking, the rapid intake of alcohol in short bursts of time, is an increasingly common pattern of drinking, costing UK taxpayers £4.9 billion a year (due to hospital admissions, road accidents and policing costs)[301, 302]. Unfortunately, the highest prevalence of binge drinking is in young adults[303, 304] who experience the direct and indirect toxic effects of alcohol on neural development. Young adults who binge drink but not those who drink without this pattern[305], partake in other detrimental behaviours, ultimately linking binge drinking with accidents, violence, suicide and alcohol-induced liver disease [306-308] as well as heightened risk for substance abuse and dependence or addiction[309].

Alcohol Misuse: Latent Circuitry Disturbance

The focus in this section is on latent or intrinsic structural or neural network features in AD and binge drinkers, rather than during any task. Findings of latent neural differences between AD or binge drinkers and healthy volunteers are briefly reviewed. Understanding resting and latent neural properties provides insight into the default or intrinsic function of the neural network as a whole without perturbation by cognition, which may differ on an

interindividual basis. As such, two levels of interindividual variability are possible: variability within the intrinsic network itself; and variability in the way in which that network is recruited during task. This distinction certainly requires further exploration and delineation. However, understanding the baseline characteristics of neural structure and networks is key, before any recruitment by task demand. Later sections (Section 3.2 and 3.3) examine the neural correlates of impulsivity and compulsivity specifically during task.

In terms of structural evidence, AD patients demonstrate significantly decreased grey matter volume in the frontal cortex, including dlpfc[310], amygdala[311], insula, dorsal hippocampus, thalamus and putamen compared to healthy individuals[310, 312]. AD subjects also show lower regional cerebral blood flow within thalamus, hippocampus, parahippocampal gyrus, amygdala and ACC compared to healthy individuals[313].

Studies of microstructure (as measured by fractional anisotropy, FA) in AD are somewhat convergent, demonstrating reduced FA, particularly in the frontal cortex. A large study examining whole brain FA in AD (N=47) demonstrated reduced FA throughout the brain, including corpus callosum, cingulum and superior longitudinal fasciculus [314]. Reduced FA seems to persist into abstinence. Lower FA in cortico-striatal and frontal fibres is observed in a small sample of AD undergoing early detox (N=10) [315] and in a larger sample of detoxified AD compared to light drinkers [316]. Later abstinence is also associated with reduced tract integrity between midbrain and pons, associated with cognitive flexibility impairments [317]. Finally, lower frontal FA predicts subsequent relapse in AD [318].

Adolescent and young adult binge drinkers feature a range of grey and white matter volume changes that coincide with cognitive impairments. White matter FA also interacts with age. FA reduces with age in healthy volunteers but AD who subsequently abstain from alcohol intake (compared to relapsers and healthy controls), show a reduced slope, indicating some recovery[314]. Mixed effects have been observed in younger populations. Teenagers with AD show reduced FA in splenium associated with large quantities of recent alcohol intake[319]. FA is however higher in the corpus callosum in

another study of adolescent AD subjects, potentially indicating enhanced myelination in that group [320]. In teenagers who developed regular alcohol use patterns in the previous year, reductions in cortical grey matter volumes have been reported, in particular of the dlpfc and premotor cortex[321]. Reduced cerebellar grey matter volume has also been associated with severity of binge-drinking in a large sample of healthy teenagers[322]. Contrastingly, higher left dlpfc grey matter volume has also been reported in this group, associated with past alcohol consumption[323]. Binge drinkers also show larger ventral striatal volumes[324].

Studies examining resting functional networks in patient populations are growing. Studies of addiction find abnormalities in reward-related and behavioural control network's. Both long and short term abstinent AD individuals primarily show reduced synchrony of the reward or limbic network (caudate, thalamus, nucleus accumbens and ACC) but increased connectivity between nucleus accumbens and dorsal ACC with the executive network (dlpfc), associated with attentional set shifting [325, 326], suggesting a shift towards behavioural control. However, amygdala connectivity with medial PFC is intact[327] suggesting that reward rather than salience networks are key in the maintenance of abstinence in AD. Indeed, resting state synchrony in reward and executive function – related regions, associated with impaired inhibitory control, differentiate those who relapse six months later compared to those who remain abstinent [328]. Binge drinkers also displays functional changes in these regions: activity in the dorsal PFC during a spatial working memory task is reduced[329] and resting state functional connectivity of the ventral striatum is disturbed and associated with impulsivity[330].

In summary, evidence for reduced frontal grey matter volume and white matter FA is consistent in AD, the latter persisting into abstinence and predicting subsequent relapse. Structural findings in younger populations are more divergent, with both increased and decreased cortical grey matter demonstrated, which could reflect early neuroadaptive responses to alcohol insult that require further delineation. There is evidence for reduced

intrinsic connectivity of reward or limbic circuits in AD that seems to interact more with executive networks in states of successful abstinence.

Alcohol Misuse: Impulsivity

The link between problematic drug or alcohol use and impulsivity is well established in both rodents[128, 182, 331, 332] and humans[63, 188, 333]. As discussed, impulsivity can be separated into several factions, including motor, decisional and waiting impulsivity. Questionnaire measures of impulsivity are also useful. The major questionnaire scales are the Barratt Impulsiveness Scale (BIS)[334] and the UPPS[335, 336]. The UPPS self-report measure can be dissociated into five subscales, including positive and negative urgency, sensation seeking, lack of planning and lack of perseverance.

Individuals with AD tend to show impairments or higher impulsivity on most of these measures. On more general self-reported measure of impulsivity, AD individuals report higher urgency [337], which predicts the magnitude of drinking severity[338], and sensation seeking, which predicts the pattern or frequency of drinking[333, 338]. Adolescents with AD[339] and early onset problem drinkers also score higher on the BIS scale[340]. Personality measures that incorporate all of: novelty seeking; impulsivity; sensation seeking; and extraversion explain the highest proportion of variance in predicting early alcohol drinking [341]. With more cognitive measures, heavy drinkers[342] and AD[343] show impairments in motor impulsivity as measured by response inhibition and performance on the SST, which acts as a predictor of subsequent alcohol dependence[342]. Impairments in response inhibition are also more apparent when alcohol related images or cues are used[343]. Increased decisional impulsivity in the form of delay discounting is observed in AD[344], which reduces with abstinence [345]. Impairments in waiting impulsivity have also recently been demonstrated in AD[188].

Neural disturbances associated with impulsivity in AD are less well understood. Two studies have demonstrated reduced OFC volumes in individuals at high risk for AD[346] that is associated with self-control or impulsivity[347]. A small sample of males with AD show reduced corpus callosum white matter microstructural integrity and a specific association between tracts linking orbitofrontal cortices and BIS scores[348]. Also, negative urgency is associated with vmpfc responses to alcohol odours in social drinkers[349].

In terms of motor impulsivity, impairments in response inhibition have been extensively investigated as a risk factor for the development of AD. AD individuals show impairments in stopping ability[350], especially during conflict[351], a process that requires error detection and behavioural adjustment. Acute alcohol intoxication reduces error detection mediated by the ACC[352] and error related brain activity is disturbed in AD[353], a disturbance that can be mediated by effective AD treatment[354]. Alongside this, hypoactivity of the inhibitory network is associated with an enhanced risk of developing AD. Children (ages 7 to 12) with a positive family history of AD who subsequently developed problem drinking showed blunting of activity of the caudate, mid-frontal cortex and ACC during a Go/NoGo task[355]. Adolescents who subsequently demonstrate problematic alcohol use also have blunted activity in the middle frontal gyrus, right IFC, putamen and motor and cingulate cortices during failed inhibition[356, 357]. Finally, heavy drinkers with a positive family history showed lower right IFC activity during inhibition compared to those with negative family history[358]. In individuals with disorders of addiction, hypoactivity of inhibitory circuits (including the ACC, IFC and dlPFC) is still observed during motor response inhibition[359].

As mentioned, decisional impulsivity can be subdivided into delay discounting and reflection impulsivity, as well as risk taking. In a large sample of 151 subjects with AD and social drinkers, greater alcohol use severity was associated with greater discounting and greater activity in SMA, OFC, IFC and insula cortex[360]. Heavy drinking AD also show greater activity in the dlPFC during delay discounting compared to heavy drinking non-AD[361]. Non-treatment seeking AD and social drinkers also showed lower right ventral

striatal 11C-raclopride binding potential (reflecting greater dopamine release or lower dopamine D2/3 receptor availability), correlating with greater impulsive choice and alcohol use severity[362]. Risk taking and the anticipation of gain and loss also mediates impulsive behaviours. Abstinent AD show blunted ventral striatal and ACC activity during anticipation of monetary gain, associated with elevated impulsivity[363].

AD individuals are impaired during several measures of risky decision making, including the Iowa Gambling Task[364] [365], the Card Playing Task[365], the Cambridge Gamble Task[167, 350] and the Game of Dice Task[364]. AD patients who subsequently relapse show preference for an immediate gain, despite the possibility of future negative consequences[366]. Similarly, substance use in adolescents has been associated with sensation seeking[367], novelty seeking[368] and risky sexual behaviours[369]. Neurally, SD individuals, including AD, show impaired decision making during a gambling task that requires intact vmpfc functioning[370] and anterior insula responses to reward and loss anticipation are associated with GABA receptor genetic polymorphism in individuals at high risk for AD[371]. During risk-taking, heavy drinkers show reduced amygdala activity[372] and social drinkers with high alcohol use show reduced activity in superior frontal gyrus and left caudate[373]. Binge drinkers also demonstrate enhanced risky behaviours towards large losses, associated with greater dlpfc and lateral OFC activity compared to healthy controls[374]. However, after receiving feedback, binge drinkers demonstrate reduced risk taking to a level similar to healthy controls, associated with greater IFC activity[374]. Finally, binge drinkers further show enhanced reflection impulsivity on the Beads task (although not on the Information Sampling Task) correlating with lower dlpfc volumes[375].

In summary, AD individuals demonstrate increased impulsivity and risky decision making in a range of measures, with seemingly stronger impairments when confronted with alcohol cues or images. Blunted neural activity during tasks of behavioural control or response inhibition also seems to precede the onset of alcohol use disorders in adolescents. Importantly, while waiting impulsivity or premature responding has been

associated with compulsive drug use in rodents[182] and humans [188], the neural correlates of this form of impulsivity has not been explored in humans.

Alcohol Misuse: Behavioural Flexibility and Compulsivity

As discussed, behavioural flexibility or compulsivity can be defined by measures of set shifting, reversal learning and habit formation. Cognitive set-shifting, can be measured by the Wisconsin Card Sorting Task (WCST) or Intra- and Extra-dimensional set shifting (IED) task. AD individuals show impairments on the WCST[364, 376], associated with medial PFC glucose hypometabolism[377] and subsequent relapse[378]. Impairments on the IED set shifting task in AD is associated with lower IFC volume[379]. Reversal learning impairments are also observed in AD[380], irrespective of outcome valence [381].

In terms of habit formation, AD individuals show reduced model-based goal-directed decision making two weeks after detoxification[382]. Self-reported alcohol-related problems in social drinkers are also associated with reduced model-based goal-directed control during decision-making[383]. Another study focusing on abstinent AD subjects did not reveal any differences in model-based control[384], although abstinence was positively associated with model-based learning. AD patients do show altered goal-directed and habitual behavior during the 'slips-of-action' task, suggesting that AD patients show a general impairment in stimulus-response-outcome learning[385]. These patients also showed decreased activity in the ventromedial PFC and anterior putamen and increased activity in the posterior putamen during the acquisition phase of the task[385]. Similarly, heavy social drinkers show greater responses in the dorsal striatum to drinking cues, whereas light drinkers showed greater prefrontal and ventral striatal responses[386]. This might indicate an overreliance on habits in the heavy drinking group[385, 386]. However, contradictory to the hypothesis that alcohol dependent patients show increased neural signatures of habit formation, fMRI studies comparing the neural representation of model-free prediction errors during instrumental learning have shown no evidence for a difference between AD patients and healthy individuals[387-

389]. Therefore to date, there is inconclusive evidence of an overreliance on habit formation in AD[390], but rather fair evidence for a disturbance in goal-directed model based behavioural control.

Aims and Hypotheses

This thesis includes three broad aims. Firstly, to map and define the organization of the intrinsic cortical – basal ganglia circuitry in humans; secondly to examine the behavioural relevance of these circuits by examining the neural correlates of discrete measures of impulsivity and compulsivity; and thirdly to examine whether the neural correlates defined are perturbed in individuals with alcohol use disorders and binge drinkers.

The majority of our understanding of cortico – basal ganglia connectivity has come from non-human primate or rodent tracer studies[62, 75, 91], with fewer representations demonstrated in humans. To address the first aim of examining the cortical – basal ganglia circuitry in its entirety, functional MRI was assessed during rest. Multi-echo resting state fMRI acquisition and denoising techniques were used, which have greater signal compared to noise for examining small, noise-susceptible subcortical structures. The utility of this method was demonstrated first by specifically focusing on the STN due to its small size, functional importance and limited human literature demonstrating functional subzones. Functional connectivity between a diverse range of cortical regions and STN was examined, mapping dissociable STN subregions. Connectivity was examined then for the entire cortical – basal ganglia circuitry, with the hypothesis that motor limbic and cognitive-associative sub-circuits would emerge.

The second aim was to assess the relationship between each segregated circuit and behaviour as measured by discrete cognitive constructs of compulsivity. Circuit connectivity was assessed in relation to performance on multiple tasks that dissociate measures of compulsivity, including model based goal-directed and model free habitual behaviors; attentional set shifting; and cognitive-behavioural flexibility in the form of reversal learning for both reward and loss. As the anatomical correlates of model-based

behavior are well-characterized[191, 391] model-based learning is expected to be associated with higher medial OFC and ventral striatal connectivity and model-free with connectivity of the motoric circuit including SMA and putamen. Probabilistic reversal learning and attentional set shifting were expected to implicate lateral OFC[392] and the associative circuit with dlpfc[25, 267, 392], respectively.

As discussed, the STN sits at a crucial position within the cortico – basal ganglia circuitry and is well poised to mediate cognitive or behavioural programs that are processing through this circuitry, including motor, associative or limbic programs[109]. The connectivity of the STN within the cortico – basal ganglia circuitry is therefore specifically examined in relation to measures of behavioural control, including both impulsivity and compulsivity. Impulsivity and compulsivity have been widely studied in terms of the cortico – basal ganglia circuitry but there has been less focus on the STN, even givens it's important role within the system. Waiting impulsivity was specifically examined due to a lack of evidence of the neural correlates of waiting impulsivity in humans. Rodent lesion studies have implicated the STN in waiting impulsivity[177-180], as well as ventral striatum[174] 6] and subgenual ACC[177-180] but studies linking these structures with waiting impulsivity are yet to be reproduced in humans. This form of impulsivity was also dissociated from motor impulsivity as measured by the SSRT. The role of the STN within the cortical – basal ganglia circuitry was further examined in terms of relationships with compulsivity, as indicated by model based goal-directed and model free habitual behaviors, with an expectation that the STN is involved with medial OFC and ventral striatal networks that mediate model based behaviour and a more motoric network for habit. Finally, specific subzones of the STN were examined, using a behavioural measure that is thought to be relevant to only the anterior medial limbic-associative portion of the STN. The Beads task measures the extent of evidence accumulation before a decision provides an index of decisional reflection impulsivity. The anterior medial limbic STN subzone and posterior lateral motor STN subzone were examined separately and as reflection impulsivity implicates the anterior STN, dlpfc, parietal and anterior insular activity and volume[375, 393], connectivity between these regions (and not including posterior STN) is expected to be associated with task performance.

The third and final aim was to examine functional and structural neural disturbances in individuals with AD and binge drinkers. Individuals with alcohol use disorders demonstrate a range of behavioural deficits, but particularly including heightened waiting impulsivity, which has been heavily linked with compulsive drug use in rodents[182] and humans [188]. Therefore, the neural correlates of waiting impulsivity, as defined from previous sections, were examined in AD individuals and binge drinkers compared to healthy volunteers, with the expectation that both groups show heightened impulsivity and that the neural circuitry that mediates waiting impulsivity is disturbed in both groups. The microstructural features of the whole brain were additionally examined in binge drinkers compared to healthy volunteers, with a specific focus on the ventral striatum, due to previous findings of changes in ventral striatal grey matter volume in binge-drinkers[324], and due to its role in neural proliferation following excessive alcohol use [394, 395]. The STN was also specifically examined due to its central role in stopping behaviours[120, 143] and behavioural control that might be pertinent to control of drinking behaviours.

Chapter 1. Showcasing Neuroimaging Methods

The aim of this Chapter was to describe and demonstrate the utility of the neuroimaging methods used in the following sections. Two forms of MRI are examined and used: resting state functional MRI and diffusion MRI. In each of the following sections a description of the method is provided and data are presented for each technique, with their utility compared to traditional techniques where possible.

MRI Background and History

Basic MRI physics

MRI harnesses the basic physical property of magnetization of the Hydrogen atom. The Hydrogen atom is ‘magnetic’, such that when placed in an external magnetic field, the net spin direction of the protons aligns with the direction of the field. The MRI scanner has a magnetic field (B0), so when Hydrogen atoms are placed within the scanner, they align with this field (most align in the parallel direction due to its lower energy state and less in an anti-parallel manner). Alignment is not perfect and stable, but the atoms process with some rotation or ‘wobbling’. The frequency of the precession is related to the magnetic field strength and defined by the Larmor equation.

An electromagnetic radiofrequency pulse is applied to one slice of the brain at a time, which provides the energy for the atoms to switch from the parallel longitudinal direction to anti-parallel. The radiofrequency pulse also tilts the spins into the transverse plane. These are two independent processes, acting to align the atom spins in both the longitudinal and transverse planes. The switch in the longitudinal plane from parallel to anti-parallel reduces the net magnetization in this direction, thereby eliminating the longitudinal magnetization signal. However, the phase alignment in the transverse plane

creates a transverse magnetization signal. Rotation in the transverse plane occurs at the Larmor frequency and engenders a detectable magnetic resonance signal.

After the radiofrequency pulse, the spins decay or relax to their ‘natural’ state. In the transverse plane, spins that were in phase (due to the pulse), become out of phase again, releasing energy and reducing the transverse magnetization (transverse relaxation, T2). T2 is unique for each tissue type and related to the chemical environment. Relaxation also occurs along the longitudinal plane (T1 recovery) in an independent manner and with unique recovery rate characteristics depending on tissue. Due to variations in the B0 field across the brain (as a result of the effects of different tissue environments on the field for example), relaxation rates and endpoints are different at different parts of the brain. Inhomogeneities in the field affect relaxation and spin dephasing, an effect that is cumulatively known as T2* relaxation. The T2* effect is smaller than T2, with more inhomogeneities creating a lower T2* signal. Thus, in regions with more inhomogeneities, the T2* signal decays faster and the signal is lower. This signal ‘drop-out’ is observed in areas of high inhomogeneity, for example around the sinuses. So the timing of image capture after a radiofrequency excitation pulse is crucial. Echo time (TE) is the time between excitation and acquisition. T1 is captured with short TE’s and T2 with longer TE’s.

To encode spatial information, a graded magnetic field is applied, for example along the x direction. So, one end of the slice (x direction) shows high spin frequency and the other shows low spin frequency. This creates a direct relationship between spatial position and spin frequency in the x direction. In the y direction, a gradient for the time of spin procession is applied, which disturbs spin procession speed at different rates along the y direction. Thus, one end of the slice (y direction) shows high spin procession speed, the other end shows low spin procession speed. After this gradient is applied, the spins relax to their ‘natural’ aligned state but are now out of phase (at different spin positions). This creates a range of phases along the y direction.

Thus, for each slice that is excited by a radiofrequency pulse, it is not excited by a uniform radiofrequency, but by a gradient. This means that across the pulse plane, target atom spin frequency and phase changes will be gradiented and therefore spatially measurable. For each slice, both the x and y plane can therefore be encoded as the frequency and phase gradients (frequency and phase encoding), together known as k-space. In sum, the process of collecting MRI data can be broadly described as the following: firstly a radiofrequency pulse of a single slice flips the spins to create traverse magnetization; secondly a phase shift pulse is applied to that slice with a gradient in the y direction; thirdly the transverse magnetization is flipped 180 degrees within the slice with a frequency encoding gradient along the x direction. Application of a Fourier transform allows the conversion from k-space to a 3D spatial image of the brain.

Neurovascular Coupling

Neurovascular coupling describes the relationship between neuronal activity and the subsequent increase in cerebral blood flow. Neural activity depends on glucose metabolism requiring oxygen, both of which are supplied by an extensive vasculature network. Due to the initial neuronal requirement of oxygen, there is a dip in oxygenated blood, followed by a delayed increase in blood flow, volume and oxygenation. This initial dip might therefore be a more specific spatial marker of neuronal activity as blood flow innervates surrounding regions too[396, 397]. The amplitude of the peak blood oxygenation and flow response following neuronal activity has a linear relationship with neuronal activity in many cases [398-400] although neuronal responses may saturate while blood flow continues [401]. Both synaptic activity, as measured by local field potentials and neuronal action potentials (or spikes), which represent neuronal input and output signals respectively, together correlate with vascular responses. There are some situations in which they are dissociated, for example when synaptic input does not lead to a neuronal spike due to a neuromodulatory function, in which case the vascular response represents the synaptic activity only[400, 402]. However, the neurovascular response mostly reflects both an increase in synaptic and spiking activity. [401]

The BOLD signal

As mentioned, inhomogeneities affect transverse relaxation and spin dephasing and is captured by the T2* effect. Macroscopic inhomogeneities can be caused by air, metal and also blood oxygen. Hemoglobin has two confirmations, for oxygenated and deoxygenated states. While oxygenated hemoglobin has similar magnetic susceptibility to tissue, deoxygenated hemoglobin is paramagnetic and interacts with the magnetic field, creating inhomogeneity. When a group of neurons or brain region is activated, glucose is metabolized and blood flow increases to that site, bringing oxygenated blood. The amount of deoxygenated blood reduces causing a reduction in field inhomogeneity, a slower signal decay and an increase in the T2* signal. This measure of blood deoxygenation in the form of the T2* signal forms the basis of functional MRI. BOLD signals depend on blood flow and volume as well as oxygenation[403] and are correlated with neuronal action potentials[404].

Resting State Functional MRI

Twenty years ago, seminal work by Biswal and colleagues[405] changed the way we use fMRI to examine the characteristic features of the living human brain. Biswal and colleagues showed that regions that are functionally similar (such as sensorimotor cortices) show highly temporally correlated spontaneous fluctuations of BOLD signal intensity during wakeful rest. The spontaneous BOLD signal time series of a single voxel in the motor cortex was examined and found to be correlated with the signal time series of the contralateral motor region. These resting state correlation maps within and across sensorimotor cortex showed substantial overlap with task activation maps during finger tapping[405]. This suggested that information processing was ongoing in these regions during rest and perhaps more importantly today, that the functional homology between these regions was measurable. Since then, hundreds of studies have been published examining fMRI during rest, addressing a wide range of questions (cognition, genetics, pharmacology) and in an array of translatable models (rodents, cats, non-human primates).

Intrinsic fluctuations of BOLD signal intensity within regions with similar function (for example, the primary and supplementary motor cortices) are highly correlated, and are described as being 'functionally connected'[405]. This temporal dependence between anatomically dissociable regions forms the basis of our understanding of functional connectivity and the emergence of a network view of the brain. Such measures of communications between regions or networks provide insight into their ability to perform neural computations or levels of cognitive ability[259]. Not only do studies of functional connectivity indicate how information is processed and transferred across the brain, but also how it is organised on the fine and gross scales.

Major resting state networks include: the default mode network (including medial frontal cortex, precuneus, inferior parietal cortex and medial temporal cortex) which is more active during rest than task, representing a baseline state[406]; the frontal-parietal attentional executive network; and primary visual and motor networks [259, 407, 408]. Although the components of these networks are anatomically separated, they demonstrate consistent functional connectivity suggesting ongoing synchronous neural processing during rest. Such networks are largely consistent across different subjects[407-409], different stages of development[410, 411], and states of consciousness[412, 413]. The functional or behavioural relevance of resting state networks has been exemplified by reports of relationships between intrinsic resting state characteristics and behavioural ability[414], and inter individual variability in cognitive task performance[415].

Furthermore, activity of nodes within the primary motor cortex are more correlated with each other than with supplementary motor cortex[405], presenting a functionally hierarchical state. Indeed, when examining the resting state brain, sub-networks become apparent, within larger scale networks like the visual network, suggesting an internal topology that reflects organization for sub-functions[259, 407, 408]. This means that not only can we understand which regions are integral in specific networks, we can start to gain an understanding of their relative strengths or weights within that network.

Together, the study of resting state functional connectivity can provide insight into neural organization that has been previously restricted to anatomical tracer or post-mortem studies. This endeavor is not simply restricted to the exploration of functional organization but also their behavioural relevancies.

Issues with rsfMRI

There are several issues that arise when studying resting state functional connectivity. For resting state data, particular interest falls on the low frequency oscillations of the time series (0.01 – 0.1 Hz) [259, 405, 416]. As functional MRI has low temporal resolution (around 0.5 Hz), more highly frequent cardiac and respiratory oscillations can be aliased back into the lower frequency signals of the resting state activity[259]. As such, there has been some ongoing suggestion that the observed resting state signals results from cardiac and respiratory oscillations. BOLD has been shown to be associated with breathing volume at lower frequencies (0.03 Hz) across highly vascularized regions like grey matter[417]. Therefore, functionally connected regions could be due to similar respiration-induced changes rather than similar underlying neuronal activity. Several methods such as removing global signal changes[417], separating the respiration-related signals as an independent component[418] and measuring respiratory changes independently[418] can help to remove these confounding effects and 'clean' the data. However, confidence that the observed resting signals reflect underlying neuronal activity can be gained from observations that patterns of functional connectivity occur in functionally or neuroanatomically related regions[259, 405].

Most convincing are studies demonstrating relationships between simultaneous physiological measures of neuronal activity and resting state signals. Shmuel and colleagues conducted intracortical neurophysiological recording and functional MRI to demonstrate that slow BOLD signal fluctuations were correlated with measured neuronal activity[419]. It is widely accepted now that the observed BOLD signal reflects, for the most part, underlying neuronal activity, but the influence of non-neuronal disturbances on

BOLD signal is still a matter of concern. Because the analysis of resting state data is largely data driven and not controlled by a task or block design, these sources of structured noise can cause spurious artefactual correlations and increase the presence of false positives.

Various methods have been and are still being developed to combat the issues of perturbation by confounding influences, like respiratory activity, cardiac activity and motion. Typical approaches include using temporal noise models, regressing out time series of noise artefacts as nuisance covariates, separating noise artefacts out in an independent component analysis and band pass filtering. However, in some cases, noise artefact components can spatially overlap with resting state networks, causing an underestimation of noise components or removal of neuronal-related fluctuations and component-based separation of artefact from network components can ultimately fail[409, 418].

Another issue for consideration is the effects of alcohol on neurovasculature, which might be expected in heavy drinking populations. Acute alcohol has been shown to slow down neurovascular coupling[420], reduce blood-brain barrier integrity[421] and both reduce and increase blood flow[422] in certain brain regions. However, while the acute effects of alcohol on neurovasculature has been studied[420, 422, 423], neuro-vascular coupling and BOLD measurements following chronic use in AD individuals has been less studied. Chronic alcohol use has been associated with hypertension and stroke[424, 425] but how chronic alcohol use affects the BOLD signal is unclear. Therefore, broad interpretations of neural function based on BOLD responses should be taken alongside complimentary examinations of cognitive processes and behaviour, to allow a more accurate depiction of the disease, rather than relying simply on neural responses measured with fMRI.

Multi-Echo rsfMRI

Due to the issues around the collection and interpretation of rsfMRI data, there are multiple ongoing avenues of development of acquisition and analysis techniques to solve the problems relating to noise, motion and respiratory signal artefacts. One promising method is using multi-echo rsfMRI acquisition and analysis[426, 427], which is described here and employed throughout the rest of this thesis.

As discussed, BOLD signal can be captured by the T2* signal. Data is typically acquired at a single TE that is equal to the average T2*. The current technique collects data at multiple TE's. Collecting data at multiple TE's allows the capture of signals that decay at different rates, for example, using shorter TE's allows the experimenter to gain more signal from regions with substantial early signal drop out. The utility of multi-echo rsfMRI mostly lies with denoising. Changes in the T2* signal (equivalent to 1/R2*) are linearly dependent on TE, whereas changes in T1 and motion have no relationship with TE. Defining this relationship for all collected data can thus determine whether the observed signal is BOLD (T2* change) or non-BOLD (T1, noise) based on its relationship with TE. Goodness of fit measures can be computed that quantify TE-dependence, effectively providing a measure of likelihood that the observed signal is neuronal (κ, BOLD) or non-neuronal (ρ, non-BOLD)[427]. By separating signal components based on these characteristics, rsfMRI data can be parsed for BOLD (high κ, low ρ) and non-BOLD (low κ, high ρ) signal. Non-BOLD signal components can be removed as noise and BOLD signals retained. This method of denoising improves the signal to noise ratio fourfold compared to traditional single echo acquisition and analysis techniques[426].

Diffusion MRI and Tractography

Diffusion MRI

Diffusion weighted MRI is a form of imaging that is sensitive to the diffusion of water in the sample (brain tissue). As water molecules diffuse freely in CSF and in a restricted

manner in white matter fibre bundles, this method can provide information on white matter integrity, size, shape, volume and boundaries. Unlike functional MRI, with diffusion imaging, the magnetic field of the scanner is spatially linearly varied with a gradient field pulse, which causes the precessions of the protons to vary in phase. A second gradient field pulse is applied that is identical but in the opposite direction to re-align or refocus the phase of the proton spins to their original positions. Static spins (non-diffusing) are cancelled out by the reverse gradient. However, between the first and second gradient field pulse's, non-static spins (diffusing) are not fully cancelled, causing residual phase and a reduction in signal compared to the baseline (baseline has no diffusion gradient). Higher attenuation equates to higher diffusion. The gradient strength and time lag between the two pulses can be varied, producing different contrast characteristics. The diffusion weighted gradients can be applied in any direction and signal attenuation perpendicular to the direction of the gradient indicates diffusion in that direction. For example, an anterior – poster gradient would produce quantifiable signal attenuation in the corpus callosum.

Diffusion within a voxel can be measured using a diffusion tensor. The diffusion tensor is a 3 x 3 matrix that quantifies diffusion along the xyz directions and the correlations between them. From this, three eigenvectors and three eigenvalues can be derived that depict the direction / orientation and the magnitude of diffusion, respectively. Together, these values are used to create a sphere or ellipsoid for each voxel that represents the diffusivity and the direction of the underlying water diffusion. In the CSF, this tensor is spherical and in coherent anisotropic white matter fibre bundles like the corpus callosum, the tensor is a long narrow ellipsoid. The diffusion tensor is a simple representation of tissue microstructure.

Neurite Orientation Dispersion and Density Imaging (NODDI)

NODDI, a recently developed diffusion MRI technique, provides higher specificity of microstructural characteristics than conventional diffusion tensor imaging. As mentioned, diffusion of water, which in an unrestricted environment is isotropic, is restricted in the

brain by tissue boundaries such as axonal membranes and as such, different microstructural environments can be assessed. Models of white matter use a diffusion ellipsoid or diffusion tensor to capture the features of white matter fiber bundles that restrict movement of water. More advanced models that work to capture directionality for tractography analysis use the ball-and-stick model [428], which represents the intracellular water diffusion component as cylinders with zero radius (stick) and extra-cellular diffusion as isotropic and unrestricted (ball). These models assume one single orientation of fibers, which limits analysis to coherently organised fiber bundles like the corpus callosum while grey matter displays substantial dispersion of fiber orientations. However, recent more model-based methods using geometric models of microstructure to predict the MR signal produced by water diffusion can explicitly represent the dispersion of axon orientation, expected in grey matter.

The NODDI approach is based on the ‘hindered and restricted model’ of white matter water diffusion that assumes that neural microstructure environments have distinct effects on the diffusion of water (hindered and restricted water diffusion). This technique uses three-compartment modeling[429] for three distinct tissue microstructural environments. Firstly, the intracellular fraction shows restricted diffusion with a non-Gaussian pattern of water displacement, in which diffusion is bounded by restricted geometries like axonal membranes. The total signal is thus a composite of diffusion restriction by a cylinder with a given orientation and weighted by all cylinders oriented in that direction. While previous models use a single, parallel orientation parameter, the current computation uses a Watson distribution (spherical analog of a Gaussian distribution) to signify axons dispersing about a central orientation, which can range from highly parallel to highly dispersed. This ultimately provides a measure of orientation dispersion index, or how dispersed fibers are, indicating the complexity of neurite or dendritic branching. Secondly, the extracellular fraction shows hindered diffusion and a Gaussian anisotropic displacement, in which water diffusion is hindered by glial and cell body (soma) membranes. Thirdly, the cerebrospinal fluid space where water diffusion is unhindered and isotropic[430]. The differentiation of such water forms provides a basis for depiction of microstructural features using diffusion MRI. From this, measures of

neurite density and orientation dispersion can be obtained, which provide a more fine-grained microstructural approach and have good scan – rescan reproducibility[431].

In grey matter, the orientation dispersion index captures sprawling dendritic processes, detailing grey matter complexity[430]. NODDI microstructural modeling has a more direct relationship with axonal orientation distribution[432], neurite density and dendritic architecture[433]. Indeed, these microstructural features have previously been associated with the hierarchy of computations performed by increasingly higher-level cortical structures[434], lower age [435] and resting state functional network connectivity [435].

Demonstrating the Utility of Multi-Echo rsfMRI and NODDI

First, in Experiment 1, the utility of the multi-echo rsfMRI acquisition and denoising technique is demonstrated by focusing on the STN. The STN was chosen due to the notorious difficulty in examining this structure thanks to its small size and positioning within a region of signal drop out and noise. In a large sample of healthy volunteers, cortical and striatal functional connectivity with STN was computed, and compared with traditional single echo rsfMRI techniques. Firstly, functional connectivity between limbic (ventral striatum) and motor (posterior putamen) striatum with STN was examined, to test whether limbic and motor subregions of STN can be broadly delineated using multi-echo rsfMRI. Secondly, functional connectivity between diverse cortical regions and STN was examined to parcellate STN subzones on a more fine-grained level and to replicate findings from non-human primate tracer studies[109].

Secondly, Experiment 2 describes and demonstrates the second major neuroimaging method employed in the latter sections of this thesis, namely neurite orientation dispersion and density imaging (NODDI), a type of diffusion MRI. Whole brain NODDI data are presented for a single healthy volunteer to aid the description of the method and to present the microstructure features obtainable. Secondly, STN-to-whole brain tractography was computed and illustrated for a combined group of healthy individuals

and binge drinkers (N=68), to increase the power of the sample. Group differences are presented later in this thesis.

Methods

Experiment 1: rsfMRI

Participants

All participants completed the Beck Depression Inventory[436] for depressive symptoms, the UPPS-P scale for impulsivity[335] and Alcohol Use Disorders Test (AUDIT)[437] / Alcohol Use Questionnaire for alcohol use severity and binge score[438].

Healthy volunteers (N=154, 71 female; age=31.3 ±12.842) were recruited from the University of Cambridge and community-based advertisements in East Anglia. Subjects aged 18 and over were tested and were excluded if they had a major psychiatric disorder, substance addiction, a history of regular or current use of substances, serious medical illness or were on psychotropic medications, and screened with the Mini International Neuropsychiatric Interview[439]. Subjects provided written informed consent before participating and were compensated for their time. The study was approved by the University of Cambridge Research Ethics Committee.

Data Acquisition and Processing

Functional MRI data was collected during rest for 10 minutes with eyes open with a Siemens 3T Tim Trio scanner with 32-channel head coil at the Wolfson Brain Imaging Centre, University of Cambridge (repetition time (TR), 2.47s; flip angle, 78°; matrix size 64 x 64; in-plane resolution, 3.75mm; field of view (FOV), 240mm; 32 oblique slices, alternating slice acquisition slice thickness 3.75mm with 10% gap; iPAT factor, 3; bandwidth (BW) = 1,698 Hz/pixel; TE = 12, 28, 44 and 60 ms). Anatomical T1-weighted

magnetization prepared rapid gradient echo (MPRAGE) (176 x 240 FOV; 1-mm in-plane resolution; inversion time (TI), 1100ms) data were also acquired.

Multi-echo independent component analysis (ME-ICA v2.5 beta10; http://afni.nimh.nih.gov) was used to denoise functional data. Data were decomposed into independent components using FastICA and independent components that strongly scaled with TE were retained as BOLD data [427]. TE independent components were assigned as non-BOLD artefacts and were removed by projection, robustly denoising data for motion, physiological and scanner artefacts based on physical principles[426]. Denoised echo planar images were coregistered with their anatomical MPRAGE data and normalized to a standard MNI template.

Data Analysis

Functional connectivity was computed using a seed-driven approach using the CONN-fMRI Functional Connectivity toolbox[440] for SPM. Functional data was temporally band-pass filtered ($0.008 < f < 0.09$ Hz) and significant principle components of white matter and cerebrospinal fluid were removed.

Functional connectivity between limbic (ventral striatum) and motor (posterior putamen) striatum was examined with STN, to test whether limbic and motor subregions of STN can be delineated. Cortical functional connectivity with STN was measured using functionally-defined cortical regions as seeds[441], which reflected primate anterograde tract tracing studies demonstrating projections to STN[109], including dlpfc (Brodmann Area (BA) 9 and 46); dorsal ACC)BA 24); pre-SMA (Rostral BA 6); SMA (Caudal BA 6) and primary motor cortex (M1, BA 4). Significance was assessed with SVC for STN, FWE $p<0.05$.

STN to whole brain functional connectivity was also examined, using the STN ROI provided by Wake Forrest University PickAtlas[442]. This has the same centre of mass

as a previously used STN ROI based on task-based fMRI[121, 156]) (xyz= 10, -14, -4 for right STN). For this, whole brain corrected FWE $p<0.05$ was used.

Seed definition

The bilateral ventral striatal anatomical ROI, previously used in other studies[443] had been hand drawn using MRIcro based on the definition of VS[444]. The putamen ROI was obtained from the Automated Anatomical Labelling (AAL) atlas. The posterior putamen was separated from anterior putamen using a vertical line passing through the anterior commissure. The caudate ROI was obtained from the AAL atlas with removal of the ventral striatal ROI.

The following seeds were manually created or altered using MarsBaR ROI toolbox[445] for SPM[445][445][445][445][445][445][58]. For the OFC, the dorsal extent was defined by the axial slice showing the disappearance of the olfactory sulcus, the medial and lateral OFC were distinguished by the crown of the gyrus rectus[446]. The lateral OFC consisted of two boxes of 14.2 x 22 x 2mm centered on coordinates ±28, 36, -18. The medial OFC ROI consisted of the combination of 2 boxes, the size of 6 x 26 x 4mm and centered on coordinates ±6, 36, -22. The vmpfc was defined anteriorly by the posterior border of the cytoarchitectonic anterior prefrontal cortex (i.e., the most anterior coronal slice in which all three frontal gyri are visible), also known as area 10p [447]; posteriorly and laterally by the cingulate cortex; dorsally by the genu of the corpus callosum; and ventrally by the superior boundary of the medial OFC described above. To make the dlpfc ROI, the masks of Brodmann areas 46 and 9 from the AAL atlas were combined, and manually restricted the mask to the boundaries of the dlpfc: the anterior border was defined by the most anterior tip of the corpus callosum (CC); the posterior extent was the posterior border of the genu of the CC; the ventral border was the inferior frontal sulcus; and the medial border defined by the cingulate sulcus[446, 448]. To create the SMA seed, the SMA ROI from the AAL atlas was modified. The posterior border of the pre-SMA is typically defined as a vertical line through the anterior commissure, the anterior border defined as a vertical line passing through the genu of the corpus callosum and the

inferior border being the superior border of the cingulate cortex [449]. The posterior border of the SMA is defined by the primary motor cortex. By respecting these boundaries, the SMA ROI was created.

Brodmann Area 25 from AAL atlas was used to create the subgenual ACC seed. For the dorsal ACC, the cingulate cortex ROI from AAL atlas was modified such that the anterior border was defined as the tip of the genu of the corpus callosum [446, 450] and the posterior was the posterior end of the genu of the corpus callosum[450]. The IFC ROI was created using the inferior frontal sulcus as the superior boundary; the precentral gyrus as the posterior boundary[446, 450]; and the rostral extent of the inferior frontal sulcus as the anterior boundary[450]. This was then restricted to those regions falling within a 300mm radius sphere on x= ±48, y=18, z=8 [451], using the anterior horizontal ramus of the Sylvian fissure to differentiate from orbital regions[446]. For the anterior PFC ROI, Brodmann area 10 from WFU PickAtlas was manually restricted the ROI posteriorly at the boundary of the anterior coronal place where the three frontal gyri are present[447, 452, 453], and dorsally by the dorsal extent of area 10p described by[447]. The dorsomedial PFC ROI was created using the dorsal boundary of the anterior PFC, the lateral boundaries described for the vmpfc and anterior boundary described for the pre-SMA.

Experiment 2: NODDI

Participants

Young adult binge-drinkers (BD) and healthy volunteers were recruited from community-based advertisements in East Anglia. BD inclusion criteria was based on the National Institute on Alcoholism and Alcohol Abuse[454] diagnostics: >8/ >6 alcohol units consumption (males/ females) within a 2 hour period at least once a week. Subjects had to have been ‘drunk’ at least once per week for the previous 6 months and reported an intention to get drunk. Subjects were carefully questioned on their patterns of alcohol consumption and last alcohol binge consumption prior to testing. Healthy volunteers were

made up of social drinkers and non-drinkers. Psychiatric disorders were screened with the Mini International Neuropsychiatric Interview[439]. Subjects were excluded if they had a major psychiatric disorder, substance addiction (including alcohol and excluding nicotine) or medical illness or were on psychotropic medications. Subjects were included if they were 18 years of age or over and had no history of regular or current use of other substances.

Neurite Orientation Dispersion and Density Imaging

NODDI data was acquired from 39 healthy volunteers and 29 binge-drinkers. Data was acquired with a Siemens 3T Tim Trio scanner using a 32-channel head coil at the Wolfson Brain Imaging Centre at the University of Cambridge with the following parameters: TE = 128 msec; TR = 11,300 msec; planar FOV = 192 mm × 192 mm; 96 matrix with 2 mm voxel and 2 mm slice thickness. There were 63 slices (b-values: 2850 and 700 sec/mm2 with 65 and 33 directions, respectively). A NODDI microstructural model was computed and fitted to the data using the NODDI toolbox for Matlab[430] (http://www.nitrc.org/projects/noddi_toolbox). Resulting parameter maps were normalized to MNI space with ANTS software (http://stnava.github.io/ANTs/). The orientation dispersion index parameter map was masked to standard grey matter and the neurite density parameter map to a standard white matter template.

Tractography

Probabilistic diffusion tractography for STN to whole brain was computed according to previously described methods[455]. Diffusion data were processed with FMRIB's Diffusion Toolbox as part of the FMRIB's Software Library (FSL; http://www.fmrib.ox.ac.uk/fsl). Images were corrected for Eddy currents with the first b0 volume as the reference and individually skull-stripped using the Brain Extraction Tool. A diffusion tensor model was then estimated for the processed and corrected data at each voxel. Estimations of probable pathways emerging from the seed point of interest were computed using Bayesian Estimation of Diffusion Parameters Obtained using Sampling Techniques (BEDPOST) as implemented in FSL. This approach runs Markov Chain

Monte Carlo sampling and estimates a probability distribution function for the main fibre direction for each voxel in the seed mask. Then, principal diffusion directions for each voxel were repetitively sampled, computing 5000 probabilistic streamline samples. A posterior distribution for the streamline location ultimately indicates the dominant path for that seed.

Results

Experiment 1: rsfMRI

Striatal Connectivity with STN

Ventral striatum had more restricted connectivity with STN, with peaks bilaterally in ventromedial anterior STN (right STN: Z=2.92, xyz= 8 -11 -7; left STN: Z=1.98, xyz=-8 -14 -9) (Figure 1.1) whereas posterior putamen had more widespread connectivity with STN with peaks bilaterally in posterior STN (right STN: Z =4.25, xyz= 10 -14 -4; left STN: Z=3.99, xyz= -10 -11 -7) (Figure 1.1).

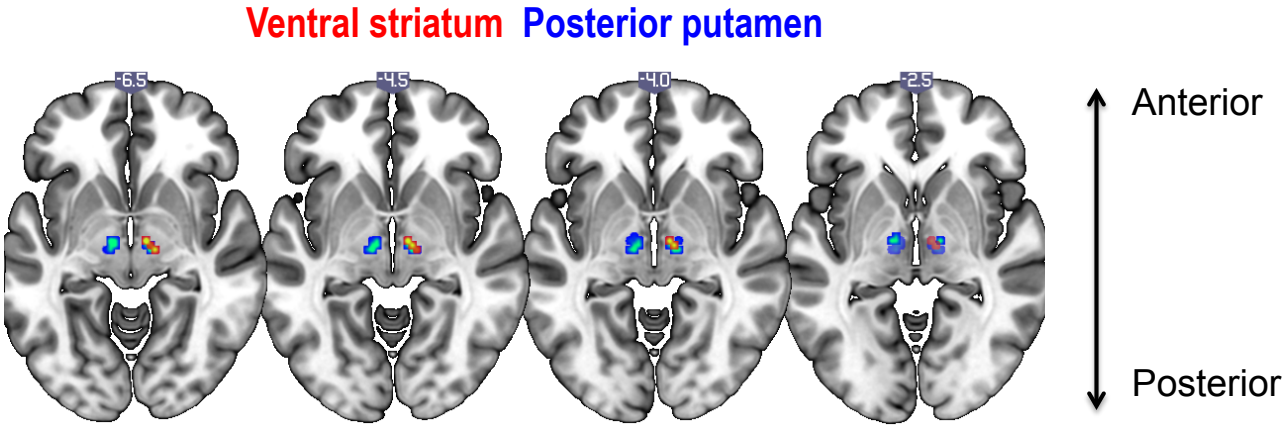

Figure 1.1. Ventral striatum and posterior putamen connectivity with Subthalamic Nucleus. *Resting state functional connectivity of ventral striatal (red) and posterior putamen (blue) seed regions with STN is demonstrated using SVC FWE correction p<0.05 on a standard MNI template.*

Cortical Connectivity with STN

Of the cortical seed regions, dorsal ACC and SMA had the strongest and most widespread functional connectivity with STN (Dorsal ACC: right STN: Z=4.92, xyz= 13 -11 -2; left STN: Z=5.39, xyz= -13 -11 -2; SMA: right STN: Z=5.32, xyz= 10 -14 -4; left STN: Z=4.28, xyz= -13 -16 -4), followed by primary motor cortex (M1) (right STN: Z=4.33, xyz= 13 -16 -4; left STN: Z=4.50, xyz= -10 -16 -4) which had the most posterior connectivity (Figure 1.2 and Figure 1.3). Dlpfc was dissociable on an anterior-posterior axis, with peaks bilaterally in anterior STN (right STN: Z=2.40, xyz= 8 -11 -4; left STN: Z=2.16, xyz= -8 -11 -7) with a posterior extent of y=-14. The pre-SMA and right IFC, both nodes within the 'stopping' network, had peaks overlapping across both anterior and posterior STN (pre-SMA: right STN: Z=3.94, xyz= 13 -11 -2; left STN: Z=2.17, xyz= -10 -16 -9; right IFC: right STN: Z=2.89, xyz= 10 -16 -9; left STN: Z=1.94, xyz= -8 -14 -4). Dorsomedial PFC and orbitofrontal cortex showed no significant functional connectivity with STN.

In sum, the peak values for the ventral striatum, dlPFC and dorsal ACC connectivity to STN were more anterior bilaterally (y=-11) whereas posterior putamen, SMA and M1 were more posterior bilaterally (y=-14 to -16).

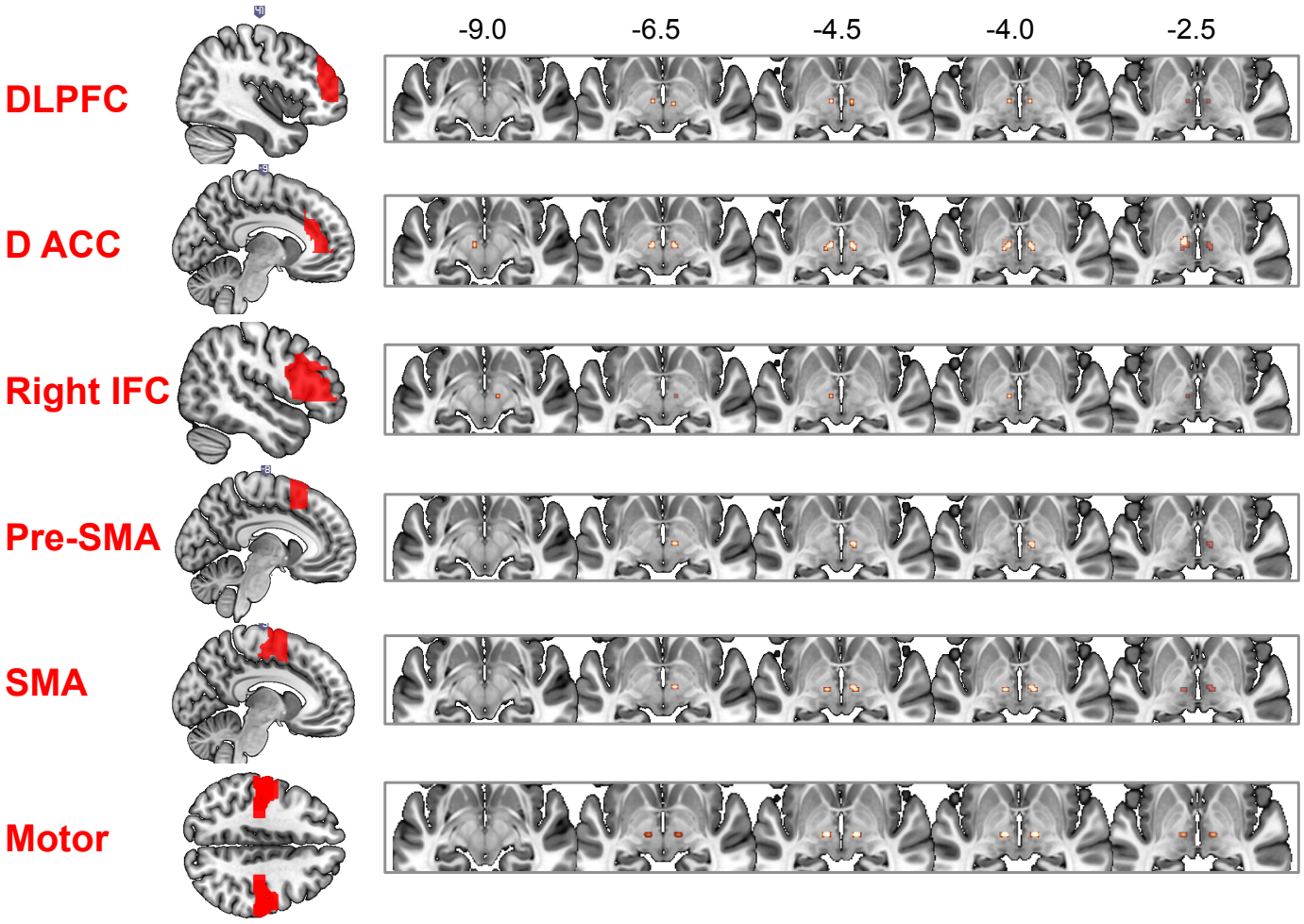

Figure 1.2. Cortical connectivity with subthalamic nucleus. *Cortical seed regions of interest were correlated with subthalamic nucleus, revealing discrete subzones of functional connectivity. Abbreviations: DLPFC, dorsolateral prefrontal cortex; D ACC, dorsal anterior cingulate cortex; IFC, inferior frontal cortex; pre-SMA, pre-supplementary motor area, SMA, supplementary motor area. Images are displayed on standard MNI template.*

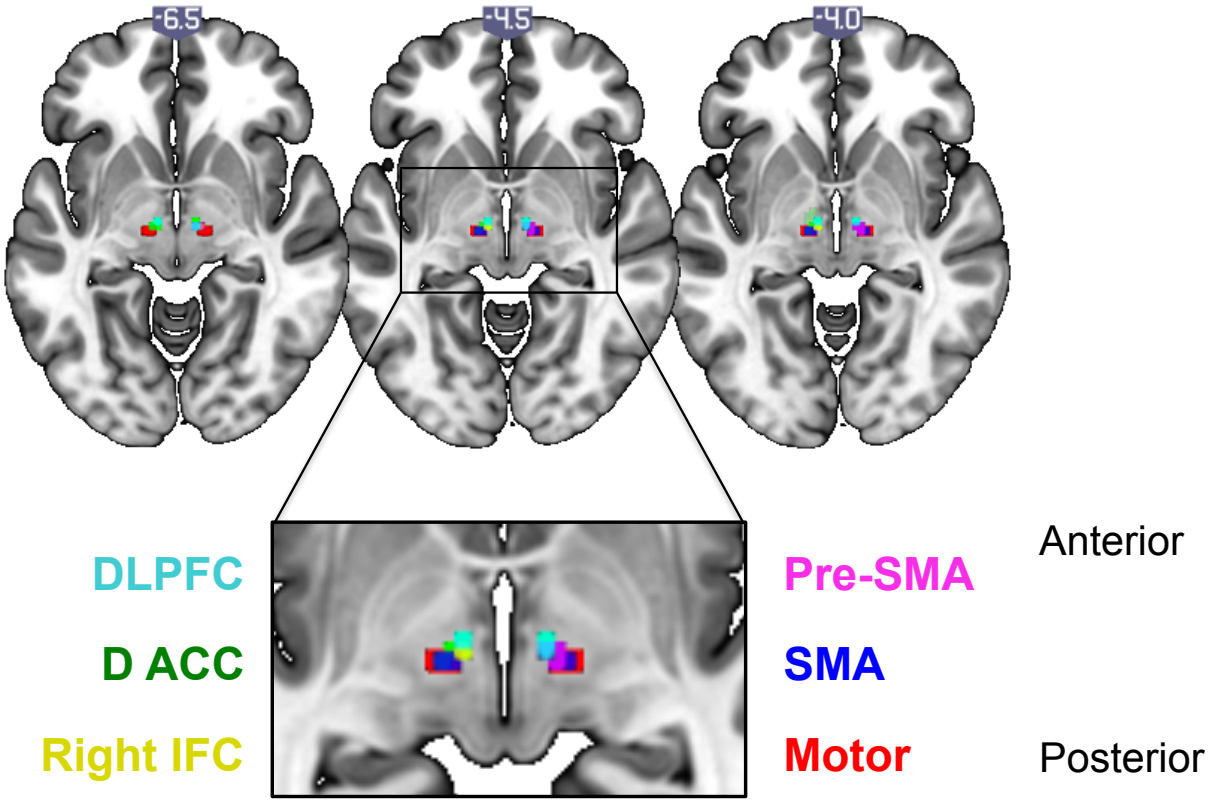

Figure 1.3. Collation of cortical connectivity with subthalamic nucleus. *Cortical region functional connectivity with STN is demonstrated on the same image, to illustrate borders in functional connectivity. Abbreviations: DLPFC, dorsolateral prefrontal cortex; D ACC, dorsal anterior cingulate cortex; IFC, inferior frontal cortex; pre-SMA, pre-supplementary motor area, SMA, supplementary motor area. Images are displayed on standard MNI template.*

STN and Whole Brain Connectivity

Controlling for age and gender, baseline functional connectivity of bilateral STN with the whole brain was examined (Figure 1.4) (Table 1.1). The STN was positively connected with thalamus, striatum, pallidum, dorsal cingulate, dorsolateral prefrontal cortex and negatively with temporal and occipital cortices.

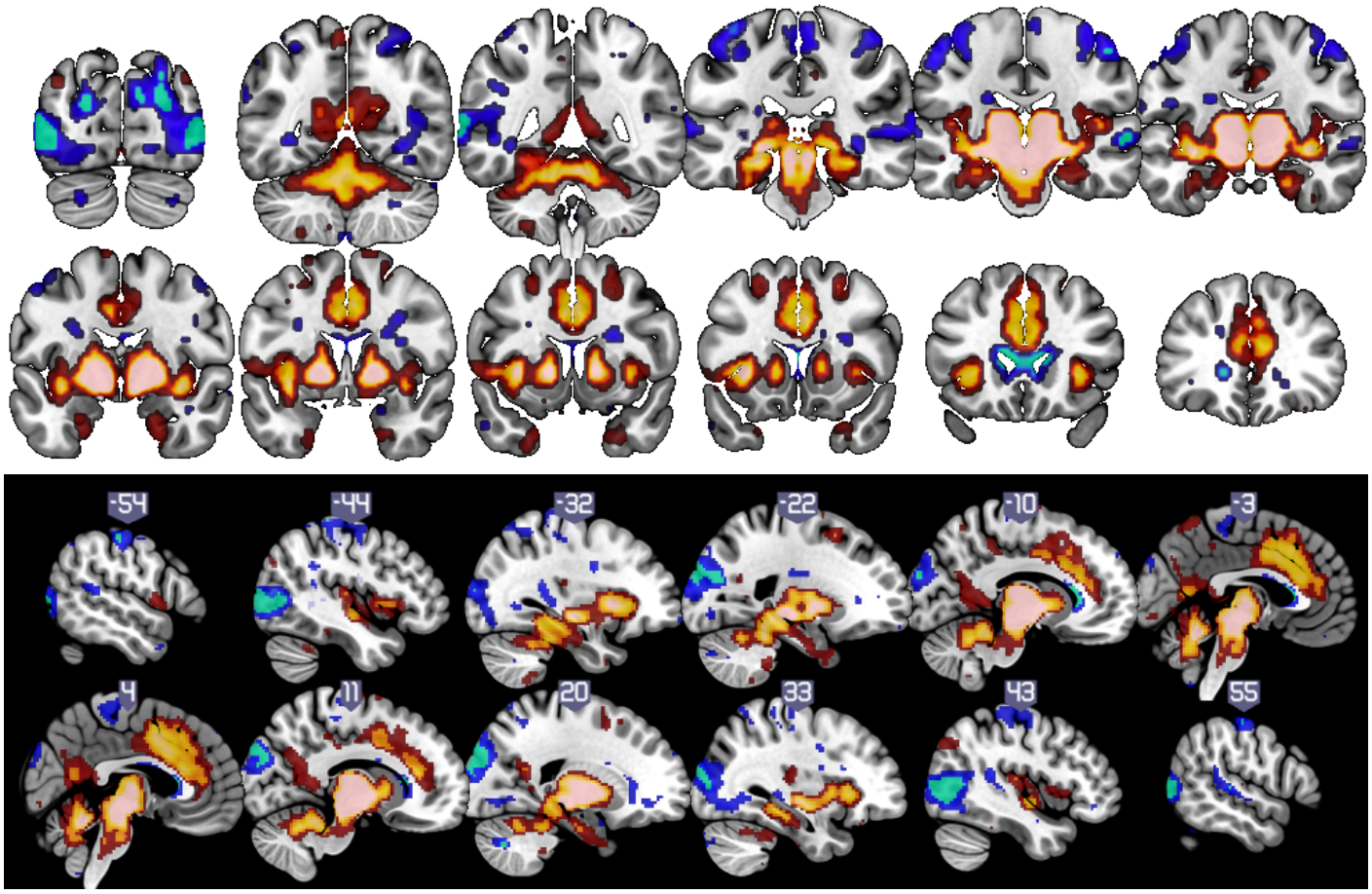

Figure 1.4. Subthalamic nucleus seed connectivity with cortex. *Functional connectivity of bilateral STN with the whole brain is illustrated. Hot colours represent positive and cold colours represent negative functional connectivity. Data is whole-brain FWE p<0.05 corrected. Images are displayed on standard MNI template*

	p(FWE-corr)	Cluster	Z	x	y	z
STN positive						
Cluster includes midbrain, thala	<0.001	6993	<8.00	10	-14	-7
			<8.00	-10	-14	-7
			<8.00	6	-27	-11
Dorsal Cingulate	<0.001	1638	7.25	3	12	33
			7.2	3	5	42
			7.02	-6	28	21
Temporal (hippocampus)	<0.001	27	5.83	22	-16	-25
Posterior Cingulate	<0.001	74	5.78	-1	-60	10
Posterior Insula	0.001	13	5.33	45	-20	10
DLPFC	0.005	7	5.14	24	12	52
Medial Parietal	0.001	14	5.13	-17	-60	19
Medial Parietal	0.001	14	5.12	17	-55	19
STN negative						
Posterior Temporal / Occipital	<0.001	435	<8.00	45	-72	5
			5.17	36	-67	-7
White matter	<0.001	220	7.15	3	19	10
			7.11	-13	26	7
Posterior Temporal / Occipital	<0.001	317	7.01	-48	-83	3
			5.81	-43	-69	5
			5.56	-48	-76	10
Occipital	<0.001	501	6.53	24	-86	28
			5.85	27	-88	10
			5.81	8	-90	35
Occipital	<0.001	202	6.05	-22	-79	21
			5.93	-20	-95	26
			5.44	-27	-93	14
Temporal	<0.001	26	5.74	62	-20	0
Cerebellum	0.005	7	5.62	20	-69	-37
Temporal	<0.001	37	5.48	-69	-44	5
Parietal	<0.001	25	5.47	-50	-25	54
Parietal	0.001	13	5.37	-41	-34	68
White matter	0.004	8	5.2	3	5	17
Parietal	0.002	10	5.08	50	-18	54

Table 1.1. Intrinsic subthalamic nucleus connectivity with whole brain. *Bilateral subthalamic nucleus (STN) seed-to-whole brain positive and negative functional connectivity was computed. Abbreviations: p(FWE-corr), whole brain family wise error corrected p value; Z, Z score; xyz, peak voxel coordinates; DLPFC, dorsolateral prefrontal cortex.*

Comparison with Single Echo rsfMRI

On an exploratory basis, this analysis was repeated in half of the sample of healthy volunteers (N=85, 31 female, age=31.247±12.546), in order to a) assess the potential for replication in a smaller sample and b) compare multi-echo independent component analysis and denoising with traditional single echo resting state data with the same preprocessing (detrending and bandpass filtering) but without removal of non-BOLD components and denoising by ME-ICA.

The findings from the larger sample are replicated, demonstrating a spatial dissociation between limbic ventral striatum and motor posterior putamen connectivity with STN using multi-echo rsfMRI, although the findings were not significant for ventral striatum (Ventral striatum: SVC p=0.473, Z=1,77, xyz= -13 -16 -4; posterior putamen: SVC p=0.011, Z=3.37, xyz= -10 -11 -7) (Figure 1.5 top). This data was also compared with data from the same 85 individuals, using traditional resting state functional MRI studies with *single* echo data and preprocessing with detrending and bandpass filtering but without denoising by ME-ICA. Traditional single echo data and analysis demonstrated a loss of clusters and significance for posterior putamen (Ventral striatum: SVC p=0.458, Z=1.70, xyz= -13 -16 -7; posterior putamen: SVC p=0.386, Z=1.82, xyz= 8 -14 -5) (Figure 1.5 bottom).

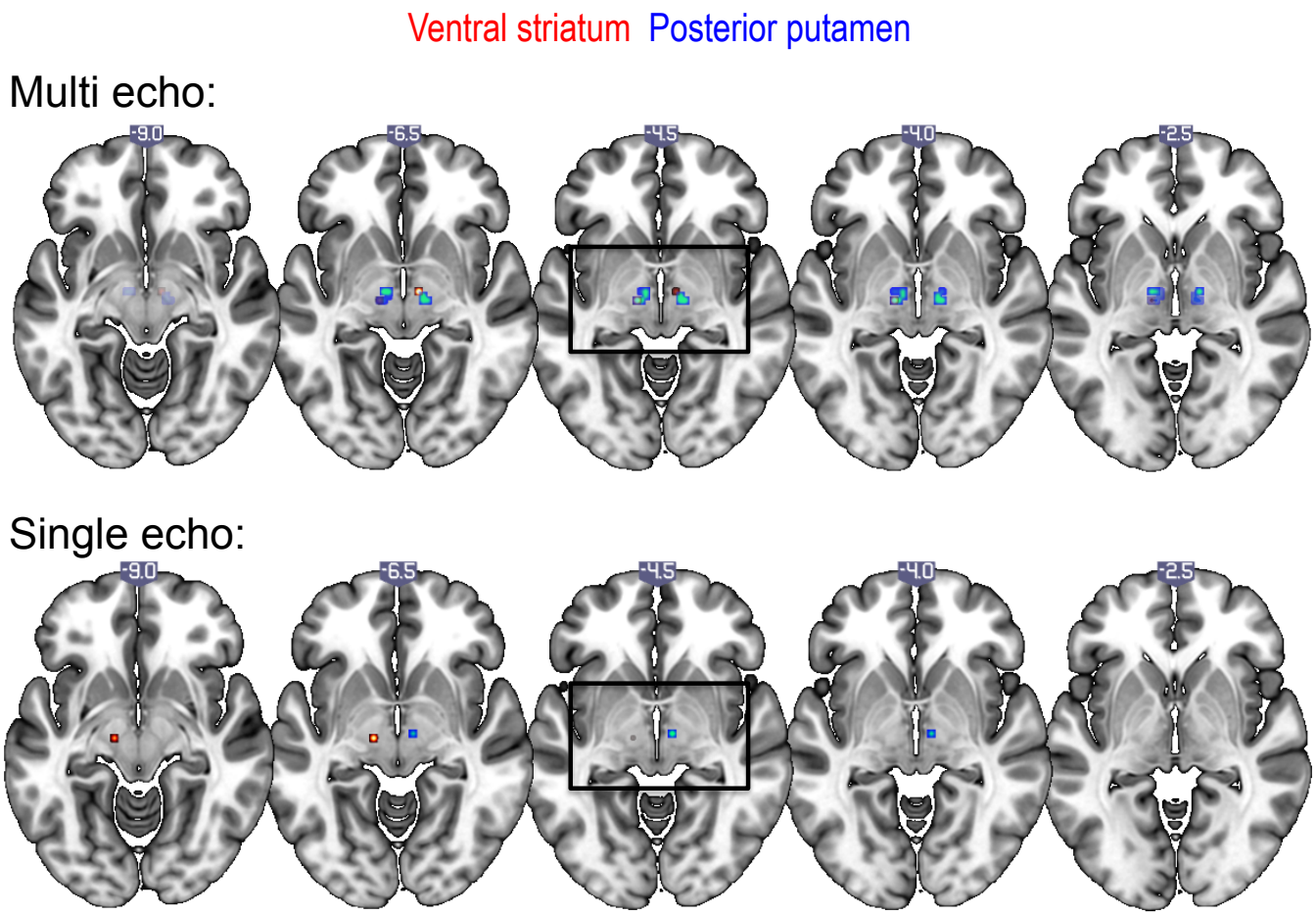

Figure 1.5. Comparison between multi-echo and traditional single-echo analyses. *Resting state functional connectivity of ventral striatal (red) and posterior putamen (blue) seed regions with STN is demonstrated for both multi-echo acquisition and denoising and single echo acquisition and traditional motion correction (SVC FWE correction p<0.05 on a standard MNI template).*

Experiment 2: NODDI

Participant Characteristics

Data was acquired from 39 healthy volunteers (HV, 24 female; age 23.64, 3.88 SD; current/occasional smokers=1/3) and 29 binge-drinkers (BD, 12 female; age 23.10, 7.33 SD; current/occasional smokers, 5/3; days since last binge, 2.85, 1.89 SD). There were no signification group differences in age (p=0.697) or gender (p=0.102).

Binge-drinkers had significantly higher 'binge score', AUDIT score and had significantly more days that they were 'drunk' and percentage that they would drink in order to get drunk in the last 12 months (Table 1.2). Binge-drinkers also had higher total UPPS total scores (Table 1.2). The two groups did not significantly differ in depressive symptoms (BD, 9.636 (8.370 SD); HV, 6.973 (7.407 SD); p=0.208). Group differences are further explored later in this thesis. The current section aims to simply demonstrate the employed neuroimaging methods.

	Mean	SD	*p*
Gender (F \ M)	24 \ 14		0.102
	11 \ 17		
Age	23.69	3.85	0.697
	22.03	4.47	
BDI	6.973	7.407	0.208
	9.636	8.37	
AUDIT	4.333	3.119	<0.001
	16.75	4.529	
Binge score	7.545	6.035	<0.001
	33.376	15.371	
Percent Drunk	0.112	0.224	<0.001
	0.47	0.291	
Amount drunk	1.5	3.121	<0.001
	15.889	14.175	
UPPS total	127.5	16.246	0.004
	141.091	16.622	

Table 1.2. Demographic data. *Data is presented for 38 healthy volunteers and 28 binge drinkers. Abbreviations: HV, healthy volunteers; BD, binge drinkers; F/M, Female/Male; BDI, Beck Depression Inventory; AUDIT, Alcohol Use Disorders Test; UPPS, urgency, premeditation, perseverance, sensation seeking, and positive urgency impulsive behavior scale; SD, standard deviation; p, independent samples t-test p value.*

Microstructure

Figure's 1.6 – 1.8 demonstrates the normalised NODDI microstructure parameter maps for a single healthy individual. Orientation dispersion index was highest in grey matter

regions, both cortically and subcortically and lowest in regions of coherent fibre bundles, like corpus callosum (Figure 1.6). Neurite density maps had the opposite pattern, with higher neurite density in corpus callosum (Figure 1.7). The isotropic parameter was highest in the ventricles as expected (Figure 1.8).

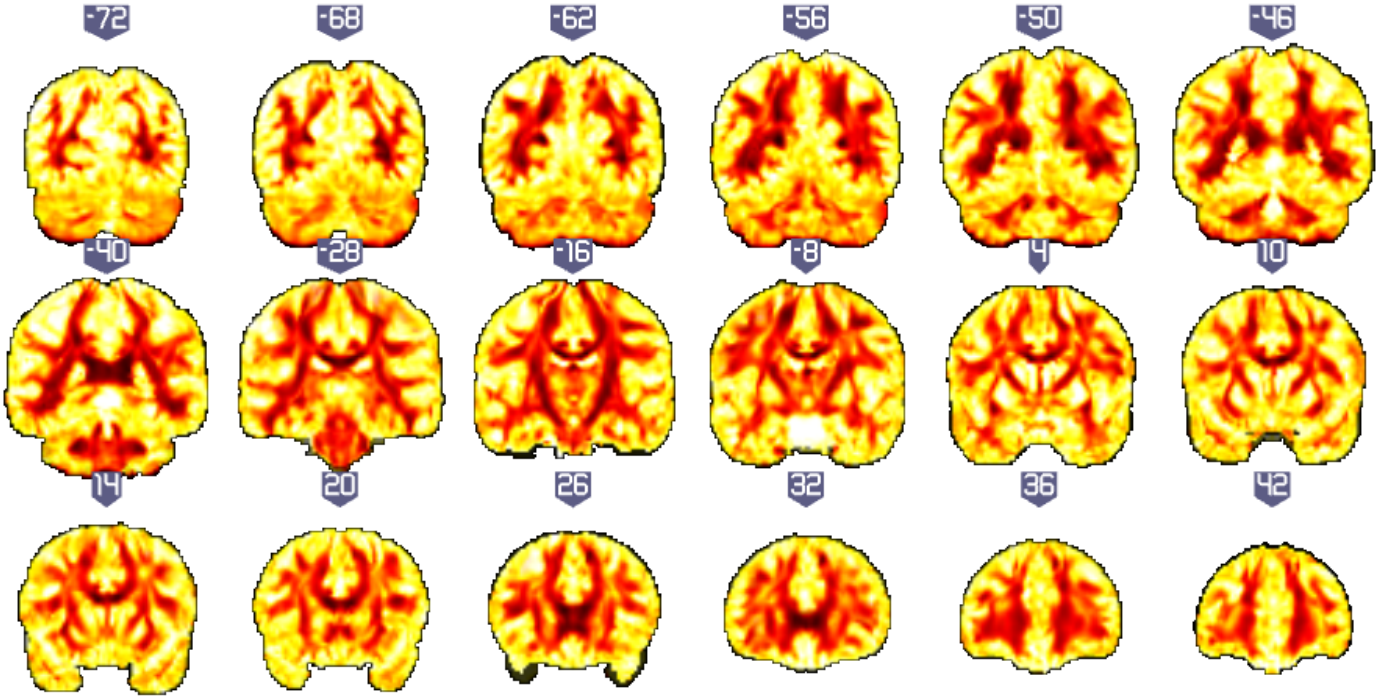

Figure 1.6. Orientation Dispersion Index. *This measure was highest (white-yellow) in grey matter and lowest (dark red) in regions of coherent fibre bundles, like corpus callosum. Data is demonstrated for a single healthy subject for illustration purposes.*

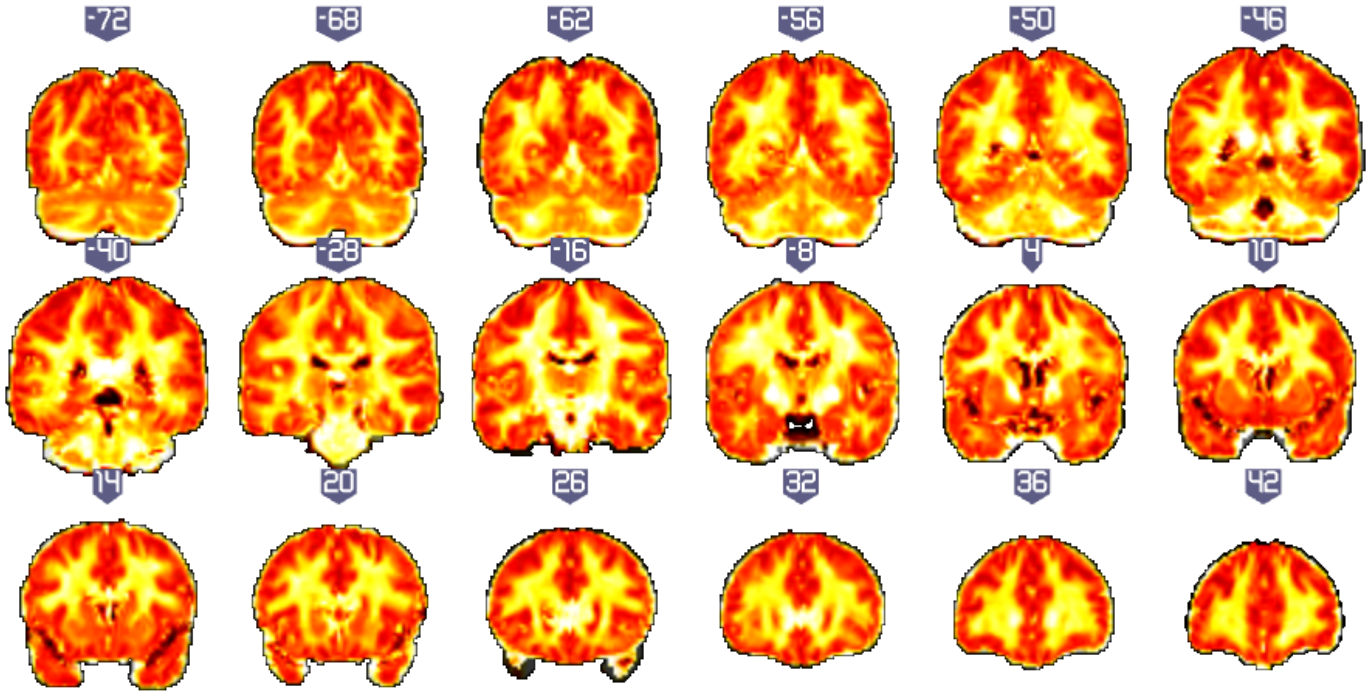

Figure 1.7. Neurite Density. *This measure arises as a product of the relationship between the intraceullar and extracellular compartments. Neurite density values are highest in corpus callosum. Data is illustrated for a single healthy subject.*

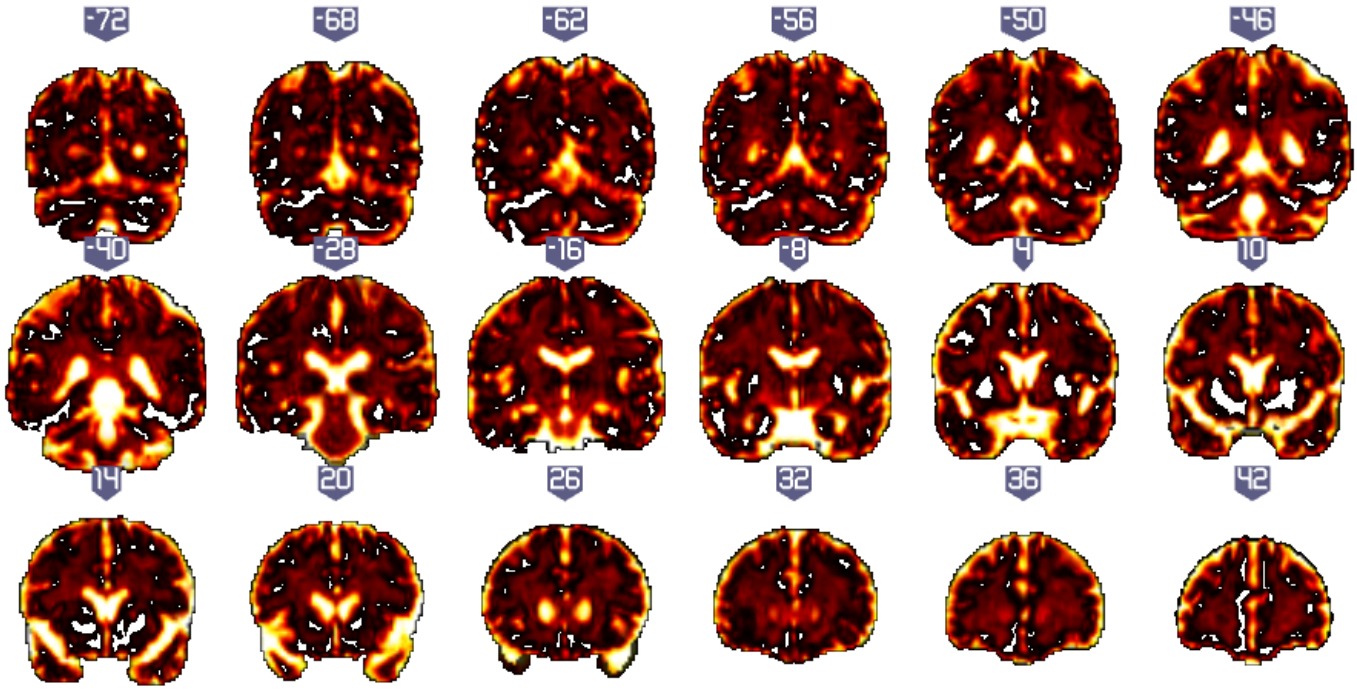

Figure 1.8. Isotropic Volume Fraction: Cerebrospinal Fluid. *Data is demonstrated for a single healthy subject.*

Tractography

Figure's 1.9 – 1.11 illustrate the tracts emerging from the bilateral STN seed to the whole brain. Fibre tracts from the STN reached key regions involved in motor preparation, planning and stopping, including up towards right lateral frontal cortex and pre-supplementary motor area, and through the motor mid cingulate cortex and premtoro cortex. Additional axial and coronal sections of the same data are displayed in Figure 1.11.

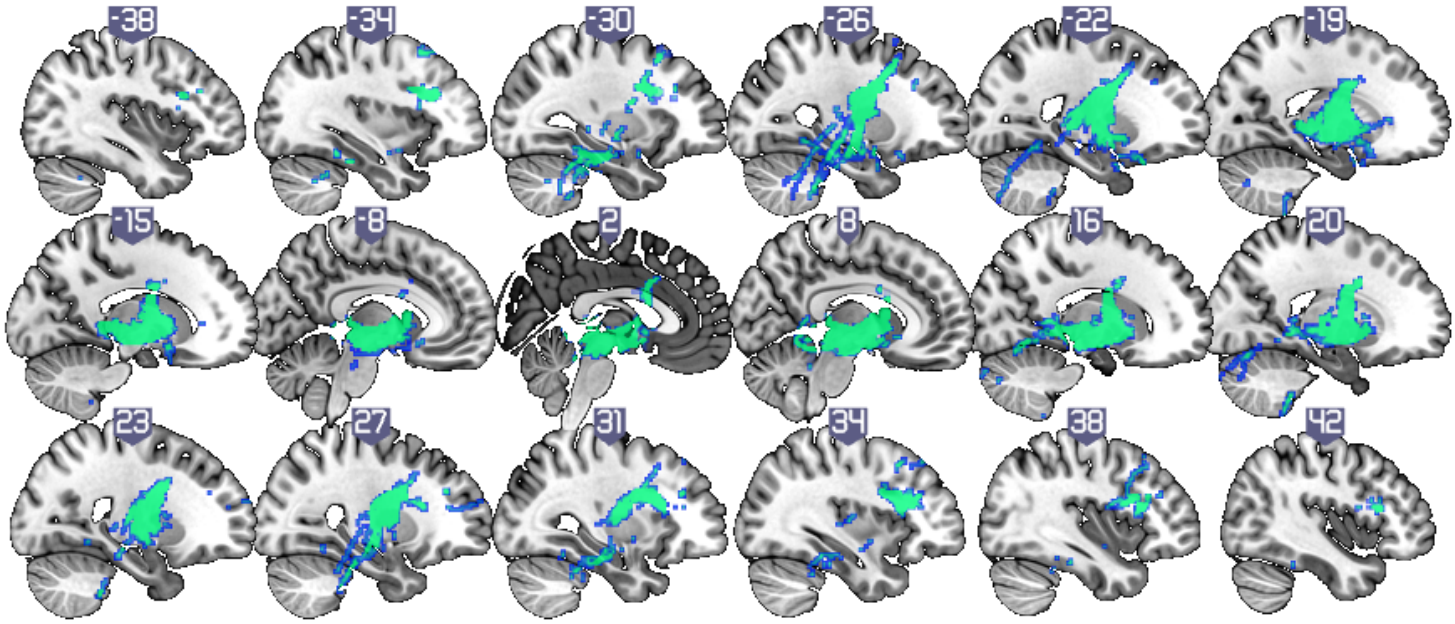

Figure 1.9. Bilateral Subthalamic Nucleus Tracts. *Fibre tracts are illustrated from bilateral STN, in a group of healthy volunteers and binge drinkers (N=68). Demonstrated on a standard MNI template.*

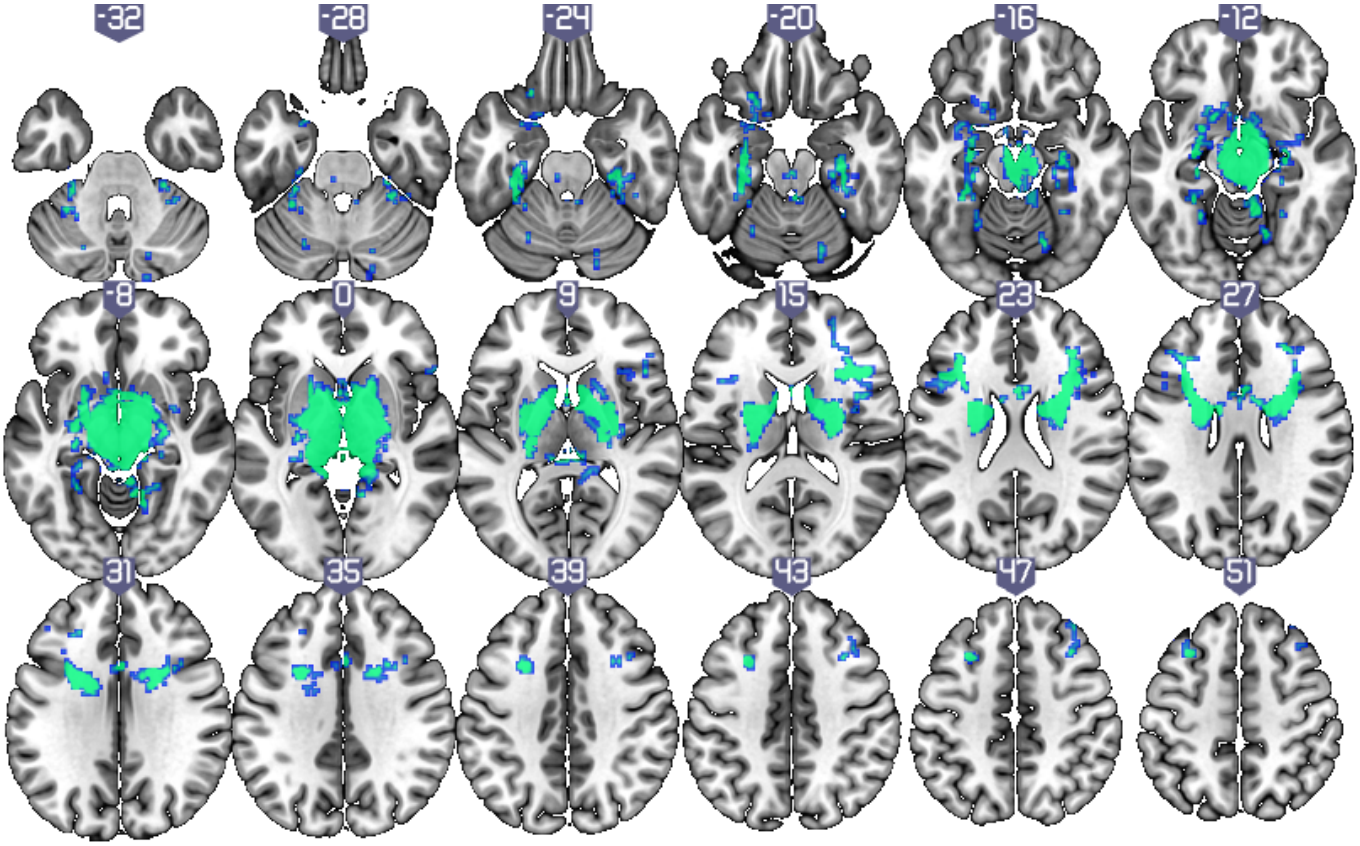

Figure 1.10. Bilateral Subthalamic Nucleus Tracts: Axial. *Lateralization of STN tracts is illustrated. A tendency towards STN fibre tracts reaching right (moreso than left) lateral frontal cortex is suggested. Data is from a group of healthy volunteers and binge drinkers (N=68) and demonstrated on a standard MNI template.*

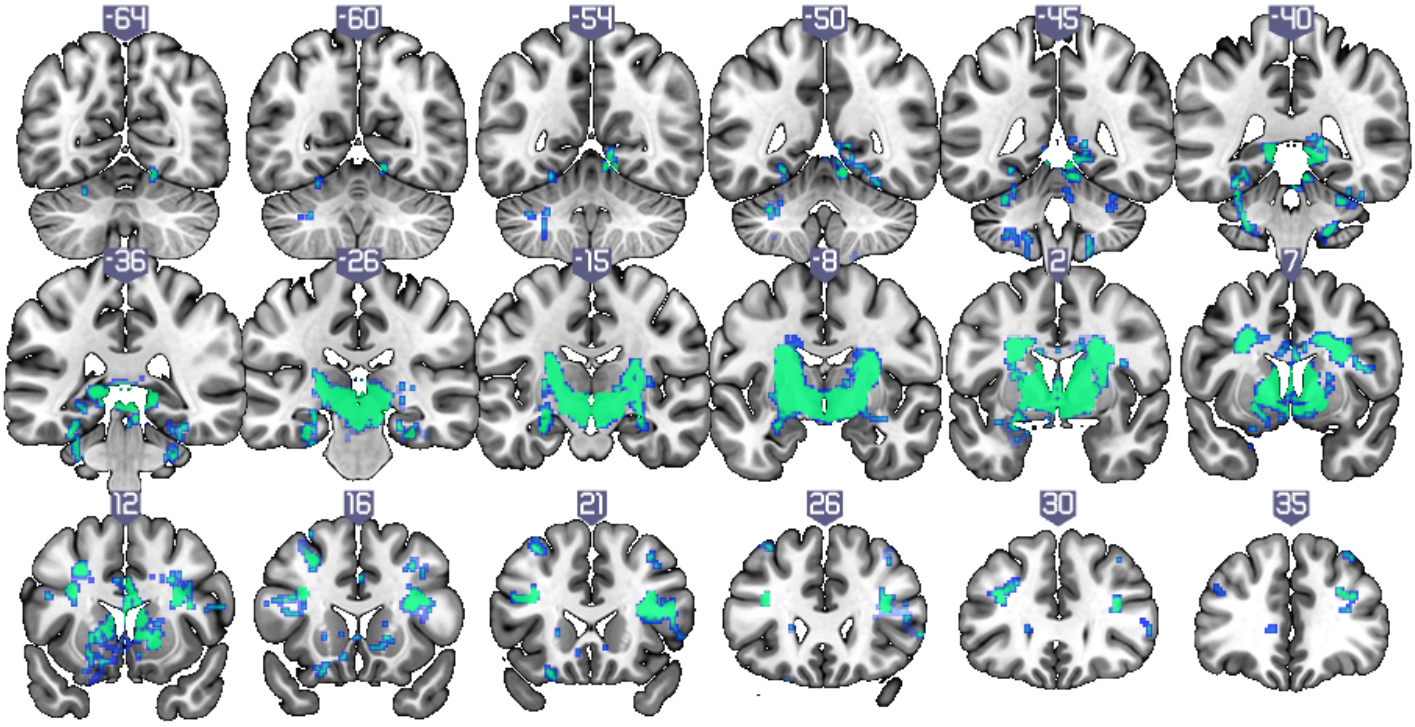

Figure 1.11. Bilateral Subthalamic Nucleus Tracts: Coronal. *A final demonstration of STN to whole brain tractography results. Data is from a group of healthy volunteers and binge drinkers (N=68) and demonstrated on a standard MNI template.*

Discussion

Multi-Echo rsfMRI

This study highlights the utility of multi-echo rsfMRI acquisition, analysis and denoising for the examination of subcortical structures that are spatially small and locations of signal drop-out. The findings replicate in humans, the tracing studies performed in non-human primate's showing prefrontal connectivity with a gradient of subregions of the STN[109]. In particular, this study demonstrates that by using resting state functional connectivity in a relatively large sample of healthy humans, it is possible to observe the most anterior medial limbic extent of the gradient and the posterior lateral motor gradient extent of the STN.

Ventral striatum and prefrontal associative regions (dlPFC (BA 9, 46) and dorsal ACC (BA 24)) showed greater connectivity with more anterior STN. However, SMA (caudal BA 6), putamen and M1 had greater connectivity with posterior STN. In contrast, the nodes of the 'stopping' network were more difficult to localize, with pre-SMA (rostro-medial BA 6) having connectivity peaks across both anterior and posterior STN, consistent with rostral BA 6 projections in the non-human primate occurring more caudally than prefrontal projections but overlapping with dlPFC (BA46) projections. Projections from the right IFC were not shown in the primate study.

The STN receives direct anatomical projections from dorsal ACC in the medial limbic tip region and the OFC converges with the ventromedial prefrontal cortex in its projections to adjacent lateral hypothalamus[109]. Interestingly, the current findings demonstrate that ventral striatum and dorsolateral prefrontal cortex (rather than ventromedial prefrontal cortex) has the strongest functional connectivity with the medial STN. The dorsal ACC however showed widespread connectivity with STN, without a local isolated anatomical cluster. Together this converges with suggestions that the STN integrates sensory and contextual information from these diffuse cortical regions to mediate decision thresholds[109] and slow or stop behaviour when behavioural adjustments are required [50, 109], mechanisms that are crucial for flexible and adaptive learning and behaviour.

The statistical power of the multi-echo technique is also demonstrated. While a smaller sample size was not able to replicate the ventral striatum and STN functional connectivity, connectivity between posterior putamen and STN was preserved. However, single echo data and traditional denoising by motion parameter regression examined in the same subjects revealed a loss of significant functional connectivity between putamen and STN. This analysis was exploratory and while the current study did not compute a power analysis of the difference in statistical power between multi and single echo acquisition and analysis, a previous study has demonstrated a four-fold increased in signal to noise ratio when using multi compared to single echo[426].

NODDI

This study demonstrates that the NODDI acquisition and analysis can be used to examine microstructural features in vivo, including neurite density and orientation dispersion index. Neurite density was highest in regions of coherent fibre bundles, including corpus callosum and cerebellar white matter bundles. Orientation dispersion index was highest in grey matter, including both cortical and subcortical grey matter.

This measure of orientation dispersion index details dendritic complexity and has previously been associated with age[435] and the hierarchy of neural computations[434]. Also, hetero-modal cortical regions required for higher level processing of information show more complex dendrite and spine features than primary and uni-modal cortical regions[434]. These associations are in line with the current demonstration of higher orientation dispersion index in higher order cortical regions. Indeed, the neurite complexity captured by the orientation dispersion index is consistent with both Golgi staining of dendritic processes[432] and microscopic detailing of grey matter dendritic architecture[433].

The diffusion MRI data collected was also used to compute anatomical white matter tracts from the STN. The STN was chosen as a small subcortical structure of interest within the cortical – basal ganglia circuitry, whose tracts and anatomical connectivity has not been extensively characterized in humans. The STN showed connectivity with primary and supplementary cortical motor regions, as well as to striatum, globus pallidus and thalamus. Connectivity with the lateral prefrontal cortex showed a tendency towards right lateralization. This is in line with demonstrations of a right-lateralized ‘stopping’ network that includes right IFC, pre-SMA and STN[121, 150].

In sum, the NODDI parameters provide a useful measure of microstructure in vivo, particularly orientation dispersion index, which probably has the most functional and behavioural relevance and which is not captured by other current diffusion or structural

measures. Traditional computations of tractography can also be performed using the NODDI data.

Chapter 2. Cortical – Basal Ganglia Circuits

The majority of our understanding of cortico – basal ganglia connectivity has come from non-human primate or rodent tracer studies[62, 75, 91] (see Introduction), with fewer representations demonstrated in humans. The utility of rsfMRI for mapping the fine-grained detail of connectivity patterns of small subcortical structures has been demonstrated for humans in this thesis (Chapter 1). The current section aims to examine the cortical – basal ganglia circuitry in its entirety using rsfMRI and assess the relationship between each segregated circuit and behavioural control.

In human studies, rsfMRI connectivity studies have used several methods to analyze cortical – basal ganglia circuitry. In one study, the striatum was split into six subregions and each was used as a seed for whole-brain functional connectivity analysis[456]. The inferior and superior ventral striatum showed functional connectivity with medial and lateral OFC respectively, the dorsal caudate was functionally connected with lateral PFC, and the putamen was connected with motor cortical regions[456]. The globus pallidus, substantia nigra and STN were excluded in this study and the findings were produced by the examination of striatal seed regions only. Another study examined the functional connectivity between subsections of the whole cortical surface and the striatum[457]. This revealed a seperation of a five-network parcellation of the striatum including motor, attention, fronto-parietal executive, default and limbic, as well as a somatomotor topolgical organisation of connectivity between striatum and somatomotor cortex[457]. A third study performed a clustering computation of striatal connectivity with the whole brain, to parcellate the striatum based on its cortical connectivity[458]. This revealed distinctions between dorsal caudate, putamen and ventral striatum, which were assocaited with cognitive, motor and affective cortical region connecitivity, respecitvely.

The aim of this Chapter is to extend these studies by developing cortical – basal ganglia connectivity maps that are based on carefully defined frontal seed regions that are defined based on function. Furthermore, functional connectivity is followed through the rest of the basal ganglia and thalamic circuit, to examine the entire pathway.

Methods

Participants

Healthy volunteers were recruited from community and University-based advertisements in the East Anglia region, United Kingdom. Participants were excluded if they had current major depression or other major psychiatric disorder, substance addiction or major medical illness or were taking psychotropic medications. Psychiatric disorders were screened with the Mini International Neuropsychiatric Interview[439]. Participants were compensated for their time and paid an additional amount depending on their performance. Written informed consent was obtained and the study was approved by the University of Cambridge Research Ethics Committee. Participants completed the Beck Depression Inventory to assess depressive symptoms. Of the 154 healthy volunteers from the baseline resting state study in Chapter 1, 66 healthy volunteers (33 male; mean age 40 (SD 13) years old; Beck Depression Inventory 8.6 (SD 8.4); verbal IQ 114.3 (SD 9.5)) were used for this study.

Resting State functional MRI Data Acquisition and Analysis

Cortical – Striatal Functional Connectivity

Acquisition parameters and seed definitions are described in Chapter 1. Intrinsic cortical – striatal connectivity was first examined by computing the functional

connectivity between each cortical seed and the striatum. For this, ROI-to-whole brain functional connectivity for each cortical seed region was computed and the observation of functional connectivity was restricted to the whole striatum, controlling for age. Statistics for whole brain corrected FWE $p<0.05$ corrected functional connectivity for striatal peak voxel's are reported in Table 2.1. Also, SVC FWE $p<0.05$ corrected statistics for different regions of the striatum (ventral striatum, caudate, anterior putamen and posterior putamen) (Table 2.2).

Exploratory analyses of gradient patterns through the striatum were performed for cortical regions of interest with heterogeneous striatal connectivity, namely dlpfc, pre-SMA and SMA. First, parameter estimates of connectivity for each frontal cortical seed with the striatum were computed at seven points along coronal slice 12 (see Figure 2.2) of the right striatum. Slice 12 was chosen from Figure 2.1 as it contained the most heterogeneity of cortical – striatal connectivity. The coordinates were chosen to be 5mm from the top of the caudate (point 1) and putamen (point 7), with approximately 8mm between each of the 7 points (point 1, xyz= 15, 12, 16; point 2, xyz=11, 12, 8; point 3, xyz=9, 12, 0; point 4, xyz=11, 12, -10; point 5, xyz=20, 12, -7; point 6, xyz= 23, 12, -2; point 7, xyz= 25, 12, 4). Thus, connectivity parameters were extracted from the following discrete striatal points: 1. Dorsal caudate; 2. Mid caudate; 3. Ventral caudate; 4. Ventral striatum; 5. Ventral putamen; 6. Mid putamen; 7. Dorsal putamen. Connectivity estimates for mid caudate (point 2), ventral striatum (point 4) and mid putamen (point 6) for named cortical regions of interest were entered into one-way ANOVA for statistical comparisons. See Figure 2.2 and Figure 2.3 for an illustration of their positioning.

A similar approach was taken to examine an anterior – posterior gradient of cortical connectivity within putamen. Five points were chosen 6mm apart along the putamen in axial plane 0 (Figure 2.4), with the most anterior position at xyz= 26, 18, 0 and posterior at xyz= 32, -6, 0 (point 1, xyz=26, 18, 0; point 2, xyz=25, 12, 0; point 3, xyz=28, 6, 0; point 4, xyz=31, 0, 0; point 5, xyz=32, -6, 0).

Connectivity estimates for anterior (point 1), mid (point 3) and posterior (point 5) putamen were entered into one-way ANOVA to compare between cortical connectivity strengths.

Basal Ganglia and Thalamic Functional Connectivity

For the mapping of connectivity patterns through the rest of the cortico – basal ganglia circuit, the three major striatal subregions were used as seeds and functional connectivity was computed for each seed with globus pallidum, substantia nigra and thalamus, using SVC FWE $p<0.05$. Functional connectivity with STN is reported in Chapter 1.

Results

Cortical – Striatal Functional Connectivity

Intrinsic cortical – basal ganglia organization was assessed by examining connectivity between carefully defined prefrontal functional regions and striatum and secondly, striatum with basal ganglia subregions and thalamus in the same healthy volunteers.

The findings demonstrate the segregation between the three separable circuits (limbic, associative, motor) based on functional connectivity between functionally defined prefrontal cortical regions and dissociable sub-regions of the striatum (Figures 2.1 – 2.3). There was predominant connectivity of ventral and mesial prefrontal cortical regions (medial and lateral OFC, vmpfc, subgenual ACC, dorsal ACC and dmpfc) with the ventral striatum; lateral prefrontal (dlpfc, IFC) with caudate; pre-SMA with anterior putamen; and SMA with posterior putamen. Statistics for functional connectivity are reported in Table 2.1 (whole brain FWE $p<0.05$ corrected) and Table 2.2 (small volume correction for striatal subregions).

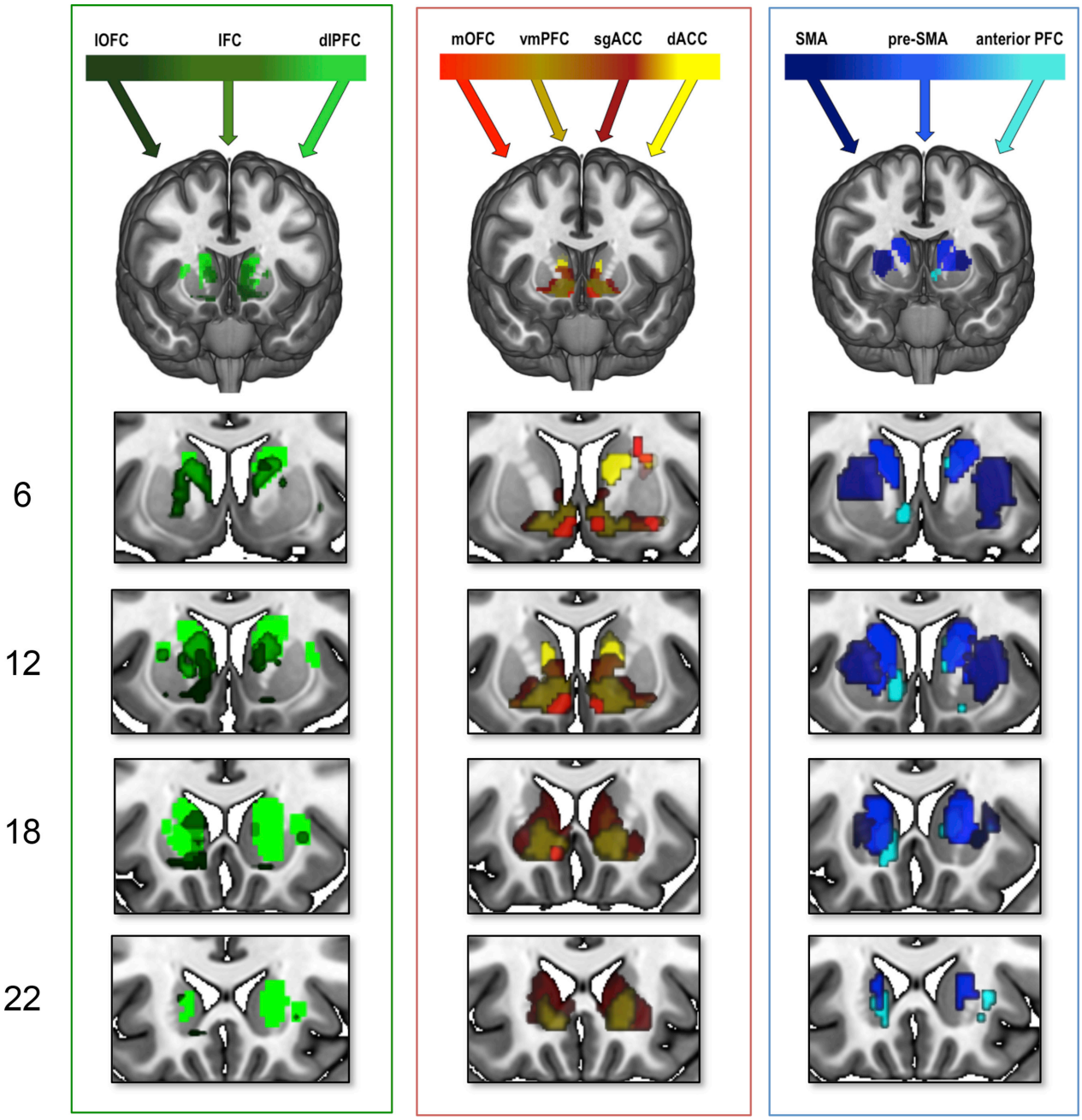

Figure 2.1. **Intrinsic fronto-striatal connectivity.** *Prefrontal seeds are illustrated (top) with striatal connectivity colour-coded to the prefrontal seeds. Several additional enlarged slices are included below each fronto-striatal connectivity map by coronal slice number along the y direction (left). The blood-oxygen-level dependent (BOLD) overlays are illustrated with a striatal mask at family wise error corrected p < .005 (medial orbitofrontal cortex shown at p < .05) for illustration purposes. Abbreviations: lFC: inferior frontal cortex, dlPFC: dorsolateral prefrontal cortex, lOFC: lateral orbitofrontal cortex, mOFC: medial orbitofrontal cortex, vmPFC: ventromedial prefrontal cortex, sgACC: subgenual*

cingulate, dACC: dorsal cingulate, SMA: supplementary motor area, pre-SMA: pre-supplementary motor area, anterior PFC: anterior prefrontal cortex.

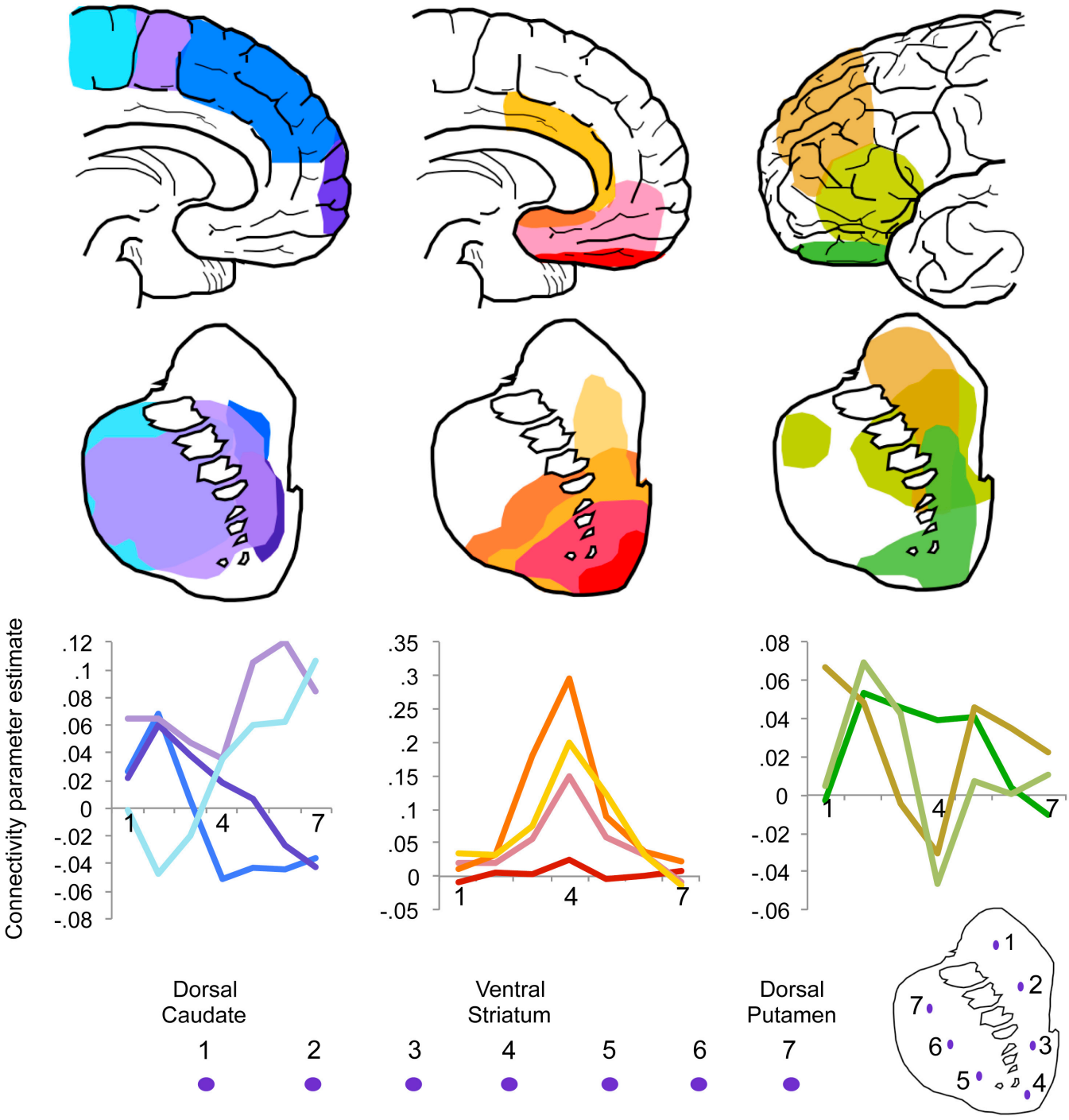

Figure 2.2. Schematic depiction of intrinsic fronto-striatal connectivity.
Top: schematic illustration of cortical seeds with regions of striatal connectivity for corresponding colour-coded cortical seeds below. For the purposes of

illustration and comparison, the maps were reproduced from images using a striatal mask set at a threshold of FWE corrected p < .005 (medial orbitofrontal cortex to ventral striatum (red) was based on a threshold of FWE corrected p < .05 and pre-supplementary motor area connectivity with putamen/caudate (light purple) was based on a threshold of FWE corrected p < .0001). Bottom: Parameter estimates of connectivity for each cortical seed are plotted in the same colour-coded system for 7 points along the striatum from dorsal caudate (point 1) to ventral striatum (point 4) to dorsal putamen (point 7).

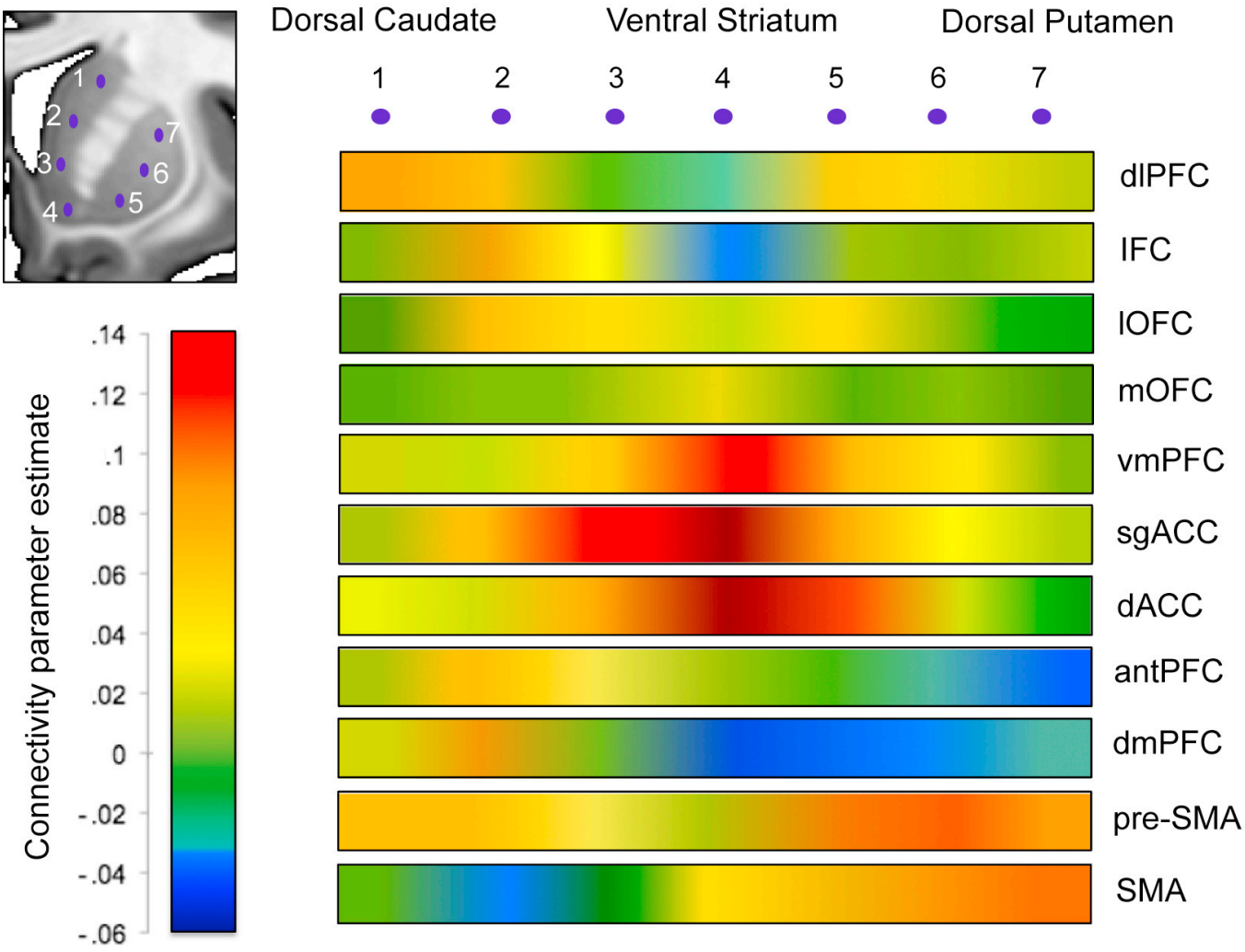

Figure 2.3. Fronto-striatal connectivity patterns as 'heat' maps. *Parameter estimates of connectivity for each cortical seed are illustrated as heat maps for 7 points along the right striatum from dorsal caudate (point 1) to ventral striatum (point 4) to dorsal putamen (point 7). Abbreviations: IFC: inferior frontal cortex, dlPFC: dorsolateral prefrontal cortex, lOFC: lateral orbitofrontal cortex, mOFC: medial orbitofrontal cortex, vmPFC: ventromedial prefrontal cortex, sgACC: subgenual cingulate, dACC: dorsal cingulate, SMA: supplementary motor area,*

pre-SMA: pre-supplementary motor area, antPFC: anterior prefrontal cortex; dmPFC, dorsomedial prefrontal cortex.

Seed	Striatal Peak Regions	Whole brain p(FWE-corr)	Z	x	y	z
dlpfc	Caudate	<0.001	5.61	31	19	0
vmpfc	Ventral striatum, cluster includes anterior cingulate cortex	<0.001	>8.0	-1	49	-7
SMA	Putamen, cluster includes pre-SMA, motor cortex, insula	<0.001	>8.0	3	-11	65
Pre-SMA	Putamen, cluster includes caudate and ventral striatum	<0.001	>8.0	-41	14	0
antrPFC	Caudate	0.024	4.97	13	17	4
IFC	Caudate	0.001	5.66	-13	10	4
sgACC	Ventral striatum, cluster extends to vmPFC, caudate and amygdala	<0.001	>8.0	-3	17	-7
dACC	Ventral striatum, cluster includes caudate, vmPFC	<0.001	>8.0	-1	35	-5

Table 2.1. **Prefrontal intrinsic resting state connectivity with striatum**. *Abbreviations: dlpfc, dorsolateral prefrontal cortex; vmpfc, ventromedial prefrontal cortex; SMA, supplementary motor area; pre-SMA, pre-supplementary motor area; antrPFC, anterior prefrontal cortex; IFC, inferior frontal cortex; sgACC, subgenual anterior cingulate cortex; dACC, dorsal anterior cingulate cortex; p(FWE-corr), whole brain (P<0.05) family-wise error P value; Z, Z-score; xyz, peak voxel coordinates.*

.

Seed	ROI	SVC p(FWE-corr)	Z	x	y	z
dlPFC	Dorsal Caudate	0.001	4.47	15	12	11
	Ventral Striatum	0.005	4.16	-13	17	0
	Anterior Putamen	ns				
	Posterior Putamen	ns				
vmPFC	Ventral Striatum	<0.001	6.64	-6	12	-10
	Anterior Putamen	0.006	4.05	-13	5	-12
	Dorsal Caudate	ns				
	Posterior Putamen	ns				
SMA	Posterior Putamen	<0.001	>8.0	-38	3	7
	Anterior Putamen	<0.001	7.01	27	0	9
	Ventral Striatum	0.019	3.8	-22	10	-3
	Dorsal Caudate	ns				
preSMA	Anterior Putamen	<0.001	7.54	17	12	4
	Posterior Putamen	<0.001	6.79	-34	7	7
	Ventral Striatum	<0.001	6.72	-13	10	0
	Dorsal Caudate	<0.001	6.26	15	10	11
mOFC	Ventral Striatum	0.001	4.55	6	12	-17
	Anterior Putamen	ns				
	Posterior Putamen	ns				
	Dorsal Caudate	ns				
lOFC	Ventral Striatum	<0.001	7.52	15	14	-17
	Dorsal Caudate	<0.001	5.37	-27	12	-14
	Anterior Putamen	ns				
	Posterior Putamen	ns				
antrPFC	Ventral Striatum	<0.001	5.04	-10	17	0
	Dorsal Caudate	<0.001	4.17	13	14	9
	Anterior Putamen	ns				
	Posterior Putamen	ns				
dmPFC	Ventral Striatum	0.001	4.66	-24	17	-14
	Dorsal Caudate	0.045	3.86	-13	14	9
	Anterior Putamen	ns				
	Posterior Putamen	ns				
lFC	Dorsal Caudate	<0.001	6.95	-27	21	0
	Posterior putamen	<0.001	6.06	-38	0	2
	Ventral Striatum	<0.001	5.59	-10	10	2
	Anterior Putamen	<0.001	5.17	15	7	4
sgACC	Ventral Striatum	<0.001	>8.0	3	21	-5
	Anterior Putamen	<0.001	7.42	-13	7	-12
	Dorsal Caudate	0.005	4	-10	21	9
	Posterior putamen	ns				
dACC	Ventral Striatum	<0.001	>8.0	8	24	-7
	Anterior Putamen	<0.001	>8.0	-13	7	-12
	Dorsal Caudate	0.009	3.82	13	14	18
	Posterior putamen	ns				

Table 2.2. *Prefrontal intrinsic resting state connectivity with striatal subregions. Reported as small volume family wise error corrected. Abbreviations: dlPFC, dorsolateral prefrontal cortex; vmPFC, ventromedial prefrontal cortex; SMA, supplementary motor area; preSMA, pre- supplementary motor area; mOFC, medial orbitofrontal cortex; lOFC, lateral orbitofrontal cortex; antrPFC, anterior prefrontal cortex; dmPFC, dorsomedial prefrontal cortex; IFC, inferior frontal cortex; sgACC, subgenual anterior cingulate cortex; dACC, dorsal anterior cingulate cortex; SVC p(FWE-corr), small volume corrected (P<0.05) family-wise error P value; Z, Z-score; xyz, peak voxel coordinates.*

Gradient patterns of connectivity through the striatum were examined for all cortical regions. Parameter estimates of connectivity were extracted from 7 points along striatum from dorsal caudate (point 1) to ventral striatum (point 4) to dorsal putamen (point 7) (Figure 2.2). Vmpfc and ACC showed similar patterns of connectivity, with peaks in ventral striatum. Regions of heterogeneous function had varied patterns of gradiented connectivity: connectivity of dlpfc, pre-SMA and SMA, as determined with one-way ANOVA, was significantly different for mid caudate (point 2, $F_{(2,188)}$= 7.660, p=0.001), ventral striatum (point 4, $F_{(2,188)}$= 4.344, p=0.014), and mid putamen (point 6, $F_{(2,188)}$= 4.001, p=0.020). Tukey post-hoc comparisons revealed that for mid caudate, connectivity for SMA was significantly lower than pre-SMA (p=0.001) and dlPFC (p=0.009). For ventral striatum, connectivity of dlPFC was lower than of pre-SMA (p=0.029) and SMA (p=0.027). For mid putamen, connectivity of pre-SMA was significantly higher than dlpfc (p=0.019).

An anterior – posterior gradient of cortical connectivity within putamen was also examined for dlpfc, pre-SMA and SMA, which all showed relatively high putaminal connectivity (Figures 2.1 – 2.3). As expected, SMA had increasing connectivity estimates with more posterior regions of the putamen, whereas pre-SMA and dlPFC had the opposite pattern (Figure 2.4). Connectivity of these cortical regions, determined with one-way ANOVA, was significantly different for anterior (point 1, $F_{(2,185)}$= 5.991, p=0.003), and posterior putamen (point 5, $F_{(2,185)}$= 7.541, p=0.001), but not mid putamen (point 3, $F_{(2,185)}$= 2.781, p=0.065).

Post-hoc Tukey test demonstrated that for the anterior putamen, the pre-SMA had higher connectivity compared to both SMA (p=0.003) and dlPFC (p=0.049), and for posterior putamen, the SMA had higher connectivity compared to both pre-SMA (p=0.013) and dlPFC (p=0.001).

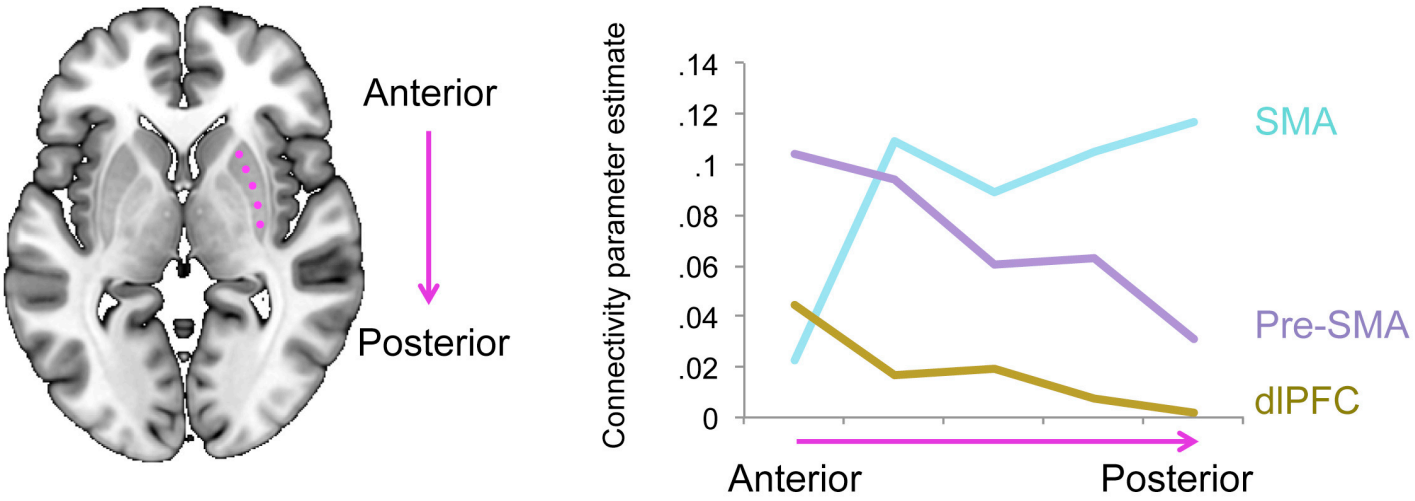

Figure 2.4. An anterior – posterior gradient of connectivity along the putamen. *Parameter estimates of connectivity for supplementary motor area (SMA), pre-supplementary motor area (pre-SMA) and dorsolateral prefrontal cortex (dlPFC) are plotted for 5 points along an anterior – posterior axis of the right putamen.*

Basal Ganglia and Thalamic Functional Connectivity

Figure 2.5 reiterates the cortical – striatal connectivity for the vmpfc with ventral striatum (red), dlpfc with caudate (yellow) and SMA with putamen (blue), representing limbic, cognitive and motor circuits respectively. Seeds were placed in ventral striatum, dorsal caudate and posterior putamen to further examine dissociations of intrinsic connectivity downstream in the cortical – basal ganglia circuitry, focusing on the globus pallidus interna, the globus pallidus externa, thalamus and substantia nigra (STN is reported earlier).

Striatal seeds were dissociable in connectivity to globus pallidus interna and externa: ventral striatal connectivity was predominantly to ventral pallidum whereas posterior putamen was predominantly to the motor posterodorsal pallidum and dorsal caudate was predominantly functionally connected to anterodorsal pallidum (Figure 2.5, Table 2.3). Also reflecting functionally relevant segregations, both posterior putaminal and dorsal caudate seeds were correlated with bilateral lateral substantia nigra and the ventral striatal seed was correlated with right mesial midbrain compatible with the ventral tegmental area. Finally, while the ventral striatum was functionally connected with the mediodorsal nucleus of the thalamus (associated with emotional, limbic processing), the posterior putamen showed connectivity with ventrolateral regions of the thalamus (associated with motor and somatomotor function). Connectivity between striatal subregions and STN is reported earlier and follows a similar dissociation of ventral striatal connectivity with mesial limbic and putaminal connectivity with motor lateral subthalamic nucleus.

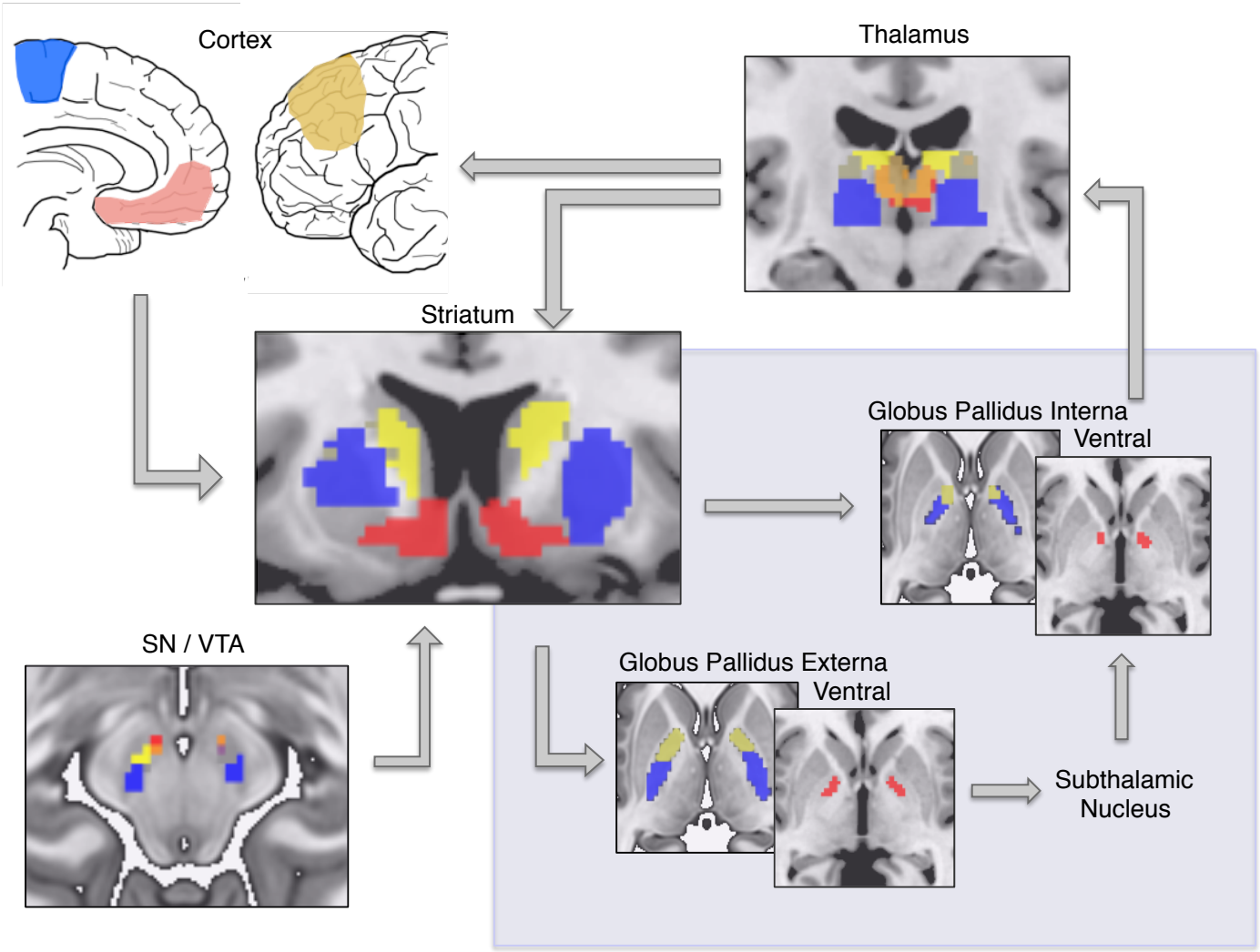

Figure 2.5. Cortico – basal ganglia – thalamic circuitry. *Connectivity of the ventromedial prefrontal cortex (red), dorsolateral prefrontal cortex (yellow) and supplementary motor are (blue) with the ventral striatum, caudate and putamen, respectively is recapitulated. Seeds in ventral striatum, posterior putamen and dorsal caudate subsequently demonstrated distinct connectivity with globus pallidus interna and externa, substantia nigra/ventral tegmental area (SN/VTA) and thalamus. The blood-oxygen-level dependent (BOLD) overlays are shown using basal ganglia subregion and thalamus masks at family wise error corrected $p < .005$ for illustration purposes. See Supplementary Table 2 for statistics.*

Seed	ROI	SVC p(FWE-corr)	Z	x	y	z
Posterior Putamen	Thalamus	<0.001	>8	22	-20	11
	Gpe	<0.001	>8	24	-7	2
	Gpi	<0.001	7.31	-13	0	2
	SN / VTA	<0.001	5.79	15	-18	-7
	STN*	<0.001	6.29	13	-16	-5
Ventral Striatum	Thalamus	<0.001	7.72	-3	-9	7
	Gpe	<0.001	>8	13	7	-5
	Gpi	<0.001	>8	-10	3	-5
	SN / VTA	0.049	2.84	6	-11	-14
	STN*	0.035	2.72	8	-11	-5
Dorsal Caudate	Thalamus	<0.001	>8	15	-9	16
	Gpe	<0.001	>8	-13	3	7
	Gpi	<0.001	>8	-10	3	2
	SN / VTA	0.047	2.48	13	-20	-12
	STN	ns				

Table 2.3. **Striatal connectivity with basal ganglia subregions and thalamus.** *Reported as small volume family wise error corrected. Abbreviations: GPe, globus pallidum externa; GPi, globus pallidum interna; SN / VTA, substania nigra / ventral tegmental area; STN, subthalamic nucleus; * previously reported; ns, not significant; SVC p(FWE-corr), small volume corrected (P<0.05) family-wise error P value; Z, Z-score; xyz, peak voxel coordinates.*

Discussion

These studies defined and demonstrated the three majorly segregated cortical – basal ganglia circuits based on intrinsic functional connectivity. This expands on previous resting state connectivity parcellation studies[456-458] by using a novel multi-echo acquisition and analysis[427], focusing on carefully defined prefrontal seed regions parcellated based on function and elucidating the pathway of the entire cortical – basal ganglia system.

These findings demonstrate dissociable intrinsic frontal – striatal connectivity with predominant connectivity between ventral and medial prefrontal regions with

ventral striatum, lateral prefrontal regions with caudate, pre-SMA with anterior putamen and SMA with posterior putamen. We further demonstrate opposing gradient patterns of connectivity for SMA and pre-SMA along an anterior – posterior axis of the putamen. Regions implicated in multiple functions have connectivity across multiple striatal subregions (e.g. pre-SMA and IFC show connectivity with all striatal subregions; subgenual and dorsal cingulate show connectivity with all subregions except posterior putamen) but limbic vmpfc and ACC regions maintain clear preference for connectivity with ventral striatum over caudate and putamen. Similarly downstream, limbic, cognitive and motor connectivity respected a mesial-lateral division of the substantia nigra / ventral tegmental area and ventral – dorsal and anterior – posterior division of the globus pallidus: motor and cognitive striatal regions connected to dorsal pallidum and limbic regions to ventral pallidum. In the thalamus, the ventral striatum was functionally connected with the mediodorsal nucleus, which, along with additional inputs from ventral pallidum and amygdala, mediates limbic processes. On the other hand, the posterior putamen connected with the ventral lateral and ventral anterior nuclei, which, via connections with cerebellum and cortical motor areas, are involved with motor feedback and planning, respectively[455, 459].

An issue with this analysis is that it assumes that there are three unique, distinct and separable circuits passing through the cortical – basal ganglia circuitry. While this is sometimes a useful framework to use to understand functional connectivity and networks, it is not entirely accurate. Previous studies have suggested there are five or even seven separable circuits [1, 68, 69] but importantly, they may not be distinct and in fact include much convergence and overlap. Choosing three sub-circuits segregates the circuits into the expected distinct functions of motor, limbic and cognitive processing [71-74]. This is a simple and powerful way of examining the whole circuit as it relates to broad behavioural and cognitive functions (as motor is different from cognitive which can be separated from limbic etc.). However, with finer techniques, the examination of overlap, convergence, divergence and specificity of circuits must be considered. The simplicity of a three-circuit model employed in the current

method therefore overlooks much information in the circuit that must be addressed. For example, examining connectivity from the ventromedial prefrontal areas with striatum demonstrates an interesting gradient pattern of connectivity in which more ventral PFC regions are connectivity with the most ventral striatum and as you move dorsally up the medial PFC wall, the connectivity pattern with striatum becomes more dispersed such that the anterior cingulate cortex has a wider spread of connectivity throughout the ventral striatum up towards dorsal striatum. Examining the functional relevance of this spread and comparing it to the functional relevance of the more specific connectivity pattern of the medial OFC would be an important focus for future studies. Furthermore, how the ACC connectivity with mid caudate differs in functional relevance from connectivity of lateral PFC regions with mid caudate, should also be examined more closely. However, this is a fair starting point for the examination broad delineations within the cortical – basal ganglia circuitry based on function.

While these studies demonstrate distinct gradients of connectivity throughout the striatum, the methods focus on a finite number of points within the striatum with which to assess 'gradients'. Indeed the entire striatum was not examined and only seven points along its dorsal-ventral axis and five points along the anterior-posterior axis of the putamen were examined. These points were somewhat arbitrary and methods that map gradients of connectivity throughout the entire striatum are warranted. Nevertheless, this simplification of specific points does highlight an interesting and somewhat expect pattern of cortical connectivity.

These results take forward previous evidence of cortical – basal ganglia circuit organization by demonstrating the ability of resting state functional MRI methods to measure their properties. By examining circuit or connectivity strength or patterns in healthy humans, the ground can be laid for understanding disturbed circuit dynamics in disordered populations.

Chapter 3. Cortical – Basal Ganglia Circuits and Behaviour

The functional relevance of the cortico – basal ganglia circuits was further examined by assessing the relationship between latent connectivity and cognitive and behavioural measures. This Chapter is split into three broad experiments: examining the neural correlates of impulsivity, compulsivity and specifically focusing on the STN in an exploratory manner.

Resting state neural properties were examined rather than task-based for several reasons. Firstly, understanding the resting and latent neural network provides insight into the default or intrinsic function of the network as a whole- without perturbation by cognition, which may differ on an interindividual basis. As such, two levels of interindividual variability are possible: variability within the intrinsic network itself; and variability in the way in which that network is recruited during task. This distinction certainly requires further exploration and delineation. However, understanding the baseline characteristics of neural networks is key, before any network recruitment by task demand. Furthermore, resting state fMRI data is quicker and easier to collect compared to task fMRI- features that are crucial in clinical settings. As the current studies are of relevance to clinicians interested in STN deep brain stimulation, we use a tool that is accessible to clinical work. This technique can therefore be expanded to other areas of clinical interest, for example for pre-surgical mapping studies based on behavioural or cognitive faculties of particular importance.

Impulsivity

First, impulsivity is examined in relation to the functional connectivity of the cortico – basal ganglia circuitry. Waiting impulsivity or premature responding is examined, a behaviour that has been extensively studied and characterized in rodents[173, 182, 183] but not humans. Lesion studies in rodents have implicated the nucleus accumbens (or human ventral

striatum), infralimbic cortex (equivalent to the human subgenual ACC) and STN in premature responding or waiting impulsivity. Lesions of the nucleus accumbens attenuate amphetamine-induced increases in premature responding[174] and highly impulsive rodents have lower dopamine D2/3 nucleus accumbens receptor availability[175] and lower left grey matter density in the nucleus accumbens core[176]. Furthermore, lesions of the rodent infralimbic cortex and the STN also enhance premature responding[177-180]. However, the neural network underlying this behaviour in humans is yet to be elucidated. The aim of this first experiment therefore was to characterize the underlying neural correlates of waiting impulsivity in healthy humans, using rsfMRI. The cortico – basal ganglia network is also examined using another measure of impulsivity, motor impulsivity, as measured by the SSRT. Studies on stopping behaviours implicate a distinct network from waiting, suggesting the hyperdirect connections to the STN from the pre-SMA and right IFC, as well as the indirect pathway output of the dorsomedial striatum (caudate)[128, 460, 461].

Compulsivity

Secondly, the relationships between circuit connectivity and behavioural control is examined, as measured by multiple tasks that assess model based goal-directed and model free habitual behaviors; attentional set shifting; and cognitive-behavioural flexibility in the form of reversal learning for both reward and loss. As the anatomical correlates of model-based behavior are well-characterized[191, 391] model-based learning is expected to be associated with higher medial OFC and ventral striatal connectivity and on an exploratory basis, model-free behavior is expected to be associated with connectivity of the motoric circuit including SMA and putamen. Probabilistic reversal learning and attentional set shifting are additionally assessed and as both processes have evidenced dissociability of frontal cortical involvement, the expectation is that lateral OFC is associated with reversal[392] whereas the dlpfc and the associative circuit is associated with attentional shifting[25, 267, 392].

Subthalamic Nucleus

The STN directly receives afferents from cortical regions involved in diverse functions[109], including executive control, motor control and limbic functioning. This allows hyperdirect control of basal ganglia output based on frontal innervations. Therefore, the positioning of the STN within the cortico – basal ganglia circuitry allows it to mediate cognitive or behavioural programs that are processed through this circuitry, whether they are motor, associative or limbic (discussed by [109]).

In the third experiment, the STN's functional connectivity is examined in relation to measures of behavioural control. While the cognitive constructs of impulsivity and compulsivity have been widely studied in terms of the cortico – basal ganglia circuitry, there has been less specific focus on the STN, even though it maintains a crucial position within this system.

STN and Compulsivity

The parallel, interactive and dissociable measures of behavioural control that distinguishes model-free compulsive behaviour from model-based goal-directed behaviour is first examined. Briefly, a fast, reactive and model-free system relies on habitual learning in which previously reinforced behaviours are repeated (compulsive) is dissociable from a slower, deliberative model-based system for more flexible goal-directed behavior that takes into account the task-structure or internalized task model. The model-based system implicates the ventral striatum[191, 462], the medial OFC[462] and the dlpfc[391]. The model-free system implicates the putamen and premotor cortex[463] and the SMA. This section aims to elucidate the role of the STN within these networks and its relationship with these behavioural measures. Compulsivity is secondly examined in the form of perseveration, which involves repetition of behaviour irrespective of the outcome (distinct from habitual behaviours, which are defined as repeated choices of previously reinforced behaviours and are hence outcome sensitive). The neural correlates of perseverative behaviours are currently unclear.

STN Subzones and Impulsivity

The implications of STN in behavioural control is then taken a step further by specifically examining anterior and posterior portions of the STN, thought to reflect more limbic and motor processing, respectively, with a measure that is relevant to the limbic-associative portion of the STN. Decisional reflection impulsivity, as measured by the Beads task is used for this analysis. Briefly, this measures the extent of evidence accumulation during probabilistic inference- the number of beads selected prior to decision provides an index of reflection impulsivity. Reflection impulsivity is associated with dlpfc, parietal and anterior insular activity and volume[375, 393].

Methods

Participants

Healthy volunteers were recruited from community-based advertisements in East Anglia. Psychiatric disorders were screened with the Mini International Neuropsychiatric Interview[439]. Subjects were excluded if they had a major psychiatric disorder, substance addiction or medical illness or were on psychotropic medications. Subjects were included if they were 18 years of age or over and had no history of regular or current use of other substances. Participants provided written informed consent and were compensated for their time. The study was approved by the University of Cambridge Research Ethics Committee. Participants underwent multi-echo rsfMRI as described in Chapter 1. Behavioural tasks were performed outside the scanner. Seeds and ROI's used are described in Chapter 1.

Of the 154 healthy volunteers from the baseline resting state study in Chapter 1, 55 participants completed the 4-choice serial reaction time task and SST (28 male; mean age 38.9 (SD 13.4); BDI 8.5 (SD 8)); An additional 11 also completed the model-free model-based task and ED shift task (N=66, 33 male; mean age 40 (SD 13) years old; BDI 8.6 (SD 8.4). Of these, 37 completed the probabilistic reversal learning task (17 male; mean age, 36.6 (SD 14.1); and 45 completed the Bead's task (27 female; mean age, 24.3 (SD 5.7)). Participants completed the resting-state functional MRI scan and behavioural testing no

more than 7 days apart.

Behavioural Tasks

4-choice Serial Reaction Time Task

Subjects were seated in front of a touch screen (a Paceblade Tablet personal computer; Paceblade Technology, Amersfoort, the Netherlands). Baseline blocks without monetary feedback were used to individualize monetary feedback amounts for subsequent blocks based on the individual's mean fastest reaction time and standard deviation. The 4 test blocks with monetary feedback were optimized to increase premature responding and varied by target duration, variability of the cue-target interval and the presence of distractors. Accurate and timely responses were followed by individualized reward magnitude outcomes depending on the speed of responding. The primary outcome measure was the premature release of the space bar prior to target onset. The task lasted 20 minutes and was programmed in Visual Basic with Visual Studio 2005. The premature responding task comprised of two baseline blocks and four test blocks. The baseline blocks were used to individualize feedback according to the individual's RT and encourage individuals to respond faster. Each baseline block had 20 trials with the final 10 trials used to calculate mean RT and SD for this calculation. Baseline Block 1 occurred at the start of the trial with the mean RT used for Test Block 1. Baseline Block 2 occurred at the end of Test Block 1 with the mean RT from both baseline blocks used for Test Blocks 2 to 4. The subjects were told to respond as quickly as possible during the baseline blocks with "Keep going" appearing on the screen as feedback. There were 4 test blocks with monetary feedback (40 trials per block). Subjects were instructed to respond as quickly as possible, that they would earn money for their responses, that it was more important to be fast rather than accurate and that they would not lose money if they were inaccurate. See Figure 3.1A for a schematic of the task.

The relationship between baseline block mean RT, SD and test block feedback were as follows: Very fast accurate responses: For very fast accurate responses in which RT during

a trial in the test blocks was less than -0.5 SD of the baseline RT, the response was followed by the text “YOU WIN!! EXCELLENT!!” along with a £1 image. If subjects won £1 in three sequential trials, the feedback increased to £2. Fast accurate responses: For accurate responses in which test RT was between -0.5 SD and +0.5 SD of the baseline RT, the response was followed by the text “Very good. Keep going.” along with a 50 pence image. Test RTs that were accurate and between +0.5 SD and +1.5 SD of the baseline RT were followed by the text “Good. Keep going.” along with a 10 pence image. Slow accurate responses: Slow but accurate responses in which trial RTs were greater than +1.5 SD of the baseline RT were penalized and followed by the text “YOU LOSE!! TOO LATE!! HURRY UP!!” and an image of -£1 with a red X over the coin. No response: If no responses were registered, the feedback was “TOO LATE!! GO FASTER!!” with an image -£1 with a red X. Premature response or incorrect responses: Neither premature responses (responding prior to target onset) nor incorrect responses (touching the incorrect box) were penalized. Following a premature response, subjects were required to touch the screen to complete the trial, which was followed by the text “Keep going”. An incorrect response was followed by the text “Keep going”.

Stop Signal Task

Response inhibition was tested using the stop signal task (Cambridge Neuropsychological Test Battery, CANTAB) (Figure 3.2)(4). Subjects were presented with a series of Go stimuli in the form of a left or right arrows and instructed to respond as quickly as possible by pressing the respective button on the two button response box. On a subset of the trials, the stimulus is followed 250 ms later (stop signal delay, SSD) by a stop signal tone. The SSD varied by 50 ms depending on performance, maintaining a staircase throughout the task resulting in approximately 50% successful and 50% unsuccessful stop trials. The key outcome measure was the SSRT. The SSRT is based on Logan’s model of a competition between the stop and go response and was calculated using the integration method[464] in which the SSD was subtracted from the integration of the finishing time as indicated by the Go reaction time distribution.

Model-Free Model-Based Task

A two-step choice task was employed[191] that has been shown to elicit engagement of goal-directed (model-based) and habitual (model-free) learning systems, as well as perseveration (p). Subjects completed extensive computer-based training before starting the task. The task involved two stages. At stage 1, participants were offered a choice between two stimuli, each leading with a fixed probability to one of two states at stage 2. At stage 2, participants were offered another choice between two stimuli, each leading, with differing probabilities, to monetary reward. The probability of reward slowly shifts over the course of the task. Each stage lasts 2 seconds, the transition between is 1.5 seconds and the outcome is shown for 2 seconds. Habit learning was modeled using a model-free reinforcement learning algorithm. However, the goal-directed learning algorithm takes into account the state transitions. A weighting factor (w) was calculated for each individual, capturing the relative contribution of either habitual model-free (w=0) or goal-directed model-based (w=1) learning. Perseveration (p) provides a measure of the tendency to select the same first stage choice irrespective of outcome. The task was programmed with Matlab 2011a. A schematic of the task structure is presented in Figure 3.3A.

Participants received extensive, self-paced training including practices demonstrating the concepts of stage transitions and probability, lasting 15-20 minutes. Choice of one stimulus at stage one led to one of two stimulus-pairs at stage two with a fixed probability (P=0.70 or 0.30). Choice of the other stimulus led to the same stage two but with the opposite fixed probability (P=0.30 or 0.70). Choice of a stimulus at stage two led to an independently varying probability of reward (between P=0.25 to 0.75). Participants had two seconds to make a decision and the transition between stages was 1.5 seconds. The chosen stimulus at stage one remained on the screen during stage two of that trial as a reminder. Participants completed 201 trials divided into three sessions. The outcome was an image of £1.

Model-Free Model-Based Computational Modeling

During the model-based model-free task, there are three states (stage-one state A (s_A); stage-two state B and C (s_B and s_C)), each with two actions (a_A and a_B). In order to model the habitual learning strategy, we used a SARSA (λ) temporal difference (TD) algorithm where each choice is based on a predicted long-run value ($Q_{TD}(s,a)$) for each action a at each stage s. In this framework, the TD reward prediction error (δ) informs subsequent predictions. For each trial t the stage-one state $s_{1,t}$ (s_A) requires an action $a_{1,t}$ choice. The stage-two state $s_{2,t}$ (s_B or s_C) also requires an action $a_{2,t}$ choice, leading to a reward $r_{2,t}$ (£1 or £0). After each stage i (1,2) of each trial t when the stage-two state is displayed and at final reward presentation, a prediction error $\delta_{i,t}$ will occur. These will update the previous states $s_{i,t}$ value Q_{TD} and action $a_{i,t}$:

$$Q_{TD}(s_{i.t},a_{i,t}) = Q_{TD}(s_{i.t},a_{i,t}) + \alpha_i\delta_{i,t}$$

where

$$\delta_{i,t} = r_{i,t} + Q_{TD}(s_{i+1,t},a_{i+1,t}) - Q_{TD}(s_{i,t}.a_{i,t})$$

This updates the action value of stage-one depending on the value following the stage-two state, $Q_{TD}(s_{2,t},a_{2,t})$. $r_{1,t}$=0 because no reward is received at this stage. The reward $r_{2,t}$ then updates the value at the second stage. Here, the terminal value $Q_{TD}(s_{3,t},a_{3,t})$=0. A separate parameter is used for the learning rate for the update of each stage (α_1, α_2). The stage-one action value is updated by the stage-one prediction error described but also according to the stage-two prediction error at the end of each trial when the reward $r_{2,t}$ is received, which is added to the previous:

$$Q_{TD}(s_{1,t}, a_{1,t}) = Q_{TD}(s_{1,t}, a_{1,t}) + \alpha_1\lambda\delta_{2,t}$$

This update extent is also determined by the eligibility trace parameter λ.

At stage-one (Q_{MB}), the model-based reinforcement learning algorithm calculated the action value per action based on the probabilities that the current action would lead to each stage two state ($P(s_B|s_A.a_A)$=0.70; ($P(s_B|s_A.a_A)$=0.30; and conversely for s_C) and the values of those states. Therefore, for each action a_j (j= A,B):

$$Q_{MB}(s_A,a_j) = P(s_B|s_A,a_j)\max_k Q_{TD}(s_B,a_k) + P(s_C|s_A,a_j)\max_k Q_{TD}(s_C,a_k)$$

The stage-two value here is equivalent to the model-free value of the optimal action as both model-free and model-based values coincide at the end state. For each stage-one action, a net action value is calculated depending on the weighted sum of both model-free and model-based values:

$$Q_{net}(s_A,a_j) = wQ_{MB}(s_A,a_j) + (1 - w)Q_{TD}(s_A,a_j)$$

where w is a weighting parameter such that higher w (w=1) indicates reliance on model-based learning strategies while lower w (w=0) indicates greater reliance on model-free. At stage two, $Q_{NET}=Q_{TD}$. For each stage, the probability of a choice is calculated using the softmax equation in Q_{net}:

$$P(a_{i,t} = a|s_{i,t}) \alpha \exp\left(\beta_i[Q_{net}(s_{i,t},a) + p * rep(a)] \right)$$

where β_i is an index of choice reliability at each stage (β_1, β_2) with higher values indicating higher reliability. p accounts for perseveration (p>0) or switching (p<0) of choices in stage one. $rep(a)$ acts as a binary indicator such that it has a value of 1 if a is an action from stage one and $a = a_{1,t-1}$, and otherwise equals 0. We estimated the free parameters of the model (w, p, α_1, α_2, β_1, β_2, p, λ) for each subject separately by maximum likelihood (over the joint probability of each choice conditional on the preceding choice and outcomes) as described in Daw et al. (2011). Complementing w, which characterizes the net contribution of model-based vs. model-free values to choice, we computed the scores MB=w β_1, and MF=(1-w) β_1,,

as the unscaled contribution of each value separately to choice, producing model-based computation (MB_c) and model-free computation (MF_c) scores. Accordingly, the relativized score $w = MB/(MF + MB)$.

Extra-Dimensional Set-Shifting Task

The Intradimensional-extradimensional shift task (IDED shift; CANTAB[269]; Figure 3.3B) involves two stimulus feature dimensions of colour-filled shapes and white lines. Simple stimuli contain just one dimension, whereas compound stimuli contain both. There are a series of stages and six successive correct trials are necessary for continuation of each stage. Stages 1-5 involve simple stimulus discrimination with the development of an attentional set to a single stimulus dimension (shapes). The complexity of the stimulus increases as irrelevant lines become compounded with the relevant shapes. Stages 6 and 7 involve the introduction of new shapes, or intra-dimensional shift and reversal, respectively. The attentional set to a single salient stimulus dimension remains. At the crucial stage 8, the previously irrelevant stimulus dimension (lines) becomes relevant and subjects must perform an extra-dimensional (ED) shift by responding to the correct line and ignore the shape. Finally, stage 9 is an ED reversal. Thus, an ED shift requires shifting of attention from a previously relevant to a previously irrelevant dimension, requiring cognitive flexibility. The primary outcome measure was the number of ED shift errors.

Probabilistic Reversal Learning Task

The probabilistic reversal learning task (Figure 3.4) comprised of an acquisition and reversal phase, each with three conditions of varying reward, neutral or loss outcomes. In the acquisition phase, subjects chose from 3 stimulus-pairs associated with probabilistic outcomes. Following 30 trials of each condition for acquisition, the contingencies for each stimulus-pair switched and were therefore followed by 30 trials per condition in the reversal phase. The stimulus phase (2.5 seconds) was followed by an outcome phase (1 second) with the feedback; “You WON!!” with an image of a £2 or £1 coin or “You LOST!!” with an image of a red cross over the money. The trial was followed by a variable inter-trial interval

of a mean of 0.75 seconds varying between 0.5 and 1 second. Subjects were instructed to choose between pairs of symbols and that one symbol within each pair was more likely to win or not lose money and that at some point the relationship between the symbols and the likelihood of winning and not losing money might change. Subjects were told to make as much money as possible of which a proportion would be paid to them at the end of the study. The primary outcome measure was the number of trials to criterion of 4 correct sequential choices. The task was coded in E-prime Version 2.

For the probabilistic reversal learning task, the acquisition phase included the following probabilistic outcomes: Loss (Stimulus A: P=0.30 Win +£1 / P=0.70 Lose -£2 (mean -£1.1); Stimulus B: P=0.70 Win +£1 / P=0.30 Lose -£2 (mean +£0.1)), Neutral (Stimulus C: P=0.70 Win +£1 / P=0.30 Lose -£1 (mean+£0.4); Stimulus D: P=0.30 Win +£1 / P=0.70 Lose -£1 (mean -£0.4)) or Reward (Stimulus E: P=0.70 Win +£2 / P=0.30 Lose -£1 (mean+£1,1); Stimulus F: P=0.30 Win +£2 / P=0.70 Lose -£1 (mean+0.1)). After 30 trials of each condition for acquisition, the contingencies were switched for the reversal phase (e.g. Stimulus A: P=0.70 Win +£1 / P=0.3 Lose -£2; Stimulus B: P=0.30 Win +£1 / P=0.70 Lose -£2). There were a total of 180 trials. The position of the stimuli within each stimulus-pair was counterbalanced on either side of the screen and the stimuli conditions were randomly presented. Subjects were given 10 practice trials of a stimuli-pair in which one stimulus was associated with P=0.70 Win +£1 / P=0.30 Lose -£1 and the other stimulus associated with P=0.30 Win +£1 / P=0.70 Lose -£1). The stimulus was 2.5 seconds during which the subjects responded with either the left arrow on the keyboard for the stimulus on the left or the right arrow on the keyboard for the stimulus on the right. If subjects were too slow, this was followed by the words: “You were too slow. Respond faster”.

Bead’s Task

Reflection impulsivity was assessed with the Beads task. Subjects were shown two jars on the computer screen with opposite ratios of red and blue beads (P=.80; P=.20) (Figure 3.6). They were informed of the bead ratio and were told that beads from one of the jars would be presented one at a time in the centre of the screen. The drawn beads were shown at the top

of screen to control for working memory effects. The subjects' goal was to infer from which jar the beads were drawn. Subjects were free to view as many beads as they wanted without time limit up to 20 before committing to their decision. Subjects pressed the 'Return' key to view more beads and the 'Space bar' when they were ready to make a decision. Following their decision, they then indicated the degree of confidence that their answer was correct on a visual analogue scale anchored at 'Not confident' to 'Very confident' using a mouse. There was no feedback. Subjects were then informed that the next block would start. The primary outcome measure was the number of beads drawn prior to a decision. Other outcome measures included confidence ratings and objective probability at the time of decision. There were three blocks of trials with the same bead order[375].

Resting State functional MRI Data Acquisition and Analysis

Acquisition parameters and seed definitions are described in Chapter 1. This section examined the relationship between functional connectivity and behavioural performance. ROI-to-ROI functional connectivity was computed for the following ROI pairs using Pearson's correlation: waiting impulsivity: STN, ventral striatum, subgenual ACC; SSRT: STN, pre-SMA, right IFC, dorsal caudate; model-based: medial OFC and ventral striatum; model-free, SMA and posterior putamen; ED shift dlpfc, dorsal caudate, ventral striatum.

For the more exploratory analyses for STN and compulsivity, STN seed-to-whole brain connectivity maps were computed and entered into second level correlation analysis with compulsivity measures model based / model free and perseveration, controlling for age and gender. The variance related to each of the other variable was controlled for (i.e. controlling for perseveration in the model free / model based analysis and vice versa), to account for multiple comparisons and to highlight unique contributions of each. Due to the exploratory nature of this analysis and the implication of several cortical and subcortical regions, whole brain voxel-wise correlations were performed and cluster extent threshold correction was used. The cluster extent correction was calculated at 15 voxels at $p<0.001$ whole brain uncorrected, which corrects for multiple comparisons at $p<0.05$ assuming an individual-voxel

Type I error of p=0.01[465]. This exploratory approach was taken for the probabilistic reversal learning task analysis, using the OFC as a seed region.

Due to the possibility of mixed signals arising from adjacent structures, we also examined the adjacent substantia nigra (SN) as a seed region to ensure specificity of the current findings to STN. Thus, the same correlation for model based / model free was performed for SN-to-whole brain functional connectivity maps.

In order to assess the relationship between anterior and posterior STN with the behavioural measures, anterior STN was dissociated based on ventral striatal and dlpfc connectivity with whole STN (Chapter 1). Both ventral striatum and dlPFC showed connectivity with anterior STN (ventral striatum to right STN; dlPFC to bilateral STN) and had a posterior extent at y=-14. As both ROIs had considerable overlap, limbic and associative anterior STN were combined and divided from motor posterior STN by dissecting the STN at y=-14, dividing STN into anterior and posterior sub-regions (Figure 3.6). Both anterior and posterior STN seed-to-whole brain functional connectivity maps were correlated with primary outcome measures. Whole brain cluster-extent threshold FWE $p<0.05$ was considered significant.

Results

Impulsivity

Fifty-five HV were examined (premature responding= 8 ±5.9, SSRT= 184.3 ±55.1, GoRT= 440.7 ±112.7) There was no significant correlation between premature responding and SSRT or GoRT ($R<0.1$, $p>0.4$). Greater premature responding was negatively correlated with connectivity between STN and right ventral striatum ($R=-0.286$, $p=0.034$, Figure 3.1B), and between STN and subgenual cingulate cortex ($R=-0.391$, $p=0.003$, Figure 3.1C). We repeated the analysis with SSRT as a covariate of no interest, which did not affect the results. Similarly, SSRT was not correlated with connectivity between STN and ventral striatum or subgenual cingulate.

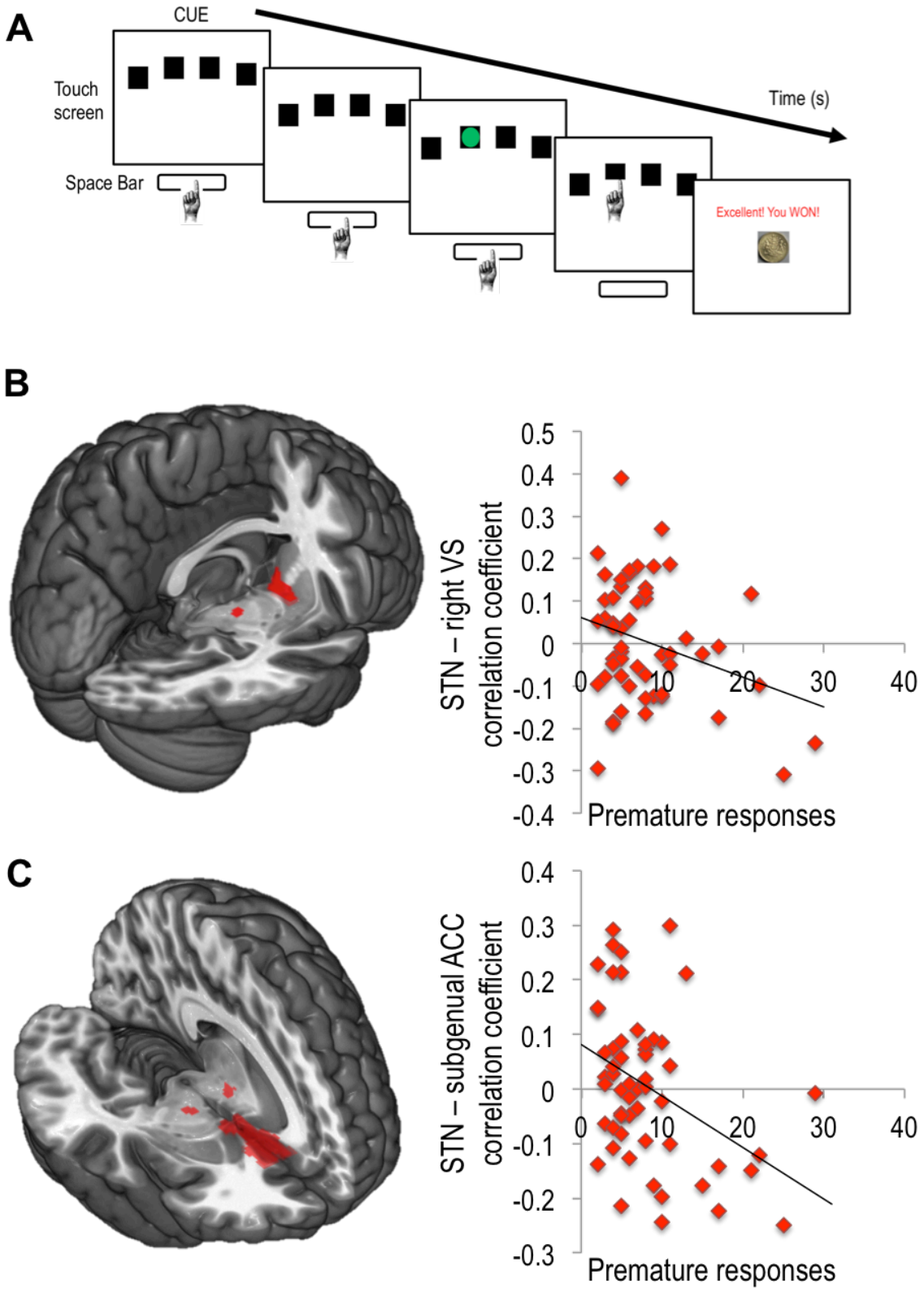

Figure 3.1. The 4-Choice Serial Reaction Time (4-CSRT) task and neural correlates of waiting impulsivity. *A, The 4-CSRT task. The cue onset prompted subjects to hold down the space bar. A green circle target appeared, to which subjects responded by releasing the*

space bar and touching the box on the touch screen in which the target appeared. Finally, monetary feedback was displayed. Premature responding was defined as release of the space bar prior to target onset. Correlation coefficients were computed between regions of interest (ROI) as a marker of their functional connectivity. Functional connectivity between subthalamic nucleus (STN) and ventral striatal (VS) seed regions (B) and STN and subgenual anterior cingulate cortex (ACC) (C) was correlated with premature responses in healthy volunteers. The seed regions for ROI-to-ROI analyses are shown overlaid on MNI152 template image.

The stop signal task data of one participant was removed as an outlier for all analyses using this measure (Go Reaction time score >3 SD above group mean). SSRT was negatively correlated with connectivity between left STN and right pre-SMA connectivity (R= -0.350, p=0.010) along with STN and dorsal caudate connectivity (R=-0.338, p=0.014)(Figure 3.2). There was no significant correlation between SSRT and connectivity between STN and right inferior frontal cortex. These hyper-direct and striatal connections with STN were also not significantly correlated with premature responding.

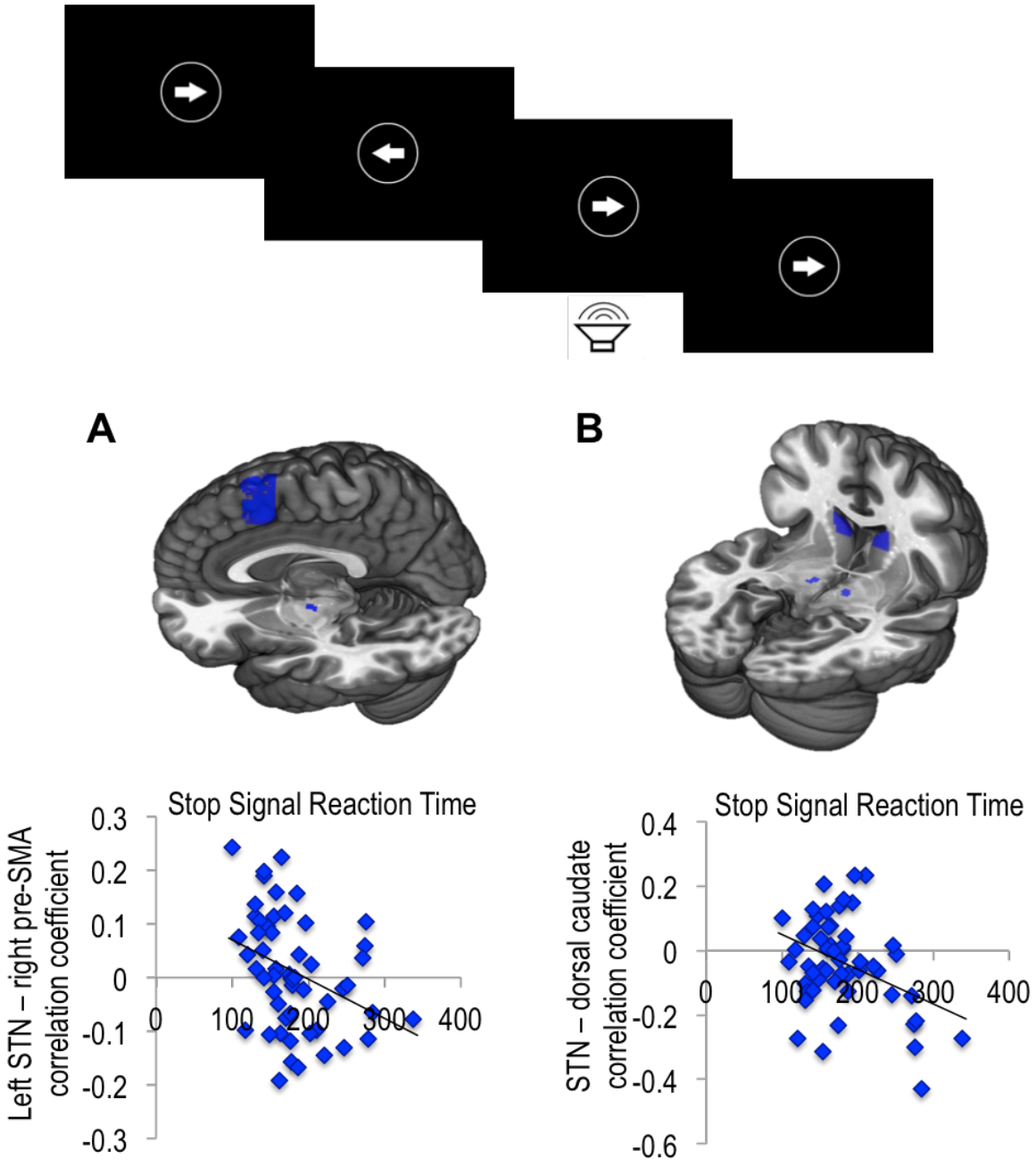

Figure 3.2. Neural correlates of motor response inhibition. *Top: Stop signal task. Functional connectivity (measured as correlation coefficients) between subthalamic nucleus (STN) and pre-supplementary motor area (pre-SMA) (A), and dorsal caudate (B), was correlated with Stop Signal Reaction Time in healthy volunteers. The regions of interest (ROI) for ROI-to-ROI analyses are shown overlaid on MNI152 template image.*

Compulsivity

The following behavioural measures were examined in healthy volunteers: *w* (group mean, 0.31; standard deviation (SD), 0.23), ED shift errors (7.92; 9.44 SD), computational measure of model-basedness (mb_c) (1.77; 1.76 SD), computational measure of model-freeness (mf_c) (3.55; 2.45 SD), reversal-learning trials to criterion for reward (345.65; 296.62 SD) and loss (3.45.51; 297.04 SD).

The primary outcome measure, *w* or more goal-directed model-based behaviour was positively correlated with connectivity between medial OFC and ventral striatum (R=0.32, p=0.01; Figure 3.3C). In the exploratory analysis, mf_c scores were positively correlated with connectivity between posterior putamen and SMA (R=0.266, p=0.033; Figure 3.3D).

There was no significant correlation between extra-dimensional errors and connectivity between dlpfc and caudate (R=0.032, p=0.811). However, extra-dimensional shift errors were correlated with connectivity between dlpfc and ventral striatum (R=-0.298, p=0.021; Figure 3.3E).

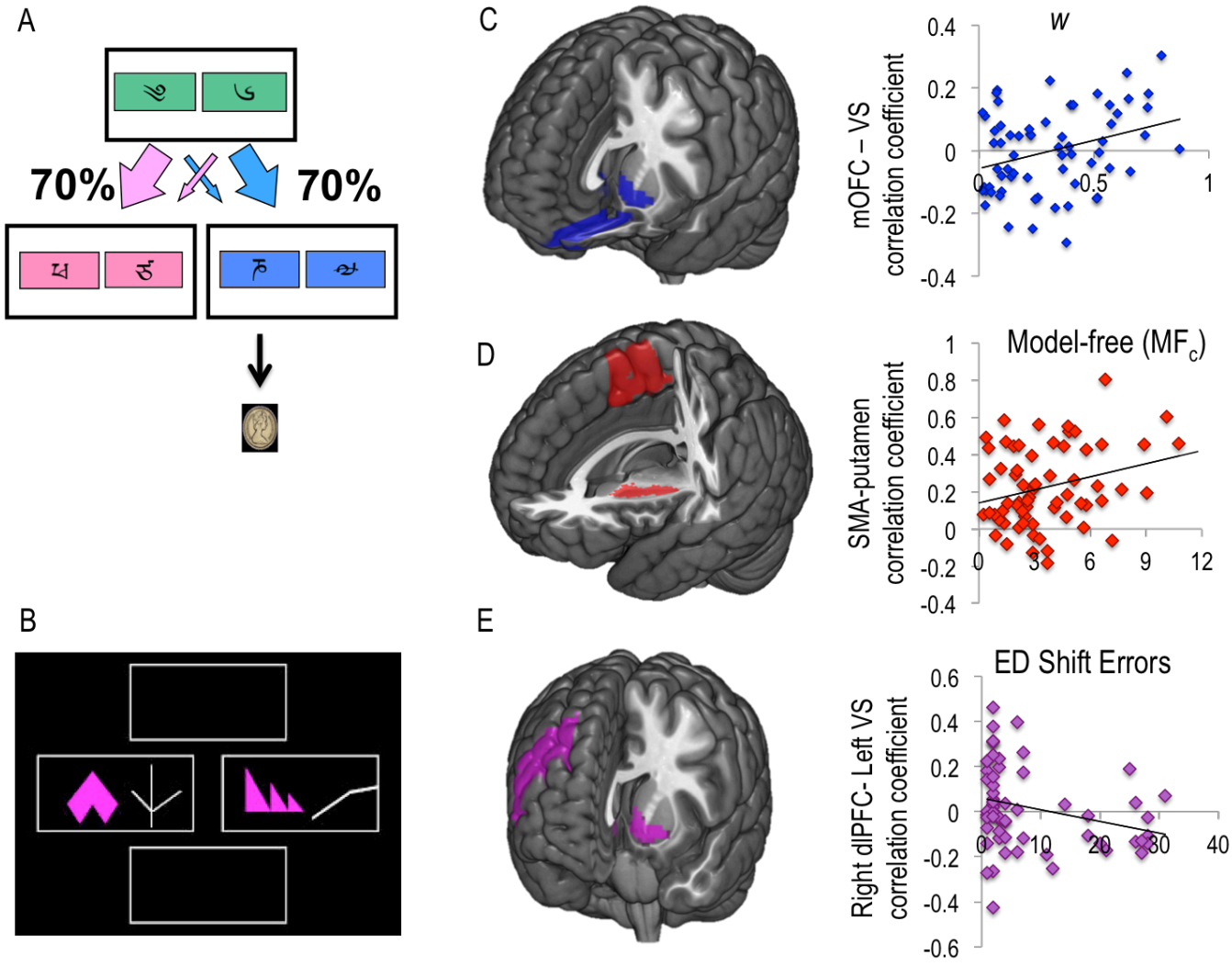

Figure 3.3. Neural connectivity correlates of behaviour. *A, Two step task: A choice between two stimuli at Stage 1 led with fixed probability (p = 70%) to one of two Stage 2 stimulus-pairs. A choice at Stage 2 probabilistically led to reward. B, Extradimensional (ED) set-shifting requires attentional shifts to a previously irrelevant stimulus (i.e., shape vs line, left). C, w, the relative contribution of either model-based (w = 1) or model-free learning (w = 0) positively correlated with connectivity between ventral striatum (VS) medial orbitofrontal cortex (mOFC). D, A computational measure of model-free learning (MF_c) positively correlated with connectivity between supplementary motor area (SMA) and posterior putamen. E, Set shifting errors negatively correlated with connectivity between dorsolateral prefrontal cortex (dlPFC) and ventral striatum (VS).*

Flexible updating of reward and loss stimulus-outcome contingencies was also examined using a probabilistic reversal learning task (Figure 3.4). In the context of reward, the number of trials to criterion for reversal learning was negatively correlated with ventral striatum seed

and lateral OFC and ventral anterior/mid insula (Figure 3.4A) and positively correlated with connectivity between the lateral OFC seed and the amygdala (Figure 3.4C). In the context of loss, slower reversal-learning also negatively correlated with ventral striatum and lateral OFC and dorsal anterior/mid insula connectivity (Figure 3.4B) (see Table 3.1 for statistics).

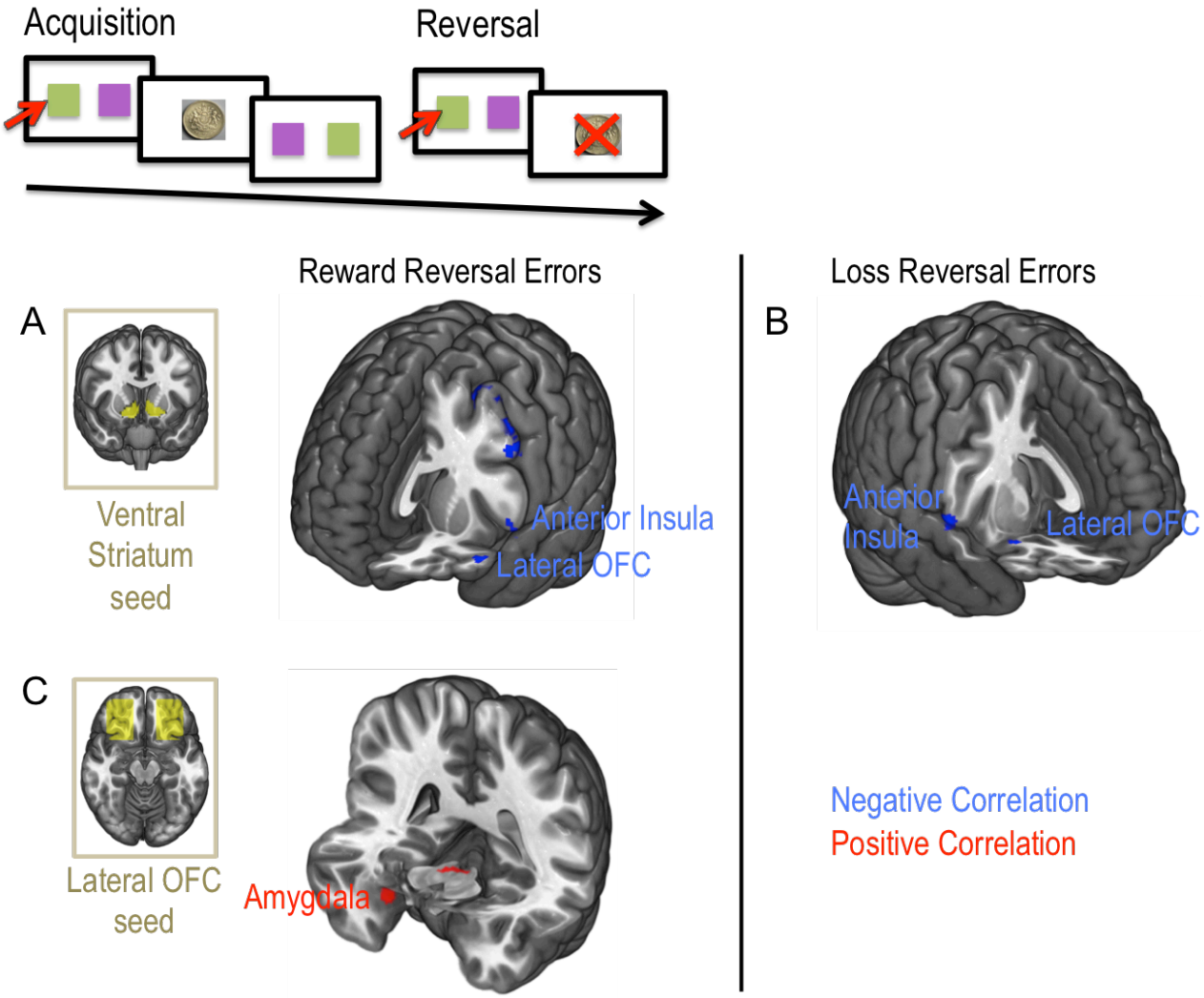

Figure 3.4. Neural correlates of reversal learning errors. *Top: Reversal learning task. Ventral striatum seed-based functional connectivity maps revealed sites of connectivity that negatively correlated with both reward reversal errors (A) and loss reversal errors (B). C. Lateral orbitofrontal (OFC) seed-based connectivity correlated positively with reward reversal learning errors in the amygdala region. Cluster extent threshold correction was used for correlations with behaviour measures.*

Seed ROI	Correlation		Cluster	Z	x	y	z
Reward Reversal errors							
Lateral OFC	Positive	Midbrain	25	4.13	6	-27	-12
		Amygdala (right)	27	4.04	20	-2	-19
	Negative	Frontal Polar	16	4.04	15	63	-12
Ventral striatum	Positive	Midbrain	18	4.01	-8	-27	-45
	Negative	Parietal	198	5.47	-50	-69	-24
		Cerebellum	26	3.94	24	-81	-45
		Insula	24	3.75	-55	17	-5
		Lateral PFC	132	3.73	-52	12	39
		Lateral OFC	23	3.5	-43	31	-14
Loss Reversal errors							
Lateral OFC	Positive	nil					
	Negative	dlPFC	23	3.45	24	45	28
Ventral striatum	Positive	nil					
	Negative	Insula	21	3.79	62	5	4
		Temporal	18	3.75	-20	-11	-47
		Lateral OFC	21	3.7	22	10	-19

Table 3.1. Neural connectivity correlates of learning errors for reward and loss. *Whole brain connectivity maps for seed regions of interest (ROI) were correlated with reversal errors for reward and loss separately. Abbreviations: PFC, prefrontal cortex; OFC, orbitofrontal cortex; dlPFC, dorsolateral prefrontal cortex; Z, Z-score statistic following cluster extent thresholding.*

Subthalamic Nucleus

For this analysis, data was available for 77 healthy controls (46 female; age=29.623 ±12.168; *w*=0.411 ±0.276; perseveration=0.191 ±0.173). The weighting factor, w, which

describes the relative contribution of either habitual (model-free, MF, w=0) or goal-directed (model-based, MB, w=1) learning tendencies, was positively correlated with STN connectivity with left ventral striatum and medial OFC and negatively with STN connectivity with left hippocampus, dorsal ACC and medial parietal cortex (Table 3.2, Figure 3.5). For comparison purposes perseveration was investigated. Perseveration was associated with reduced connectivity between STN and left premotor cortex and left lateral prefrontal cortex (Figure 3.5).

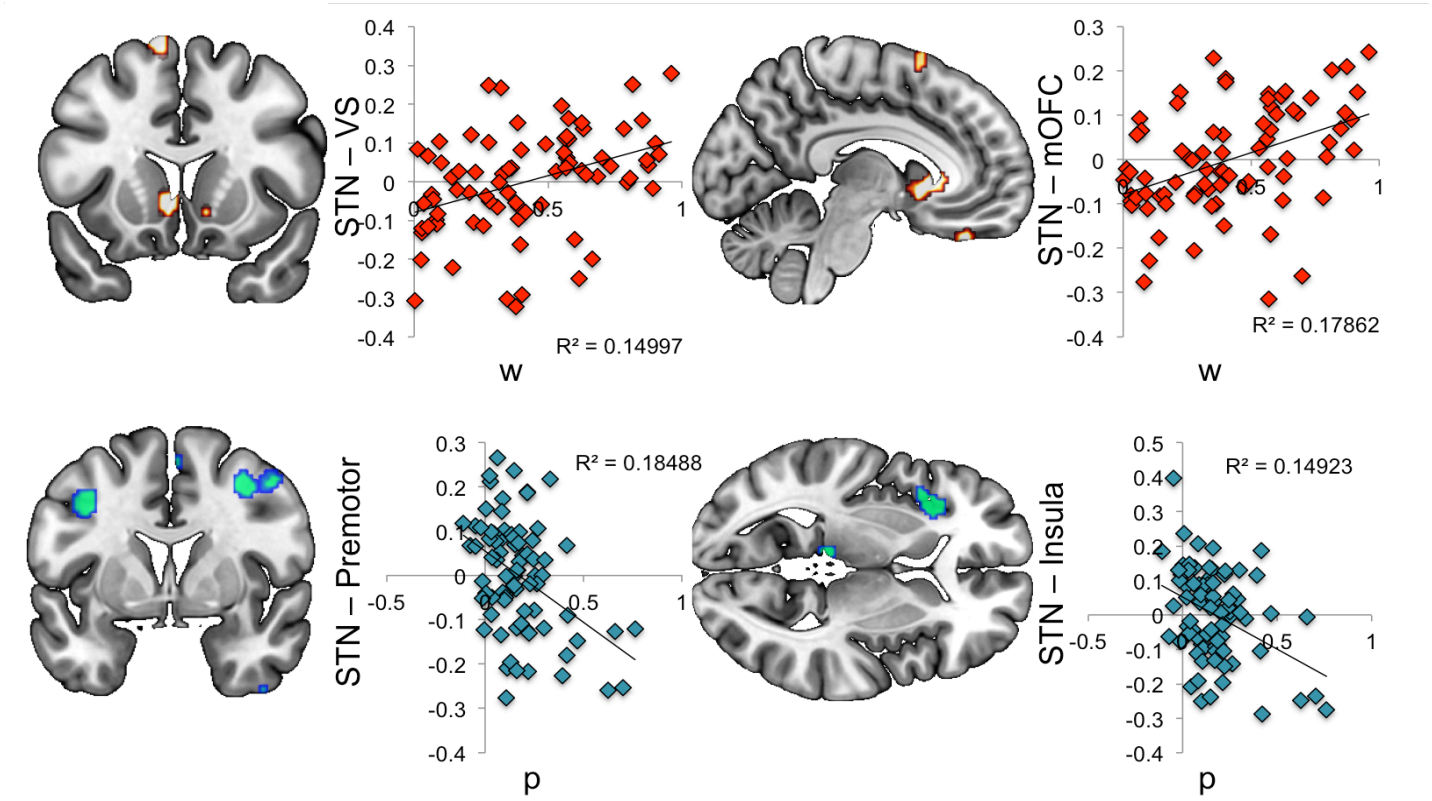

Figure 3.5. Subthalamic nucleus connectivity and model based versus model free learning. *Subthalamic nucleus (STN) connectivity with whole brain was computed and correlated with w, the relative contribution of model-free (w=0) or model-based (w=1) learning tendencies (top) and perseveration (p, bottom). Abbreviations: VS, ventral striatum; mOFC, medial orbitofrontal cortex; dACC, dorsal anterior cingulate cortex. Displayed at p<0.005 whole brain uncorrected for illustration on standard MNI template.*

	Cluster	Z	x	y	z
w positive					
Bilateral ventral Striatum	65	4.35	13	24	-4
	89	4.26	-6	14	-2
Left medial OFC	29	4.22	-6	38	-30
Right temporal	29	3.76	64	-30	-23
	19	3.56	-66	-32	17
w negative					
Dorsal ACC	31	4.87	8	28	19
Left hippocampus	38	4.44	-31	-20	-18
Posterior Cingulate	26	4.12	-13	-23	33
Medial Parietal	34	3.92	-10	-65	49
		3.4	-8	-74	49
	21	3.66	1	-74	56
Cerebellum	19	3.63	-41	-58	-53
Midbrain	17	3.58	3	-25	-18
		3.32	8	-20	-23
Perseveration positive					
Left Cerebellum	17	3.58	-8	-48	-9
Perseveration negative					
Left Occipital	24	4.58	-27	-76	12
Left Premotor Cortex	23	4.52	-38	3	45
Left Lateral PFC	20	4.06	-20	19	35

Table 3.2. Statistics of subthalamic nucleus connectivity and compulsivity. *Statistics for the bilateral subthalamic nucleus (STN) seed-to-whole brain connectivity correlations with measures of compulsivity. Cluster extent threshold correction of 15 voxels at p<0.001 whole brain uncorrected was used. Abbreviations: Z, Z score; xyz, peak voxel coordinates; w, weighting of model based (w=1) and model free (w=0) learning; OCI, obsessive compulsive index; OFC, orbitofrontal cortex; ACC, anterior cingulate cortex; PFC, prefrontal cortex; IFC, inferior frontal cortex.*

To examine the specificity of the STN findings to arising from STN rather than adjacent structures, the substantia nigra was examined. There were no overlapping regions whose connectivity with substantia nigra was correlated with w (positive correlation cluster size>16, with occipital cortex Z=4.39, Cerebellum Z=4.28, and inferior temporal cortex Z=4.06). To examine whether adjacent substantia nigra contributed to the current findings for STN, SN connectivity was computed with the regions and peak coordinates implicated in the main study (ventral striatum (xyz=13,24,-4), medial orbitofrontal cortex (OFC, xyz=-6,38,-30), dorsal anterior cingulate cortex (ACC, xyz=8,28,19), hippocampus (xyz=-31,-20,-18). These connectivity measures were correlated with *w* and no significant correlations were observed (substantia nigra and ventral striatum functional connectivity correlated with w, R=-0.018, p=0.877; SN and medial OFC, R=-0.009, p=0.937; SN and dorsal ACC, R=-0.201, p=0.078; SN and hippocampus, R=-0.134, p=0.242).

The behavioural relevance of subregions of STN was examined. Forty-five HV completed the Beads Task (Figure 3.6) outside the scanner (Beads=8.063 ±4.824). Number of beads positively correlated with anterior STN connectivity with right dlPFC (p=0.015, K=128, Z=4.33, xyz= 20 21 52) and right anterolateral PFC (p<0.001, K=47, Z=4.62, xyz= 38 56 -2), confirmed with small volume corrected FWE p<0.05 for dlPFC: p=0.012, Z=4.33) (Figure 3.6). Number of beads negatively correlated with posterior STN connectivity with temporal cortex (p=0.016, K=124, Z=3.90, xyz= 57 -55 10), with no correlations with dlpfc.

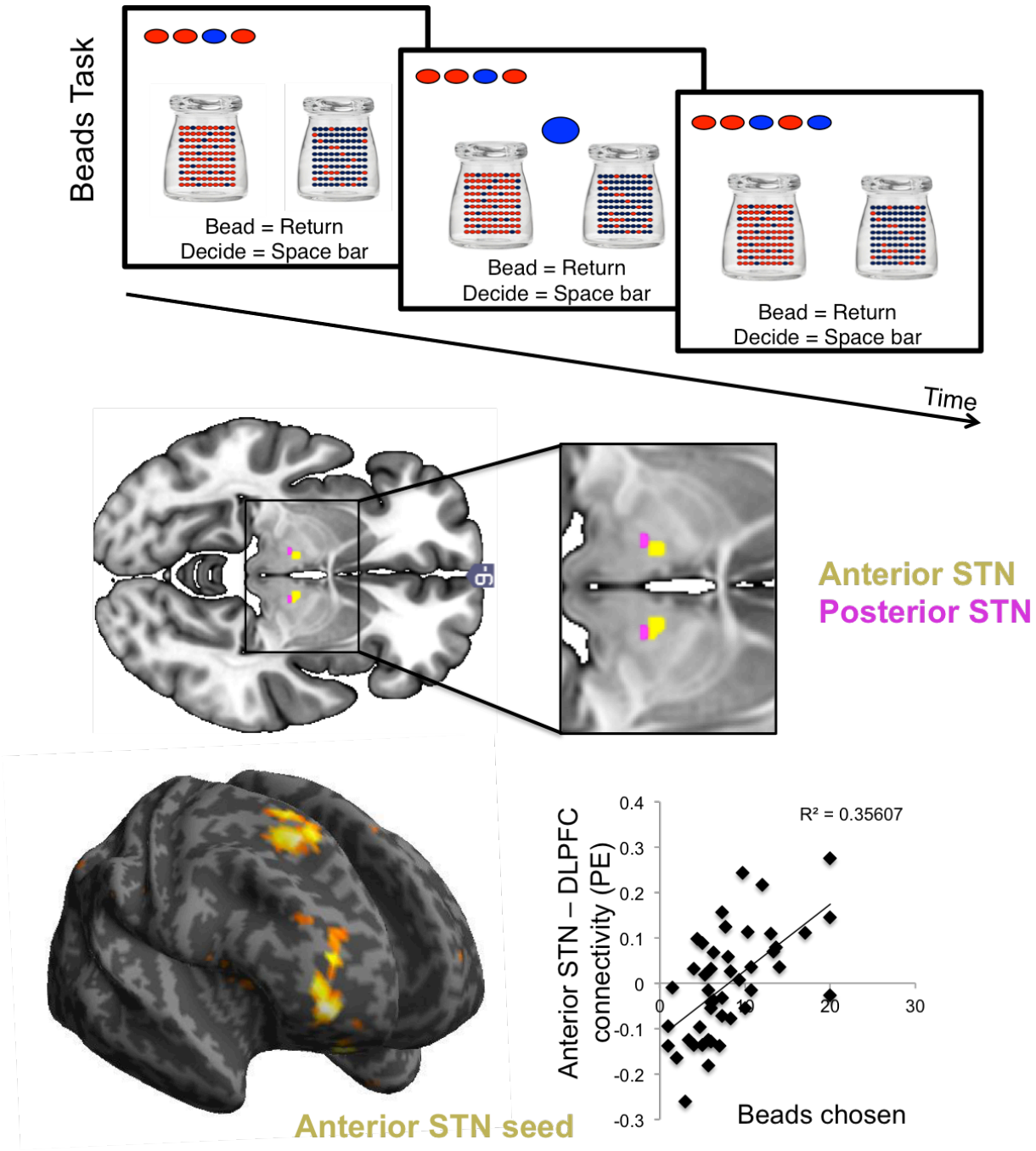

Figure 3.6. Anterior and posterior subthalamic nucleus and decisional impulsivity. *Top: Beads task: Subjects viewed two jars with opposing ratios of red and blue beads (P=.80; P=.20). Based on the sequential viewing of beads selected from a jar, participants were to make a decision from which jar the beads were selected. The selected beads were shown at the top to control for working memory effects. Middle: The anterior (yellow) and posterior (pink) subthalamic nucleus (STN) seeds are shown. Bottom: Anterior STN seed-to-whole brain functional connectivity maps were correlated with the primary outcome measure from the Beads Task, the number of beads drawn prior to a decision. The scatter plots shows the parameter estimates for the correlation in the STN with beads chosen in the*

right dorsolateral prefrontal cortex (DLPFC). Displayed at p<0.005 whole brain uncorrected for illustration on standard MNI template. Abbreviations: DLPFC, dorsolateral prefrontal cortex; IFC, inferior frontal cortex.

Discussion

Impulsivity

Greater premature responding in humans was associated with lower intrinsic connectivity of bilateral STN with bilateral subgenual cingulate and right ventral striatum. This implicates the more limbic subcircuit within the cortico – basal ganglia circuitry in waiting impulsivity. This is distinct from the findings for motor response inhibition or action cancellation as captured by SSRT, which was associated with lower connectivity between hyperdirect projections of the right pre-SMA and left STN along with dorsal caudate and STN connectivity, thereby implicating the more motoric cortico – basal ganglia circuit, both via the indirect and hyperdirect pathways.

The findings demonstrating the neural correlates of waiting impulsivity provide translational evidence in humans for a similar network implicated in rodents (STN, ventral striatum and subgenual ACC or infralimbic cortex). That this form of waiting impulsivity implicates the limbic circuit is interesting given the relationships between the more motoric circuit with impulsivity[156]. However, the current task is distinct from traditional measures of motor impulsivity. The task ties the waiting period to rewarding outcomes, linking reward and action control or inhibition, which is not the case during the SST, which has no monetary reward outcomes. Thus, the current demonstration of an implication for the ventral striatum coincides with its role in reward anticipation, prediction, reinforcement, and motivation[28, 40, 41, 466]. The subgenual ACC has also been implicated in reward sensitivity[467], and regulation of behavioural responses in light of learned or salient environments[468, 469]. The role of the subgenual cingulate in the cortico – basal ganglia circuitry is less pivotal, although there are extensive and unique projections from subgenual cingulate to nucleus

accumbens shell[470, 471], which establishes its position as a modulator of striatal and basal ganglia limbic processing.

For response inhibition or regulation of motor impulsivity, the STN works via the indirect and hyper-direct pathways to critically mediate responses. Indeed, STN lesions in rodents are associated with a generalized impairment in response inhibition with greater errors in the SST but no specific prolongation of SSRT[155]. The current findings support studies on stopping behaviours that implicate the hyper-direct connections to the STN from pre-SMA and the indirect pathway through the dorsomedial striatum or caudate[128, 460, 461]. There was no relationship between motor impulsivity and right IFC connectivity with STN. This may be related to the functional characteristic demonstrated in Chapter 1 of lower intrinsic, resting functional connectivity between IFC and STN (compared to between pre-SMA and STN). Further studies with larger sample sizes might therefore be necessary to elucidate this expected relationship.

The current findings of separable neural networks underlying premature responding and action cancellation (SSRT) converge with rodent and human studies in demonstrating that the two measures are unrelated[188, 472]. In rodents, action restraint as measured using commission errors in go/no-go type tasks is similarly unrelated to premature responding[472, 473]. The STN is believed to influence response suppression via both reactive (in response to an internal or external cue) and proactive (preparatory inhibition) models[50, 474]. The current findings suggest that premature responding is likely dissociable from fast reactive stopping which is mediated via the hyperdirect pre-SMA to STN projection.

Compulsivity

Prospective model-based goal-directed learning was associated with the latent biomarker of medial OFC and ventral striatal intrinsic connectivity. These findings suggest a neural network for model-based learning involving integration of instrumental performance (ventral striatum) and flexible, computationally-driven updating of outcome value based on changing internal motivational states and external feedback (medial OFC). The results dovetail with findings using structural and on-task functional neuroimaging, including a report of

correlations between model-based learning and higher medial OFC volume[191, 219, 391, 475, 476].

On an exploratory basis, a dissociation between model-based and retrospective model-free habit learning was demonstrated, implicating functional connectivity between the putamen and SMA. The dissociability of the networks underlying model-based and model-free learning supports the intrinsic parcellation of cortical – basal ganglia circuitry. Most previous findings from studies of computational learning behavior have focused on the neural correlates of model-based learning or higher *w* scores[391], with fewer clear correlates of model-free learning. Consistent with the hypothesis that model-free learning gives rise to habits, the current findings emphasize the similarities in the neural correlates underlying model-free learning as operationalized computationally, with that for conventional habit learning in rodent lesion studies[231] and human imaging studies[250, 251] based on overtraining and testing of sensitivity to devaluation. These results also converge with a report of on-task functional neuroimaging using a three-step decision tree task, related to the current task in which model-free values were shown to be encoded by the putamen[212].

Extra-dimensional shift errors, indicating conceptual attentional shifting, were associated with reduced functional connectivity between dlpfc and ventral striatum. The role of the dlpfc in extra-dimensional shifting is well-established implicating a capacity for storing multiple choice options during outcome evaluation[25, 217, 267]. The present finding converges with non-human primate studies showing only a limited role of the caudate nucleus in extra-dimensional shifting[477] and rodent studies showing that nucleus accumbens lesions can impair strategy shifting[478]. Specifically, nucleus accumbens core lesions impair the later stage of acquisition and maintenance of a new strategy rather than the capacity to shift away from previously learned contingencies[479]. Thus, the current findings may represent this later stage of acquisition and maintenance of a new strategy. Furthermore, slower reversal learning across both reward and loss valences was negatively correlated with lateral OFC and ventral striatum connectivity. Several lines of evidence implicate the lateral OFC specifically in reversal learning. Depletion of serotonin in primate OFC is associated with reversal impairments[480] and deep brain stimulation of the lateral OFC in rodents impairs

spatial reversal learning but not acquisition learning[481]. In human studies, activation of the lateral OFC is specifically involved with reversal implementation[392].

Together, this study demonstrates a parcellation of discrete and dissociable cortico – basal ganglia circuits, providing evidence of anatomical segregation of functional regions of this circuitry with connectivity of functionally defined prefrontal cortical regions projecting to dissociable motor, limbic and associative striatal regions[482, 483].

Subthalamic Nucleus

The relationship between model-basedness and STN connectivity with OFC and ventral striatum dovetails with the previous finding of a relationship between medial OFC and ventral striatal connectivity with model-basedness. In contrast, greater habitual model-free learning was associated with greater connectivity of the STN with dorsal ACC and hippocampus. The neural correlates of model-freeness have been less well established. Previous studies assessing habitual behaviour in humans have implicated the putamen and premotor cortex using the 'slips of action' task[463] and the SMA in the current Chapter. Traditionally, there has been a dissociation between dorsal striatal habit and hippocampal declarative or cognitive memories driving behaviour[484-486]. However, the hippocampus has been shown to encode reward prediction[163], which is necessary for the reinforcement learning that drives model-free behaviour[475]. The dorsal ACC receives extensive projections from dopaminergic midbrain projections and is also implicated in reward prediction and prediction error for guiding reinforcement driven behaviour[487, 488]. Links between the STN and dorsal ACC have been exemplified by studies in PD patients, which show that STN DBS reduces cerebral blood flow in the dorsal ACC[474, 489]. STN DBS affects habitual behaviour, as measured by the generation of a sequence of random numbers (requiring habit suppression), although DBS has been shown to both improve[490] and impair[489] performance during this task. STN DBS has also been shown to consistently hasten responding in the context of conflict or competing responses related to mesial prefrontal theta activity[122]. In the context of habit learning, conflict resolution may be relevant in resolving choices that involve switching between strategies. Thus, the STN may mediate the shift between automatic habit learning from enhanced reliance on previously encoded

reward prediction mediated via dorsal ACC and hippocampal structures to control goal-directed learning via the representation of goals in the medial OFC to flexibly guide responding.

Both w and perseveration capture similar repeated choices but are dissociated as a function of relevance of previously learned outcomes. Perseveration was associated with STN connectivity with premotor cortex, a region responsible for action ownership and recognition[491, 492]. Changes in perseveration for reward[493-495] are observed following STN DBS in PD. Thus, whereas habit learning implicates regions involved in the encoding of reward prediction, perseveration implicates motor preparatory regions.

Anterior and Posterior STN and Reflection Impulsivity

Lower evidence accumulation, a marker of greater impulsivity, was associated with lower resting state functional connectivity between the anterior STN and dlpfc in healthy controls, suggesting that connectivity between the dlpfc and the anterior but not the posterior portion of the STN is associated with this measure of impulsivity.

Reflection impulsivity as tested in this probabilistic inference task includes several elements such as evidence accumulation, integration and decision in the context of probabilistic uncertainty[168, 393]. This study demonstrates that connectivity of the more limbic-associative portion of the STN with right dlpfc and not the more motoric STN with dlpfc is related to greater evidence accumulation. Less evidence accumulation (higher impulsivity) as measured using the same Beads task has been previously associated with lower dlpfc volumes, as well as reduced volumes of the lateral parietal cortex and insular cortices[375]. Further support for the role of the dlpfc in the information processing required for the task comes from task-based fMRI studies. The dlpfc is involved in both the evidence seeking and the decision phases of the Beads task[168]. In another fMRI study focusing on evidence accumulation using differing proportions of coloured cards, greater uncertainty during decision execution was associated with greater activity in lateral frontal and parietal regions[393]. Similarly, in a study involving a series of rapidly shifting shapes, decision-

making in the context of uncertainty was associated with greater dlpfc and posterior parietal activity[496]. While the current finding is not direct evidence for a role of the anterior STN only, the dlpfc is widely implicated in this form of behavioural control, so the implication of anterior STN connectivity with dlpfc suggests a functional role for anterior STN and dlpfc connectivity in this type of impulsivity. Indeed, when DBS to the STN specifically targets the more motoric subzones in patients with PD, decisional impulsivity is not affected[118].

While the dlpfc has also been implicated in working memory, the current version of the Beads task controlled for working memory. Therefore, the findings suggest that active evidence accumulation under probabilistic uncertainty implicates the right dlpfc and anterior STN.

Conclusions and Limitations

The current studies demonstrate how underlying and latent neural networks that persist during rest, without any functional cognitive activation, are associated with patterns of behaviour.

There are several limitations to the current methods that might hinder any conclusions drawn. Firstly, it is difficult to consistently and definitively locate the STN in humans using the MR resolution currently employed. A recent publication suggests that reported findings for the STN can be some millimeters off a high resolution parcellation of the STN[497] and that overlap across subjects in STN location is little over 50%[498]. Reports of signals expected to be STN might therefore include significant contributions from neighbouring substantia nigra and other tissue[497]. The left STN was shown to be on average around 1mm off a high resolution map of the STN, whereas the right STN was on average up to 3.7mm off [497]. This limitation assumes that the high-resolution parcellation of the STN was perfect, although there was only around 50% overlap across the 30 participants scanned, meaning that even that would be subject to issues around inter-individual variability. While registration of all native brains to MNI space can combat this issue in some ways, there is still some

inter-individual variability in the location of the STN. These studies used the STN ROI provided by WFU PickAtlas SPM toolbox (9). This seed has overlap with a previous study focusing on the STN, which used a sphere with 3 mm radius centered on the coordinates x y z = 10, -14, -4 mm for the right STN which was selected based on an fMRI task study on stopping ability (10). Furthermore, this seed has been previously confirmed with anatomical tracings of the STN using R2* and magnetization transfer anatomical sequences (11) for 16 healthy volunteers, traced by two researchers[330]. The centers of mass for the manually traced STN (0.5, -13.5, -6.7 mm) and the STN ROI from WFU PickAtlas (0.6, -13.6, -5.6 mm) were similar. In addition, the coordinates of this STN ROI (right STN xyz= 10 -14 -4) is in the bounds of the high-resolution manually traced right STN ROI (x~ 6 to 12, y~ -11 t0 -15, z~ -4 to -10) [497].

Furthermore in the current studies, a control region was examined to asses whether the same patterns of connectivity and relationships with behaviour expected from STN were observed (reflection impulsivity). The substantia nigra is adjacent to the STN but has different connectivity and functional profiles. By demonstrating that the neighbouring substantia nigra did not show the same relationship between connectivity and behavioural performance as STN, a conclusion can be drawn that at least compared to this neighbouring region, the STN showed a distinct connectivity profile that resembles the network recruited for this task performance (reflection impulsivity). Still, by demonstrating the neighbouring substantia nigra does not show a connectivity profile associated with this task performance, does not mean that the results from the STN are true. Nonetheless, this suggests that neighbouring regions aren't contributing to the results obtained for STN. Furthermore, as these analyses were done in a large sample of healthy individuals and as normalizing registration was used, it is more likely that the signal observed to be STN is truly STN. However, there might be some contribution from other adjacent untested regions and tissue.

Another limitation is that for the analysis of anterior and poster STN, a boundary has been instigated on the STN in a hypothesis-driven manner and not demonstrated in a data-driven analysis. Imposition of a somewhat arbitrary cluster segregation influences any results and conclusions. For example, if 3 clusters were chosen instead of two then different conclusions

could be drawn. In this study, two clusters of anterior and posterior STN were chosen as representing the most motor versus limbic-associative potential subzones of STN. Previous data in this thesis suggest that there is no 'hard' boundary but that there are gradient patterns of function or connectivity throughout the STN across its multiple axes. However, for the purposes of the current analysis, a hard boundary was devised based on the posterior boundary of the functional connectivity from ventral striatum and dorsolateral PFC, two key nodes in the limbic and associative-cognitive pathways, respectively. The collation of an 'anterior limbic-associative' subdivision of STN can be useful for determining whether the most ventromedial, the most limbic-associative portions of the STN shows any functional relationship in its connectivity. indeed, as mentioned, the network previously associated with the examined behavioural measure (reflection impulsivity) was associated with anterior STN connectivity and not posterior STN connectivity. Nonetheless, these findings do not empirically demonstrate that the chosen posterior STN is not involved with this process, just that the expected 'reflection impulsivity' network links with anterior STN only when examining correlates of behavioural performance.

There are other limitations around the behavioural tasks used. There is a lot of overlap in these tasks, for example, the reversal learning task and two-step model-free model-based task both require working memory and have been linked to IQ[499, 500]. A shared or common mechanism driving behaviour on these tasks means that they are not entirely dissociable and may not implicate unique or specific processes. This is less the case for the model-free learning parameter as it is an operation of a specific computational process and its subsequent measurable effect on behaviour. However, as discussed, the reversal learning measure is a composite of acquisition learning, behavioural inhibition, and re-learning, each requiring separate but overlapping sets of cognitive processes that cannot be fully deconstructed into their constituent parts. Therefore, while the model-free model-based measures have been operationalized computationally and mark a specific cognitive processes, the reversal learning measure is less specific. There is also overlap between reversal learning and ED shifting but the ED shift requires a different set of cognitive processes, rather than what could be attributed to 'learned irrelevance'[196, 197]. During the ED shift, a novel stimulus dimension is introduced in place of the

previously irrelevant stimulus, so disengaging from learned irrelevance is not driving behavioural responses to this stimulus dimension. Repeated responding to the novel stimulus therefore indicates perseveration rather than a problem with learning that the previously irrelevant stimulus is now relevant [196, 197].

While the current study did not directly address the neural correlates of impulsivity or compulsivity at the time of the behaviour (in-scanner testing), the intrinsic neural correlates are highlighted. This elucidation of links between latent neural characteristics and behavioural or cognitive traits is interesting and important, as an understanding of the latent neural network provides insight into the default state of the system as a whole, without perturbation by cognition. Understanding the baseline characteristics of neural networks is key, before any network recruitment by task demand.

Chapter 4. Cortical Basal Ganglia Circuit Integrity and Alcohol Use

Individuals with alcohol use disorders demonstrate a range of behavioural deficits, including heightened impulsivity. As waiting impulsivity has been heavily linked with the transition towards compulsive drug intake in rodents[182], and elevated in humans with compulsive drug use[188], Experiment 1 of this section aimed to specifically examine the neural correlates of waiting impulsivity (STN, ventral striatum and subgenual ACC) in alcohol dependent individuals and binge drinkers compared to healthy volunteers, with the expectation that both groups show elevated impulsivity and abnormal functional connectivity of the associated circuit.

In Experiment 2, the microstructural features of the whole brain were examined in binge drinkers compared to healthy volunteers. Specific focus was also applied to the ventral striatum, due to previous findings of larger ventral striatal grey matter volume in binge-drinkers[324], and its role in neural proliferation associated with excessive alcohol use or motivation for reward and heightened response to rewards[394, 395] in young adults. The STN was also specifically examined. The STN has been understudied in pathological drinking groups, which is interesting given its central role in stopping behaviours[120, 143] and behavioural control that might be pertinent to control of drinking behaviours.

Methods

Experiment 1: Resting State fMRI

The STN, ventral striatal and subgenual ACC functional neural network, regions implicated in waiting impulsivity, were examined in abstinent subjects with alcohol

dependence and binge drinkers compared to healthy volunteers. The capacity for machine learning models to distinguished between pathological drinking groups and healthy volunteers based on the STN intrinsic network was also assessed.

Participants

Abstinent subjects with AD were recruited via community and university-based advertisements in Cambridge. Psychiatric disorders were screened with the Mini International Neuropsychiatric Interview. Participants were excluded if they had a current major depression or another major psychiatric disorder including substance addiction, major medical illness, or were taking psychotropic medication. Participants completed the Beck Depression Inventory [436]. Participants were reimbursed for their time and written informed consent was obtained. The study was approved by the University of Cambridge Research Ethics Committee.

Binge-drinking criteria have been previously described. Primary AD diagnoses were confirmed by a psychiatrist using the Diagnostic and Statistical Manual of Mental Disorders, Version IV criteria for substance dependence(3). The AD subjects were tested 2 weeks–1 year after abstinence and 1 week after discontinuation of long-acting benzodiazepines used during detoxification. Subjects were excluded if they had positive urine drug screens or alcohol breathalyzer test on testing day.

STN connectivity maps of 36 abstinent subjects with AD and 32 BD who underwent scanning were compared with matched HV. Age-matched HV were separately tested for each patient group (for AD, 34 HV's; for BD, 32 HV's). The BD and their matched healthy volunteers are the same as the subjects in the microstructural analysis of Chapter 1. Subject characteristics are reported in Table 4.1.

Group	M/F	Age (SD)	Verbal IQ (SD)	BDI (SD)	AUDIT (SD)
HV for BD	16/16	24.1 (3.4)	116.3 (6.3)	4.5 (4.9)	4.2 (4.6)
HV for AUD	17/17	41.4 (12.5)	117.6 (7.3)	6.3 (7.9)	3.9 (2.2)
BD	18/14	22.1 (3.3)	116.5 (5.3)	7.13 (5.4)	15.7 (5.4)
AUD	21/15	40.6 (12.1)	113.5 (6.2)	12.1 (9.1)	

Table 4.1. Subject characteristics. *Abbreviations: AUD, alcohol use disorders; AUDIT, Alcohol Use Disorders Test; BD, binge drinkers; BDI, Beck Depression Inventory; HV, healthy volunteers; M/F, male/female; SD, standard deviation; STN, subthalamic nucleus.*

Data Acquisition and Analysis

Multi-echo resting state functional MRI data was collected and analysed as described in Chapter 1. For the estimation of differences between pathological drinkers and HV's, ROI-to-voxel whole brain connectivity maps were computed for STN. These connectivity maps were entered into full factorial general linear models to compare whole-brain connectivity between groups. Whole brain voxel-wise group comparisons were performed using cluster extent threshold correction at 15 voxels at $p<0.001$ whole brain uncorrected, which corrects for multiple comparisons at $p<0.05$ assuming an individual-voxel Type I error of $p=0.01$[465]. Secondarily, for strong a priori hypothesized regions (ventral striatum and subgenual ACC), SVC analysis was used with FWE threshold of $p<0.05$. The relationship between the neural network associated with waiting impulsivity and severity of alcohol use was also examined in a proportion of the healthy volunteers (social drinkers, N=38) and binge-drinkers (N=32).

For exploratory supervised machine learning classification analysis, support vector machine was employed with Pattern Recognition for Neuroimaging Toolbox (PRoNTo) for SPM[501]. Supervised machine learning methods that automatically extract information from the data were used for classification analysis, remaining sensitive to subtle spatial differences. Support vector machine initially uses example training data that have previously been classified (i.e., patient or healthy volunteer) to identify an

optimum boundary that distinguishes the training data into the groups. This is followed by a testing phase in which the computed boundary is used to predict which group the new data belongs to in a blind manner. Finally its performance in doing this is evaluated. All patients and matched HV's were entered as two classes into one support vector machine analysis with the STN ROI-to-voxel whole brain connectivity maps as inputs. Cross validation of leave one subject out was used. This method uses data from all subjects except one from each group to train the classifier. The two data that were left out are then used to test the ability of the machine to classify between "new" data. This is repeated for all subjects allowing an unbiased estimate of generalizability. Statistical significance of classification was tested using permutation testing with 1000 permutations with random assignment of group class to input image. Significance was assigned at $p<0.05$ for the combined pathological drinking groups compared to HVs. Each drinking group was then compared to their own age-matched HV in two separate support vector machine analyses with the same parameters.

Experiment 2: Microstructure

Cortical and basal ganglia microstructural features were examined in binge drinkers compared to healthy volunteers, with a particular focus on ventral striatum and STN. Tractography was also computed for STN and compared between groups.

Methods, including participant details, data acquisition and tractography analysis descriptions are reported in detail in Data Chapter 1. Briefly, data were collected from 39 healthy volunteers and 29 binge-drinkers. The Alcohol Use Disorders Test (AUDIT)[437] and Alcohol Use Questionnaire were used to measure alcohol use severity and binge score[438]. The binge score is less susceptible to self-report estimation distortions[438]. This score incorporates the speed of drinking, the amount of times being 'drunk' in the previous 6 months and the percentage of times that an individual drinks to get drunk. This provides a measure of the pattern of drinking as

opposed to simply the amount of alcohol consumed. Therefore, one may have relatively low alcohol intake but a high binge score.

NODDI parameter maps for neurite density and orientation dispersion index were computed and entered into independent samples t-test analysis to compare between groups, controlling for age and gender. Whole-brain corrected FWE $p<0.05$ was considered significant for these group comparisons and thresholded at cluster extent of <10 contiguous voxels to remove contributions from small spurious clusters. Microstructure was correlated with drinking severity measures. Whole brain parameter maps were entered into correlation analysis with AUDIT and binge scores, separately for healthy volunteers and binge drinkers and whole-brain FWE $p<0.05$ was considered significant. To examine whether there were group differences in the ventral striatum and STN ODI specifically based on a priori hypotheses, SVC ROI analysis ($p<0.05$) was computed for ventral striatum and STN for both group difference analyses and correlations with drinking measures.

Tractography was computed for STN and compared between groups. STN-to-whole brain tracts were also correlated with alcohol use severity measures in binge drinkers. Nonparametric permutation inference estimation was performed using FSL's randomize tool[502] for both the group comparison and correlation. Significance was computed in a voxelwise FWE-corrected $p<0.05$ manner using Threshold-Free Cluster Enhancement (TFCE).

Results

Experiment 1: Resting State fMRI

The number of premature responses in the 4-CSRT task was greater in BD subjects (10.86 (SD 7.21)) compared to healthy volunteers (7.81 (SD 6.77); $p=0.041$) (Figure 4.1). There were no differences in SSRT (HV: 165.65 (SD 57.46); BD: 160.92 (SD 27.37); $p=0.320$).

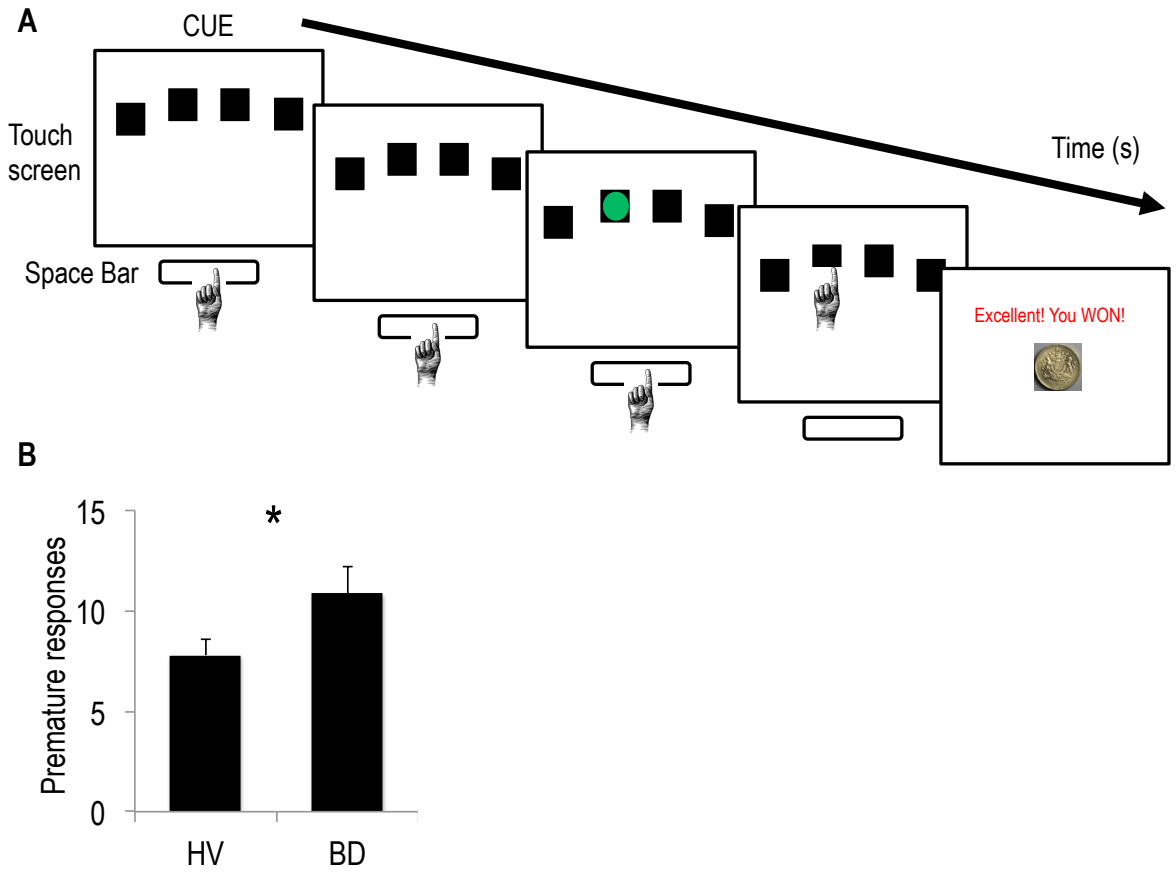

Figure 4.1. Waiting impulsivity in binge drinkers. *A. The 4-Choice Serial Reaction Time (4-CSRT) task. The cue onset prompted subjects to hold down the space bar. A green circle target appeared, to which subjects responded by releasing the space bar and touching the box on the touch screen in which the target appeared. Finally, monetary feedback was displayed. Premature responding was defined as release of the space bar prior to target onset. B. Number of premature responses of healthy volunteers (HV) and binge drinkers (BD), error bars are standard error of the mean * indicates p<0.05.*

Subthalamic Nucleus Connectivity

To establish whether STN connectivity differs with clinically-relevant alcohol misuse, STN connectivity was compared between 36 abstinent subjects with AD (Table 4.1. includes subject characteristics; reported in mean: weeks abstinent 15.78 ±17.13,

range 2-52; years heavy use 13.29 ±8.31; Units/day 29.44 ±15.31; on the following medications, acamprosate 2 and disulfiram 1) and 32 young adult subjects with BD compared to age and gender matched HV (for AD, 34 HV's; for BD, 32 HV's). Smoking status: current/ex-smokers/never: AD, 21/3/8; BD, 12/5/13; HV for BD 4/3/21; HV for AD, 5/7/19).

Group differences in STN connectivity with ventral striatum and subgenual ACC were specifically examined. Compared to HV's, both BD and AD had reduced connectivity of STN with subgenual ACC ($Z=4.32$, $p=0.002$). Both BD and AD also exhibit reduced connectivity of STN with ventral striatum ($Z=4.10$, $p=0.006$). As the combined group was significant overall, the groups were then separately compared with age-matched HVs. Relative to their matched HVs, AD subjects had reduced STN and subgenual ACC connectivity ($Z=3.47$, $p=0.040$) and BD had reduced ventral striatum ($Z=3.97$, $p=0.010$) and subgenual ACC ($Z= 3.96$, $p=0.008$) connectivity. The neural correlates of SSRT were also examined. STN connectivity with pre-SMA or dorsal caudate did not differ between groups ($p>0.05$).

Since smoking affects premature responding[188], smoking status (current or never/ex-smoker) was added as a covariate of no interest in the main group difference analysis. The main findings of reduced STN connectivity with VS and subgenual ACC in pathological drinkers remained significant. Connectivity of the STN with VS or subgenual ACC was also not different between current versus never and ex-smokers in the HV group ($p>0.05$).

STN ROI-to-whole brain voxel connectivity maps were entered into independent samples t-tests to compare groups. Group comparisons were performed using cluster extent threshold correction, calculated at 15 voxels at $p<0.001$ whole brain uncorrected, correcting for multiple comparisons at $p<0.05$ assuming an individual-voxel Type I error of $p=0.01$[465]. Cluster-extent threshold analysis revealed that both AD and BD had reduced STN connectivity with subgenual cingulate cortex (peak coordinate xyz = -45 -41 42 mm; Cluster size=45; $Z= 4.32$; $p=0.036$, Figure 4.2), and

inferior parietal cortex (xyz = 1 19 -10 mm; Cluster size=58; Z= 4.83; p=0.019) compared to HV.

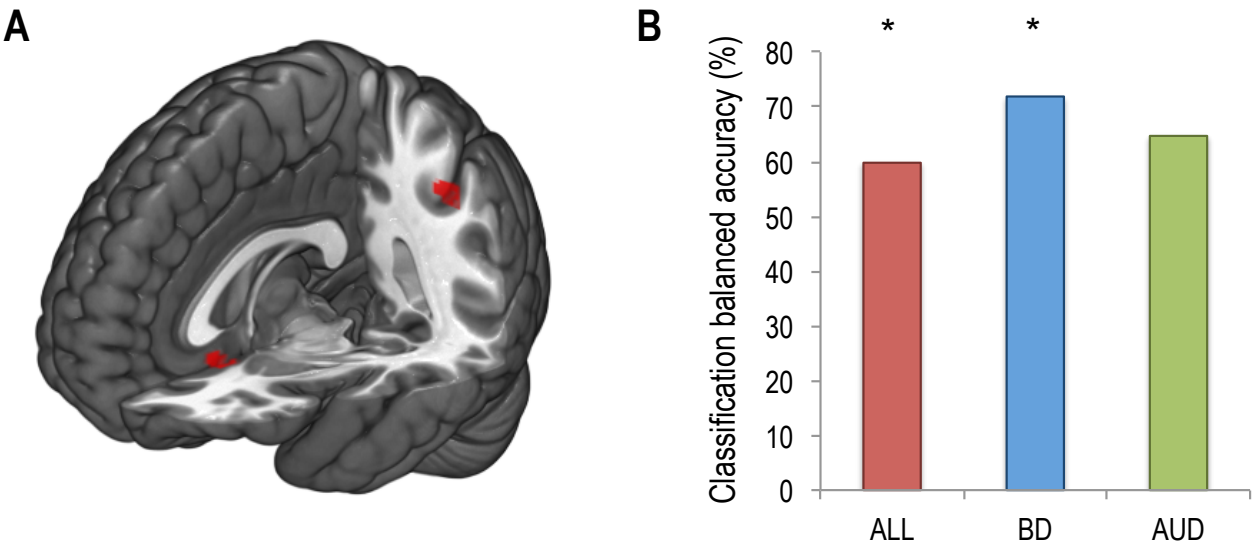

Figure 4.2. Subthalamic nucleus connectivity in binge drinkers and alcohol use disorders. *A. Independent samples t-test to compare ROI-to-whole brain voxel connectivity maps for subthalamic nucleus (STN) between groups revealed reduced connectivity of the STN with both the subgenual cingulate cortex and the inferior parietal cortex (cluster-extent threshold analysis p<0.05) compared to age- matched healthy volunteers. B. Exploratory supervised machine learning (support vector machine) significantly classified between all patient groups compared to healthy volunteers based on STN-to-whole brain functional connectivity. This was significant when comparing binge drinkers (BD) but not alcohol use disorders (AUD) individuals separately to healthy volunteers.*

Machine Learning Analysis

On an exploratory basis, supervised machine learning methods (support vector machine) were applied to STN seed ROI-to-whole brain voxel connectivity maps to determine whether patterns in the data could be used to classify between groups. Correct classification was achieved for all pathological drinking groups versus HV's with a significant balanced accuracy of 59.8% (p=0.039, Figure 4.2). AD and BD were then separately compared to their own age-matched HV: correct classification was

achieved for BD with significant balanced accuracy of 71.9% (p=0.026). AD showed an elevated balanced accuracy of 64.7% that was not significant (p>0.05).

Alcohol Use Severity and Abstinence

The neural network associated with waiting impulsivity and severity of alcohol use was examined in social drinkers (N=38) and binge-drinkers (N=32). Across both groups, AUDIT scores negatively correlated with connectivity between STN and subgenual ACC (R=-0.391, p=0.001, Figure 4.3) and with a trend correlation with connectivity between right STN and right ventral striatum (R=-0.236, p=0.052). To determine whether this represented an underlying biomarker, the HV group were examined alone. In HVs, AUDIT scores negatively correlated with connectivity between STN and subgenual ACC (R=-0.421, p=0.010) but not STN and ventral striatum (R=-0.267, p=0.11). In AD, there was a positive correlation trend between the number of weeks abstinent and STN connectivity with right VS (R=0.411, p=0.058, Figure 4.3) and no correlations with units/day or total units consumed.

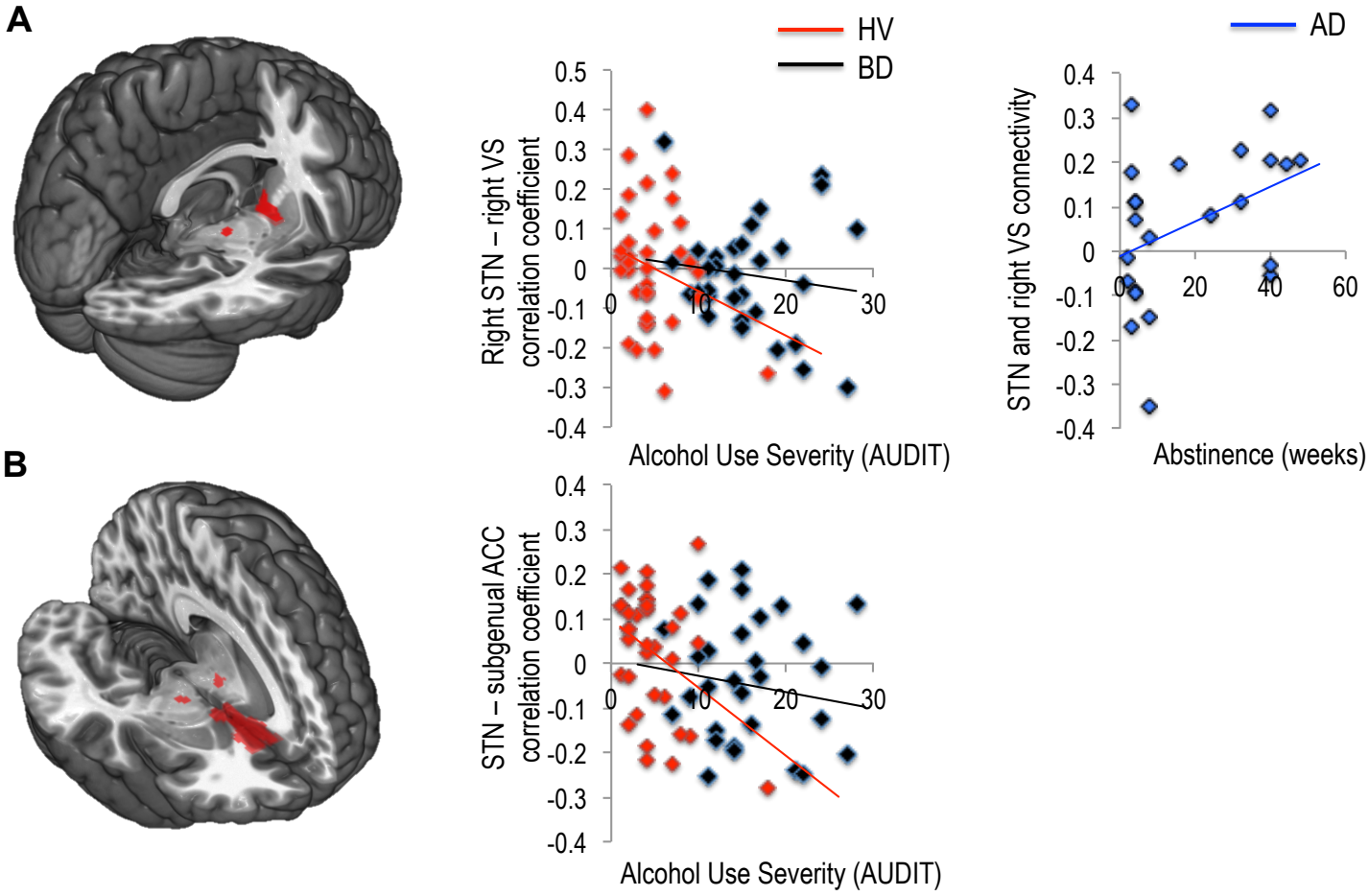

Figure 4.3. Neural correlates of waiting impulsivity and alcohol use severity. *Correlation coefficients were computed between regions of interest (ROI) as a marker of their functional connectivity. Functional connectivity between subthalamic nucleus (STN) and ventral striatal (VS) seed regions (A) and STN and subgenual anterior cingulate cortex (ACC) (B) was correlated with alcohol use disorders test (AUDIT) scores in healthy volunteers and binge drinkers and connectivity between STN and ventral striatal VS was correlated with abstinence in alcohol dependent (AD) individuals. The seed regions for ROI-to-ROI analyses are shown overlaid on MNI152 template image.*

Experiment 2: Microstructure

Participants

Participant characteristics are described in Data Chapter 1. Briefly, data from 39 healthy volunteers and 29 binge-drinkers was acquired, with no signification group

differences in age (p=0.697) or gender (p=0.102). Binge-drinkers had significantly higher 'binge score', AUDIT score and had significantly more days that they were 'drunk' and percentage that they would drink in order to get drunk in the last 12 months (see Data Chapter 1). The two groups did not significantly differ in depressive symptoms (BD, 9.636 (8.370 SD); HV, 6.973 (7.407 SD); p=0.208).

Whole Brain Microstructure

Binge-drinkers had lower grey matter orientation dispersion index (ODI) in several regions, including right dlpfc and higher adjacent white matter neurite density (whole-brain FWE corrected $p<0.05$, see Table 4.2 for further statistics) (Figure 4.4). Binge drinkers also had decreased ODI and increased neurite density in regions throughout the parietal cortex (Table 4.2). There were no differences between males and females across both groups in ODI or neurite density (FWE $p>0.05$).

	p(FWE-corr)	K	Z	x	y	z
Orientation Dispersion Index						
HV>BD						
Right Inferior Parietal Cortex	<0.001	14	>8	50	-64	22
Right Superior Frontal Gyrus (DLPFC)	<0.001	27	7.75	24	40	38
Left Middle Occipital Gyrus	<0.001	12	7.06	-28	-82	36
			6.44	-32	-78	30
	<0.001	10	6.94	-28	-74	44
Right Postcentral Gyrus	<0.001	22	7.05	34	-34	58
Left Superior Parietal Lobule	<0.001	10	6.42	-24	-58	62
BD>HV						
Right Angular Gyrus	<0.001	26	7.84	50	-60	26
	<0.001	15	7.33	-40	-76	32
	<0.001	12	6.43	42	-58	40
	<0.001	10	5.74	-42	-62	20
Left Superior Parietal Lobule	<0.001	22	7.19	-22	-64	52
Right SupraMarginal Gyrus	<0.001	22	6.95	56	-42	40
Left Inferior Parietal Lobule	<0.001	12	6.89	-40	-40	46
	<0.001	16	6.06	30	-42	56
Neurite Density						
HV>BD						
Right Angular Gyrus	<0.001	19	7.77	46	-58	26
	<0.001	12	6.61	54	-48	30
Left Middle Occipital Gyrus	<0.001	16	6.59	-38	-74	32
Right Postcentral Gyrus	<0.001	15	6.08	32	-38	48
BD>HV						
Inferior Parietal Cortex	<0.001	20	>8	48	-64	22
	<0.001	13	6.82	34	-84	22
			5.68	36	-76	22
	<0.001	10	6.04	44	-76	12
Right Superior Frontal Gyrus (DLPFC)	<0.001	27	7.71	24	38	38
Left Middle Frontal Gyrus (DLPFC)	<0.001	21	7.44	-28	40	26
	<0.001	20	6.6	-22	30	38
Right SupraMarginal Gyrus	<0.001	29	7.57	54	-44	32
			6.06	54	-46	42
Right Middle Frontal Gyrus	<0.001	19	6.33	38	12	48
Right Superior Frontal Gyrus	<0.001	12	6.18	26	-8	58

Table 4.2. Statistics of group differences for neurite density and orientation dispersion. *Abbreviations: p(FWE-corr), whole brain (P<0.05) family-wise error corrected P value; K, cluster size; Z, Z-score; xyz, peak voxel coordinates; BD, binge-drinkers; HV, healthy volunteers; DLPFC, dorsolateral prefrontal cortex.*

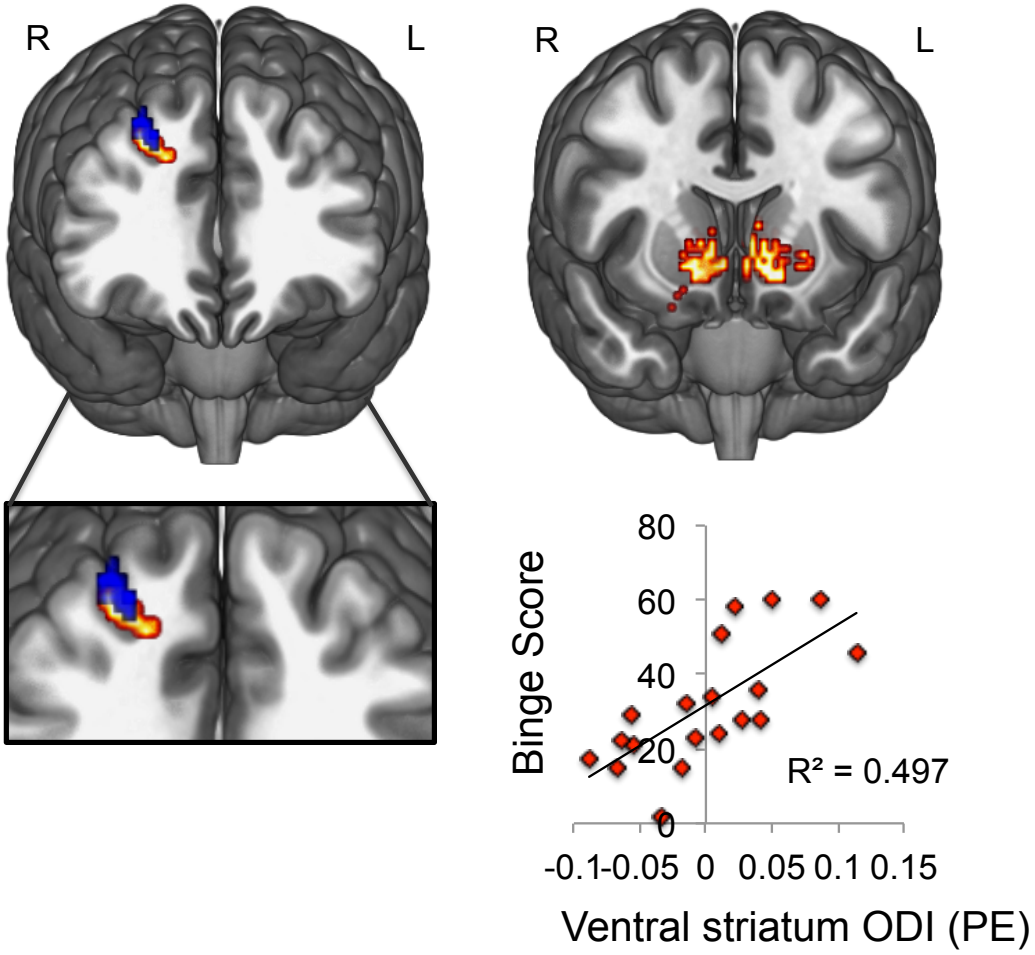

Figure 4.4. Lower dorsolateral prefrontal cortex (dlpfc) but higher ventral striatal orientation dispersion in binge-drinkers. *Left: Clusters illustrate regions of significantly higher white matter neurite density (red) and lower grey matter orientation dispersion index (ODI, blue) in dlpfc of binge drinkers compared to healthy volunteers (displayed at p<0.001 uncorrected threshold for visualization purposes). Right: Small volume corrected family-wise error p<0.05 analyses revealed that binge drinkers had reduced orientation dispersion index (ODI) in ventral striatum (VS) compared to matched controls. Left sided peak ventral striatal ODI (peak coordinates, xyz= -6 12 0) positively correlated with binge score in binge drinkers. Images are displayed on a standard MNI152 template; R, right; L, left.*

Binge-drinkers had higher bilateral ventral striatal orientation dispersion compared to healthy volunteers (peak coordinate at left ventral striatum, xyz= -6 12 0; VS small volume corrected (SVC) FWE p=0.003; Z=4.62)(Figure 4.4). Binge drinkers had higher STN ODI (SVC FWE, p=0.039, Z=3.06, xyz= -12 -12 -2) (Figure 4.5) compared to HV.

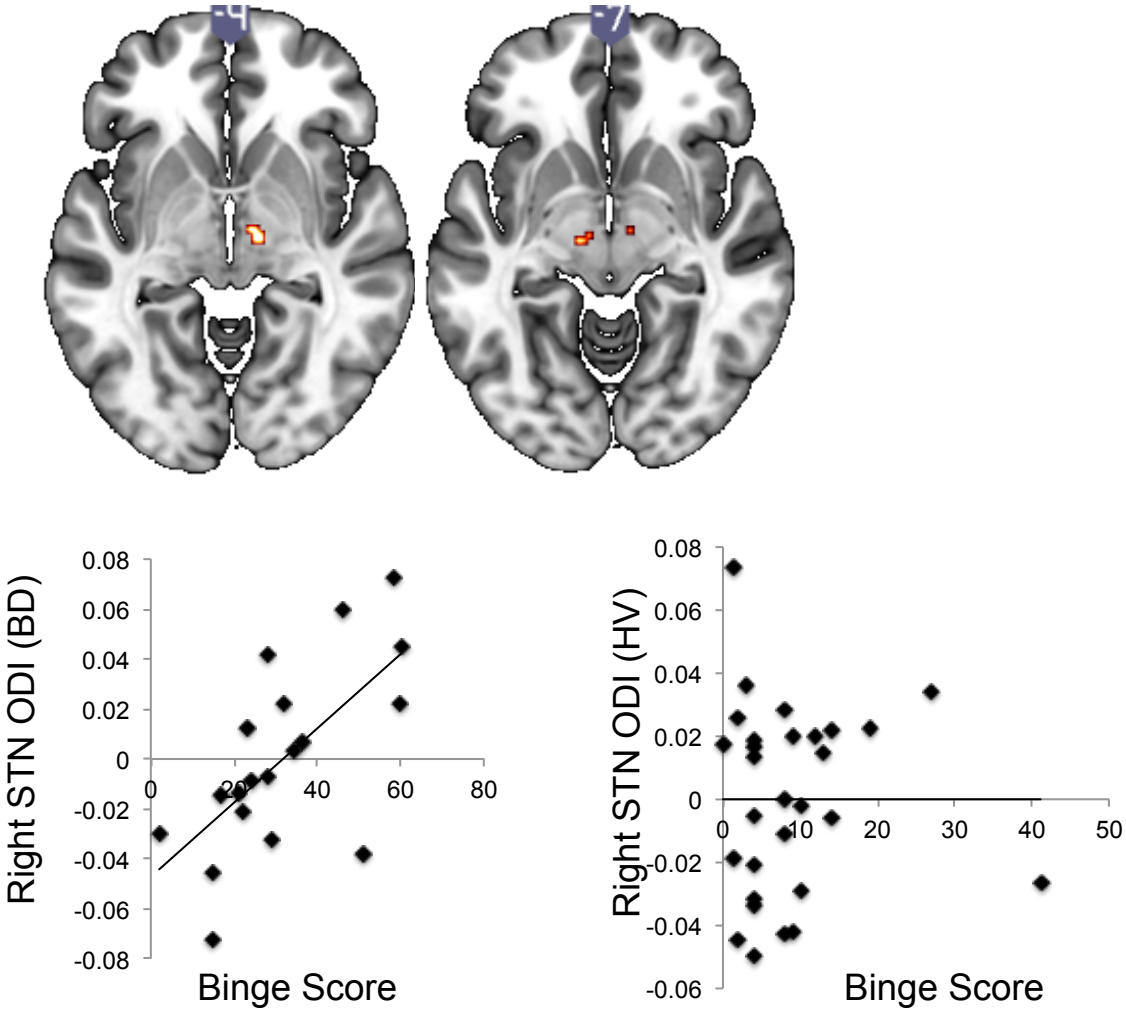

Figure 4.5. Higher subthalamic nucleus (STN) orientation dispersion in binge-drinkers. *Top: Binge drinkers (BD) had higher orientation dispersion index (ODI) of the STN compared to healthy individuals (HV). Bottom: STN ODI was positively correlated with binge score in BD but not in HV.*

Binge drinkers show a positive correlation between ventral striatal ODI and binge score (bilateral ventral striatum SVC FWE p=0.011; Z=4.32, peak xyz= 12 14 -8)

(Figure 4.4) but not AUDIT (p>0.05). To explore the specificity of these findings, we controlled for AUDIT in the binge score correlation, which did not affect the significance of the findings (positive correlation between right ventral striatum ODI and binge score controlling for AUDIT in binge drinkers: SVC FWE p=0.012). Binge drinkers also showed a positive correlation between right STN ODI and binge score, controlling for AUDIT (bilateral STN SVC FWE p=0.010, Z=3.51, xyz=12 -14 -6) (Figure 4.5). There was no relationship between STN ODI and AUDIT in binge drinkers (p=0.567) or healthy volunteers (p=0.505). No significant correlations between ventral striatal or STN ODI and drinking severity were observed in healthy volunteers.

Tractography

In binge drinkers only, there was a negative correlation between STN connectivity with ventral striatum and binge score (Figure 4.6, TFCE p<0.05). Across both groups, binge score positively correlated with anatomical connectivity between STN and right inferior parietal cortex (Figure 4.7, TFCE p<0.05).

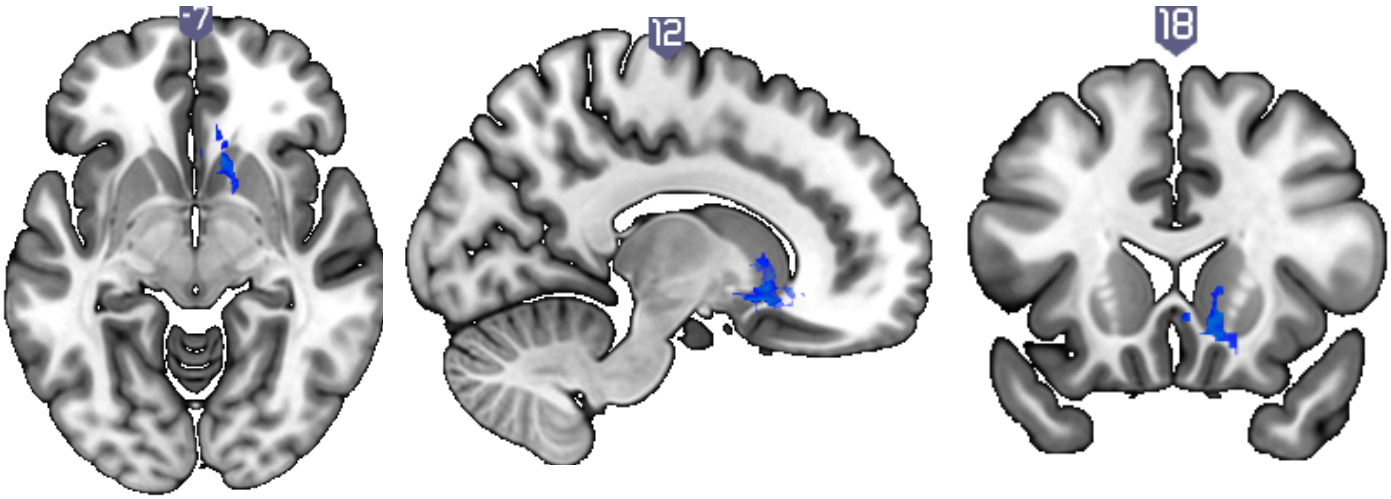

Figure 4.6. Subthalamic nucleus tracts and binge score. *Tracts from bilateral subthalamic nucleus reaching ventral striatum were negatively correlated with binge score in binge drinkers (Threshold-Free Cluster Enhancement p<0.05). Displayed at p<0.1 for illustration purposes.*

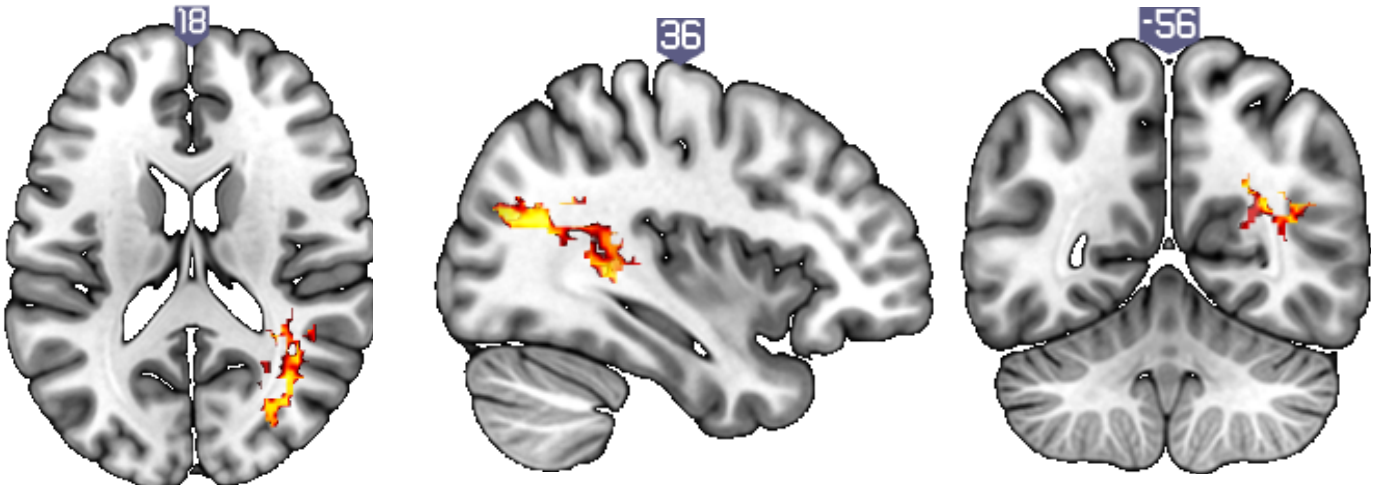

Figure 4.7. Subthalamic nucleus tracts and binge score. *Tracts from bilateral subthalamic nucleus reaching inferior parietal cortex were positively correlated with binge score across both binge drinkers and healthy volunteers (Threshold-Free Cluster Enhancement p<0.05).*

Discussion

Functional Connectivity

Due to the strong relationship between waiting impulsivity and compulsive drug use[128, 182, 188], the neural correlates of waiting impulsivity were examined in individuals with BD and AD. Intrinsic resting state functional connectivity between STN, ventral striatum and subgenual ACC were found to be disturbed in these pathological drinking groups. There was decreased connectivity between the STN and subgenual ACC and ventral striatum in BD and AD compared to healthy volunteers. Furthermore, in healthy social drinkers, the degree of alcohol severity correlated negatively with connectivity between the bilateral STN and subgenual cingulate. This suggests this circuit as a potential early clinical marker or underlying endophenotype.

Machine-learning classification revealed that patient groups can be distinguished from healthy individuals simply based on their STN-to- whole brain functional connectivity, a finding that has key clinical relevance given that the requirements for this test are a

single MRI scan, rather than group data (once the machine has been trained). STN connectivity differentiated the combined group of BD plus AD from social drinkers (healthy volunteers) and while STN and whole brain connectivity classified pathological drinking groups versus healthy volunteers, it was not sufficient to classify between AD alone and healthy volunteers. Also, the accuracy for both groups was low, around 58%. This might be due to the combination of both groups together and while there are shared deficits across these groups, they are also very different. The AD group were older and were diagnosed with alcohol dependence, a stringent criteria to meet, indicating higher severity of alcohol use. The binge drinkers were younger and not diagnosed with any alcohol or substance use disorders. Therefore to combine them as one homogenous group is inaccurate. When separating the groups, both groups were more accurately classified, with binge drinkers reaching 72%, an interesting classification level given that they have not been diagnosed with any psychiatric or neurological condition and are generally healthy. The balanced accuracy in AD, while elevated, failed to reach significance. This may be related to abstinence in this group as there was a trend towards stronger connectivity between STN and ventral striatum with longer abstinence. This may also explain why there were no significant group differences of STN and ventral striatal connectivity for AD. Leave-one-out cross-validation reduces over-fitting issues by splitting the data into the training and testing sets, using the testing data as ‘new’ data to test the validity of the model[276]. There is however room for improvement on the current findings, for example by including more modalities, clinical or behavioural data, or from advancements in algorithmic design[276]. Incorporating more measures into the model would provide improved classification accuracy, although there is a balance of over-fitting that must be considered. That STN-to-whole brain functional connectivity only can distinguish patients from controls above chance is promising, as it is one [3D] measure that can be quickly acquired. Separating the STN-to-whole brain resting state connectivity and running SVM on that data combines theory and data –driven approaches. Further studies should examine how adding behavioural measures and data from other imaging modalities might improve classification accuracy.

Together, the findings suggest that the neural correlates of premature responding, particularly connectivity between the STN and subgenual ACC, may be endophenotypic markers of alcohol misuse but that STN and ventral striatal connectivity may act as a neuroadaptive marker.

Microstructure and Anatomical Connectivity

This is the first study demonstrating reduced orientation dispersion index, a proxy of neurite complexity, in the frontal cortical grey matter of binge drinkers. Neurite density was higher in cortical white matter in adjacent regions of lower orientation dispersion index in binge drinkers. Thus, while there is a weak relationship between orientation dispersion index and neurite density [430], the current study suggests their joint disturbance in binge drinkers. The ventral striatum and STN showed higher orientation dispersion index that was associated with binge severity in binge drinkers.

As discussed previously (Chapter 1), the current measure of orientation dispersion index or dendritic complexity relates to higher order computaions in grey matter[434]. Thus, lower dlpfc orientation dispersion index in binge-drinkers may reflect a reduction in the highly dispersed dendritic tree organization expected in high-level cortical regions. Indeed, this converges with observations that binge-drinking in young adults is associated with significant attentional and executive functioning deficits subserved by dlpfc[503-505]. Furthermore, alcohol craving is associated with dlpfc activity[506] and modulation of dlpfc with transcranial direct current stimulation reduces craving in individuals with alcohol use disorders[507].

Previous studies of grey matter volume in pathological drinkers have yielded mixed results. There have been reports of lower ventral striatal volume in AD[508-510] and of an association between higher incidence of familial AD and greater left ventral striatal volume[511]. Binge-drinkers seem to have enlarged ventral striatal volume[324] influenced by gender[512]. However, the current measure is distinct from volume and an increase in ventral striatal orientation dispersion index could indicate enhanced cell

proliferation due to neuroplastic responses to alcohol insult or higher recruitment of this region that drives motivation for alcohol. For example, chronic psychostimulant use increases dendritic arborization in the ventral striatum of rodents[513] and plasticity of nucleus accumbens mediates the reinforcing effects of ethanol[514]. The link between ventral striatal dendritic complexity and binge drinking score but not general alcohol use severity suggests that the behavioural binge pattern of alcohol intake (rapid and frequent bouts of heavy drinking) is associated with ventral striatal neurite integrity.

Furthermore, lower anatomical connectivity between STN and ventral striatum was associated with more severe binge drinking behaviour in binge drinkers. This relationship between binge drinking and increased STN and ventral striatum complexity but reduced connectivity potentially suggests enhanced functioning or plasticity of these regions (that either drive motivation for drinking or are a result of repeated drinking cycles) but a disconnection between them. Thus, the more limbic basal ganglia indirect pathway integrity might be reduced or disconnected, potentially suggesting reduced inhibitory control in the limbic or reward-motivation domain.

Discussion

This thesis explored three major aims. The first was to map the intrinsic cortical – basal ganglia circuitry in healthy humans, using multi-echo rsfMRI. The second aim was to elucidate the functional relevance of these dissociable circuits by examining their relationship with discrete measures of impulsivity and compulsivity, which should implicate dissociable systems. Finally, the third aim was to examine which of these circuits might be disturbed in a disorder characterized by increased impulsivity and compulsivity, AD and in binge drinkers. The experiments maintain a specific focus on the STN throughout, due to several reasons: its pivotal role directing the information flow of the cortical – basal ganglia circuitry by modulating basal ganglia output; due to infrequent characterization of the role of the STN in non-motor faculties, possibly due to lack of technical capability to examine such a small subcortical structure; and due to its implication in several facets of impulsivity (waiting[177-180] and stopping[128, 460, 461]); and compulsivity (habit suppression[489, 490] and perseveration[493-495]). The multi-echo resting state fMRI method employed provides improved signal and data quality for examining this small subcortical structure.

Mappings

Segregated intrinsic cortical – basal ganglia circuits were first demonstrated, alongside a more detailed mapping of cortical connectivity with STN. This important replication of non-human primate tracer studies[109] demonstrates that more fine-grained connectivity mapping can be performed in healthy humans and that multi-echo rsfMRI provides enhanced data quality for this task. Demonstrating discrete subzones of functional connectivity is important not only for basic physiological questions around functional organization, but also provides a means of examining potential disruption of specific functional organization. For example, detailed characterizations of functional organization in healthy humans will illuminate sites of disorganization in patient

populations. By defining the behavioural relevance of these connections, a model can be built of how connectivity changes in some groups might disturb specific behavioural or cognitive faculties too. Applications of these findings include transcranial magnetic stimulation, which when applied to target surface cortical regions, can modulate the connectivity of those regions with other cortical and subcortical structures[515, 516]. The more fine grained mapping of specifically defined seed regions in the current studies will provide more directed targets for stimulation intervention.

The mapping of cortical – basal ganglia circuits followed expected patterns and these results take forward previous evidence of cortical – basal ganglia circuit organization by demonstrating the ability of resting state functional MRI methods to measure their properties. By examining circuit or connectivity strength or patterns in healthy humans, the ground can be laid for understanding disturbed circuit dynamics in disordered populations.

The more novel and interesting demonstration of limbic and associative-motor subzones of STN shows the possibility of dissociating small regional subzones based on functional connectivity that are behaviourally relevant. Interestingly, the ACC had the strongest functional connectivity with STN. This is surprising given the more general role of the STN in motor functions and stopping[120, 121, 156]. However, if considering the STN as a more global 'halt' system that mediates information flow through the cortical – basal ganglia circuitry, to guide cognitive or motor programs in light of changing or new environmental information, the relationship between ACC and STN connectivity is more understandable. The dorsal ACC has widespread connections with other cortical regions involved with affective, cognitive and motor processing, with a more general role in monitoring these processes in situations of conflict[217]. As the ACC does not necessarily predict behavioural choice responses[217] it must engage a downstream structure (that receives convergent sensorimotor information) to modulate behaviour. Indeed, a discrete population of STN neurons responds to errors[517] and conflict during decision making[518]. Mechanistically, STN stop-related excitation signals to substantia nigra are needed before striatal movement-initiating inhibition reaches substantia nigra, in order to successfully inhibit movement[145], creating a

‘race’ between these inputs to substantia nigra. Therefore, the STN serves as halt system that includes motor stopping but extends beyond motor function to the more cognitive and decision making realm. Evidence for this is demonstrated by links between the STN and medial PFC (that could include ACC[518]) when response adjustments are needed in situations of high conflict[518].

Together, the current findings support a model whereby the STN receives extensive and diverse cortical innervations carrying information that is vital for choice or action updating, with the STN acting at a crucial site to modulate motor or cognitive programs passing through the cortical – basal ganglia circuitry. This suggests that the STN, via inputs and directives from dorsal ACC based on error detection and correction information, pauses behaviour or cognition in situations of conflict, allowing new, updated information to guide dynamic behaviour (for example including valuation or motivational state updating from OFC[519]). The question of where action, choice and decision values are computed is not addressed in the current studies but the expected locus of convergence of sufficient information to pause or drive pre-selected behaviours is seemingly the STN. The current findings and suggestions coincide with the high degree of convergence of diverse cortical inputs to STN observed in non-human primates, where diffuse projections allow extended interfaces between sites of cortical innervations, for complex processing and information integration by the STN[109].

The STN is of course accompanied by myriad other cortical and subcortical structures that mediate the regulation of behaviour. Importantly, the adjacent substantia nigra is a source of contamination of the observed STN signal in fMRI experiments[497]. The current studies took steps to ensure that the observed data was not due to contamination by neighboring signals by demonstrating that the substantia nigra did not display any similar correlations with measures of compulsivity as STN. Furthermore, there are hundreds of unique subcortical structures or nuclei yet to be explored in humans due to low resolution functional imaging[520]. The current studies demonstrate that while voxel size is still rather too large to delineate subzones of structures smaller than the STN, some signal compared to noise can be regained by use of multi-echo

acquisition and denoising. This will inevitably be helpful as the emergence and use of ultra high field MRI continues to improve voxel size and spatial resolution.

Functions

The main experimental findings of this thesis regard behavioural or cognitive neural correlates. There was some broad separation between limbic, associative-cognitive and motor circuits implicated in divergent behavioural measures, although there was also some convergence, discussed below. This is the first presentation of the neural correlates of waiting impulsivity in healthy humans.

Reward-Motivated Goal-Directed Behaviour

There was some convergence of the neural networks implicated in goal-directed model based behaviour and waiting impulsivity, in that they implicated limbic indirect pathways. Model based behaviour was associated with medial OFC, ventral striatum and STN connectivity and waiting impulsivity with subgenual ACC, ventral striatum and STN connectivity. While both involved STN and ventral striatum, they diverged in the cortical node of origin (and/or target, as directionality is not tested in the current studies). These measures of goal-directedness and impulsivity are divergent but they do converge on the common processes of reward-related action choice and restraint. During the model-based task, participants must select between stimulus-pairs and in order to be more ‘model-based’, they must withhold responses for choices that have been previously rewarded, maintaining an understanding of overall task structure rather than simply choosing the most recently reinforced action. This type of response inhibition is necessary when other cognitive information must be incorporated into response choice, a mechanism that can be ascribed to STN. As such, the STN might receive future or state-relevant information from the OFC to ensure responding is not biased to the previously reinforced choice. Indeed, while the OFC responds to magnitudes of rewards and punishments[210], it updates valuations in line with current motivational states, rather than object reversal learning per se[519]. Re-evaluating

changing outcomes recruits OFC in mice and OFC inhibition and activation impairs and enhances goal-directed behaviour, respectively[521]. Furthermore, while learned stimulus – response – outcome associations important for goal-directed behaviour may not necessarily be represented by OFC[522], this structure seems to be recruited when that learned information is needed for mediating behavioural adjustments[522].

On the other hand, the subgenual ACC was implicated in waiting impulsivity. The waiting impulsivity measure similarly tests an ability to withhold responding for the ultimate purpose of obtaining a goal (monetary reward) but the participant does not need to update choices or responses for a dynamic goal and as such, valuation computations are not necessary to guide behaviour. Therefore the valuation-updating function of the OFC is not needed during this task. The dissociation between the OFC-limbic circuit and subgenual ACC-limbic circuit in goal-directed control and waiting impulsivity, respectively, is reflected by a study demonstrating that OFC but not infralimbic (equivalent to human subgenual ACC) lesions in non-human primates impairs devaluation for food rewards[523], meaning that the OFC but not subgenual ACC is involved with flexibly updating behaviour in response to changing choice-outcome contingencies.

A unique behavioural process accessed during the waiting impulsivity task is the holding or active inhibition of behavioural responses during the expectation of a positive, rewarding outcome. This process can be facilitated by subgenual rather than dorsal ACC. While the dorsal ACC is involved with more effortful task processing than the subgenual ACC, the subgenual ACC is involved with autonomic control and the parasympathetic drive of arousal responses that support cognition[524]. Indeed, recent evidence indicates that the subgenual ACC maintains arousal states during the expectation of a positive outcome[525]. Together, these findings suggest that the subgenual ACC might recruit the behavioural ‘pause’ function of the STN when it is necessary to wait for an upcoming reward, and that it acts to maintain elevated arousal levels to facilitate the ongoing inhibition of a response, and potentially the initiation of a response when it is ultimately due.

Both measures of goal directed behaviour and waiting impulsivity implicated ventral striatum and STN. Dopaminergic afferents to the ventromedial striatum arising from the VTA[7, 32, 33], can act as a 'Go' signal for foraging or exploration[34] and striatal dopamine has been shown to encode rewarding properties of unconditioned and conditioned stimuli, as well as an unexpected presence or absence of reward and its magnitude[40-43]. Encoding of reward outcome related information in the ventral striatum is thus crucial for directing motivated behaviour towards an apparent environmental goal. Environmental stimuli that can trigger VTA release of dopamine to the ventral striatum include natural rewards (food, sex) and drug rewards (cocaine, nicotine)[33, 35, 36], which engender appetitive approach behaviours that are necessary for both tasks. Since the current studies used ROI based methods, or the STN as a seed, they were unable to assess which subzones of STN were involved in the measures of goal-directed and waiting behaviours. While discrete subzones have been demonstrated in the current healthy populations, adding correlational analyses to examine differences in clusters of very few voxels would be problematic. Further studies at higher field MRI that provide finer anatomical detail and smaller voxel size are needed to dissociate STN functional subzones on this more subtle, behavioural level.

Motor Control

Findings from other behavioural measures were less dissociable on a circuit-based level. For example, motor stopping included both motor (pre-SMA) and cognitive-associative (dorsal caudate) involvement, as well as STN. Perseveration similarly included motor (premotor cortex) and cognitive-associative (lateral PFC) regions, again converging with STN. This suggests involvement of traditionally dissociable functional circuits (motor and cognitive-associative) as well as dissociable pathways (indirect and hyperdirect). The involvement of the pre-SMA and premotor cortex in stopping and perseveration was expected as they are traditionally considered motor preparatory and initiatory regions[491, 492, 526]. The pre-SMA is more involved in updating motor

plans[527], pertinent to a sudden need to stop during the SST rather than continuation of a current choice or action as measured by perseveration. Indeed the perseveration measure is not a purely motor process by any means. Perseveration as measured here is defined as a continued choice (plus response) that requires cognitive control of response selection (or lack thereof), rather than only a continued motor response. The implication of a cortical cognitive node in this behaviour is therefore more expected. The lateral PFC has a well-established role in instigating cognitive control of behaviour by mediating premotor and other posterior associative regions, selecting appropriate premotor and associative representations[528] and linking with short term memory stores[529] to guide behaviour. As discussed previously, subzones within the lateral PFC serve discrete cognitive roles, with dorsal regions monitoring and selecting goal-directed representations and the ventral regions maintaining them in working memory[530]. Again, both processes converge on STN as a mediator of diverse behavioural control systems. However, there was no functional connectivity between right IFC and STN related to stopping. This was surprising given previous demonstrations of anatomical connectivity between right IFC and STN and the functional role they together play in stopping[120, 121, 156]. This lack of finding may be related to the functional characteristic demonstrated in Chapter 1 of lower intrinsic, resting functional connectivity between IFC and STN (compared to between pre-SMA and STN). While previous evidence suggests that the right IFC mediates the hyperdirect control of the STN by pre-SMA[531], further evidence is required to tease apart the relative contribution of each cortical region to motor stopping.

Cognitive Flexibility

There was similar ‘mixing’ of neural pathway involvement with the more cognitive measures, which implicated cognitive-associative and limbic circuits. The current findings reflect previous demonstrations that attentional control and cognitive set shifting are associated with dlpfc integrity[265, 532, 533] and reversal with the OFC[200, 265, 534]. The dlpfc is largely recruited when stimulus dimensions change and engender a required shift in attention or valuation[25, 535]. In the current work,

shifting and reversal learning converged on ventral striatum and not dorsal caudate, the latter having been previously implicated in ED shift errors but this was in patients with OCD[536]. However as discussed previously, the nucleus accumbens has also been implicated in set shifting[479] and as both shifting and reversal learning require behavioural adjustments for an ultimate monetary goal, it fits that this reward-monitoring structure is involved.

The demonstration of the involvement of lateral OFC and ventral striatal connectivity in reversal learning for both monetary gain and loss is interesting given dissociations in their roles in processing valence. The ventral striatum has been implicated in reward or gain processing[537] whereas the posterior striatum[538] and anterior insula[539] have been more associated with loss. However, the ventral striatum still seems to play a role in loss processing as the presentation of a monetary loss engenders a sharp drop in both caudate and ventral striatal activity[537]. Indeed the striatum encodes predication errors for both reward and loss[538, 540], but with more anterior striatum encoding reward prediction errors and more posterior regions encoding loss[538]. The lateral OFC has also been preferentially implicated in loss rather than reward processing (the latter subserved by more medial regions of the OFC)[210] but plays a significant role in reversal learning in general. Studies of inhibition and reversal often employ negative feedback, meaning that it is less clear whether the OFC processes punishment-related information or inhibition itself. However, a recent study did also demonstrate that the lateral OFC was involved with reversal learning for both monetary reward and shock punishment[534].

The current studies also demonstrated that connectivity between the anterior associative-limbic STN and dlpfc was associated with greater evidence accumulation or reflection impulsivity. Reflection impulsivity as tested in this probabilistic inference task includes several processes including evidence accumulation, integration and decision in the context of probabilistic uncertainty[168, 393]. Uncertainty has been associated with greater activity in lateral frontal and parietal cortices[393] and implementing a decision in a state of uncertainty has been associated with greater dlpfc activity[496]. Less

evidence accumulation (higher impulsivity) in the Beads task has been associated with lower dlpfc, parietal cortex and insular cortex volume[375] and the dlpfc is recruited during evidence seeking and the decision phase during this task[168]. Similarly, the STN has been associated with early responding and lower evidence accumulation in the context of conflict or competing responses[50, 541-543]. Interestingly, STN DBS to the motor portion in patients with PD has no effect on evidence accumulation during the Beads tasks[544]. However, recent evidence indicates that DBS to the limbic-associative portion decreases evidence accumulation during probabilistic inference in patients with OCD[117]. This, together with the current implication of anterior-limbic STN and dlpfc connectivity in reflection impulsivity, highlights a dissociation in function between the limbic-associative and motor STN for decisional impulsivity.

Habit

The least convergent evidence is for the neural correlates of habit formation or habit learning. Model free habit learning implicated connectivity between posterior putamen and SMA, as well as STN with dorsal ACC and hippocampus. Traditionally, there has been a dissociation between hippocampal goal-directed navigation and dorsal striatal reinforcement driven behaviour[545-547]. For example, hippocampal damage is associated with impairment in a win-shift task, whereas dorsal striatum damage is linked with win-stay task impairments, demonstrating the importance of these structures for behavioural updating and repeating previously rewarded behaviours, respectively[546]. Goal-directed behaviour can be directed by representations of future paths encoded in the hippocampus[548] and representation of future reward by the ventral striatum[549]. However, the dorsal striatum encodes neither of these types of information and instead seems to encode action-relevant state representations[550] and has been implicated in more model-free habitual learning and responding[463].

An explanation for the potential role of the hippocampus in model-free behaviour can come from an understanding of its role in directing behaviour during earlier stages of learning. The hippocampus encodes upcoming paths of a decision tree, at points when

an animal pauses before choosing the next steps[550]. Thus, by linking with the STN to pause behaviour or action at the necessary time, the hippocampus can have time to search potential paths to inform current decision making. The dorsal striatum does not show this type of 'future path' information processing[550] and in early stages of model-free learning, when the cue-response association has not been fully learned yet (and therefore behaviour is not wholly driven by stimulus-response associations), the hippocampus might be involved with guiding choice behaviour down a path associated with previous rewards, a process that the dorsal striatum is not equipped to carry out. Indeed the hippocampus has been shown to encode reward prediction[163], which is necessary for the reinforcement learning that drives model-free behaviour[475]. Therefore there might be different neural mechanisms driving early and late stages of model free learning. The hippocampus might be recruited more than dorsal striatum at early stages before stimulus-response associations have fully formed and when future path outcome information is needed to guide a decision. On the other hand, at later stages of model-free learning, the dorsal striatum can take over when more established stimulus-response learning can drive habitual behaviour.

As discussed, there is strong intrinsic connectivity between dorsal ACC and STN and a potential functional role for this connection is highlighted here. As mentioned, the dorsal ACC can monitor a range of cognitive processes in situations of conflict or effortful task processing[217, 524] and could link with the STN to pause cognitive or motor processing when behaviour must be adjusted. In the context of habit learning, conflict resolution may be relevant in resolving choices that involve switching between strategies. Furthermore, the dorsal ACC receives extensive projections from dopaminergic midbrain projections and is also implicated in reward prediction and prediction error for guiding reinforcement driven behaviour[487, 488], which is necessary for guiding model-free behaviour. Links between the STN and dorsal ACC have been exemplified by studies in PD patients, whereby STN DBS reduces cerebral blood flow in the dorsal ACC[474, 489]. Finally, STN hyperactivity in PD is associated with more habitual behaviour as measured by random number generation that requires habit suppression[551], and this impairment is improved by STN DBS in this

group[490]. Therefore, the STN may play a role in mediating the shift from goal directed behaviour modulated by flexible valuation processing by ventral striatum and OFC, to more behavioural choice paths driven by reward and reinforcement mediated by hippocampus and dorsal ACC, and that in later stages of habit learning the dorsal striatum and motoric cortical regions take over to drive behaviour based on strongly learned stimulus-response associations.

Problematic Drinking

The third and final aim was to examine which of the explored circuits might be disturbed in individuals with AD and in binge drinkers, who have deficits in impulsive and compulsive behavioural control (heightened waiting impulsivity demonstrated in Chapter 3 and [188]). Several stages of alcohol addiction have been proposed, each associated with alterations in both cortical and subcortical regions. An initial binge-intoxication stage, subserved by the mesolimbic dopamine system (VTA/ ventral striatum) is followed by compulsive habitual responding[63], withdrawal and negative reinforcement (amygdala/ ventral striatum) and craving and preoccupation (prefrontal cortex) which together facilitate the maintenance of alcohol use[552].

The main findings centre on the neural correlates of waiting impulsivity, which has been repeatedly and reliably demonstrated as being elevated in compulsive drug use[128, 182, 188]. Connectivity between the STN, ventral striatum and subgenual ACC underlies the behaviour of waiting impulsivity in healthy humans. Functional connectivity within this circuit was significantly reduced in individuals with AD and binge drinkers. Indeed, STN centric functional connectivity with the whole brain was sufficient to accurately classify between healthy and pathological drinking groups, driven in part by the connectivity between STN and subgenual ACC. The neural correlates of stopping (connectivity between STN, pre-SMA and dorsal caudate) did not differ between groups, implicating the relevance of the ‘waiting’ circuit instead. The role of the ventral striatum in excessive alcohol use and heighted motivation for rewards is well documented in young adults[394, 395] but the STN has been understudied in

pathological drinking groups. These findings highlight an intrinsic control role for the STN in modulating reward seeking behaviours that is disturbed in binge drinkers and individuals with AD.

The current demonstration of the relevance of the waiting impulsivity 'circuit' dysfunction in both AD subjects and binge drinkers coincides with the Research Domain Criteria project that includes impulsivity as a behavioural risk factor for alcohol and substance dependence and compulsivity more generally[63, 182-184, 217]. Further evidence for the role of impulsivity as a premorbid neuropsychological risk factor comes from familial studies indicating that even siblings of chronic drug users show higher trait impulsivity[278, 279]. The current findings of not just a behavioural deficit in both groups but a circuit deficit links this important neuropsychological measure to neural function, providing a platform for further development of neurobiological markers of disease propensity. These studies suggest that functional connectivity of the basal ganglia represents a neurocognitive or neurophysiological risk state for binge drinking or AD.

Furthermore, STN and subgenual ACC functional connectivity was associated with more severe alcohol use in the healthy population alone suggesting a potential premorbid risk factor. Connectivity between STN and ventral striatum was somewhat normalized in AD individuals who had already undergone prolonged abstinence. Reduced NAc volume in alcohol dependent subjects has been previously shown to increase with prolonged abstinence[509], suggesting structural repair in this region when alcohol insult is removed. These findings were further corroborated by the demonstration of disturbed microstructure in ventral striatum and STN of current binge drinkers and that anatomical connectivity between the two was associated with more severe binge drinking behaviour. Together these findings suggest the potential sub-clinical neurobiological markers of alcohol use severity that persists into binge drinking, alcohol dependence and remains in late abstinence but that some elements of the system (ventral striatal integrity and connectivity) are able to normalize during abstinence.

As discussed, the measure of waiting impulsivity can be conceptualized as a goal-directed behavioural control faculty, driven by an expected reward. This process would be expected to be disturbed in AD and binge drinking where there is an apparent deficit in controlling behaviour in light of an expected reward (alcohol). The subgenual ACC maintains arousal during expectation of positive outcomes[525] and may link with the STN to pause or actively inhibit behaviour for ultimate goals. The reduced connectivity between these regions therefore suggests that the system that controls a behavioural pause function during reward anticipation is perturbed and may not be sufficiently controlling or inhibiting drinking behaviours in these groups. That subgenual ACC and STN connectivity seemed to be the most disturbed in these pathological drinking groups is interesting as their functional connectivity seems to specifically regulate behaviour during anticipation of a reward, rather than more motoric response inhibition (stopping, pre-SMA) or valuation-updating (goal-directedness, OFC). In binge drinkers and individuals with AD, the behavioural deficit might therefore be related to an inability to adequately inhibit responses when a reward (alcoholic beverage) looms. In fact, the behavioural 'Go' response outweighs the 'Stop' function during anticipation of such a reward, rendering the individual unable to stop.

The current studies did not specifically examine the neural correlates of other cognitive measures as waiting impulsivity has been most reliably and robustly implicated. For example, one study showed no association between model free and model based learning behaviour and alcohol consumption in young social drinkers (18 years), or ventral striatal or vmpfc neural activity during this type of learning[553]. In this relatively large study (N=188), only impulsivity was related to alcohol consumption[553] and therefore remained the focus of the current studies.

That machine learning classifications can distinguish between groups is key given the clinical relevance of this technique. Once a machine has been trained, this means that a single subject's data can be input and classified with around 70% accuracy, rather than requiring whole group data like traditional fMRI studies. The classification accuracy

isn't necessarily very strong, compared to studies of dementia for example where accuracy can reach up to 95%[554, 555]. However, dementia is associated with significant and robust brain atrophy and elucidating the neural correlates of more elusive psychiatric disorders is notoriously difficult, for example in early-stage binge drinkers. Therefore, while the current accuracy is not very high, it is likely that other variables could be incorporated, perhaps measures of impulsivity or familial histories, which would be expected to improve the accuracy greatly. Regardless, the demonstration that a single type of data (STN to whole brain functional connectivity) is sufficient to significantly classify between these groups is promising, both diagnostically and from a basic science perspective.

In binge drinkers, both STN and ventral striatum had increased orientation dispersion, a measure that details dendritic complexity. The orientation dispersion index is consistent with Golgi staining of dendritic processes[432] and microscopic detailing of grey matter dendritic architecture[433] and has previously been associated with age[435], the hierarchy of neural computations[434], and higher level cortical regions required for more complex information processing[434]. Increased dendritic proliferation might suggest excessive recruitment or activity of these regions. The finding of increased ventral striatal orientation dispersion is at odds with reports of decreased ventral striatal volume in individuals with alcohol use disorders[508-510]. However, two recent reports have demonstrated an association between higher incidence of familial AD and increased left ventral striatal volume[511] and enlarged ventral striatal volume in binge drinkers[324]. The increased complexity may thus reflect a neuroadaptive capacity. In line with this hypothesis, chronic psychostirmulant use increases dendritic arborization in the ventral striatum of rodents[513] and plasticity of nucleus accumbens receptor expression mediates the reinforcing effects of ethanol[514]. Furthermore, repeated cycles of intoxication and withdrawal in binge drinkers might facilitate neural proliferation. In rats, chronic ethanol withdrawal can result in more than a 2-fold increase in striatal glutamate after 12 hours, at which time an ethanol challenge reduces glutamate and the behavioural signs of withdrawal[286]. This ethanol-induced amelioration of adverse physical symptoms implicates the glutamate system in the

negative reinforcement cycle of addiction[556]. Magnetic resonance spectroscopy studies in humans and rats have further revealed increases in glutamate during acute withdrawal in the prefrontal cortex[557] and nucleus accumbens, the latter being associated with craving[558].

However, this does not necessarily coincide with the finding of reduced connectivity between these regions, associated with impaired behavioural control and binge drinking. Given the hypothesis of reduced STN-mediated pause or behavioural control functions, it would be expected that this region was recruited less in binge drinkers and therefore show a reduction in neural proliferation. It is possible however that the orientation dispersion index measure is capturing neuroinflammatory or glia support cell proliferation. Rats treated with chronic intermittent ethanol have increased markers of neuroinflammation, including activated microglia in the hippocampus alongside increased glutamate levels[559]. The increased excitotoxicity induced by excessive glutamate may activate phagocytes which in turn release inflammatory cytokines, causing and facilitating neuroinflammation[559]. Therefore with excessive alcohol neural insult, as well as intermittent withdrawal, it is possible that neural adaptations in these regions to compensate for excessive stimulation (and restructuring during withdrawal), leads to enhanced proliferation of neuronal support cells.

Finally, cortical microstructure was also disturbed in binge drinkers, in frontal and parietal regions typically associated with executive control of behaviour. This included the dlpfc, a region associated with executive and flexible behavioural regulation and decision making[166, 560, 561], with more anterior regions associated with attention and action inhibition but more posterior dlpfc with action execution[562]. The dlpfc is recruited during times of decision conflict, to guide decision choice[563]. Binge drinkers show a tendency towards impulsive behaviour and seem to be impaired at regulating drinking behaviours, despite possible negative consequences[438, 504, 564]. The current finding suggests that a disturbance in dlpfc microstructure might underlie behavioural control difficulties observed in this group. These findings coincide with a previous study demonstrating reduced glial cell size and density in the dlpfc of

individuals with AD[565] that might be related to the cytotoxic effects of alcohol[566]. Furthermore, connectivity between dlpfc and striatum has been previously shown to be associated with impairments in learning and craving in AD subjects[387]. However, just like a how balloon animal can be shaped and adapted to suit its purpose, the neural architecture underling behavioural control deficits and craving can be similarly adapted. A key example of this for future exploration is transcranial stimulation, which can modulate functional connectivity between relevant sites and when applied to the dlpfc can reduce alcohol craving in AD subjects[507, 567, 568].

Limitations

There are some drawbacks of the current studies. These experiments used mainly a seed-driven approach. It is important to note therefore that several neural regions were not included in the ROI-based analyses, for example the amygdala (relevant for conditioning as well as goal-directed behaviour), insula (reversal learning, internal state monitoring) and other regions like the parietal cortex and cerebellum. The current studies instead focused on seed based methods based on strong hypotheses from established literature. This is a benefit and an issue. On the one hand, directing research questions allows yes/no answers to a discrete, relevant and supported questions. On the other hand, other relevant and unknown or unexpected regional involvement might be missed. This is the delicate balance between examining the brain as one system and as a series of isolated and interlinked systems. Both are necessary. However, neuroscience has moved away from studying brain regions in isolation and future work will use novel and developing methods to examine networks and systems rather that pairs or groups of connections.

Furthermore, these studies did not take into account positive and negative functional connectivity, which could have distinct functional relevance. Positive connectivity might facilitate integration between neural systems. On the other hand, negative or anti-correlations might be inhibitory or regulatory in function, acting to segregate discrete or opposing neural processes[569-571]. Indeed, there is a shift between childhood and

adolescence from positive PFC and amygdala connectivity, to negative connectivity, the latter associated with reduced amygdala-related emotional reactivity[572], implicating the negative correlation in a more regulatory role. Examining which regions might have negative functional connectivity with STN will be important for future research as it would indicate which regions have more of a regulatory role over the STN. However, interpretations of the differences between positive and negative functional connectivity should be made with caution, as our understanding of their functional roles is still developing.

Another issue with these analyses is the assumption that there are three distinct cortical – basal ganglia circuits. Previous studies have suggested there are five or even seven separable circuits [1, 68, 69] but they are likely to include much convergence and overlap. Other studies have separated these circuits into three, representing motor, limbic and cognitive processing [71-74]. This is a simple and powerful way of examining the whole circuit as it relates to broad behavioural and cognitive functions (as motor is different from cognitive which can be separated from limbic etc.). However, with finer techniques, the examination of overlap, convergence, divergence and specificity of circuits must be considered but this is a fair starting point for the examination broad delineations within the cortical – basal ganglia circuitry based on function. There are also limitations of the behavioural tasks used. There is a lot of overlap in these tasks and a shared or common mechanism driving behaviour on these tasks means that they are not entirely dissociable and may not implicate unique or specific processes. This is less the case for the model-free learning parameter as it is an operation of a specific computational process and its subsequent measurable effect on behaviour. However, as discussed, the reversal learning measure is a composite of multiple cognitive processes that cannot be fully deconstructed into their constituent parts. Therefore, while the model-free model-based measures have been operationalized computationally, the reversal learning measure is less specific.

Finally, the findings were mostly correlational and as such, direct causation cannot be established. Conclusions can be drawn about associations between networks and behaviour or psychopathology, rather than about the neural cause of aberrant behaviours. Experiments that induce a direct perturbation of network connectivity, for example with transcranial stimulation, and subsequent monitoring of connectivity and behavioural change would more appropriately answer questions about causality between network dynamics and behaviour. As mentioned, stimulation to the dlpfc can reduce craving in AD subjects[507, 567, 568], but the neural mechanisms underlying this shift should be further characterized. From the current findings, a disturbance in connectivity of the dlpfc with downstream regions such as the ventral striatum or STN could potentially alter attentional shifting capacity or decisional impulsivity, which might relate to a reduction in alcohol craving. These questions about causality warrant thorough future investigation.

Summary

In summary, this thesis demonstrated several novel findings. Of note, it provides a detailed map of cortical connectivity with STN, a small and technically inaccessible structure that has a diverse and pivotal role in cortical – basal ganglia systems. This work demonstrated that dissociable behavioural systems map onto the cortical – basal ganglia circuitry, showing both overlap in functional neural correlates (waiting impulsivity and goal-directed learning both implicate the limbic indirect pathway), and divergence in neural recruitment by a single behaviour (habit implicates both traditional motor pathways as well as navigation and conflict monitoring networks). This highlights instances of shared cognitive or neural functionality and demonstrates the complexities of certain cognitive systems.

The importance and relevance of waiting impulsivity was demonstrated by the characterization of its neural correlates for the first time in humans (STN, subgenual ACC and ventral striatum). Waiting impulsivity was dissociable from another form of

impulsivity, motor impulsivity, demonstrating that this cognitive construct can be successfully separated into discrete neural functional circuits, important for the precise delineation of neural and behavioural aberrancy in psychiatric conditions. Furthermore functional connectivity, microstructural integrity and anatomical connectivity of the regions underlying waiting impulsivity were associated with problematic drinking behaviours. Defining both the baseline functional network organization underlying a particular behaviour and demonstrating its disturbance and relevance in a psychiatric group is crucial for the progression of a basic understanding of function – behaviour relationships and will inform both diagnostic and treatment development.

References

1. Alexander, G.E., DeLong, M. R., & Strick, P. L. , *Parallel organization of functionally segregated circuits linking basal ganglia and cortex. .* Annual review of neuroscience, 9(1), 357-381., 1986.
2. Mega, M.S. and J.L. Cummings, *Frontal-subcortical circuits and neuropsychiatric disorders.* J Neuropsychiatry Clin Neurosci, 1994. **6**(4): p. 358-70.
3. Knowlton, B.J., J.A. Mangels, and L.R. Squire, *A neostriatal habit learning system in humans.* Science, 1996. **273**(5280): p. 1399-402.
4. Stocco, A. and C.S. Prat, *Bilingualism trains specific brain circuits involved in flexible rule selection and application.* Brain Lang, 2014. **137**: p. 50-61.
5. Ravizza, S.M. and R.B. Ivry, *Comparison of the basal ganglia and cerebellum in shifting attention.* J Cogn Neurosci, 2001. **13**(3): p. 285-97.
6. Anderson, J.R., *Human symbol manipulation within an integrated cognitive architecture.* Cogn Sci, 2005. **29**(3): p. 313-41.
7. Bolam, J.P., et al., *Synaptic organisation of the basal ganglia.* J Anat, 2000. **196 (Pt 4)**: p. 527-42.
8. Cohen, M.X. and M.J. Frank, *Neurocomputational models of basal ganglia function in learning, memory and choice.* Behav Brain Res, 2009. **199**(1): p. 141-56.
9. Arnsten, A.F. and K. Rubia, *Neurobiological circuits regulating attention, cognitive control, motivation, and emotion: disruptions in neurodevelopmental psychiatric disorders.* J Am Acad Child Adolesc Psychiatry, 2012. **51**(4): p. 356-67.
10. Parent, A. and F. Cicchetti, *The current model of basal ganglia organization under scrutiny.* Mov Disord, 1998. **13**(2): p. 199-202.
11. Ring, H.A. and J. Serra-Mestres, *Neuropsychiatry of the basal ganglia.* J Neurol Neurosurg Psychiatry, 2002. **72**(1): p. 12-21.
12. Alvarez, J.A. and E. Emory, *Executive function and the frontal lobes: a meta-analytic review.* Neuropsychol Rev, 2006. **16**(1): p. 17-42.
13. Bonelli, R.M. and J.L. Cummings, *Frontal-subcortical circuitry and behavior.* Dialogues Clin Neurosci, 2007. **9**(2): p. 141-51.
14. Eickhoff, S.B., et al., *A new SPM toolbox for combining probabilistic cytoarchitectonic maps and functional imaging data.* Neuroimage, 2005. **25**(4): p. 1325-35.
15. Petrides, M. and D.N. Pandya, *Dorsolateral prefrontal cortex: comparative cytoarchitectonic analysis in the human and the macaque brain and corticocortical connection patterns.* Eur J Neurosci, 1999. **11**(3): p. 1011-36.
16. Petrides, M. and D.N. Pandya, *Comparative cytoarchitectonic analysis of the human and the macaque ventrolateral prefrontal cortex and corticocortical connection patterns in the monkey.* Eur J Neurosci, 2002. **16**(2): p. 291-310.

17. Cox, D.D. and R.L. Savoy, *Functional magnetic resonance imaging (fMRI) "brain reading": detecting and classifying distributed patterns of fMRI activity in human visual cortex.* Neuroimage, 2003. **19**(2 Pt 1): p. 261-70.
18. Eickhoff, S.B., et al., *Co-activation patterns distinguish cortical modules, their connectivity and functional differentiation.* Neuroimage, 2011. **57**(3): p. 938-49.
19. Fox, M.D. and M.E. Raichle, *Spontaneous fluctuations in brain activity observed with functional magnetic resonance imaging.* Nat Rev Neurosci, 2007. **8**(9): p. 700-11.
20. Yeo, B.T., et al., *The organization of the human cerebral cortex estimated by intrinsic functional connectivity.* J Neurophysiol, 2011. **106**(3): p. 1125-65.
21. Arnsten, A.F., *The Emerging Neurobiology of Attention Deficit Hyperactivity Disorder: The Key Role of the Prefrontal Association Cortex.* J Pediatr, 2009. **154**(5): p. I-S43.
22. Derrfuss, J., et al., *Involvement of the inferior frontal junction in cognitive control: meta-analyses of switching and Stroop studies.* Hum Brain Mapp, 2005. **25**(1): p. 22-34.
23. Price, J.L., S.T. Carmichael, and W.C. Drevets, *Networks related to the orbital and medial prefrontal cortex; a substrate for emotional behavior?* Prog Brain Res, 1996. **107**: p. 523-36.
24. Iversen, S.D. and M. Mishkin, *Perseverative interference in monkeys following selective lesions of the inferior prefrontal convexity.* Exp Brain Res, 1970. **11**(4): p. 376-86.
25. Dias, R., T.W. Robbins, and A.C. Roberts, *Dissociation in prefrontal cortex of affective and attentional shifts.* Nature, 1996. **380**(6569): p. 69-72.
26. Stocco, A., C. Lebiere, and J.R. Anderson, *Conditional routing of information to the cortex: a model of the basal ganglia's role in cognitive coordination.* Psychol Rev, 2010. **117**(2): p. 541-74.
27. Dayan, P. and B.W. Balleine, *Reward, motivation, and reinforcement learning.* Neuron, 2002. **36**(2): p. 285-98.
28. O'Doherty, J., et al., *Dissociable roles of ventral and dorsal striatum in instrumental conditioning.* Science, 2004. **304**(5669): p. 452-4.
29. Gunaydin, L.A. and A.C. Kreitzer, *Cortico-Basal Ganglia Circuit Function in Psychiatric Disease.* Annu Rev Physiol, 2016. **78**: p. 327-50.
30. Alexander, G.E., & Crutcher, M. D. , *Functional architecture of basal ganglia circuits: neural substrates of parallel processing. .* Trends in neurosciences, 13(7), 266-271., 1990.
31. Tachibana, Y., et al., *Motor cortical control of internal pallidal activity through glutamatergic and GABAergic inputs in awake monkeys.* Eur J Neurosci, 2008. **27**(1): p. 238-53.
32. O'Donnell, P., et al., *Modulation of cell firing in the nucleus accumbens.* Ann N Y Acad Sci, 1999. **877**: p. 157-75.
33. Ikemoto, S., *Dopamine reward circuitry: two projection systems from the ventral midbrain to the nucleus accumbens-olfactory tubercle complex.* Brain Res Rev, 2007. **56**(1): p. 27-78.
34. Chambers, R.A. and M.N. Potenza, *Neurodevelopment, impulsivity, and adolescent gambling.* J Gambl Stud, 2003. **19**(1): p. 53-84.

35. Wise, R.A., *Dopamine, learning and motivation.* Nat Rev Neurosci, 2004. **5**(6): p. 483-94.
36. Wise, R.A., *The Neurobiology of Craving - Implications for the Understanding and Treatment of Addiction.* Journal of Abnormal Psychology, 1988. **97**(2): p. 118-132.
37. Chambers, R.A., J.H. Krystal, and D.W. Self, *A neurobiological basis for substance abuse comorbidity in schizophrenia.* Biol Psychiatry, 2001. **50**(2): p. 71-83.
38. Rommelfanger, K.S. and T. Wichmann, *Extrastriatal dopaminergic circuits of the Basal Ganglia.* Front Neuroanat, 2010. **4**: p. 139.
39. Gerfen, C.R., K.A. Keefe, and E.B. Gauda, *D1 and D2 dopamine receptor function in the striatum: coactivation of D1- and D2-dopamine receptors on separate populations of neurons results in potentiated immediate early gene response in D1-containing neurons.* J Neurosci, 1995. **15**(12): p. 8167-76.
40. Schultz, W., et al., *Neuronal activity in monkey ventral striatum related to the expectation of reward.* J Neurosci, 1992. **12**(12): p. 4595-610.
41. Schultz, W., P. Dayan, and P.R. Montague, *A neural substrate of prediction and reward.* Science, 1997. **275**(5306): p. 1593-9.
42. Tobler, P.N., C.D. Fiorillo, and W. Schultz, *Adaptive coding of reward value by dopamine neurons.* Science, 2005. **307**(5715): p. 1642-5.
43. O'Doherty, J.P., et al., *Neural responses during anticipation of a primary taste reward.* Neuron, 2002. **33**(5): p. 815-26.
44. AG, B., *Adaptive Critics and the Basal Ganglia.* Models of information processing in the basal ganglia (1995): 215., 1995.
45. Sutton RS, B.A., *Reinforcement learning: An introduction.* Vol. 1. No. 1. Cambridge: MIT press, 1998.
46. van Schouwenburg, M., E. Aarts, and R. Cools, *Dopaminergic modulation of cognitive control: distinct roles for the prefrontal cortex and the basal ganglia.* Curr Pharm Des, 2010. **16**(18): p. 2026-32.
47. Mink, J.W., *The basal ganglia: focused selection and inhibition of competing motor programs.* Prog Neurobiol, 1996. **50**(4): p. 381-425.
48. Frank, M.J., *Dynamic dopamine modulation in the basal ganglia: a neurocomputational account of cognitive deficits in medicated and nonmedicated Parkinsonism.* J Cogn Neurosci, 2005. **17**(1): p. 51-72.
49. Frank, M.J. and E.D. Claus, *Anatomy of a decision: striato-orbitofrontal interactions in reinforcement learning, decision making, and reversal.* Psychol Rev, 2006. **113**(2): p. 300-26.
50. Frank, M.J., et al., *Hold your horses: impulsivity, deep brain stimulation, and medication in parkinsonism.* Science, 2007. **318**(5854): p. 1309-12.
51. Leber, A.B., N.B. Turk-Browne, and M.M. Chun, *Neural predictors of moment-to-moment fluctuations in cognitive flexibility.* Proc Natl Acad Sci U S A, 2008. **105**(36): p. 13592-7.
52. Cools, R., L. Clark, and T.W. Robbins, *Differential responses in human striatum and prefrontal cortex to changes in object and rule relevance.* J Neurosci, 2004. **24**(5): p. 1129-35.
53. Hardman, C.D., et al., *Comparison of the basal ganglia in rats, marmosets, macaques, baboons, and humans: volume and neuronal number for the output,*

internal relay, and striatal modulating nuclei. J Comp Neurol, 2002. **445**(3): p. 238-55.
54. Holt, D.J., L.B. Hersh, and C.B. Saper, *Cholinergic innervation in the human striatum: a three-compartment model.* Neuroscience, 1996. **74**(1): p. 67-87.
55. Holt, D.J., A.M. Graybiel, and C.B. Saper, *Neurochemical architecture of the human striatum.* J Comp Neurol, 1997. **384**(1): p. 1-25.
56. Meredith, G.E., et al., *Shell and core in monkey and human nucleus accumbens identified with antibodies to calbindin-D28k.* J Comp Neurol, 1996. **365**(4): p. 628-39.
57. Haber, S.N. and N.R. McFarland, *The concept of the ventral striatum in nonhuman primates.* Ann N Y Acad Sci, 1999. **877**: p. 33-48.
58. Sturm, V., et al., *The nucleus accumbens: a target for deep brain stimulation in obsessive-compulsive- and anxiety-disorders.* J Chem Neuroanat, 2003. **26**(4): p. 293-9.
59. Brauer, K., et al., *The core-shell dichotomy of nucleus accumbens in the rhesus monkey as revealed by double-immunofluorescence and morphology of cholinergic interneurons.* Brain Res, 2000. **858**(1): p. 151-62.
60. Nambu, A., et al., *Excitatory cortical inputs to pallidal neurons via the subthalamic nucleus in the monkey.* J Neurophysiol, 2000. **84**(1): p. 289-300.
61. Takada, M., et al., *Elucidating information processing in primate basal ganglia circuitry: a novel technique for pathway-selective ablation mediated by immunotoxin.* Front Neural Circuits, 2013. **7**: p. 140.
62. Haber, S.N., et al., *Topographic organization of the ventral striatal efferent projections in the rhesus monkey: an anterograde tracing study.* J Comp Neurol, 1990. **293**(2): p. 282-98.
63. Everitt, B.J. and T.W. Robbins, *Neural systems of reinforcement for drug addiction: from actions to habits to compulsion.* Nat Neurosci, 2005. **8**(11): p. 1481-9.
64. Spencer, H.J., *Antagonism of cortical excitation of striatal neurons by glutamic acid diethyl ester: Evidence for glutamic acid as an excitatory transmitter in the rat striatum.* Brain Research, 102(1), 91-101., 1976.
65. Selemon, L.D. and P.S. Goldman-Rakic, *Longitudinal topography and interdigitation of corticostriatal projections in the rhesus monkey.* J Neurosci, 1985. **5**(3): p. 776-94.
66. Carter, C.J., *Topographical distribution of possible glutamatergic pathways from the frontal cortex to the striatum and substantia nigra in rats.* Neuropharmacology, 1982. **21**(5): p. 379-83.
67. DeLong, M.R., Georgopoulos, A. P., *Motor functions of the basal ganglia.* Handb. Physiol., Sect. 1 , The Nervous System, Vol. 2, Motor Control, Part 2. M. Brookhart, V. B. Mountcastle, V. B. Brooks. Bethesda: Am. Physiol. Soc., 1981.
68. Kelly, R.M. and P.L. Strick, *Macro-architecture of basal ganglia loops with the cerebral cortex: use of rabies virus to reveal multisynaptic circuits.* Prog Brain Res, 2004. **143**: p. 449-59.
69. DeLong, M.R. and T. Wichmann, *Circuits and circuit disorders of the basal ganglia.* Archives of Neurology, 2007. **64**(1): p. 20-24.
70. Haber, S.N., *The primate basal ganglia: parallel and integrative networks.* J Chem Neuroanat, 2003. **26**(4): p. 317-30.

71. Redgrave, P., et al., *Goal-directed and habitual control in the basal ganglia: implications for Parkinson's disease.* Nat Rev Neurosci, 2010. **11**(11): p. 760-72.
72. Jahanshahi, M., et al., *A fronto-striato-subthalamic-pallidal network for goal-directed and habitual inhibition.* Nat Rev Neurosci, 2015. **16**(12): p. 719-32.
73. Krack, P., et al., *Deep brain stimulation: from neurology to psychiatry?* Trends Neurosci, 2010. **33**(10): p. 474-84.
74. Obeso, J.A., et al., *The expanding universe of disorders of the basal ganglia.* Lancet, 2014. **384**(9942): p. 523-31.
75. Haber, S.N., *The primate basal ganglia: parallel and integrative networks.* Journal of Chemical Neuroanatomy, 2003. **26**(4): p. 317-330.
76. Groenewegen, H.J., et al., *Convergence and segregation of ventral striatal inputs and outputs.* Advancing from the Ventral Striatum to the Extended Amygdala, 1999. **877**: p. 49-63.
77. Joel, D. and I. Weiner, *The connections of the primate subthalamic nucleus: indirect pathways and the open-interconnected scheme of basal ganglia-thalamocortical circuitry.* Brain Res Brain Res Rev, 1997. **23**(1-2): p. 62-78.
78. Cummings, J.L., *Frontal-subcortical circuits and human behavior.* Arch Neurol, 1993. **50**(8): p. 873-80.
79. Divac, I., H.E. Rosvold, and M.K. Szwarcbart, *Behavioral effects of selective ablation of the caudate nucleus.* J Comp Physiol Psychol, 1967. **63**(2): p. 184-90.
80. Lichter DG, C.J., *Frontal- Subcortical Circuits in Psychiatric and Neurological Disorders.* New York, NY: Guilford Press; 2001:1-43., 2001.
81. Kirkby RJ, P.S., *Active avoidance in the laboratory rat following lesions of the dorsal or ventral caudate nucleus.* S. Psychobiology 2: 301. doi:10.3758/BF03333025, 1974.
82. Thompson, R.L., *Effects of lesions in the caudate nuclei and dorsofrontal cortex on conditioned avoidance behavior in cats.* J Comp Physiol Psychol, 1959. **52**: p. 650-9.
83. Bokura, H. and R.G. Robinson, *Long-term cognitive impairment associated with caudate stroke.* Stroke, 1997. **28**(5): p. 970-5.
84. Kemp, J., et al., *Caudate nucleus and social cognition: neuropsychological and SPECT evidence from a patient with focal caudate lesion.* Cortex, 2013. **49**(2): p. 559-71.
85. Jones, E.G., et al., *Cells of origin and terminal distribution of corticostriatal fibers arising in the sensory-motor cortex of monkeys.* J Comp Neurol, 1977. **173**(1): p. 53-80.
86. Kunzle, H., *Bilateral projections from precentral motor cortex to the putamen and other parts of the basal ganglia. An autoradiographic study in Macaca fascicularis.* Brain Res, 1975. **88**(2): p. 195-209.
87. Haber, S.N. and R. Calzavara, *The cortico-basal ganglia integrative network: the role of the thalamus.* Brain Res Bull, 2009. **78**(2-3): p. 69-74.
88. Parent, A., C. Bouchard, and Y. Smith, *The striatopallidal and striatonigral projections: two distinct fiber systems in primate.* Brain Res, 1984. **303**(2): p. 385-90.

89. Kim, R., et al., *Projections of the globus pallidus and adjacent structures: an autoradiographic study in the monkey.* J Comp Neurol, 1976. **169**(3): p. 263-90.
90. Kievit, J. and H.G. Kuypers, *Organization of the thalamo-cortical connexions to the frontal lobe in the rhesus monkey.* Exp Brain Res, 1977. **29**(3-4): p. 299-322.
91. Haber, S.N., et al., *Reward-related cortical inputs define a large striatal region in primates that interface with associative cortical connections, providing a substrate for incentive-based learning.* J Neurosci, 2006. **26**(32): p. 8368-76.
92. Mendez, M.F., N.L. Adams, and K.S. Lewandowski, *Neurobehavioral changes associated with caudate lesions.* Neurology, 1989. **39**(3): p. 349-54.
93. Sandson, T.A., et al., *Frontal lobe dysfunction following infarction of the left-sided medial thalamus.* Arch Neurol, 1991. **48**(12): p. 1300-3.
94. Stuss, D.T., et al., *The neuropsychology of paramedian thalamic infarction.* Brain Cogn, 1988. **8**(3): p. 348-78.
95. Stefanacci, L. and D.G. Amaral, *Some observations on cortical inputs to the macaque monkey amygdala: An anterograde tracing study.* Journal of Comparative Neurology, 2002. **451**(4): p. 301-323.
96. Mega, M.S., et al., *The limbic system: an anatomic, phylogenetic, and clinical perspective.* J Neuropsychiatry Clin Neurosci, 1997. **9**(3): p. 315-30.
97. Eslinger, P.J. and A.R. Damasio, *Severe disturbance of higher cognition after bilateral frontal lobe ablation: patient EVR.* Neurology, 1985. **35**(12): p. 1731-41.
98. Johnson, T.N. and H.E. Rosvold, *Topographic projections on the globus pallidus and the substantia nigra of selectively placed lesions in the precommissural caudate nucleus and putamen in the monkey.* Exp Neurol, 1971. **33**(3): p. 584-96.
99. Smith, Y., L.N. Hazrati, and A. Parent, *Efferent projections of the subthalamic nucleus in the squirrel monkey as studied by the PHA-L anterograde tracing method.* J Comp Neurol, 1990. **294**(2): p. 306-23.
100. Tengvar, C., B. Johansson, and J. Sorensen, *Frontal lobe and cingulate cortical metabolic dysfunction in acquired akinetic mutism: a PET study of the interval form of carbon monoxide poisoning.* Brain Inj, 2004. **18**(6): p. 615-25.
101. Oberndorfer, S., et al., *Akinetic mutism caused by bilateral infiltration of the fornix in a patient with astrocytoma.* Eur J Neurol, 2002. **9**(3): p. 311-3.
102. Bogousslavsky, J., et al., *Manic delirium and frontal-like syndrome with paramedian infarction of the right thalamus.* J Neurol Neurosurg Psychiatry, 1988. **51**(1): p. 116-9.
103. Ungerstedt, U., *Adipsia and aphagia after 6-hydroxydopamine induced degeneration of the nigro-striatal dopamine system.* Acta Physiol Scand Suppl, 1971. **367**: p. 95-122.
104. Giguere, M. and P.S. Goldman-Rakic, *Mediodorsal nucleus: areal, laminar, and tangential distribution of afferents and efferents in the frontal lobe of rhesus monkeys.* J Comp Neurol, 1988. **277**(2): p. 195-213.
105. Goldman-Rakic, P.S. and L.J. Porrino, *The primate mediodorsal (MD) nucleus and its projection to the frontal lobe.* J Comp Neurol, 1985. **242**(4): p. 535-60.

106. Haber, S.N., E. Lynd-Balta, and S.J. Mitchell, *The organization of the descending ventral pallidal projections in the monkey.* J Comp Neurol, 1993. **329**(1): p. 111-28.
107. Parent, A. and L.N. Hazrati, *Functional anatomy of the basal ganglia. II. The place of subthalamic nucleus and external pallidum in basal ganglia circuitry.* Brain Res Brain Res Rev, 1995. **20**(1): p. 128-54.
108. Ewert, S., Plettig, P., Li, N., Chakravarty, M., Collins, L., Herrington, T., ... & Horn, A. , *Toward defining deep brain stimulation targets in MNI space: A subcortical atlas based on multimodal MRI, histology and structural connectivity.* Neuroimage, 2017.
109. Haynes, W.I. and S.N. Haber, *The organization of prefrontal-subthalamic inputs in primates provides an anatomical substrate for both functional specificity and integration: implications for Basal Ganglia models and deep brain stimulation.* J Neurosci, 2013. **33**(11): p. 4804-14.
110. Karachi, C., et al., *The pallidosubthalamic projection: an anatomical substrate for nonmotor functions of the subthalamic nucleus in primates.* Mov Disord, 2005. **20**(2): p. 172-80.
111. Keuken, M.C., et al., *Are there three subdivisions in the primate subthalamic nucleus?* Front Neuroanat, 2012. **6**: p. 14.
112. Temel, Y., et al., *The functional role of the subthalamic nucleus in cognitive and limbic circuits.* Prog Neurobiol, 2005. **76**(6): p. 393-413.
113. Plantinga, B.R., et al., *Individualized parcellation of the subthalamic nucleus in patients with Parkinson's disease with 7T MRI.* Neuroimage, 2016.
114. Lambert, C., et al., *Confirmation of functional zones within the human subthalamic nucleus: patterns of connectivity and sub-parcellation using diffusion weighted imaging.* Neuroimage, 2012. **60**(1): p. 83-94.
115. Lambert, C., et al., *Do we need to revise the tripartite subdivision hypothesis of the human subthalamic nucleus (STN)? Response to Alkemade and Forstmann.* Neuroimage, 2015. **110**: p. 1-2.
116. Mallet, L., et al., *Subthalamic nucleus stimulation in severe obsessive-compulsive disorder.* N Engl J Med, 2008. **359**(20): p. 2121-34.
117. Voon, V., et al., *Decisional impulsivity and the associative-limbic subthalamic nucleus in obsessive-compulsive disorder: stimulation and connectivity.* Brain, 2017. **140**(Pt 2): p. 442-456.
118. Evens, R., et al., *The impact of Parkinson's disease and subthalamic deep brain stimulation on reward processing.* Neuropsychologia, 2015. **75**: p. 11-9.
119. Seinstra, M., et al., *No Effect of Subthalamic Deep Brain Stimulation on Intertemporal Decision-Making in Parkinson Patients.* eNeuro, 2016. **3**(2).
120. Aron, A.R., *The neural basis of inhibition in cognitive control.* Neuroscientist, 2007. **13**(3): p. 214-28.
121. Aron, A.R., et al., *Triangulating a cognitive control network using diffusion-weighted magnetic resonance imaging (MRI) and functional MRI.* J Neurosci, 2007. **27**(14): p. 3743-52.
122. Cavanagh, J.F., et al., *Subthalamic nucleus stimulation reverses mediofrontal influence over decision threshold.* Nat Neurosci, 2011. **14**(11): p. 1462-7.
123. Brittain, J.S., et al., *A role for the subthalamic nucleus in response inhibition during conflict.* J Neurosci, 2012. **32**(39): p. 13396-401.

124. Mansfield, E.L., et al., *Adjustments of response threshold during task switching: a model-based functional magnetic resonance imaging study.* J Neurosci, 2011. **31**(41): p. 14688-92.
125. Robbins, T.W., et al., *Neurocognitive endophenotypes of impulsivity and compulsivity: towards dimensional psychiatry.* Trends Cogn Sci, 2012. **16**(1): p. 81-91.
126. Fineberg, N.A., et al., *New developments in human neurocognition: clinical, genetic, and brain imaging correlates of impulsivity and compulsivity.* CNS Spectr, 2014. **19**(1): p. 69-89.
127. Moeller, F.G., et al., *Psychiatric aspects of impulsivity.* American Journal of Psychiatry, 2001. **158**(11): p. 1783-1793.
128. Dalley, J.W., B.J. Everitt, and T.W. Robbins, *Impulsivity, compulsivity, and top-down cognitive control.* Neuron, 2011. **69**(4): p. 680-94.
129. Harnishfeger, K.K., *The development of cognitive inhibition. Interference and inhibition in cognition, 175-204.* 1995.
130. Desimone, R. and J. Duncan, *Neural mechanisms of selective visual attention.* Annu Rev Neurosci, 1995. **18**: p. 193-222.
131. Colzato, L.S., et al., *How does bilingualism improve executive control? A comparison of active and reactive inhibition mechanisms.* J Exp Psychol Learn Mem Cogn, 2008. **34**(2): p. 302-12.
132. Logan, G.D., *On the ability to inhibit thought and action: a users' guide to the stop signal paradigm.* 1994.
133. MacLeod C. , D.M., Sheard E. , Wilson D. , Bibi U., *In opposition to inhibition. In: Ross B , editor. The psychology of learning and motivation . Vol 43. San Diego: Elsevier Science p 163-214.* 2003.
134. van den Wildenberg, W.P., et al., *Mechanisms and dynamics of cortical motor inhibition in the stop-signal paradigm: a TMS study.* J Cogn Neurosci, 2010. **22**(2): p. 225-39.
135. Watanabe, J., et al., *The human prefrontal and parietal association cortices are involved in NO-GO performances: an event-related fMRI study.* Neuroimage, 2002. **17**(3): p. 1207-16.
136. Pfefferbaum, A., et al., *ERPs to response production and inhibition.* Electroencephalogr Clin Neurophysiol, 1985. **60**(5): p. 423-34.
137. Horn, N.R., et al., *Response inhibition and impulsivity: an fMRI study.* Neuropsychologia, 2003. **41**(14): p. 1959-66.
138. Kawashima, R., et al., *Functional anatomy of GO/NO-GO discrimination and response selection--a PET study in man.* Brain Res, 1996. **728**(1): p. 79-89.
139. Simmonds, D.J., J.J. Pekar, and S.H. Mostofsky, *Meta-analysis of Go/No-go tasks demonstrating that fMRI activation associated with response inhibition is task-dependent.* Neuropsychologia, 2008. **46**(1): p. 224-32.
140. Logan, G.D., W.B. Cowan, and K.A. Davis, *On the ability to inhibit simple and choice reaction time responses: a model and a method.* J Exp Psychol Hum Percept Perform, 1984. **10**(2): p. 276-91.
141. Li, C.S., et al., *Subcortical processes of motor response inhibition during a stop signal task.* Neuroimage, 2008. **41**(4): p. 1352-63.
142. Hanes, D.P., W.F. Patterson, 2nd, and J.D. Schall, *Role of frontal eye fields in countermanding saccades: visual, movement, and fixation activity.* J Neurophysiol, 1998. **79**(2): p. 817-34.

143. Aron, A.R., et al., *Converging evidence for a fronto-basal-ganglia network for inhibitory control of action and cognition.* J Neurosci, 2007. **27**(44): p. 11860-4.
144. Bevan, M.D., J.P. Bolam, and A.R. Crossman, *Convergent synaptic input from the neostriatum and the subthalamus onto identified nigrothalamic neurons in the rat.* Eur J Neurosci, 1994. **6**(3): p. 320-34.
145. Schmidt, R., et al., *Canceling actions involves a race between basal ganglia pathways.* Nat Neurosci, 2013. **16**(8): p. 1118-24.
146. Wiecki, T.V. and M.J. Frank, *A computational model of inhibitory control in frontal cortex and basal ganglia.* Psychol Rev, 2013. **120**(2): p. 329-55.
147. Leotti, L.A. and T.D. Wager, *Motivational influences on response inhibition measures.* J Exp Psychol Hum Percept Perform, 2010. **36**(2): p. 430-47.
148. Morein-Zamir, S. and A. Kingstone, *Fixation offset and stop signal intensity effects on saccadic countermanding: a crossmodal investigation.* Exp Brain Res, 2006. **175**(3): p. 453-62.
149. Coxon, J.P., C.M. Stinear, and W.D. Byblow, *Intracortical inhibition during volitional inhibition of prepared action.* J Neurophysiol, 2006. **95**(6): p. 3371-83.
150. Aron, A.R., et al., *Stop-signal inhibition disrupted by damage to right inferior frontal gyrus in humans.* Nat Neurosci, 2003. **6**(2): p. 115-6.
151. Rieger, M., S. Gauggel, and K. Burmeister, *Inhibition of ongoing responses following frontal, nonfrontal, and basal ganglia lesions.* Neuropsychology, 2003. **17**(2): p. 272-82.
152. Chambers, C.D., et al., *Executive "brake failure" following deactivation of human frontal lobe.* J Cogn Neurosci, 2006. **18**(3): p. 444-55.
153. Floden, D. and D.T. Stuss, *Inhibitory control is slowed in patients with right superior medial frontal damage.* J Cogn Neurosci, 2006. **18**(11): p. 1843-9.
154. Nachev, P., et al., *The role of the pre-supplementary motor area in the control of action.* Neuroimage, 2007. **36 Suppl 2**: p. T155-63.
155. Eagle, D.M., et al., *Stop-signal reaction-time task performance: Role of prefrontal cortex and subthalamic nucleus.* Cerebral Cortex, 2008. **18**(1): p. 178-188.
156. Aron, A.R. and R.A. Poldrack, *Cortical and subcortical contributions to Stop signal response inhibition: role of the subthalamic nucleus.* J Neurosci, 2006. **26**(9): p. 2424-33.
157. Wittmann, M., D.S. Leland, and M.P. Paulus, *Time and decision making: differential contribution of the posterior insular cortex and the striatum during a delay discounting task.* Exp Brain Res, 2007. **179**(4): p. 643-53.
158. Cardinal, R.N., et al., *Impulsive choice induced in rats by lesions of the nucleus accumbens core.* Science, 2001. **292**(5526): p. 2499-501.
159. Mobini, S., et al., *Effects of lesions of the orbitofrontal cortex on sensitivity to delayed and probabilistic reinforcement.* Psychopharmacology (Berl), 2002. **160**(3): p. 290-8.
160. Kable, J.W. and P.W. Glimcher, *The neural correlates of subjective value during intertemporal choice.* Nat Neurosci, 2007. **10**(12): p. 1625-33.
161. Ballard, K. and B. Knutson, *Dissociable neural representations of future reward magnitude and delay during temporal discounting.* Neuroimage, 2009. **45**(1): p. 143-50.

162. Hariri, A.R., et al., *Preference for immediate over delayed rewards is associated with magnitude of ventral striatal activity.* J Neurosci, 2006. **26**(51): p. 13213-7.
163. Tanaka, S.C., et al., *Prediction of immediate and future rewards differentially recruits cortico-basal ganglia loops.* Nat Neurosci, 2004. **7**(8): p. 887-93.
164. Luhmann, C.C., et al., *Neural dissociation of delay and uncertainty in intertemporal choice.* J Neurosci, 2008. **28**(53): p. 14459-66.
165. Kim, S. and D. Lee, *Prefrontal cortex and impulsive decision making.* Biol Psychiatry, 2011. **69**(12): p. 1140-6.
166. Hare, T.A., C.F. Camerer, and A. Rangel, *Self-control in decision-making involves modulation of the vmPFC valuation system.* Science, 2009. **324**(5927): p. 646-8.
167. Lawrence, A.J., et al., *Problem gamblers share deficits in impulsive decision-making with alcohol-dependent individuals.* Addiction, 2009. **104**(6): p. 1006-1015.
168. Furl, N. and B.B. Averbeck, *Parietal cortex and insula relate to evidence seeking relevant to reward-related decisions.* J Neurosci, 2011. **31**(48): p. 17572-82.
169. Gold, J.I. and M.N. Shadlen, *The neural basis of decision making.* Annu Rev Neurosci, 2007. **30**: p. 535-74.
170. Schall, J.D., *Neural basis of deciding, choosing and acting.* Nat Rev Neurosci, 2001. **2**(1): p. 33-42.
171. Bogacz, R., et al., *The neural basis of the speed-accuracy tradeoff.* Trends Neurosci, 2010. **33**(1): p. 10-6.
172. Banca, P., et al., *Reflection impulsivity in binge drinking: behavioural and volumetric correlates.* Addict Biol, 2016. **21**(2): p. 504-15.
173. Robbins, T.W., *The 5-choice serial reaction time task: behavioural pharmacology and functional neurochemistry.* Psychopharmacology (Berl), 2002. **163**(3-4): p. 362-80.
174. Cole, B.J. and T.W. Robbins, *Effects of 6-hydroxydopamine lesions of the nucleus accumbens septi on performance of a 5-choice serial reaction time task in rats: implications for theories of selective attention and arousal.* Behav Brain Res, 1989. **33**(2): p. 165-79.
175. Dalley, J.W., et al., *Nucleus accumbens D2/3 receptors predict trait impulsivity and cocaine reinforcement.* Science, 2007. **315**(5816): p. 1267-70.
176. Caprioli, D., et al., *Gamma Aminobutyric Acidergic and Neuronal Structural Markers in the Nucleus Accumbens Core Underlie Trait-like Impulsive Behavior.* Biol Psychiatry, 2013.
177. Chudasama, Y., et al., *Dissociable aspects of performance on the 5-choice serial reaction time task following lesions of the dorsal anterior cingulate, infralimbic and orbitofrontal cortex in the rat: differential effects on selectivity, impulsivity and compulsivity.* Behav Brain Res, 2003. **146**(1-2): p. 105-19.
178. Baunez, C., A. Nieoullon, and M. Amalric, *In a rat model of parkinsonism, lesions of the subthalamic nucleus reverse increases of reaction time but induce a dramatic premature responding deficit.* J Neurosci, 1995. **15**(10): p. 6531-41.

179. Baunez, C. and T.W. Robbins, *Bilateral lesions of the subthalamic nucleus induce multiple deficits in an attentional task in rats.* Eur J Neurosci, 1997. **9**(10): p. 2086-99.
180. Aleksandrova, L.R., et al., *Deep brain stimulation of the subthalamic nucleus increases premature responding in a rat gambling task.* Behav Brain Res, 2013. **245**: p. 76-82.
181. Desbonnet, L., et al., *Premature responding following bilateral stimulation of the rat subthalamic nucleus is amplitude and frequency dependent.* Brain Res, 2004. **1008**(2): p. 198-204.
182. Belin, D., et al., *High impulsivity predicts the switch to compulsive cocaine-taking.* Science, 2008. **320**(5881): p. 1352-1355.
183. Diergaarde, L., et al., *Impulsive choice and impulsive action predict vulnerability to distinct stages of nicotine seeking in rats.* Biol Psychiatry, 2008. **63**(3): p. 301-8.
184. Diergaarde, L., et al., *Trait impulsivity predicts escalation of sucrose seeking and hypersensitivity to sucrose-associated stimuli.* Behav Neurosci, 2009. **123**(4): p. 794-803.
185. Oliver, Y.P., T.L. Ripley, and D.N. Stephens, *Ethanol effects on impulsivity in two mouse strains: similarities to diazepam and ketamine.* Psychopharmacology (Berl), 2009. **204**(4): p. 679-92.
186. Walker, S.E., Y. Pena-Oliver, and D.N. Stephens, *Learning not to be impulsive: disruption by experience of alcohol withdrawal.* Psychopharmacology (Berl), 2011. **217**(3): p. 433-42.
187. Sanchez-Roige, S., et al., *Exaggerated Waiting Impulsivity Associated with Human Binge Drinking, and High Alcohol Consumption in Mice.* Neuropsychopharmacology, 2014.
188. Voon, V., et al., *Measuring "waiting" impulsivity in substance addictions and binge eating disorder in a novel analogue of rodent serial reaction time task.* Biol Psychiatry, 2014. **75**(2): p. 148-55.
189. Voon, V., *Models of impulsivity with a focus on waiting impulsivity: translational potential to neuropsychiatric disorders.* Curr Addict Rep, in press.
190. Robbins, T.W., *The 5-choice serial reaction time task: behavioural pharmacology and functional neurochemistry.* Psychopharmacology, 2002. **163**(3-4): p. 362-380.
191. Daw, N.D., et al., *Model-based influences on humans' choices and striatal prediction errors.* Neuron, 2011. **69**(6): p. 1204-15.
192. Yin, H.H., S.B. Ostlund, and B.W. Balleine, *Reward-guided learning beyond dopamine in the nucleus accumbens: the integrative functions of cortico-basal ganglia networks.* Eur J Neurosci, 2008. **28**(8): p. 1437-48.
193. Ashby, F.G., B.O. Turner, and J.C. Horvitz, *Cortical and basal ganglia contributions to habit learning and automaticity.* Trends Cogn Sci, 2010. **14**(5): p. 208-15.
194. Yin, H.H., et al., *The role of the dorsomedial striatum in instrumental conditioning.* Eur J Neurosci, 2005. **22**(2): p. 513-23.
195. Dayan, P. and Y. Niv, *Reinforcement learning: the good, the bad and the ugly.* Curr Opin Neurobiol, 2008. **18**(2): p. 185-96.

196. Lawrence, A.D., et al., *Discrimination, reversal, and shift learning in Huntington's disease: mechanisms of impaired response selection.* Neuropsychologia, 1999. **37**(12): p. 1359-74.
197. NJ., M., *Conditioning and associative learning. Oxford: Clarendon Press.* 1983.
198. Cools, R., et al., *Defining the neural mechanisms of probabilistic reversal learning using event-related functional magnetic resonance imaging.* J Neurosci, 2002. **22**(11): p. 4563-7.
199. Clark, L., R. Cools, and T.W. Robbins, *The neuropsychology of ventral prefrontal cortex: decision-making and reversal learning.* Brain Cogn, 2004. **55**(1): p. 41-53.
200. Ghahremani, D.G., et al., *Neural components underlying behavioral flexibility in human reversal learning.* Cereb Cortex, 2010. **20**(8): p. 1843-52.
201. Tricomi, E.M., M.R. Delgado, and J.A. Fiez, *Modulation of caudate activity by action contingency.* Neuron, 2004. **41**(2): p. 281-292.
202. Kawagoe, R., Y. Takikawa, and O. Hikosaka, *Expectation of reward modulates cognitive signals in the basal ganglia.* Nature Neuroscience, 1998. **1**(5): p. 411-416.
203. Lauwereyns, J., et al., *A neural correlate of response bias in monkey caudate nucleus.* Nature, 2002. **418**(6896): p. 413-7.
204. Pasupathy, A. and E.K. Miller, *Different time courses of learning-related activity in the prefrontal cortex and striatum.* Nature, 2005. **433**(7028): p. 873-6.
205. Balleine, B.W. and J.P. O'Doherty, *Human and rodent homologies in action control: corticostriatal determinants of goal-directed and habitual action.* Neuropsychopharmacology, 2010. **35**(1): p. 48-69.
206. Balleine, B.W. and A. Dickinson, *Goal-directed instrumental action: contingency and incentive learning and their cortical substrates.* Neuropharmacology, 1998. **37**(4-5): p. 407-19.
207. Corbit, L.H. and B.W. Balleine, *The role of prelimbic cortex in instrumental conditioning.* Behav Brain Res, 2003. **146**(1-2): p. 145-57.
208. Corbit, L.H., J.L. Muir, and B.W. Balleine, *Lesions of mediodorsal thalamus and anterior thalamic nuclei produce dissociable effects on instrumental conditioning in rats.* Eur J Neurosci, 2003. **18**(5): p. 1286-94.
209. Morris, J.S. and R.J. Dolan, *Involvement of human amygdala and orbitofrontal cortex in hunger-enhanced memory for food stimuli.* Journal of Neuroscience, 2001. **21**(14): p. 5304-5310.
210. O'doherty, J., et al., *Abstract reward and punishment representations in the human orbitofrontal cortex.* Nature Neuroscience, 2001. **4**(1): p. 95-102.
211. Valentin, V.V., A. Dickinson, and J.P. O'Doherty, *Determining the neural substrates of goal-directed learning in the human brain.* Journal of Neuroscience, 2007. **27**(15): p. 4019-4026.
212. Wunderlich, K., P. Dayan, and R.J. Dolan, *Mapping value based planning and extensively trained choice in the human brain.* Nat Neurosci, 2012. **15**(5): p. 786-91.
213. Tanaka, S.C., B.W. Balleine, and J.P. O'Doherty, *Calculating consequences: Brain systems that encode the causal effects of actions.* Journal of Neuroscience, 2008. **28**(26): p. 6750-6755.

214. Glascher, J., A.N. Hampton, and J.P. O'Doherty, *Determining a role for ventromedial prefrontal cortex in encoding action-based value signals during reward-related decision making.* Cereb Cortex, 2009. **19**(2): p. 483-95.
215. Kringelbach, M.L. and E.T. Rolls, *Neural correlates of rapid reversal learning in a simple model of human social interaction.* Neuroimage, 2003. **20**(2): p. 1371-83.
216. Shin, N.Y., et al., *Impaired body but not face perception in patients with obsessive-compulsive disorder.* J Neuropsychol, 2013. **7**(1): p. 58-71.
217. Haber, S.N. and B. Knutson, *The reward circuit: linking primate anatomy and human imaging.* Neuropsychopharmacology, 2010. **35**(1): p. 4-26.
218. Elliott, R., K.J. Friston, and R.J. Dolan, *Dissociable neural responses in human reward systems.* Journal of Neuroscience, 2000. **20**(16): p. 6159-65.
219. Voon, V., et al., *Disorders of compulsivity: a common bias towards learning habits.* Mol Psychiatry, 2014.
220. Pessiglione, M., et al., *Dopamine-dependent prediction errors underpin reward-seeking behaviour in humans.* Nature, 2006. **442**(7106): p. 1042-1045.
221. Corbit, L.H., J.L. Muir, and B.W. Balleine, *The role of the nucleus accumbens in instrumental conditioning: Evidence of a functional dissociation between accumbens core and shell.* Journal of Neuroscience, 2001. **21**(9): p. 3251-3260.
222. Talmi, D., et al., *Human pavlovian-instrumental transfer.* J Neurosci, 2008. **28**(2): p. 360-8.
223. Belin, D., et al., *Parallel and interactive learning processes within the basal ganglia: relevance for the understanding of addiction.* Behav Brain Res, 2009. **199**(1): p. 89-102.
224. Nauta, W.J., et al., *Efferent connections and nigral afferents of the nucleus accumbens septi in the rat.* Neuroscience, 1978. **3**(4-5): p. 385-401.
225. Miyachi, S., O. Hikosaka, and X. Lu, *Differential activation of monkey striatal neurons in the early and late stages of procedural learning.* Exp Brain Res, 2002. **146**(1): p. 122-6.
226. Lehericy, S., et al., *Distinct basal ganglia territories are engaged in early and advanced motor sequence learning.* Proc Natl Acad Sci U S A, 2005. **102**(35): p. 12566-71.
227. Poldrack, R.A., et al., *The neural correlates of motor skill automaticity.* J Neurosci, 2005. **25**(22): p. 5356-64.
228. Miyachi, S., et al., *Differential roles of monkey striatum in learning of sequential hand movement.* Exp Brain Res, 1997. **115**(1): p. 1-5.
229. Belin, D. and B.J. Everitt, *Cocaine seeking habits depend upon dopamine-dependent serial connectivity linking the ventral with the dorsal striatum.* Neuron, 2008. **57**(3): p. 432-41.
230. Ito, R., et al., *Dopamine release in the dorsal striatum during cocaine-seeking behavior under the control of a drug-associated cue.* J Neurosci, 2002. **22**(14): p. 6247-53.
231. Yin, H.H., B.J. Knowlton, and B.W. Balleine, *Lesions of dorsolateral striatum preserve outcome expectancy but disrupt habit formation in instrumental learning.* Eur J Neurosci, 2004. **19**(1): p. 181-9.

232. Vanderschuren, L.J., P. Di Ciano, and B.J. Everitt, *Involvement of the dorsal striatum in cue-controlled cocaine seeking.* J Neurosci, 2005. **25**(38): p. 8665-70.
233. Dickinson, A., *Actions and Habits - the Development of Behavioral Autonomy.* Philosophical Transactions of the Royal Society of London Series B-Biological Sciences, 1985. **308**(1135): p. 67-78.
234. Wickens, J.R., J.N. Reynolds, and B.I. Hyland, *Neural mechanisms of reward-related motor learning.* Curr Opin Neurobiol, 2003. **13**(6): p. 685-90.
235. Horvitz, J.C., *Stimulus-response and response-outcome learning mechanisms in the striatum.* Behav Brain Res, 2009. **199**(1): p. 129-40.
236. Wickens, J.R., et al., *Striatal contributions to reward and decision making: making sense of regional variations in a reiterated processing matrix.* Ann N Y Acad Sci, 2007. **1104**: p. 192-212.
237. Horvitz, J.C., et al., *A "good parent" function of dopamine: transient modulation of learning and performance during early stages of training.* Ann N Y Acad Sci, 2007. **1104**: p. 270-88.
238. Choi, W.Y., P.D. Balsam, and J.C. Horvitz, *Extended habit training reduces dopamine mediation of appetitive response expression.* J Neurosci, 2005. **25**(29): p. 6729-33.
239. Bespalov, A.Y., et al., *AMPA receptor antagonists reverse effects of extended habit training on signaled food approach responding in rats.* Psychopharmacology (Berl), 2007. **195**(1): p. 11-8.
240. Tzschentke, T.M., *Pharmacology and behavioral pharmacology of the mesocortical dopamine system.* Prog Neurobiol, 2001. **63**(3): p. 241-320.
241. Seamans, J.K. and C.R. Yang, *The principal features and mechanisms of dopamine modulation in the prefrontal cortex.* Prog Neurobiol, 2004. **74**(1): p. 1-58.
242. Kelly, A.M. and H. Garavan, *Human functional neuroimaging of brain changes associated with practice.* Cereb Cortex, 2005. **15**(8): p. 1089-102.
243. Poldrack, R.A. and J.D. Gabrieli, *Characterizing the neural mechanisms of skill learning and repetition priming: evidence from mirror reading.* Brain, 2001. **124**(Pt 1): p. 67-82.
244. Raichle, M.E., et al., *Practice-related changes in human brain functional anatomy during nonmotor learning.* Cereb Cortex, 1994. **4**(1): p. 8-26.
245. de Wit, S., et al., *Differential engagement of the ventromedial prefrontal cortex by goal-directed and habitual behavior toward food pictures in humans.* J Neurosci, 2009. **29**(36): p. 11330-8.
246. Amemori, K. and T. Sawaguchi, *Contrasting effects of reward expectation on sensory and motor memories in primate prefrontal neurons.* Cereb Cortex, 2006. **16**(7): p. 1002-15.
247. Honda, M., et al., *Dynamic cortical involvement in implicit and explicit motor sequence learning. A PET study.* Brain, 1998. **121 (Pt 11)**: p. 2159-73.
248. Karni, A., et al., *Functional MRI evidence for adult motor cortex plasticity during motor skill learning.* Nature, 1995. **377**(6545): p. 155-8.
249. Floyer-Lea, A. and P.M. Matthews, *Distinguishable brain activation networks for short- and long-term motor skill learning.* J Neurophysiol, 2005. **94**(1): p. 512-8.

250. Tricomi, E., B.W. Balleine, and J.P. O'Doherty, *A specific role for posterior dorsolateral striatum in human habit learning.* Eur J Neurosci, 2009. **29**(11): p. 2225-32.
251. de Wit, S., et al., *Corticostriatal connectivity underlies individual differences in the balance between habitual and goal-directed action control.* J Neurosci, 2012. **32**(35): p. 12066-75.
252. Chen, L.L. and S.P. Wise, *Supplementary eye field contrasted with the frontal eye field during acquisition of conditional oculomotor associations.* J Neurophysiol, 1995. **73**(3): p. 1122-34.
253. Nachev, P., C. Kennard, and M. Husain, *Functional role of the supplementary and pre-supplementary motor areas.* Nat Rev Neurosci, 2008. **9**(11): p. 856-69.
254. Alexander, G.E., M.R. DeLong, and P.L. Strick, *Parallel organization of functionally segregated circuits linking basal ganglia and cortex.* Annu Rev Neurosci, 1986. **9**: p. 357-81.
255. Kreitzer, A.C. and R.C. Malenka, *Striatal Plasticity and Basal Ganglia Circuit Function.* Neuron, 2008. **60**(4): p. 543-554.
256. Brown, S.M., et al., *Neural basis of individual differences in impulsivity: contributions of corticolimbic circuits for behavioral arousal and control.* Emotion, 2006. **6**(2): p. 239-45.
257. Soeiro-De-Souza, M.G., et al., *Association of the COMT Met(1)(5)(8) allele with trait impulsivity in healthy young adults.* Mol Med Rep, 2013. **7**(4): p. 1067-72.
258. Guerrieri, R., et al., *The influence of trait and induced state impulsivity on food intake in normal-weight healthy women.* Appetite, 2007. **49**(1): p. 66-73.
259. van den Heuvel, M.P. and H.E. Hulshoff Pol, *Exploring the brain network: a review on resting-state fMRI functional connectivity.* Eur Neuropsychopharmacol, 2010. **20**(8): p. 519-34.
260. Gillan, C.M., et al., *Characterizing a psychiatric symptom dimension related to deficits in goal-directed control.* Elife, 2016. **5**.
261. Stein, D.J., Fineberg, N.A., Bienvenu, O.J., Denys, D., Lochner, C., Nestadt, G., Leckman, J.F., Rauch, S.L. and Phillips, K.A., *Should OCD be classified as an anxiety disorder in DSM‐V?. Depression and anxiety, 27(6), pp.495-506.* 2010.
262. Nestadt, G., et al., *The relationship between obsessive-compulsive disorder and anxiety and affective disorders: results from the Johns Hopkins OCD Family Study.* Psychol Med, 2001. **31**(3): p. 481-7.
263. van den Heuvel, O.A., et al., *Frontal-striatal abnormalities underlying behaviours in the compulsive-impulsive spectrum.* J Neurol Sci, 2010. **289**(1-2): p. 55-9.
264. Elliott, R., R.J. Dolan, and C.D. Frith, *Dissociable functions in the medial and lateral orbitofrontal cortex: evidence from human neuroimaging studies.* Cereb Cortex, 2000. **10**(3): p. 308-17.
265. Hornak, J., et al., *Reward-related reversal learning after surgical excisions in orbito-frontal or dorsolateral prefrontal cortex in humans.* J Cogn Neurosci, 2004. **16**(3): p. 463-78.
266. Chamberlain, S.R., et al., *Orbitofrontal dysfunction in patients with obsessive-compulsive disorder and their unaffected relatives.* Science, 2008. **321**(5887): p. 421-2.

267. Manes, F., et al., *Decision-making processes following damage to the prefrontal cortex.* Brain, 2002. **125**(Pt 3): p. 624-39.
268. Dickstein, D.P., et al., *Neuropsychological performance in pediatric bipolar disorder.* Biological Psychiatry, 2004. **55**(1): p. 32-9.
269. Downes, J.J., et al., *Impaired extra-dimensional shift performance in medicated and unmedicated Parkinson's disease: evidence for a specific attentional dysfunction.* Neuropsychologia, 1989. **27**(11-12): p. 1329-43.
270. McAlonan, K. and V.J. Brown, *Orbital prefrontal cortex mediates reversal learning and not attentional set shifting in the rat.* Behavioural Brain Research, 2003. **146**(1-2): p. 97-103.
271. Belin-Rauscent, A., et al., *From impulses to maladaptive actions: the insula is a neurobiological gate for the development of compulsive behavior.* Mol Psychiatry, 2016. **21**(4): p. 491-9.
272. Koob, G.F. and M. Le Moal, *Drug abuse: hedonic homeostatic dysregulation.* Science, 1997. **278**(5335): p. 52-8.
273. Everitt, B.J., A. Dickinson, and T.W. Robbins, *The neuropsychological basis of addictive behaviour.* Brain Res Brain Res Rev, 2001. **36**(2-3): p. 129-38.
274. Association, A.P., *Diagnostic and statistical manual of mental disorders (5th ed.).* Arlington, VA: American Psychiatric Publishing., 2013.
275. Singh, I. and N. Rose, *Biomarkers in psychiatry.* Nature, 2009. **460**(7252): p. 202-7.
276. Huys, Q.J., T.V. Maia, and M.J. Frank, *Computational psychiatry as a bridge from neuroscience to clinical applications.* Nat Neurosci, 2016. **19**(3): p. 404-13.
277. Insel, T., et al., *Research domain criteria (RDoC): toward a new classification framework for research on mental disorders.* Am J Psychiatry, 2010. **167**(7): p. 748-51.
278. Ersche, K.D., et al., *Drug addiction endophenotypes: impulsive versus sensation-seeking personality traits.* Biol Psychiatry, 2010. **68**(8): p. 770-3.
279. Ersche, K.D., et al., *Cognitive dysfunction and anxious-impulsive personality traits are endophenotypes for drug dependence.* Am J Psychiatry, 2012. **169**(9): p. 926-36.
280. Di Chiara, G. and A. Imperato, *Drugs abused by humans preferentially increase synaptic dopamine concentrations in the mesolimbic system of freely moving rats.* Proc Natl Acad Sci U S A, 1988. **85**(14): p. 5274-8.
281. Vengeliene, V., et al., *Neuropharmacology of alcohol addiction.* British Journal of Pharmacology, 2008. **154**(2): p. 299-315.
282. Singh, A.N., S. Srivastava, and A.K. Jainar, *Pharmacotherapy of chronic alcoholism: a review.* Drugs Today (Barc), 1999. **35**(1): p. 27-33.
283. Theile, J.W., R.A. Gonzales, and R.A. Morrisett, *Ethanol Modulation of GABAergic Inhibition in Midbrain Dopamine Neurons: Implications for the Development of Alcohol-Seeking Behaviors.* Inhibitory Synaptic Plasticity, 2011: p. 75-88.
284. Golovko, A.I., et al., *The influence of ethanol on the functional status of GABA(A) receptors.* Biochemistry-Moscow, 2002. **67**(7): p. 719-729.
285. Gass, J.T. and M.F. Olive, *Glutamatergic substrates of drug addiction and alcoholism.* Biochemical Pharmacology, 2008. **75**(1): p. 218-265.

286. Rossetti, Z.L. and S. Carboni, *Ethanol Withdrawal Is Associated with Increased Extracellular Glutamate in the Rat Striatum.* European Journal of Pharmacology, 1995. **283**(1-3): p. 177-183.
287. Chen, G., et al., *Striatal Involvement in Human Alcoholism and Alcohol Consumption, and Withdrawal in Animal Models.* Alcoholism-Clinical and Experimental Research, 2011. **35**(10): p. 1739-1748.
288. Malcolm, R.J., *GABA systems, benzodiazepines, and substance dependence.* J Clin Psychiatry, 2003. **64 Suppl 3**: p. 36-40.
289. Krupitsky, E.M., et al., *Antiglutamatergic strategies for ethanol detoxification: comparison with placebo and diazepam.* Alcohol Clin Exp Res, 2007. **31**(4): p. 604-11.
290. Rolland, B., et al., *Pharmaceutical approaches of binge drinking.* Curr Pharm Des, 2011. **17**(14): p. 1333-42.
291. Castro, L.A. and D.A. Baltieri, *[The pharmacologic treatment of the alcohol dependence].* Rev Bras Psiquiatr, 2004. **26 Suppl 1**: p. S43-6.
292. White, N.M. and M. Viaud, *Localized intracaudate dopamine D2 receptor activation during the post-training period improves memory for visual or olfactory conditioned emotional responses in rats.* Behav Neural Biol, 1991. **55**(3): p. 255-69.
293. Carr, G.D. and N.M. White, *Effects of systemic and intracranial amphetamine injections on behavior in the open field: a detailed analysis.* Pharmacol Biochem Behav, 1987. **27**(1): p. 113-22.
294. Ito, R., et al., *Dissociation in conditioned dopamine release in the nucleus accumbens core and shell in response to cocaine cues and during cocaine-seeking behavior in rats.* J Neurosci, 2000. **20**(19): p. 7489-95.
295. Yin, H.H., B.J. Knowlton, and B.W. Balleine, *Inactivation of dorsolateral striatum enhances sensitivity to changes in the action-outcome contingency in instrumental conditioning.* Behav Brain Res, 2006. **166**(2): p. 189-96.
296. Goldstein, R.Z. and N.D. Volkow, *Dysfunction of the prefrontal cortex in addiction: neuroimaging findings and clinical implications.* Nat Rev Neurosci, 2011. **12**(11): p. 652-69.
297. Volkow, N.D., et al., *Imaging dopamine's role in drug abuse and addiction.* Neuropharmacology, 2009. **56 Suppl 1**: p. 3-8.
298. *Statistics on alcohol.* Alcohol concern. **https://**http://www.alcoholconcern.org.uk/help-and-advice/statistics-on-alcohol/.
299. Lim, S.S., et al., *A comparative risk assessment of burden of disease and injury attributable to 67 risk factors and risk factor clusters in 21 regions, 1990-2010: a systematic analysis for the Global Burden of Disease Study 2010.* Lancet, 2012. **380**(9859): p. 2224-60.
300. *Health and Social Care Information Centre Statistics on Alcohol, England.* 2015
301. *The cost of binge drinking in the UK.* Institute of Policy Research, 2015.
302. James, J., Francesconi, M, *The Cost of Binge Drinking.* Bath Economics Research Papers No. 36/15, 2015.
303. Grucza, R.A., K.E. Norberg, and L.J. Bierut, *Binge Drinking Among Youths and Young Adults in the United States: 1979-2006.* Journal of the American Academy of Child and Adolescent Psychiatry, 2009. **48**(7): p. 692-702.

304. Kuntsche, E., J. Rehm, and G. Gmel, *Characteristics of binge drinkers in Europe.* Soc Sci Med, 2004. **59**(1): p. 113-27.
305. Miller, J.W., et al., *Binge drinking and associated health risk behaviors among high school students.* Pediatrics, 2007. **119**(1): p. 76-85.
306. Mathurin, P. and P. Deltenre, *Effect of binge drinking on the liver: an alarming public health issue?* Gut, 2009. **58**(5): p. 613-7.
307. Stolle, M., P.M. Sack, and R. Thomasius, *Binge drinking in childhood and adolescence: epidemiology, consequences, and interventions.* Dtsch Arztebl Int, 2009. **106**(19): p. 323-8.
308. Nutt, D.J. and J. Rehm, *Doing it by numbers: A simple approach to reducing the harms of alcohol.* Journal of Psychopharmacology, 2014. **28**(1): p. 3-7.
309. Chassin, L., S.C. Pitts, and J. Prost, *Binge drinking trajectories from adolescence to emerging adulthood in a high-risk sample: predictors and substance abuse outcomes.* J Consult Clin Psychol, 2002. **70**(1): p. 67-78.
310. Mechtcheriakov, S., et al., *A widespread distinct pattern of cerebral atrophy in patients with alcohol addiction revealed by voxel-based morphometry.* J Neurol Neurosurg Psychiatry, 2007. **78**(6): p. 610-4.
311. Dager, A.D., et al., *Shared genetic factors influence amygdala volumes and risk for alcoholism.* Neuropsychopharmacology, 2015. **40**(2): p. 412-20.
312. van Holst, R.J., et al., *A voxel-based morphometry study comparing problem gamblers, alcohol abusers, and healthy controls.* Drug Alcohol Depend, 2012. **124**(1-2): p. 142-8.
313. Suzuki, Y., et al., *Atrophy of the parahippocampal gyrus and regional cerebral blood flow in the limbic system in chronic alcoholic patients.* Alcohol, 2010. **44**(5): p. 439-45.
314. Pfefferbaum, A., et al., *White matter microstructural recovery with abstinence and decline with relapse in alcohol dependence interacts with normal ageing: a controlled longitudinal DTI study.* Lancet Psychiatry, 2014. **1**(3): p. 202-12.
315. Yeh, P.H., et al., *Tract-Based Spatial Statistics (TBSS) of diffusion tensor imaging data in alcohol dependence: abnormalities of the motivational neurocircuitry.* Psychiatry Res, 2009. **173**(1): p. 22-30.
316. Wang, J.J., et al., *MRSI and DTI: a multimodal approach for improved detection of white matter abnormalities in alcohol and nicotine dependence.* NMR Biomed, 2009. **22**(5): p. 516-22.
317. Chanraud, S., et al., *Diffusion tensor tractography in mesencephalic bundles: relation to mental flexibility in detoxified alcohol-dependent subjects.* Neuropsychopharmacology, 2009. **34**(5): p. 1223-32.
318. Sorg, S.F., et al., *Frontal white matter integrity predictors of adult alcohol treatment outcome.* Biol Psychiatry, 2012. **71**(3): p. 262-8.
319. Tapert s, T.R., Schweinsburg A, Yafai S, Frank L, *Reduced Fractional Anisotropy in the Splenium of Adolescents with Alcohol Use Disorder.* Proc. Intl. Soc. Mag. Reson. Med. 11 2003.
320. De Bellis, M.D., et al., *Diffusion tensor measures of the corpus callosum in adolescents with adolescent onset alcohol use disorders.* Alcohol Clin Exp Res, 2008. **32**(3): p. 395-404.
321. Luciana, M., et al., *Effects of alcohol use initiation on brain structure in typically developing adolescents.* American Journal of Drug and Alcohol Abuse, 2013. **39**(6): p. 345-355.

322. Lisdahl, K.M., et al., *Recent binge drinking predicts smaller cerebellar volumes in adolescents.* Psychiatry Research-Neuroimaging, 2013. **211**(1): p. 17-23.
323. Doallo, S., et al., *Larger Mid-Dorsolateral Prefrontal Gray Matter Volume in Young Binge Drinkers Revealed by Voxel-Based Morphometry.* Plos One, 2014. **9**(5).
324. Howell, N.A., et al., *Increased ventral striatal volume in college-aged binge drinkers.* PLoS One, 2013. **8**(9): p. e74164.
325. Camchong, J., A. Stenger, and G. Fein, *Resting-state synchrony in long-term abstinent alcoholics.* Alcohol Clin Exp Res, 2013. **37**(1): p. 75-85.
326. Camchong, J., V.A. Stenger, and G. Fein, *Resting-state synchrony in short-term versus long-term abstinent alcoholics.* Alcohol Clin Exp Res, 2013. **37**(5): p. 794-803.
327. Orban, C., et al., *Resting state synchrony in anxiety-related circuits of abstinent alcohol-dependent patients.* Am J Drug Alcohol Abuse, 2013. **39**(6): p. 433-40.
328. Camchong, J., A. Stenger, and G. Fein, *Resting-state synchrony during early alcohol abstinence can predict subsequent relapse.* Cereb Cortex, 2013. **23**(9): p. 2086-99.
329. Squeglia, L.M., et al., *Adolescent binge drinking linked to abnormal spatial working memory brain activation: differential gender effects.* Alcohol Clin Exp Res, 2011. **35**(10): p. 1831-41.
330. Morris, L.S., et al., *Jumping the Gun: Mapping Neural Correlates of Waiting Impulsivity and Relevance Across Alcohol Misuse.* Biol Psychiatry, 2015.
331. Poulos, C.X., A.D. Le, and J.L. Parker, *Impulsivity predicts individual susceptibility to high levels of alcohol self-administration.* Behav Pharmacol, 1995. **6**(8): p. 810-814.
332. Dalley, J.W., et al., *Nucleus Accumbens D2/3 receptors predict trait impulsivity and cocaine reinforcement.* Science, 2007. **315**(5816): p. 1267-1270.
333. Dick, D.M., et al., *Understanding the construct of impulsivity and its relationship to alcohol use disorders.* Addict Biol, 2010. **15**(2): p. 217-26.
334. Barratt, E.S., *Factor Analysis of Some Psychometric Measures of Impulsiveness and Anxiety.* Psychol Rep, 1965. **16**: p. 547-54.
335. Whiteside, S.P. and D.R. Lynam, *The Five Factor Model and impulsivity: using a structural model of personality to understand impulsivity.* Personality and Individual Differences, 2001. **30**(4): p. 669-689.
336. Whiteside, S.P., et al., *Validation of the UPPS impulsive behaviour scale: a four-factor model of impulsivity.* European Journal of Personality, 2005. **19**(7): p. 559-574.
337. Whiteside, S.P. and D.R. Lynam, *Understanding the role of impulsivity and externalizing psychopathology in alcohol abuse: application of the UPPS impulsive behavior scale.* Exp Clin Psychopharmacol, 2003. **11**(3): p. 210-7.
338. Cyders, M.A., et al., *The role of personality dispositions to risky behavior in predicting first-year college drinking.* Addiction, 2009. **104**(2): p. 193-202.
339. von Diemen, L., et al., *Impulsivity, age of first alcohol use and substance use disorders among male adolescents: a population based case-control study.* Addiction, 2008. **103**(7): p. 1198-205.
340. Dom, G., W. Hulstijn, and B. Sabbe, *Differences in impulsivity and sensation seeking between early- and late-onset alcoholics.* Addict Behav, 2006. **31**(2): p. 298-308.

341. Nees, F., et al., *Determinants of Early Alcohol Use In Healthy Adolescents: The Differential Contribution of Neuroimaging and Psychological Factors.* Neuropsychopharmacology, 2012. **37**(4): p. 986-995.
342. Rubio, G., et al., *The role of behavioral impulsivity in the development of alcohol dependence: A 4-year follow-up study.* Alcoholism-Clinical and Experimental Research, 2008. **32**(9): p. 1681-1687.
343. Noel, X., et al., *Alcohol cues increase cognitive impulsivity in individuals with alcoholism.* Psychopharmacology (Berl), 2007. **192**(2): p. 291-8.
344. Bickel, W.K., et al., *Behavioral and neuroeconomics of drug addiction: competing neural systems and temporal discounting processes.* Drug Alcohol Depend, 2007. **90 Suppl 1**: p. S85-91.
345. Petry, N.M., *Delay discounting of money and alcohol in actively using alcoholics, currently abstinent alcoholics, and controls.* Psychopharmacology, 2001. **154**(3): p. 243-250.
346. Hill, S.Y., et al., *Disruption of orbitofrontal cortex laterality in offspring from multiplex alcohol dependence families.* Biol Psychiatry, 2009. **65**(2): p. 129-36.
347. Lejuez, C.W., et al., *Behavioral and biological indicators of impulsivity in the development of alcohol use, problems, and disorders.* Alcohol Clin Exp Res, 2010. **34**(8): p. 1334-45.
348. I-Chao Liu, C.-H.C., Chih-Jui Chen, Li-Wei Kuo, Yu-Chun Lo, Wen-Yih Isaac Tseng, *The microstructural integrity of the corpus callosum and associated impulsivity in alcohol dependence: A tractography-based segmentation study using diffusion spectrum imaging.* Psychiatry Research: Neuroimaging, 2010. **184**(2): p. 128-134.
349. Cyders, M.A., et al., *Negative urgency and ventromedial prefrontal cortex responses to alcohol cues: FMRI evidence of emotion-based impulsivity.* Alcohol Clin Exp Res, 2014. **38**(2): p. 409-17.
350. Lawrence, A.J., et al., *Impulsivity and response inhibition in alcohol dependence and problem gambling.* Psychopharmacology (Berl), 2009. **207**(1): p. 163-72.
351. Fillmore, M.T. and M. Vogel-Sprott, *Response inhibition under alcohol: effects of cognitive and motivational conflict.* J Stud Alcohol, 2000. **61**(2): p. 239-46.
352. Ridderinkhof, K.R., et al., *Alcohol consumption impairs detection of performance errors in mediofrontal cortex.* Science, 2002. **298**(5601): p. 2209-11.
353. Schellekens, A.F., et al., *Alcohol dependence and anxiety increase error-related brain activity.* Addiction, 2010. **105**(11): p. 1928-34.
354. Kuhn, J., et al., *Successful deep brain stimulation of the nucleus accumbens in severe alcohol dependence is associated with changed performance monitoring.* Addict Biol, 2011. **16**(4): p. 620-3.
355. Hardee, J.E., et al., *Development of impulse control circuitry in children of alcoholics.* Biol Psychiatry, 2014. **76**(9): p. 708-16.
356. Mary M. Heitzeg, J.T.N., Jillian E. Hardee, Mary Soules, Davia Steinberg, Jon-Kar Zubieta, Robert A. Zucker, *Left middle frontal gyrus response to inhibitory errors in children prospectively predicts early problem substance use.* Drug and Alcohol Dependence, 2014. **141**: p. 51-57.
357. Norman, A.L., et al., *Neural activation during inhibition predicts initiation of substance use in adolescence.* Drug Alcohol Depend, 2011. **119**(3): p. 216-23.

358. Kareken, D.A., et al., *Family history of alcoholism interacts with alcohol to affect brain regions involved in behavioral inhibition.* Psychopharmacology (Berl), 2013. **228**(2): p. 335-45.
359. Luijten, M., et al., *Systematic review of ERP and fMRI studies investigating inhibitory control and error processing in people with substance dependence and behavioural addictions.* J Psychiatry Neurosci, 2014. **39**(3): p. 149-69.
360. Claus, E.D., K.A. Kiehl, and K.E. Hutchison, *Neural and behavioral mechanisms of impulsive choice in alcohol use disorder.* Alcohol Clin Exp Res, 2011. **35**(7): p. 1209-19.
361. Amlung, M., et al., *Dissociable brain signatures of choice conflict and immediate reward preferences in alcohol use disorders.* Addict Biol, 2014. **19**(4): p. 743-53.
362. Oberlin, B.G., et al., *Monetary discounting and ventral striatal dopamine receptor availability in nontreatment-seeking alcoholics and social drinkers.* Psychopharmacology (Berl), 2015. **232**(12): p. 2207-16.
363. Beck, A., et al., *Ventral striatal activation during reward anticipation correlates with impulsivity in alcoholics.* Biol Psychiatry, 2009. **66**(8): p. 734-42.
364. Kim, Y.T., H. Sohn, and J. Jeong, *Delayed transition from ambiguous to risky decision making in alcohol dependence during Iowa Gambling Task.* Psychiatry Research, 2011. **190**(2-3): p. 297-303.
365. Goudriaan, A.E., et al., *Decision making in pathological gambling: A comparison between pathological gamblers, alcohol dependents, persons with Tourette syndrome, and normal controls.* Cognitive Brain Research, 2005. **23**(1): p. 137-151.
366. Bowden-Jones, H., et al., *Risk-taking on tests sensitive to ventromedial prefrontal cortex dysfunction predicts early relapse in alcohol dependency: a pilot study.* Journal of Neuropsychiatry and Clinical Neurosciences, 2005. **17**(3): p. 417-420.
367. Wagner, M.K., *Behavioral characteristics related to substance abuse and risk-taking, sensation-seeking, anxiety sensitivity, and self-reinforcement.* Addictive Behaviors, 2001. **26**(1): p. 115-120.
368. Wills, T.A., D. Vaccaro, and G. McNamara, *Novelty seeking, risk taking, and related constructs as predictors of adolescent substance use: an application of Cloninger's theory.* J Subst Abuse, 1994. **6**(1): p. 1-20.
369. Fergusson, D.M. and M.T. Lynskey, *Alcohol misuse and adolescent sexual behaviors and risk taking.* Pediatrics, 1996. **98**(1): p. 91-96.
370. Bechara, A., et al., *Decision-making deficits, linked to a dysfunctional ventromedial prefrontal cortex, revealed in alcohol and stimulant abusers.* Neuropsychologia, 2001. **39**(4): p. 376-89.
371. Villafuerte, S., et al., *Impulsiveness and insula activation during reward anticipation are associated with genetic variants in GABRA2 in a family sample enriched for alcoholism.* Molecular Psychiatry, 2012. **17**(5): p. 511-519.
372. Yan, P. and C.S. Li, *Decreased amygdala activation during risk taking in non-dependent habitual alcohol users: A preliminary fMRI study of the stop signal task.* Am J Drug Alcohol Abuse, 2009. **35**(5): p. 284-9.

373. Bednarski, S.R., et al., *Neural processes of an indirect analog of risk taking in young nondependent adult alcohol drinkers-an FMRI study of the stop signal task.* Alcohol Clin Exp Res, 2012. **36**(5): p. 768-79.
374. Worbe, Y., et al., *Neuronal correlates of risk-seeking attitudes to anticipated losses in binge drinkers.* Biol Psychiatry, 2014. **76**(9): p. 717-24.
375. Banca, P., et al., *Reflection impulsivity in binge drinking: behavioural and volumetric correlates.* Addict Biol, 2015.
376. Joyce, E.M. and T.W. Robbins, *Frontal-Lobe Function in Korsakoff and Non-Korsakoff Alcoholics - Planning and Spatial Working Memory.* Neuropsychologia, 1991. **29**(8): p. 709-723.
377. Adams, K.M., et al., *Neuropsychological deficits are correlated with frontal hypometabolism in positron emission tomography studies of older alcoholic patients.* Alcohol Clin Exp Res, 1993. **17**(2): p. 205-10.
378. Pothiyil, D.I. and J. Alex, *Self–regulation and Set–shifting in Alcohol Dependence Syndrome.* Indian Journal of Applied Research, 2013. **III**(III).
379. Trick, L., et al., *Impaired fear recognition and attentional set-shifting is associated with brain structural changes in alcoholic patients.* Addict Biol, 2014. **19**(6): p. 1041-54.
380. Fortier, C.B., et al., *Delay discrimination and reversal eyeblink classical conditioning in abstinent chronic alcoholics.* Neuropsychology, 2008. **22**(2): p. 196-208.
381. Vanes, L.D., et al., *Contingency learning in alcohol dependence and pathological gambling: learning and unlearning reward contingencies.* Alcoholism, clinical and experimental research, 2014. **38**(6): p. 1602-10.
382. Sebold, M., et al., *Model-based and model-free decisions in alcohol dependence.* Neuropsychobiology, 2014. **70**(2): p. 122-31.
383. Gillan, C.M., et al., *Characterizing a psychiatric symptom dimension related to deficits in goal-directed control.* eLife, 2016. **5**: p. e11305.
384. Voon, V., et al., *Disorders of compulsivity: a common bias towards learning habits.* Mol Psychiatry, 2014. **20**: p. 345-352.
385. Sjoerds, Z., et al., *Behavioral and neuroimaging evidence for overreliance on habit learning in alcohol-dependent patients.* Transl Psychiatry, 2013. **3**: p. e337.
386. Vollstadt-Klein, S., et al., *Initial, habitual and compulsive alcohol use is characterized by a shift of cue processing from ventral to dorsal striatum.* Addiction, 2010. **105**(10): p. 1741-9.
387. Park, S.Q., et al., *Prefrontal cortex fails to learn from reward prediction errors in alcohol dependence.* J Neurosci, 2010. **30**(22): p. 7749-53.
388. Deserno, L., et al., *Chronic alcohol intake abolishes the relationship between dopamine synthesis capacity and learning signals in the ventral striatum.* Eur J Neurosci, 2015. **41**(4): p. 477-86.
389. Reiter, A.M.F., et al., *Behavioral and neural signatures of reduced updating of alternative options in alcohol-dependent patients during flexible decision-making.* The Journal of Neuroscience, in press.
390. Huys, Q.J., et al., *Model-free temporal-difference learning and dopamine in alcohol dependence: Examining concepts from theory and animals in human imaging.* Biological Psychiatry: Cognitive Neuroscience and Neuroimaging, 2016. **1**(5): p. 401-410.

391. Smittenaar, P., et al., *Disruption of dorsolateral prefrontal cortex decreases model-based in favor of model-free control in humans.* Neuron, 2013. **80**(4): p. 914-9.
392. Hampshire, A., et al., *Dissociable roles for lateral orbitofrontal cortex and lateral prefrontal cortex during preference driven reversal learning.* Neuroimage, 2012. **59**(4): p. 4102-4112.
393. Stern, E.R., et al., *Updating beliefs for a decision: neural correlates of uncertainty and underconfidence.* J Neurosci, 2010. **30**(23): p. 8032-41.
394. Braams, B.R., et al., *Longitudinal changes in adolescent risk-taking: a comprehensive study of neural responses to rewards, pubertal development, and risk-taking behavior.* J Neurosci, 2015. **35**(18): p. 7226-38.
395. Hill, S.Y., et al., *Factors predicting the onset of adolescent drinking in families at high risk for developing alcoholism.* Biological Psychiatry, 2000. **48**(4): p. 265-275.
396. Yacoub, E., et al., *Investigation of the initial dip in fMRI at 7 Tesla.* NMR Biomed, 2001. **14**(7-8): p. 408-12.
397. Thompson, J.K., M.R. Peterson, and R.D. Freeman, *Single-neuron activity and tissue oxygenation in the cerebral cortex.* Science, 2003. **299**(5609): p. 1070-2.
398. Li, B. and R.D. Freeman, *Neurometabolic coupling in the lateral geniculate nucleus changes with extended age.* J Neurophysiol, 2010. **104**(1): p. 414-25.
399. Li, B. and R.D. Freeman, *High-resolution neurometabolic coupling in the lateral geniculate nucleus.* J Neurosci, 2007. **27**(38): p. 10223-9.
400. Logothetis, N.K., et al., *Neurophysiological investigation of the basis of the fMRI signal.* Nature, 2001. **412**(6843): p. 150-7.
401. Sheth, S.A., et al., *Linear and nonlinear relationships between neuronal activity, oxygen metabolism, and hemodynamic responses.* Neuron, 2004. **42**(2): p. 347-55.
402. Rauch, A., G. Rainer, and N.K. Logothetis, *The effect of a serotonin-induced dissociation between spiking and perisynaptic activity on BOLD functional MRI.* Proc Natl Acad Sci U S A, 2008. **105**(18): p. 6759-64.
403. Logothetis, N.K., *The underpinnings of the BOLD functional magnetic resonance imaging signal.* J Neurosci, 2003. **23**(10): p. 3963-71.
404. Rees, G., K. Friston, and C. Koch, *A direct quantitative relationship between the functional properties of human and macaque V5.* Nat Neurosci, 2000. **3**(7): p. 716-23.
405. Biswal, B., et al., *Functional connectivity in the motor cortex of resting human brain using echo-planar MRI.* Magn Reson Med, 1995. **34**(4): p. 537-41.
406. Raichle, M.E. and A.Z. Snyder, *A default mode of brain function: a brief history of an evolving idea.* Neuroimage, 2007. **37**(4): p. 1083-90; discussion 1097-9.
407. Beckmann, C.F., et al., *Investigations into resting-state connectivity using independent component analysis.* Philos Trans R Soc Lond B Biol Sci, 2005. **360**(1457): p. 1001-13.
408. Damoiseaux, J.S., et al., *Consistent resting-state networks across healthy subjects.* Proc Natl Acad Sci U S A, 2006. **103**(37): p. 13848-53.
409. Cole, D.M., S.M. Smith, and C.F. Beckmann, *Advances and pitfalls in the analysis and interpretation of resting-state FMRI data.* Front Syst Neurosci, 2010. **4**: p. 8.

410. Fair, D.A., et al., *Development of distinct control networks through segregation and integration.* Proc Natl Acad Sci U S A, 2007. **104**(33): p. 13507-12.
411. Fransson, P., et al., *Resting-state networks in the infant brain.* Proc Natl Acad Sci U S A, 2007. **104**(39): p. 15531-6.
412. Greicius, M.D., et al., *Persistent default-mode network connectivity during light sedation.* Hum Brain Mapp, 2008. **29**(7): p. 839-47.
413. Boly, M., et al., *Intrinsic brain activity in altered states of consciousness: how conscious is the default mode of brain function?* Ann N Y Acad Sci, 2008. **1129**: p. 119-29.
414. Fox, M.D., et al., *Intrinsic fluctuations within cortical systems account for intertrial variability in human behavior.* Neuron, 2007. **56**(1): p. 171-84.
415. Kelly, A.M., et al., *Competition between functional brain networks mediates behavioral variability.* Neuroimage, 2008. **39**(1): p. 527-37.
416. Biswal, B.B., J. Van Kylen, and J.S. Hyde, *Simultaneous assessment of flow and BOLD signals in resting-state functional connectivity maps.* NMR Biomed, 1997. **10**(4-5): p. 165-70.
417. Birn, R.M., et al., *Separating respiratory-variation-related fluctuations from neuronal-activity-related fluctuations in fMRI.* Neuroimage, 2006. **31**(4): p. 1536-48.
418. Birn, R.M., et al., *The respiration response function: the temporal dynamics of fMRI signal fluctuations related to changes in respiration.* Neuroimage, 2008. **40**(2): p. 644-54.
419. Shmuel, A. and D.A. Leopold, *Neuronal correlates of spontaneous fluctuations in fMRI signals in monkey visual cortex: Implications for functional connectivity at rest.* Hum Brain Mapp, 2008. **29**(7): p. 751-61.
420. Luchtmann, M., et al., *Alcohol induced region-dependent alterations of hemodynamic response: implications for the statistical interpretation of pharmacological fMRI studies.* Exp Brain Res, 2010. **204**(1): p. 1-10.
421. Haorah, J., et al., *Alcohol-induced oxidative stress in brain endothelial cells causes blood-brain barrier dysfunction.* J Leukoc Biol, 2005. **78**(6): p. 1223-32.
422. Volkow, N.D., et al., *Effects of acute alcohol intoxication on cerebral blood flow measured with PET.* Psychiatry Res, 1988. **24**(2): p. 201-9.
423. Luchtmann, M., et al., *Ethanol modulates the neurovascular coupling.* Neurotoxicology, 2013. **34**: p. 95-104.
424. Altura, B.M. and B.T. Altura, *Alcohol, the cerebral circulation and strokes.* Alcohol, 1984. **1**(4): p. 325-31.
425. Gill, J.S., et al., *Alcohol consumption--a risk factor for hemorrhagic and non-hemorrhagic stroke.* Am J Med, 1991. **90**(4): p. 489-97.
426. Kundu, P., et al., *Integrated strategy for improving functional connectivity mapping using multiecho fMRI.* Proceedings of the National Academy of Sciences of the United States of America, 2013. **110**(40): p. 16187-16192.
427. Kundu, P., et al., *Differentiating BOLD and non-BOLD signals in fMRI time series using multi-echo EPI.* Neuroimage, 2012. **60**(3): p. 1759-70.
428. Behrens, T.E., et al., *Characterization and propagation of uncertainty in diffusion-weighted MR imaging.* Magn Reson Med, 2003. **50**(5): p. 1077-88.
429. Panagiotaki, E., et al., *Compartment models of the diffusion MR signal in brain white matter: a taxonomy and comparison.* Neuroimage, 2012. **59**(3): p. 2241-54.

430. Zhang, H., et al., *NODDI: practical in vivo neurite orientation dispersion and density imaging of the human brain.* Neuroimage, 2012. **61**(4): p. 1000-16.
431. Tariq M, S.T., Alexander DC, Wheeler-Kingshott CAM, Zhang H, *Scan-rescan reproducibility of neurite microstructure estimates using NODDI.* Medical Image Understanding and Analysis 2012: Proceedings of the 16th Conference on Medical Image Understanding and Analysis, 2012: p. 255 - 261.
432. Jespersen, S.N., et al., *Determination of axonal and dendritic orientation distributions within the developing cerebral cortex by diffusion tensor imaging.* IEEE Trans Med Imaging, 2012. **31**(1): p. 16-32.
433. Jespersen, S.N., et al., *Neurite density from magnetic resonance diffusion measurements at ultrahigh field: comparison with light microscopy and electron microscopy.* Neuroimage, 2010. **49**(1): p. 205-16.
434. Jacobs, B., et al., *Regional dendritic and spine variation in human cerebral cortex: a quantitative Golgi study.* Cerebral Cortex, 2001. **11**(6): p. 558-571.
435. Nazeri, A., et al., *Functional consequences of neurite orientation dispersion and density in humans across the adult lifespan.* J Neurosci, 2015. **35**(4): p. 1753-62.
436. Beck, A.T., et al., *An Inventory for Measuring Depression.* Archives of General Psychiatry, 1961. **4**(6): p. 561-&.
437. Saunders, J.B., et al., *Development of the Alcohol Use Disorders Identification Test (AUDIT): WHO Collaborative Project on Early Detection of Persons with Harmful Alcohol Consumption--II.* Addiction, 1993. **88**(6): p. 791-804.
438. Townshend, J.M. and T. Duka, *Patterns of alcohol drinking in a population of young social drinkers: a comparison of questionnaire and diary measures.* Alcohol Alcohol, 2002. **37**(2): p. 187-92.
439. Sheehan, D.V., et al., *The Mini-International Neuropsychiatric Interview (M.I.N.I.): the development and validation of a structured diagnostic psychiatric interview for DSM-IV and ICD-10.* J Clin Psychiatry, 1998. **59 Suppl 20**: p. 22-33;quiz 34-57.
440. Whitfield-Gabrieli, S. and A. Nieto-Castanon, *Conn: a functional connectivity toolbox for correlated and anticorrelated brain networks.* Brain Connect, 2012. **2**(3): p. 125-41.
441. Morris, L.S., et al., *Fronto-striatal organization: defining functional and microstructural substrates of behavioural flexibility.* Cortex, 2015.
442. Maldjian, J.A., et al., *An automated method for neuroanatomic and cytoarchitectonic atlas-based interrogation of fMRI data sets.* NeuroImage, 2003. **19**(3): p. 1233-1239.
443. Murray, G.K., et al., *Substantia nigra/ventral tegmental reward prediction error disruption in psychosis.* Mol Psychiatry, 2008. **13**(3): p. 239, 267-76.
444. Martinez, D., et al., *Imaging human mesolimbic dopamine transmission with positron emission tomography. Part II: amphetamine-induced dopamine release in the functional subdivisions of the striatum.* J Cereb Blood Flow Metab, 2003. **23**(3): p. 285-300.
445. Brett M, A.J., Valabregue R, Poline JB, *Region of interest analysis using an SPM toolbox [abstract].* Presented at the 8th International Conferance on Functional Mapping of the Human Brain, 2002. **Available on CD-ROM in NeuroImage, Vol 16, No 2, abstract 497**.

446. Cox, S.R., et al., *A systematic review of brain frontal lobe parcellation techniques in magnetic resonance imaging.* Brain Struct Funct, 2014. **219**(1): p. 1-22.
447. Ongur, D., A.T. Ferry, and J.L. Price, *Architectonic subdivision of the human orbital and medial prefrontal cortex.* J Comp Neurol, 2003. **460**(3): p. 425-49.
448. Sanches, M., et al., *An MRI-based approach for the measurement of the dorsolateral prefrontal cortex in humans.* Psychiatry Res, 2009. **173**(2): p. 150-4.
449. Kim, J.H., et al., *Defining functional SMA and pre-SMA subregions in human MFC using resting state fMRI: functional connectivity-based parcellation method.* Neuroimage, 2010. **49**(3): p. 2375-86.
450. Desikan, R.S., et al., *An automated labeling system for subdividing the human cerebral cortex on MRI scans into gyral based regions of interest.* Neuroimage, 2006. **31**(3): p. 968-80.
451. Johnson-Frey, S.H., et al., *Actions or hand-object interactions? Human inferior frontal cortex and action observation.* Neuron, 2003. **39**(6): p. 1053-1058.
452. Ramnani, N. and A.M. Owen, *Anterior prefrontal cortex: insights into function from anatomy and neuroimaging.* Nat Rev Neurosci, 2004. **5**(3): p. 184-94.
453. Ongur, D. and J.L. Price, *The organization of networks within the orbital and medial prefrontal cortex of rats, monkeys and humans.* Cereb Cortex, 2000. **10**(3): p. 206-19.
454. (NIAAA), N.I.o.A.A.a.A., *NIAAA council approves definition of binge drinking. .* NIAAA Newsletter 3., 2004.
455. Behrens, T.E., et al., *Non-invasive mapping of connections between human thalamus and cortex using diffusion imaging.* Nat Neurosci, 2003. **6**(7): p. 750-7.
456. Di Martino, A., et al., *Functional connectivity of human striatum: a resting state FMRI study.* Cereb Cortex, 2008. **18**(12): p. 2735-47.
457. Choi, E.Y., B.T. Yeo, and R.L. Buckner, *The organization of the human striatum estimated by intrinsic functional connectivity.* J Neurophysiol, 2012. **108**(8): p. 2242-63.
458. Jung, W.H., et al., *Unravelling the intrinsic functional organization of the human striatum: a parcellation and connectivity study based on resting-state FMRI.* PLoS One, 2014. **9**(9): p. e106768.
459. Alexander, G.E. and M.D. Crutcher, *Functional architecture of basal ganglia circuits: neural substrates of parallel processing.* Trends Neurosci, 1990. **13**(7): p. 266-71.
460. Swick, D., V. Ashley, and U. Turken, *Are the neural correlates of stopping and not going identical? Quantitative meta-analysis of two response inhibition tasks.* Neuroimage, 2011. **56**(3): p. 1655-65.
461. Aron, A.R., *From reactive to proactive and selective control: developing a richer model for stopping inappropriate responses.* Biol Psychiatry, 2011. **69**(12): p. e55-68.
462. Morris, L.S., et al., *Fronto-striatal organization: Defining functional and microstructural substrates of behavioural flexibility.* Cortex, 2015. **74**: p. 118-133.

463. de Wit, S., et al., *Corticostriatal Connectivity Underlies Individual Differences in the Balance between Habitual and Goal-Directed Action Control.* Journal of Neuroscience, 2012. **32**(35): p. 12066-12075.
464. Logan GD, C.W., *On the ability to inhibit thought and action: A theory of an act of control.* Psychological Review. 1984;91:295–327.
465. Slotnick, S.D., et al., *Distinct prefrontal cortex activity associated with item memory and source memory for visual shapes.* Brain Res Cogn Brain Res, 2003. **17**(1): p. 75-82.
466. Cardinal, R.N., et al., *Emotion and motivation: the role of the amygdala, ventral striatum, and prefrontal cortex.* Neurosci Biobehav Rev, 2002. **26**(3): p. 321-52.
467. Elliott, R., K.J. Friston, and R.J. Dolan, *Dissociable neural responses in human reward systems.* J Neurosci, 2000. **20**(16): p. 6159-65.
468. Drevets, W.C., J. Savitz, and M. Trimble, *The subgenual anterior cingulate cortex in mood disorders.* CNS Spectr, 2008. **13**(8): p. 663-81.
469. Phelps, E.A., et al., *Extinction learning in humans: role of the amygdala and vmPFC.* Neuron, 2004. **43**(6): p. 897-905.
470. Kopell, B.H. and B.D. Greenberg, *Anatomy and physiology of the basal ganglia: implications for DBS in psychiatry.* Neurosci Biobehav Rev, 2008. **32**(3): p. 408-22.
471. Haber, S.N., et al., *The orbital and medial prefrontal circuit through the primate basal ganglia.* J Neurosci, 1995. **15**(7 Pt 1): p. 4851-67.
472. Robinson, E.S., et al., *Behavioural characterisation of high impulsivity on the 5-choice serial reaction time task: specific deficits in 'waiting' versus 'stopping'.* Behav Brain Res, 2009. **196**(2): p. 310-6.
473. Young, J.W., et al., *The 5-choice continuous performance test: evidence for a translational test of vigilance for mice.* PLoS One, 2009. **4**(1): p. e4227.
474. Ballanger, B., et al., *Stimulation of the subthalamic nucleus and impulsivity: release your horses.* Ann Neurol, 2009. **66**(6): p. 817-24.
475. Glascher, J., et al., *States versus rewards: dissociable neural prediction error signals underlying model-based and model-free reinforcement learning.* Neuron, 2010. **66**(4): p. 585-95.
476. Lucantonio, F., et al., *The impact of orbitofrontal dysfunction on cocaine addiction.* Nat Neurosci, 2012. **15**(3): p. 358-66.
477. Collins, P., et al., *The effect of dopamine depletion from the caudate nucleus of the common marmoset (Callithrix jacchus) on tests of prefrontal cognitive function.* Behavioral Neuroscience, 2000. **114**(1): p. 3-17.
478. Block, A.E., et al., *Thalamic-prefrontal cortical-ventral striatal circuitry mediates dissociable components of strategy set shifting.* Cereb Cortex, 2007. **17**(7): p. 1625-36.
479. Floresco, S.B., et al., *Dissociable roles for the nucleus accumbens core and shell in regulating set shifting.* J Neurosci, 2006. **26**(9): p. 2449-57.
480. Groman, S.M., et al., *Monoamine levels within the orbitofrontal cortex and putamen interact to predict reversal learning performance.* Biological Psychiatry, 2013. **73**(8): p. 756-62.
481. Klanker, M., et al., *Deep brain stimulation in the lateral orbitofrontal cortex impairs spatial reversal learning.* Behavioural brain research, 2013. **245**: p. 7-12.

482. Parent, A. and L.N. Hazrati, *Functional anatomy of the basal ganglia. I. The cortico-basal ganglia-thalamo-cortical loop.* Brain Res Brain Res Rev, 1995. **20**(1): p. 91-127.
483. Middleton, F.A. and P.L. Strick, *Basal ganglia and cerebellar loops: motor and cognitive circuits.* Brain Res Brain Res Rev, 2000. **31**(2-3): p. 236-50.
484. Wingard, J.C. and M.G. Packard, *The amygdala and emotional modulation of competition between cognitive and habit memory.* Behav Brain Res, 2008. **193**(1): p. 126-31.
485. Broadbent, N.J., L.R. Squire, and R.E. Clark, *Rats depend on habit memory for discrimination learning and retention.* Learn Mem, 2007. **14**(3): p. 145-51.
486. Packard, M.G., L. Cahill, and J.L. McGaugh, *Amygdala modulation of hippocampal-dependent and caudate nucleus-dependent memory processes.* Proc Natl Acad Sci U S A, 1994. **91**(18): p. 8477-81.
487. Holroyd, C.B. and N. Yeung, *Motivation of extended behaviors by anterior cingulate cortex.* Trends Cogn Sci, 2012. **16**(2): p. 122-8.
488. Kennerley, S.W., et al., *Optimal decision making and the anterior cingulate cortex.* Nat Neurosci, 2006. **9**(7): p. 940-7.
489. Thobois, S., et al., *STN stimulation alters pallidal-frontal coupling during response selection under competition.* J Cereb Blood Flow Metab, 2007. **27**(6): p. 1173-84.
490. Witt, K., et al., *Deep brain stimulation of the subthalamic nucleus improves cognitive flexibility but impairs response inhibition in Parkinson disease.* Arch Neurol, 2004. **61**(5): p. 697-700.
491. Ehrsson, H.H., C. Spence, and R.E. Passingham, *That's my hand! Activity in premotor cortex reflects feeling of ownership of a limb.* Science, 2004. **305**(5685): p. 875-7.
492. Rizzolatti, G., et al., *Premotor cortex and the recognition of motor actions.* Brain Res Cogn Brain Res, 1996. **3**(2): p. 131-41.
493. Albuquerque, L., et al., *STN-DBS does not change emotion recognition in advanced Parkinson's disease.* Parkinsonism Relat Disord, 2014. **20**(2): p. 166-9.
494. Herzog, J., et al., *Influence of subthalamic deep brain stimulation versus levodopa on motor perseverations in Parkinson's disease.* Mov Disord, 2009. **24**(8): p. 1206-10.
495. Houeto, J.L., et al., *Behavioural disorders, Parkinson's disease and subthalamic stimulation.* J Neurol Neurosurg Psychiatry, 2002. **72**(6): p. 701-7.
496. Huettel, S.A., A.W. Song, and G. McCarthy, *Decisions under uncertainty: probabilistic context influences activation of prefrontal and parietal cortices.* J Neurosci, 2005. **25**(13): p. 3304-11.
497. de Hollander, G., M.C. Keuken, and B.U. Forstmann, *The subcortical cocktail problem; mixed signals from the subthalamic nucleus and substantia nigra.* PLoS One, 2015. **10**(3): p. e0120572.
498. Keuken, M.C., et al., *Quantifying inter-individual anatomical variability in the subcortex using 7 T structural MRI.* Neuroimage, 2014. **94**: p. 40-6.
499. Schad, D.J., et al., *Processing speed enhances model-based over model-free reinforcement learning in the presence of high working memory functioning.* Front Psychol, 2014. **5**: p. 1450.

500. van der Schaaf, M.E., et al., *Working memory capacity predicts effects of methylphenidate on reversal learning.* Neuropsychopharmacology, 2013. **38**(10): p. 2011-8.
501. Schrouff, J., et al., *PRoNTo: pattern recognition for neuroimaging toolbox.* Neuroinformatics, 2013. **11**(3): p. 319-37.
502. Winkler, A.M., et al., *Permutation inference for the general linear model.* Neuroimage, 2014. **92**: p. 381-97.
503. Parada, M., et al., *Executive functioning and alcohol binge drinking in university students.* Addictive Behaviors, 2012. **37**(2): p. 167-172.
504. Scaife, J.C. and T. Duka, *Behavioural measures of frontal lobe function in a population of young social drinkers with binge drinking pattern.* Pharmacology Biochemistry and Behavior, 2009. **93**(3): p. 354-362.
505. Mota, N., et al., *Binge drinking trajectory and neuropsychological functioning among university students: A longitudinal study.* Drug and Alcohol Dependence, 2013. **133**(1): p. 108-114.
506. Olbrich, H.M., et al., *Brain activation during craving for alcohol measured by positron emission tomography.* Australian and New Zealand Journal of Psychiatry, 2006. **40**(2): p. 171-178.
507. Boggio, P.S., et al., *Prefrontal cortex modulation using transcranial DC stimulation reduces alcohol craving: A double-blind, sham-controlled study.* Drug and Alcohol Dependence, 2008. **92**(1-3): p. 55-60.
508. Wrase, J., et al., *Amygdala volume associated with alcohol abuse relapse and craving.* Am J Psychiatry, 2008. **165**(9): p. 1179-84.
509. Makris, N., et al., *Decreased volume of the brain reward system in alcoholism.* Biol Psychiatry, 2008. **64**(3): p. 192-202.
510. Sullivan, E.V., et al., *Striatal and forebrain nuclei volumes: contribution to motor function and working memory deficits in alcoholism.* Biol Psychiatry, 2005. **57**(7): p. 768-76.
511. Cservenka, A., et al., *Family history density of alcoholism relates to left nucleus accumbens volume in adolescent girls.* J Stud Alcohol Drugs, 2015. **76**(1): p. 47-56.
512. TL Kvamme, C.S., D Strelchuk, YC Chang-Webb, K Baek, V Voon, *Sexually dimorphic brain volume interaction in college-aged binge drinkers.* Neuroimage: Clinical, 2016. **10**: p. 310-317.
513. Robinson, T.E. and B. Kolb, *Structural plasticity associated with exposure to drugs of abuse.* Neuropharmacology, 2004. **47 Suppl 1**: p. 33-46.
514. Rassnick, S., L. Pulvirenti, and G.F. Koob, *Oral Ethanol Self-Administration in Rats Is Reduced by the Administration of Dopamine and Glutamate Receptor Antagonists into the Nucleus-Accumbens.* Psychopharmacology, 1992. **109**(1-2): p. 92-98.
515. Fox, M.D., et al., *Efficacy of Transcranial Magnetic Stimulation Targets for Depression Is Related to Intrinsic Functional Connectivity with the Subgenual Cingulate.* Biological Psychiatry, 2012. **72**(7): p. 595-603.
516. Fox, M.D., H. Liu, and A. Pascual-Leone, *Identification of reproducible individualized targets for treatment of depression with TMS based on intrinsic connectivity.* Neuroimage, 2013. **66**: p. 151-60.

517. Lardeux, S., et al., *Beyond the reward pathway: coding reward magnitude and error in the rat subthalamic nucleus.* J Neurophysiol, 2009. **102**(4): p. 2526-37.
518. Zavala, B.A., et al., *Midline frontal cortex low-frequency activity drives subthalamic nucleus oscillations during conflict.* J Neurosci, 2014. **34**(21): p. 7322-33.
519. Rudebeck, P.H., et al., *Prefrontal mechanisms of behavioral flexibility, emotion regulation and value updating.* Nat Neurosci, 2013. **16**(8): p. 1140-5.
520. Forstmann, B.U., et al., *Towards a mechanistic understanding of the human subcortex.* Nat Rev Neurosci, 2016. **18**(1): p. 57-65.
521. Gremel, C.M. and R.M. Costa, *Orbitofrontal and striatal circuits dynamically encode the shift between goal-directed and habitual actions.* Nat Commun, 2013. **4**: p. 2264.
522. Zwosta, K., H. Ruge, and U. Wolfensteller, *Neural mechanisms of goal-directed behavior: outcome-based response selection is associated with increased functional coupling of the angular gyrus.* Front Hum Neurosci, 2015. **9**: p. 180.
523. Rhodes, S.E. and E.A. Murray, *Differential effects of amygdala, orbital prefrontal cortex, and prelimbic cortex lesions on goal-directed behavior in rhesus macaques.* J Neurosci, 2013. **33**(8): p. 3380-9.
524. Critchley, H.D., *The human cortex responds to an interoceptive challenge.* Proc Natl Acad Sci U S A, 2004. **101**(17): p. 6333-4.
525. Rudebeck, P.H., et al., *A role for primate subgenual cingulate cortex in sustaining autonomic arousal.* Proc Natl Acad Sci U S A, 2014. **111**(14): p. 5391-6.
526. Halsband, U., Y. Matsuzaka, and J. Tanji, *Neuronal activity in the primate supplementary, pre-supplementary and premotor cortex during externally and internally instructed sequential movements.* Neurosci Res, 1994. **20**(2): p. 149-55.
527. Shima, K., et al., *Role for cells in the presupplementary motor area in updating motor plans.* Proc Natl Acad Sci U S A, 1996. **93**(16): p. 8694-8.
528. Koechlin, E., C. Ody, and F. Kouneiher, *The architecture of cognitive control in the human prefrontal cortex.* Science, 2003. **302**(5648): p. 1181-5.
529. Ridderinkhof, K.R., et al., *Neurocognitive mechanisms of cognitive control: the role of prefrontal cortex in action selection, response inhibition, performance monitoring, and reward-based learning.* Brain Cogn, 2004. **56**(2): p. 129-40.
530. Wagner, A.D., et al., *Prefrontal contributions to executive control: fMRI evidence for functional distinctions within lateral Prefrontal cortex.* Neuroimage, 2001. **14**(6): p. 1337-47.
531. Rae, C.L., et al., *Atomoxetine restores the response inhibition network in Parkinson's disease.* Brain, 2016. **139**(Pt 8): p. 2235-48.
532. Rogers, R.D., et al., *Contrasting cortical and subcortical activations produced by attentional-set shifting and reversal learning in humans.* J Cogn Neurosci, 2000. **12**(1): p. 142-62.
533. Remijnse, P.L., et al., *Neural correlates of a reversal learning task with an affectively neutral baseline: an event-related fMRI study.* Neuroimage, 2005. **26**(2): p. 609-18.
534. Xue, G., et al., *Common neural mechanisms underlying reversal learning by reward and punishment.* PLoS One, 2013. **8**(12): p. e82169.

535. Rudorf, S. and T.A. Hare, *Interactions between dorsolateral and ventromedial prefrontal cortex underlie context-dependent stimulus valuation in goal-directed choice.* J Neurosci, 2014. **34**(48): p. 15988-96.
536. Vaghi, M.M., et al., *Specific Frontostriatal Circuits for Impaired Cognitive Flexibility and Goal-Directed Planning in Obsessive-Compulsive Disorder: Evidence From Resting-State Functional Connectivity.* Biol Psychiatry, 2016.
537. Delgado, M.R., et al., *Tracking the hemodynamic responses to reward and punishment in the striatum.* J Neurophysiol, 2000. **84**(6): p. 3072-7.
538. Seymour, B., et al., *Differential encoding of losses and gains in the human striatum.* J Neurosci, 2007. **27**(18): p. 4826-31.
539. Palminteri, S., et al., *Critical roles for anterior insula and dorsal striatum in punishment-based avoidance learning.* Neuron, 2012. **76**(5): p. 998-1009.
540. Tom, S.M., et al., *The neural basis of loss aversion in decision-making under risk.* Science, 2007. **315**(5811): p. 515-8.
541. Jahanshahi, M., et al., *The impact of deep brain stimulation on executive function in Parkinson's disease.* Brain, 2000. **123 (Pt 6)**: p. 1142-54.
542. Schroeder, U., et al., *Subthalamic nucleus stimulation affects striato-anterior cingulate cortex circuit in a response conflict task: a PET study.* Brain, 2002. **125**(Pt 9): p. 1995-2004.
543. Green, N., et al., *Reduction of influence of task difficulty on perceptual decision making by STN deep brain stimulation.* Curr Biol, 2013. **23**(17): p. 1681-4.
544. Djamshidian, A., et al., *Increased reflection impulsivity in patients with ephedrone-induced Parkinsonism.* Addiction, 2013. **108**(4): p. 771-9.
545. White, N.M., M.G. Packard, and R.J. McDonald, *Dissociation of memory systems: The story unfolds.* Behav Neurosci, 2013. **127**(6): p. 813-34.
546. McDonald, R.J. and N.M. White, *A triple dissociation of memory systems: hippocampus, amygdala, and dorsal striatum.* Behav Neurosci, 1993. **107**(1): p. 3-22.
547. McDonald, R.J. and N.M. White, *Parallel information processing in the water maze: evidence for independent memory systems involving dorsal striatum and hippocampus.* Behav Neural Biol, 1994. **61**(3): p. 260-70.
548. Redish, A.D. and A. Johnson, *A computational model of craving and obsession.* Ann N Y Acad Sci, 2007. **1104**: p. 324-39.
549. van der Meer, M.A. and A.D. Redish, *Covert Expectation-of-Reward in Rat Ventral Striatum at Decision Points.* Front Integr Neurosci, 2009. **3**: p. 1.
550. van der Meer, M.A., et al., *Triple dissociation of information processing in dorsal striatum, ventral striatum, and hippocampus on a learned spatial decision task.* Neuron, 2010. **67**(1): p. 25-32.
551. Obeso, I., et al., *Deficits in inhibitory control and conflict resolution on cognitive and motor tasks in Parkinson's disease.* Exp Brain Res, 2011. **212**(3): p. 371-84.
552. Koob, G.F. and N.D. Volkow, *Neurocircuitry of addiction.* Neuropsychopharmacology, 2010. **35**(1): p. 217-38.
553. Nebe, S., et al., *No association of goal-directed and habitual control with alcohol consumption in young adults.* Addict Biol, 2017.
554. Magnin, B., et al., *Support vector machine-based classification of Alzheimer's disease from whole-brain anatomical MRI.* Neuroradiology, 2009. **51**(2): p. 73-83.

555. Dukart, J., et al., *Meta-analysis based SVM classification enables accurate detection of Alzheimer's disease across different clinical centers using FDG-PET and MRI.* Psychiatry Res, 2013. **212**(3): p. 230-6.
556. Koob, G.F. and M. Le Moal, *Plasticity of reward neurocircuitry and the 'dark side' of drug addiction.* Nat Neurosci, 2005. **8**(11): p. 1442-4.
557. Hermann, D., et al., *Translational Magnetic Resonance Spectroscopy Reveals Excessive Central Glutamate Levels During Alcohol Withdrawal in Humans and Rats.* Biological Psychiatry, 2012. **71**(11): p. 1015-1021.
558. Bauer, J., et al., *Craving in Alcohol-Dependent Patients After Detoxification Is Related to Glutamatergic Dysfunction in the Nucleus Accumbens and the Anterior Cingulate Cortex.* Neuropsychopharmacology, 2013. **38**(8): p. 1401-1408.
559. Ward, R.J., et al., *Neuro-inflammation induced in the hippocampus of 'binge drinking' rats may be mediated by elevated extracellular glutamate content.* J Neurochem, 2009. **111**(5): p. 1119-28.
560. Steinbeis, N., B.C. Bernhardt, and T. Singer, *Impulse control and underlying functions of the left DLPFC mediate age-related and age-independent individual differences in strategic social behavior.* Neuron, 2012. **73**(5): p. 1040-51.
561. Krain, A.L., et al., *Distinct neural mechanisms of risk and ambiguity: a meta-analysis of decision-making.* Neuroimage, 2006. **32**(1): p. 477-84.
562. Cieslik, E.C., et al., *Is there "one" DLPFC in cognitive action control? Evidence for heterogeneity from co-activation-based parcellation.* Cereb Cortex, 2013. **23**(11): p. 2677-89.
563. Badre, D. and A.D. Wagner, *Selection, integration, and conflict monitoring; assessing the nature and generality of prefrontal cognitive control mechanisms.* Neuron, 2004. **41**(3): p. 473-87.
564. Sanchez-Roige, S., et al., *Exaggerated waiting impulsivity associated with human binge drinking, and high alcohol consumption in mice.* Neuropsychopharmacology, 2014. **39**(13): p. 2919-27.
565. Miguel-Hidalgo, J.J., et al., *Glia pathology in the prefrontal cortex in alcohol dependence with and without depressive symptoms.* Biol Psychiatry, 2002. **52**(12): p. 1121-33.
566. Miguel-Hidalgo, J.J. and G. Rajkowska, *Comparison of prefrontal cell pathology between depression and alcohol dependence.* J Psychiatr Res, 2003. **37**(5): p. 411-20.
567. Mishra, B.R., et al., *Efficacy of repetitive transcranial magnetic stimulation in alcohol dependence: a sham-controlled study.* Addiction, 2010. **105**(1): p. 49-55.
568. da Silva, M.C., et al., *Behavioral effects of transcranial direct current stimulation (tDCS) induced dorsolateral prefrontal cortex plasticity in alcohol dependence.* J Physiol Paris, 2013. **107**(6): p. 493-502.
569. Fox, M.D., et al., *The human brain is intrinsically organized into dynamic, anticorrelated functional networks.* Proc Natl Acad Sci U S A, 2005. **102**(27): p. 9673-8.
570. Margulies, D.S., et al., *Mapping the functional connectivity of anterior cingulate cortex.* Neuroimage, 2007. **37**(2): p. 579-88.

571. Uddin, L.Q., et al., *Functional connectivity of default mode network components: correlation, anticorrelation, and causality.* Hum Brain Mapp, 2009. **30**(2): p. 625-37.
572. Gee, D.G., et al., *A developmental shift from positive to negative connectivity in human amygdala-prefrontal circuitry.* J Neurosci, 2013. **33**(10): p. 4584-93.